MODELING AND OPTIMIZATION FOR ELECTRIC CARSHARING SERVICES

WU TING

PhD

The Hong Kong Polytechnic University

2022

The Hong Kong Polytechnic University

Department of Industrial and Systems Engineering

Modeling and Optimization for Electric Carsharing Services

WU Ting

A thesis submitted in partial fulfillment of the requirements for the degree of Doctor of Philosophy

July 2022

CERTIFICATE OF ORIGINALITY

I hereby declare that this thesis is my own work and that, to the best of my knowledge and belief, it reproduces no material previously published or written, nor material that has been accepted for the award of any other degree or diploma, except where due acknowledgement has been made in the text.

_____(Signed)

WU Ting_____(Name of student)

ABSTRACT

The era of shared mobility has prompted the emergence of many alternative transportation modes. A prominent one of them is carsharing, which allows users to access private cars without paying ownership costs. Driven by regulations and incentive programs exerted by governments for vehicle electrification, carsharing is undergoing electrification. However, vehicle electrification in carsharing inevitably poses new challenges to decision-makings faced by carsharing operators. These challenges generally come from the limited driving range, frequent charging needs, long charging times, and nonlinear charging profile of EVs. Efforts are highly anticipated to overcome these challenges such that carsharing services (CSSs) can be operated smoothly.

In this thesis, one tactical-level and two operational-level decision-making problems are addressed for electric CSSs: fleet size problem, real-time vehicle relocation and charging strategy (RT-VR&CS) problem, and real-time vehicle relocation and staff rebalancing (RT-VR&SR) problem. The objectives of the three problems are to maximize the profit for carsharing operators. By solving the three problems, this study helps carsharing operators to overcome the decision-making challenges caused by vehicle electrification.

The tactical fleet size problem aims to determine the number of electric vehicles (EVs) put into use for CSSs while considering battery degradation, on-demand charging strategy, and operational vehicle relocation as well as trip assignment. Due to the incorporation of battery wear cost, a mixed-integer nonlinear programming (MINLP) model with both concave and convex terms in the objective function is developed. A piecewise linear approximation approach and an outer-approximation method are employed to linearize the model. The resultant mixed-integer linear programming (MILP) model can be solved by state-of-the-art solvers like Gurobi to obtain an ε-optimal solution.

The operational RT-VR&CS problem seeks to develop a fast yet robust algorithm to determine the real-time vehicle relocation and charging strategies. A dynamic algorithmic framework based on a rolling time horizon is established, through which the complicated RT-VR&CS problem is transformed into solving a series of static vehicle relocation and charging strategy (S-VR&CS) problems. A set-packing-type formulation and a column-generation-based solution method are adopted to solve each static problem. Based on the investigated RT-VR&CS problem, the operational RT-VR&SR problem makes an extension by including staff

rebalancing. A Markov Decision Process (MDP) is formulated and an efficient concurrent-scheduler-based policy is proposed.

The models and solution methods proposed for the three problems are all tested in a real-world case study. Their applicability is validated. The managerial insights are also explored.

PUBLICATIONS ARISING FROM THE THESIS

Journal Publications

1. **Wu, T.**, Xu, M., Eltoukhy, A.E., 2022. Real-time vehicle relocation and staff rebalancing problem for electric and shared vehicle systems. *Transportation Research Part C: Emerging Technologies*. (under 1st round review)
2. Xu, M., **Wu, T.**, 2022. Real-time vehicle relocation and charging optimization for one-way electric carsharing systems. *Transportation Research Part B: Methodological*. (under 2nd round review)
3. **Wu, T.**, Xu, M., 2022. Modeling and optimization for carsharing services: A literature review. *Multimodal Transportation* 1, 100028.
4. Xu, M., **Wu, T.**, Tan, Z., 2021. Electric vehicle fleet size for carsharing services considering on-demand charging strategy and battery degradation. *Transportation Research Part C: Emerging Technologies* 127, 103146.

Conference Proceedings and Presentations

1. Yan, X., **Wu, T.**, Xu, M., 2022. Truck routing and platooning problem considering time-varying traffic conditions. *Proceedings of the 22nd COTA International Conference of Transportation Professionals*. (Best Paper Award)
2. **Wu, T.**, Xu, M., 2022. Dynamic vehicle relocation and charging problem in electric and shared systems under demand uncertainty. *Proceedings of the 101st Annual Meeting of Transportation Research Board*.
3. Ouyang, X., Xu, M., **Wu, T.**, 2021. Vehicle routing for shared autonomous electric vehicles considering passengers' uncertain waiting time tolerance and acceptable stopover. *Proceedings of the 100th Annual Meeting of Transportation Research Board*.
4. **Wu, T.**, Xu, M., 2021. Real-time vehicle relocation and staff rebalancing in one-way electric carsharing systems considering demand uncertainty and nonlinear charging profile. *Presentation at the 4th International Symposium on Multimodal Transportation*.
5. **Wu, T.**, Xu, M., Ouyang, X., Po Yu, Y., 2020. Empirical evidence from China: what contributes to airline customers' positive behavioral intentions? *Proceedings of the 2nd International Conference on Robotics Systems and Vehicle Technology*.

ACKNOWLEDGEMENTS

My deepest gratitude goes first and foremost to my Ph.D. supervisor, Assistant Professor Min Xu, for her persistent supervision, insightful comments, valuable suggestions, and kind encouragement during my three years of research in The Hong Kong Polytechnic University. I have benefited a lot from her strict and high requirement for research. I have also been deeply influenced by her passion and dedication to research. Being a Ph.D. student of her is a lucky thing for me, as pursuing Ph.D. under her supervision ignites my interest in research. I will take her as an example to inspire myself in my future research career and I hope to become a good researcher like her.

I would like to express my sincere appreciation to my Ph.D. committee members for providing me valuable comments on my research work as well as my thesis: Professor Xiaowen Fu, Dr. Jingzheng Ren, Professor Yangmin Li, Professor Chi Xie, and Professor W.Y. Szeto. Many thanks to The Hong Kong Polytechnic University for providing financial support to my Ph.D. study.

I feel grateful to my friends and colleagues for their accompany during my three years of Ph.D. study, especially in the hard times of Hong Kong unrest and outbreak of COVID 19: Ms. Yonghuan He, Ms. Diwan Li, Mr. Xu Ouyang, Mr. Yanlin Xie, Ms. Siyang An, Ms. Tingting Han, Ms. Tana Siqin, Ms. Xiaoyan Xu, Ms. Shengfang Lu, Dr. Li Wang, Ms. Yige Sun, Dr. Nan Huang, Dr. Haohan Xiao, Ms. Yilin Wang, and Ms. Qingqing Zhang. Thanks are also given to my teammates for their encouragement and help: Mr. Shouguo Peng, Ms. Xiaoyuan Yan, Ms. Jiangyan Huang, and Mr. Lu Yang.

Last but not the least, I want to thank my parents for their upbringing, dedication, and support. Finally, I would like to thank the man who has always stood behind me as the most solid backing, silently supported me, tolerated me, and understood me: my beloved husband Yu. Thank you for giving me so much love!

TABLE OF CONTENTS

LIST OF FIGURES

LIST OF TABLES

LIST OF ABBREVIATIONS

CSS	Carsharing service
EV	Electric vehicle
APP	Application
SOC	State of charge
SOS2	Special ordered sets of type 2
EVFS	Electric vehicle fleet size
RT-VR&CS	Real-time vehicle relocation and charging strategy
S-VR&CS	Static vehicle relocation and charging strategy
CC-CV	Constant current-constant voltage
CP-CV	Constant power-constant voltage
B&P	Branch-and-price
LP	Linear programming
RT-VR&SR	Real-time vehicle relocation and staff rebalancing
MDP	Markov Decision Process
CNCS	Constrained non-dominated charging strategy
MINLP	Mixed-integer nonlinear programming
MILP	Mixed-integer linear programming
ILP	Integer linear programming
IP	Integer programming

CHAPTER 1 INTRODUCTION

1.1 Background

The concept of shared mobility has been prevailing over the past decade as an effective way to alleviate traffic congestion and reduce transportation costs. The technology-enabled shared mobility allows users to access mobility as a service on an as-needed basis in a short term (Jittrapirom et al., 2017; Shaheen et al., 2015). It has spawned a number of variants, such as ridesharing, carpooling, vanpooling, carsharing, and dial-a-ride. As an important variant of shared mobility, carsharing has attracted a lot of users around the world. This section will introduce the practice state of carsharing, vehicle electrification in carsharing, and emerging decision-making challenges faced by electric carsharing operators.

1.1.1 Practice state of carsharing

This subsection will start by first stating the basic facts about carsharing, followed by its service features. Last, a global outlook of carsharing will be presented.

1.1.1.1 Basic facts about carsharing

(i) History, definition, and relationship to other modes

Early attempts of carsharing can be traced back to 1948, when a program named ‘Sefage’ was established in Zurich, Switzerland. Later, a number of programs, e.g., ‘Procotip’ in Montpelier, France, ‘Green Cars’ in multiple places of Britain, and ‘Vivalla Bil’ in Örebro, Sweden, were subsequently opened during the period from 1940s to 1980s. However, all these early programs ended with failure within a few years due to a variety of reasons, such as inadequate planning and financial management, small size of the service area, and lack of support from the local government (Board et al., 2005). In fact, all these causes of failure can be ultimately attributed to the mismatch between the excessive ambition and the underdeveloped technology at that time. At the late 1980s, the modern form of carsharing began to sprout and carsharing ushered in its development period. More specifically, in 1987, two companies, i.e., Auto Teilet Genossenschaft and Sharecom Genossenschaft, were founded in Switzerland, which indicated the emerging of the first large-scale professional carsharing system. Shortly after, in 1988, a German carsharing company StattAuto was set up in Berlin. Since then, carsharing spread across European countries in a short time, subsequently appeared in North America from 1994, arrived in Asia in 1997, and more recently started in Australia and Latin America in 2003 and 2009 respectively (Jung, 2014).

Along with the development of carsharing over the past decades, the definition of it has never been standard. Instead of defining it formally, most of the published studies on carsharing gave a description, which may encompass a wide range of programs. Board et al. (2005) collated definitions adopted or proposed by various agencies, which included City of Toronto, State of Washington, State of Oregon, District of Columbia, State of Minnesota, Belgium, Swedish National Road Administration, etc., and found that the definitions generally shared the common themes:

- requirements for users to be members;
- access to a common fleet;
- billing in hourly increments;
- exclusion of traditional car rental.

Based on these common themes, Board et al. (2005) recommended a definition introduced by State of Washington as a standard:

> A membership program intended to offer an alternative to car ownership under which persons or entities that become members are permitted to use vehicles from a fleet on an hourly basis.

This definition was explicitly provided for business, organizational members, and individuals.

Figure 1.1 illustrates the relationship between carsharing and other transportation modes. It can be seen that carsharing mainly caters to the needs for mid-distance trips, where flexibility has to be ensured. To distinguish carsharing from its two closest substitutes, i.e., traditional car rental and taxi, the differences between them are discussed as follows. First, carsharing belongs to hour-based short-term rental, possesses a decentralized and self-accessing network of vehicles, and bunds source of power and insurance into rates, while traditional car rental is day-based long-term rental, has centralized facilities, and requires a staff member to check the vehicle out (Board et al., 2005). Hence, in comparison to traditional car rental, carsharing is less attractive to user groups who need a car to replace a private car. Second, the vehicles in carsharing are driven by the end users and the users generally utilize the vehicles on a personal basis, whereas taxis are driven by professional drivers and the users only enjoy the service carried by the vehicles. Therefore, compared with taxi, carsharing has higher requirements for users in terms of age, driving qualification, and driving record; carsharing is less suitable for short-distance and long-duration trips as users must pay for vehicle reservations.

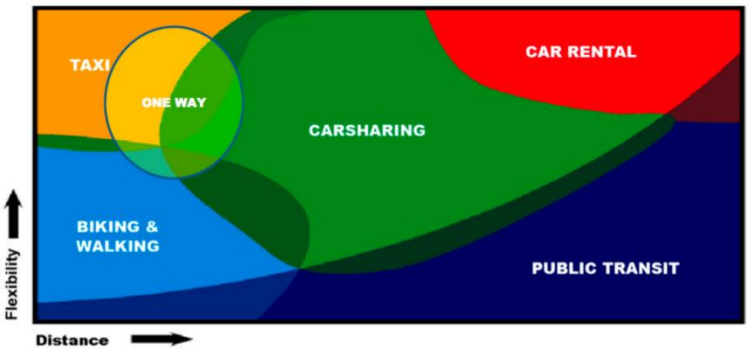

(Source: Jung (2014))

Figure 1.1 Relationship between carsharing and other transportation modes

(ii) Business background and business model

Golalikhani et al. (2021b) made a survey about the carsharing operators throughout the world and they divided them into three categories based on their business background. The first category concerns those established by automobile manufacturers, e.g., EVCARD by SAIC; the second category involves the ones expanded from traditional car-rental companies, e.g., Liandongyun; the third category refers to those without any background in automobile industry or shared mobility, e.g., BlueSG. As for the business model of carsharing operators, there are mainly three types: for-profit, non-profit, and cooperative (Shaheen et al., 2006). Specifically, the for-profit carsharing operators are often self-funded and have profit as their primary goal, and most of carsharing operators in the world such as Zipcar and ShareNow belong to this type; the non-profit carsharing operators, e.g., eGo CarShare, in general, have financial support from government and are usually tax-exempt, aiming to achieving some social or environmental objectives; cooperative carsharing operators, e.g., Som Mobilitat, are mostly financed by their members and same with the non-profit carsharing operators, target social or environmental benefits.

(iii) Service type

Broadly speaking, there are two main types of carsharing services (CSSs), i.e., business-to-consumer and peer-to-peer services (Golalikhani et al., 2021a; Kim et al., 2017; Münzel et al., 2020). The business-to-consumer CSSs can be divided into round-trip and one-way services. Further, one-way CSSs can be categorized into station-based and free-floating services. In some cases, a carsharing operators may provide more than one type of services. For example, Communauto in Canada and Stadtmobil in Germany deliver both round-trip and one-way free-floating services. In the following, these four types of CSSs are elaborated.

Round-trip carsharing. In round-trip CSSs, a user picks up a vehicle parked at a designated station, i.e., a pre-defined parking space owned by the carsharing operator or reserved by the local authority, and has to return the vehicle to the same station (Ferrero et al., 2018; Machado et al., 2018). Since the users have to pay for the entire time period during which they access vehicles, this kind of CSS is less friendly to short-distance and long-duration trips, e.g., daily commuting. Figure 1.2 gives an illustration of round-trip CSSs.

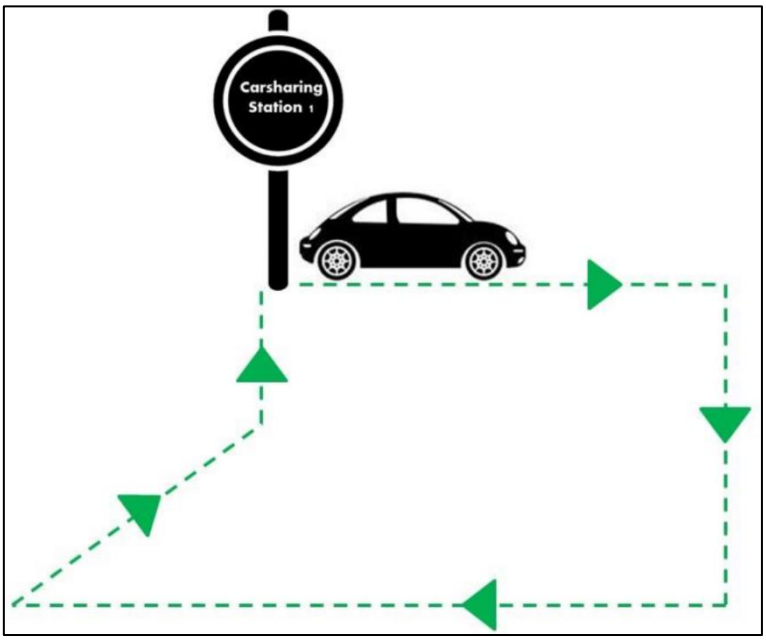

(Source: Lage et al. (2018))

Figure 1.2 Round-trip carsharing

One-way station-based carsharing & One-way free-floating carsharing. One-way station-based CSSs are similar to the round-trip CSSs, but they allow vehicles to be picked up and dropped off at different stations. Based on the one-way station-based CSSs, one-way free-floating services further relaxes vehicles to be picked up and dropped off anywhere in an operation area (e.g., along street), i.e., a non-designated station (Balac et al., 2017; Li et al., 2018). In comparison to round-trip CSSs, one-way CSSs are more flexible and convenient. Nevertheless, due to the gravitational effect caused by dynamic vehicle stock at each station and the tide phenomenon resulting from demand oscillation, one-way CSSs come at the cost of vehicle imbalance issue across stations, i.e., the mismatch between the number of vehicles/parking spots available at a specific station and the user demand over a particular period (Waserhole and Jost, 2012; Xu et al., 2018). Figure 1.3 and Figure 1.4 illustrate the one-way station-based and one-way free-floating CSSs.

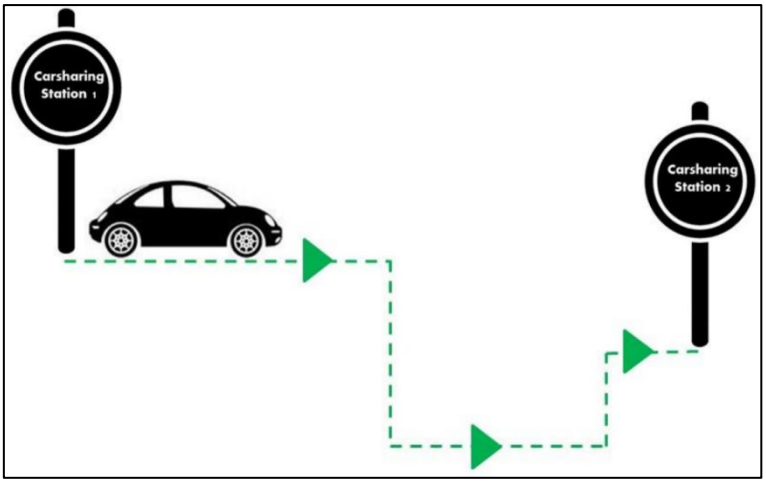

(Source: Lage et al. (2018))

Figure 1.3 One-way station-based carsharing

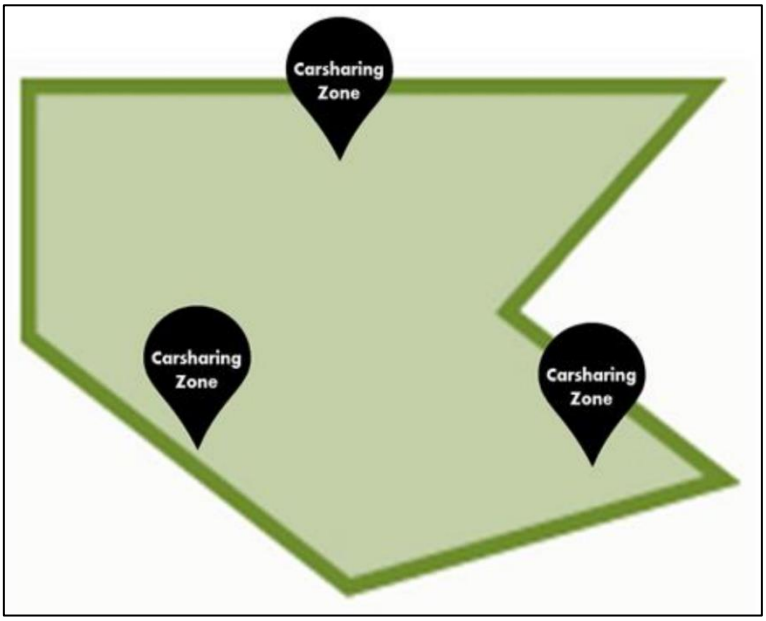

(Source: Lage et al. (2018))

Figure 1.4 One-way free-floating carsharing

Peer-to-peer carsharing. Unlike business-to-consumer CSSs, where the fleet is owned and managed by the carsharing operator, in peer-to-peer CSSs, the shared fleet is privately owned by individuals. These individuals choose to make their private vehicles available for use through the peer-to-peer carsharing platforms and receive payments after the vehicles are rented out. Peer-to-peer carsharing operators act as the intermediates connecting vehicle owners and potential lessees. They regulate the transaction process, cover the vehicle insurance expenses, and in exchange, charge the vehicle owners a portion of rent. Vehicle owners may be required to hand over the car keys to lessees in person or be provided smartcards, which can be used to transact remotely with lessees by accessing vehicles equipped with telematics

devices. Compared with the business-to-consumer CSSs, peer-to-peer CSSs provide a more diverse selection of vehicles in terms of location, type, and price, as the fleet is decentralised-managed. Figure 1.5 shows the online platform of Autonetzer, a peer-to-peer carsharing operator.

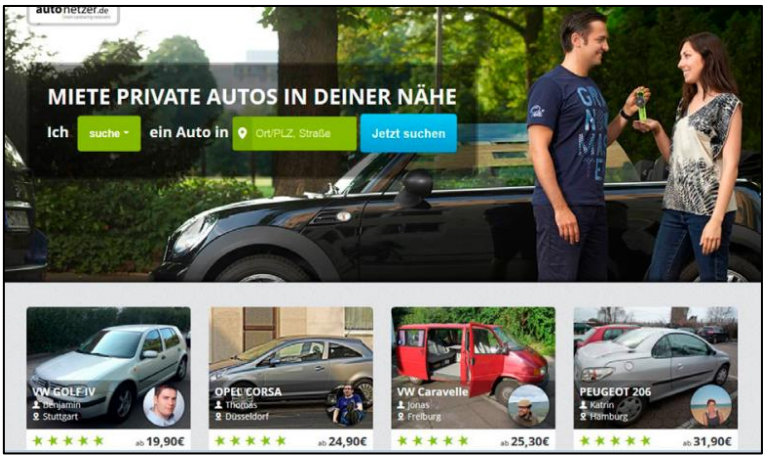

(Source: http://www.carsharing-experten.de/autonetzer-test.html)

Figure 1.5 Peer-to-peer carsharing

Since this study focuses on the business-to-consumer CSSs, unless stated otherwise, the following discussions are dedicated for the business-to-consumer CSSs.

1.1.1.2 Usage features of carsharing

Registration. To access CSSs, potential users should first become members of a carsharing operator by making a registration. The registration can be completed via a dedicated website or a mobile application (APP). In some but not all cases, a single registration fee has to be paid. The potential users are generally required to have driving licenses and keep no bad driving records. The survey by Golalikhani et al. (2021b) revealed that carsharing operators will constantly check users' records to monitor their driving behaviour.

Reservation. After the registration process, users further need to make reservations. Reservations can also be done through the website or mobile APP either in advance (e.g., three hours in advance) or spontaneously. The website or mobile APP provides the information of vehicles in terms of their availability, locations, brands, etc. Users choose vehicles they prefer, and they may be required to specify pick-up and drop-off times. They are allowed to extend the drop-off times if necessary. Before picking up vehicles, users usually need to check vehicles' conditions by opening them via a mobile phone or a chip card. Ignition keys are commonly stored inside the cars.

Pricing. Different carsharing operators may adopt different pricing strategies. However, these pricing strategies are generally developed based on usage time, or driving distance, or combination of both. To attract as many users as possible, a carsharing operator may introduce more than one pricing strategy. For example, a carsharing operator may provide two options for users to choose from: high time rate & low mileage fee and low time rate & high mileage fee. Trips with long-duration and short-distance can benefit from the pricing strategy of low time rate & high mileage fee, while trips with short-duration and long-distance will be more cost-effective by choosing the pricing strategy of high time rate & low mileage fee. To improve vehicle utilization, a carsharing operator may offer discounted usage rate for vehicle usage at off-peak times. Particularly, for a carsharing operator providing one-way services, it may propose differential pricing to encourage users to pick up vehicles at stations with surplus vehicles and drop of them at stations with deficient vehicles such that vehicle imbalance issue can be mitigated.

Returning. After enjoying the CSS, a user should return a vehicle by parking it at either a designed or a non-designed station, contingent on the service type. A penalty fee may be charged for a non-compliant cancellation, returning the vehicle later than the reserved drop-off time, parking the vehicle at an unqualified location, and any other violation of service usage principles. In contrast, a bonus or some trip credits may be offered if a user performs some kind of task, such as washing the vehicle.

1.1.1.3 Global outlook of carsharing

Carsharing has experienced rapid growth all over the world in the past decade. Figure 1.6 shows the global carsharing market trend from 2006 to 2018. It can be seen that the number of users registered for CSSs had grown significantly particularly during the period of 2012-2018. By 2018, this number had been more than 31 million. The compound annual member growth rate reaches as high as 76% from 2014 to 2016. To accommodate the increase in the number of registered members, the number of vehicles put into the carsharing market also rose accordingly. However, the compound annual fleet growth rates were all lower than the compound annual member growth rates. As a result, the member-vehicle ratio exceeded 160 in 2018. These reflect the great development potential of the carsharing market.

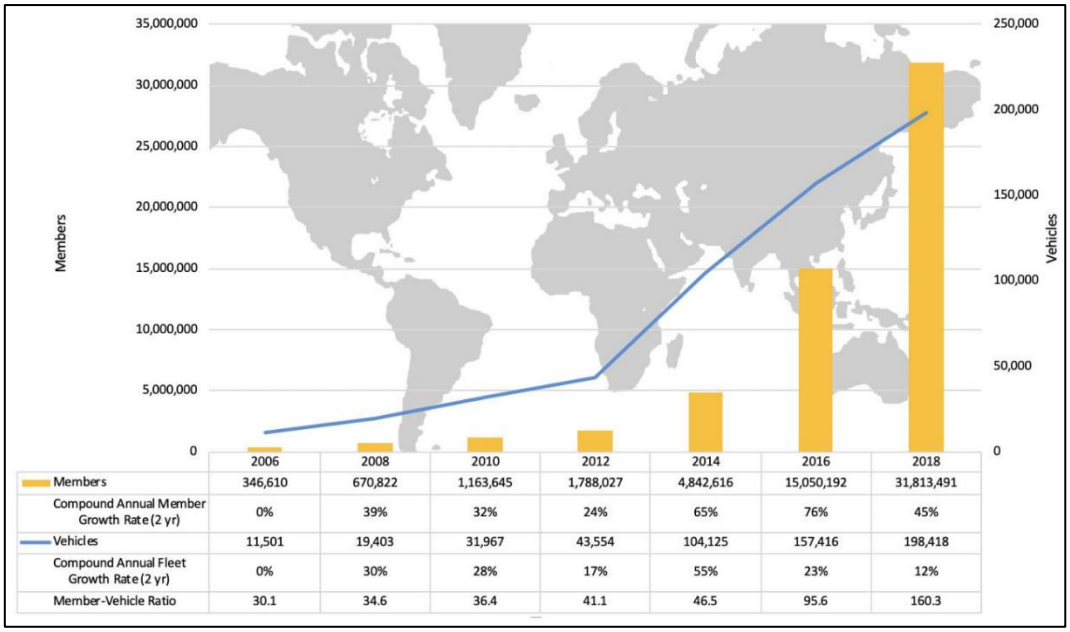

	2006	2008	2010	2012	2014	2016	2018
Members	346,610	670,822	1,163,645	1,788,027	4,842,616	15,050,192	31,813,491
Compound Annual Member Growth Rate (2 yr)	0%	39%	32%	24%	65%	76%	45%
Vehicles	11,501	19,403	31,967	43,554	104,125	157,416	198,418
Compound Annual Fleet Growth Rate (2 yr)	0%	30%	28%	17%	55%	23%	12%
Member-Vehicle Ratio	30.1	34.6	36.4	41.1	46.5	95.6	160.3

(Source: Shaheen et al. (2018))

Figure 1.6 Global carsharing market trend

Despite the momentum of the carsharing market, there are significant differences in the development between countries. This can be reflected in the global comparison of predicted carsharing revenue in 2022, which is shown in Figure 1.7. Figure 1.7 reveals that the top five countries in the predicted carsharing revenue in 2022 will be United States, China, United Kingdom, Italy, and Japan. In addition, most revenue will be generated in United States (USD 2,629.00 million) and China (USD 1,783.00 million), and some countries, e.g., Egypt, may even have not introduced CSSs because the predicted carsharing revenue is almost zero.

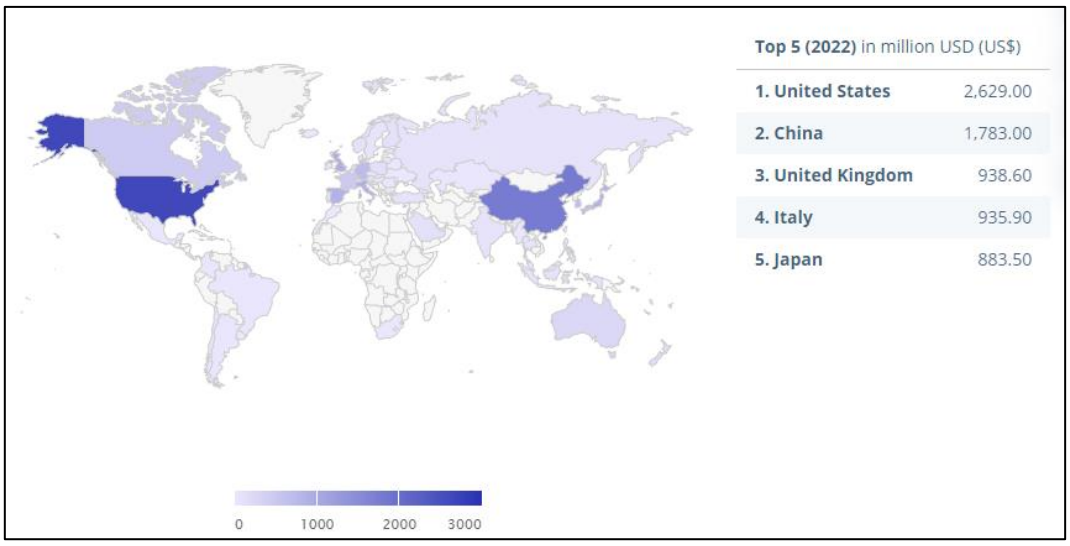

(Source: Statista (2022))

Figure 1.7 Global comparison of predicted carsharing revenue in 2022

In addition to the regional differences, different types of CSSs also show different development status. Golalikhani et al. (2021b) conducted a sample survey of carsharing operators around the world. Totally 34 carsharing operators are considered in their survey. Figure 1.8 illustrates the survey result. It shows that the vast majority of carsharing operators provided the most rigid round-trip services (56%), or the most flexible one-way free-floating services (32%), or both of them (9%). Only 3% carsharing operators offered the one-way station-based services. The reason why there were so few carsharing operators offering the one-way station-based services may be as follows. The moderate flexibility of one-way station-based services result in its significantly higher management cost in comparison to the round-trip services and remarkably lower revenue from users against with the one-way free-floating services. Therefore, the profitability performance of one-way station-based services may be inferior to the other two types of services, and thus carsharing operators were reluctant to provide this kind of services. To attract as many users with different travel needs as possible by improving the willingness of carsharing operators to offer one-way station-based services, more research efforts should be made to enhance the profitability performance of one-way station-based services.

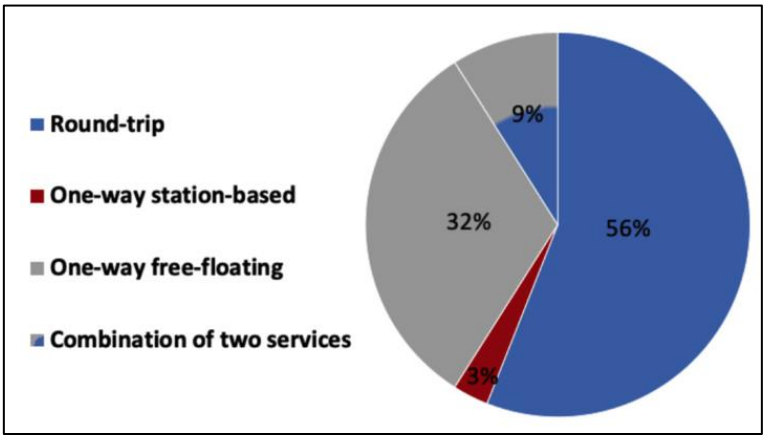

(Source: Golalikhani et al. (2021b))

Figure 1.8 Service type comparison of carsharing

1.1.2 Vehicle electrification in carsharing

To working towards achieving climate goals by reducing greenhouse gas emissions, countries around the world are setting ambitious goals for vehicle electrification in the coming decades. For example, China is planning to have full public transportation electrification by 2035 (IEA, 2021b); India aims to electrify all new vehicles by 2030 (Condliffe, 2017); Norway is determined to realize 100% penetration of electric vehicles (EVs) or plug-in hybrid units by 2025 (Crabtree, 2019). Guided by these goals for vehicle electrification, a series of policy-

oriented financial supports have been proposed by local governments to encourage the purchase of EVs. According to IEA (2021a), public spending on subsidies and incentives for EVs nearly doubled in 2021 to nearly USD 30 billion. Meanwhile, the deployment of EV charging infrastructure has also been implemented on a large scale. For instance, governments of China, United States, Japan, and many European countries have deployed considerable charging stations across their countries (Xu, 2018). As a result, the global sales of EVs have kept rising strongly. IEA (2021a) indicated that 6.6 million EVs were sold out in 2021, twice the sales in 2020. Furthermore, as shown in Figure 1.9, the global stock of EVs is projected to increase exponentially, in sharp contrast to the slowing upward trend and the gradual decline of the conventional light-duty vehicles, i.e., gasoline vehicles, diesel vehicles, etc., before and after 2038.

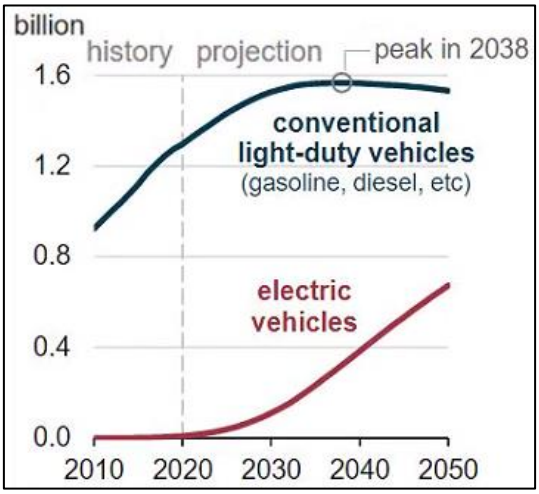

(Source: EIA (2021))

Figure 1.9 Global vehicle stock

Electrification of carsharing is one of the important achievements made by governments for electrifying vehicles. Figure 1.10 shows an overview of EV charging infrastructure, policies, and electric carsharing operators across major cities in the world. It indicates that most of the major cities in the world are providing electric CSSs, mainly driven by the governments' policies favoring vehicle electrification and practical actions for construction of EV infrastructure. In fact, by 2019, 66% of carsharing operators worldwide, e.g., EVCARD in China and BlueSG in Singapore, have introduced either all-electric or partial-electric fleets, and 25% of countries had cities where carsharing fleets consisted exclusively of EVs (Nicholas and Bernard, 2021).

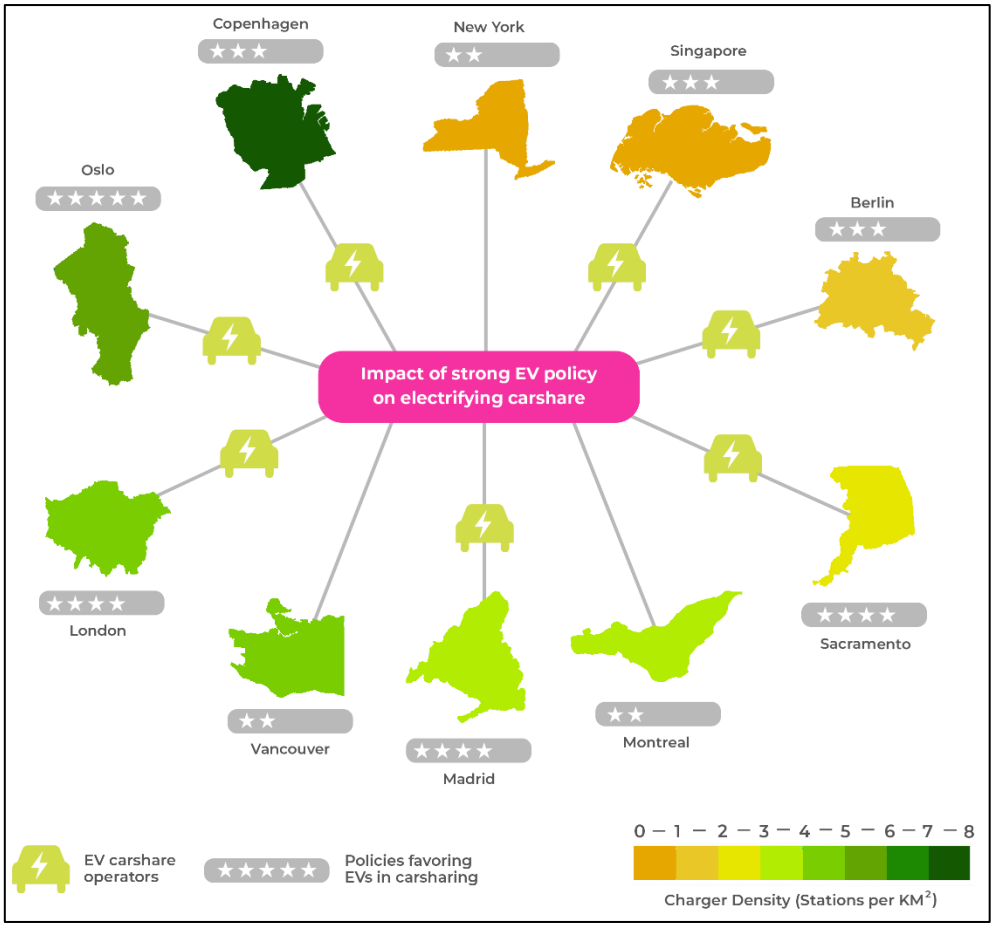

(Source: Phillips et al. (2021))

Figure 1.10 Overview of EV charging infrastructure, policies, and electric carsharing operators across major cities in the world

1.1.3 Decision-making challenges faced by electric carsharing operators

Vehicle electrification in carsharing inevitably poses new challenges for decision-makings faced by carsharing operators. This is because compared to the traditional gasoline vehicles, EVs have unique characteristics, which generally include the limited driving range, frequent charging needs, long charging times, and nonlinear charging profile, i.e., the state of charge (SOC) of an EV growing nonlinearly concerning the charging duration (Marra et al., 2012; Pelletier et al., 2017). To guarantee that EVs will not get stagnant en route, additional efforts need to be made in the decision-makings of CSSs such that these unique characteristics can be factored in.

In addition, EV batteries will suffer from serious degradation, e.g., a loss of battery capacity and a decrease of EV's driving range, caused by unhealthy charging and discharging processes (Barré et al., 2013; Pelletier et al., 2017). According to Pelletier et al. (2017), an EV battery is typically considered to have reached the end of its life when its available capacity

decreases by 20% of its original value. Since the battery cost generally accounts for up to 35% of the total cost of an EV, battery degradation will lead to high battery wear cost and ultimately a reduction of overall profitability of CSSs, if not taken seriously. Therefore, special attention should be given to the battery degradation of EVs in the decision-makings of electric CSSs. This topic is challenging, as considering battery degradation in the decision-makings of electric CSSs is not an easy task.

1.2 Research Scope and Objectives

The objective of the thesis is to address the decision-making challenges faced by carsharing operators due to vehicle electrification through mathematical modeling and optimization methods. In more detail, three classic decision-making problems arising from CSSs, i.e., fleet size, vehicle relocation, and vehicle relocation & staff rebalancing, will be investigated in the context of vehicle electrification. The fleet size problem will take into account on-demand charging strategy and battery degradation, and the latter two problems will consider demand dynamics and practical nonlinear charging profile. For each decision-making problem, both mathematical optimization models and solution algorithms will be proposed. The models and solution algorithms will be numerically evaluated.

1.3 Thesis Organization

The thesis is organized as follows.

Chapter 1 introduces the state of practice in carsharing, identifies the decision-making challenges faced by carsharing operators due to vehicle electrification, and outlines research scope, objectives, and organization of the thesis.

Chapter 2 provides a comprehensive literature review on decision-making problems arising from CSSs. These decision-making problems include strategic station planning, tactical fleet size, staff size, and trip pricing, and operational vehicle relocation. Limitations of the existing studies are identified.

Chapter 3 addresses the fleet size problem considering on-demand charging strategy and battery degradation. Vehicle assignment and vehicle relocation are also taken into account. The novelty of this study lies in the incorporation of nonlinear battery wear cost incurred during the battery charging and discharging processes. A mixed-integer nonlinear programming (MINLP) model with both concave and convex terms in the objective function is first developed for the problem. A piecewise linear approximation approach and an outer-approximation method are

employed to linearize the proposed model. Numerical experiments based on a one-way electric carsharing operator in China are conducted to demonstrate the efficiency of the proposed solution method and prove the necessity of incorporating the battery degradation into the fleet size determination of electric CSSs. Sensitivity analysis is also performed.

Chapter 4 aims to develop a fast yet robust algorithm to determine the real-time relocation and charging strategies for EVs in pursuit of profit maximization of carsharing operators. A dynamic algorithmic framework based on a rolling time horizon is first established. Specifically, the entire planning horizon is divided into a series of sub-horizons, and a static vehicle relocation and vehicle charging problem is subsequently addressed over each sub-horizon in regard to the latest demand information known up to the beginning of the sub-horizon. For each static problem, a set-packing-type formulation and a column-generation-based solution method are employed. In particular, a multi-label method is developed to generate activity trajectories (i.e., columns) incorporating vehicle relocation and charging strategy for the first static problem, whereas the activity trajectories for the subsequent static problems are efficiently generated in an online environment by leveraging the existing activity trajectories generated for the previous static problem and employing a reactive column generation process. Numerical experiments based on randomly generated instances and a case study of a one-way carsharing company in China are performed to demonstrate the efficiency of the proposed solution method and explore the managerial insights of an electric carsharing system.

Chapter 5 extends the study in Chapter 4 by including staff rebalancing. The investigated problem determines the strategies of vehicle relocation, vehicle charging, and staff rebalancing in a real-time fashion by maximizing the profit of carsharing operators. A Markov Decision Process (MDP) is first formulated. Subsequently, an efficient concurrent-scheduler-based policy is proposed. Given the nonlinear charging profile, an innovative constrained non-dominated charging strategy considering scheduling restriction of staff is put up to facilitate the implementation of the policy. Numerical experiments based on randomly generated instances and a case study of a one-way carsharing company in China are carried out to evaluate the efficiency of the proposed policy, analyse the impact of staff rebalancing, and examine the effects of several key parameters on the performance of one-way electric carsharing systems.

Chapter 6 draws conclusions and recommends future research works.

CHAPTER 2 LITERATURE REVIEW

Considering the research scope of the thesis, this chapter comprehensively reviews mathematical modeling-based studies on carsharing. Although the focus of the thesis is electric carsharing, the studies on the traditional gasoline-powered carsharing are also reviewed, as they are the cornerstone of electric carsharing research. In addition, the thesis considers carsharing with human-driven vehicles, but some of the newly emerging studies on autonomous carsharing are also reviewed in the literature review, which provide guidance for future research. Interested readers can also refer to the review paper by Hao and Yamamoto (2018). Figure 2.1 shows that decision-makings involved in CSS operations can be classified into three levels: strategic, tactical, and operational (Golalikhani et al., 2021a). At the strategic level, a carsharing operator makes long-term planning of station location, station capacity, and station number. At the tactical level, fleet size, staff size, and trip pricing are determined in the medium term. At the operational level, a carsharing operator needs to determine the short-term strategies of vehicle relocation and staff rebalancing. There is interplay between decision-makings at the three levels. For example, station information is necessary input for fleet size determination, and vehicle relocation is subject to fleet size. Studies on carsharing are grouped into three categories according to the level of the major targeted decision-making(s). A study is likely to be classified into more than one category as the major focused decision-making(s) may involve different levels. In the following, the literature review is conducted based on these three categories. In each category, decision-makings are first explained in detail if necessary, followed by the review of the related studies.

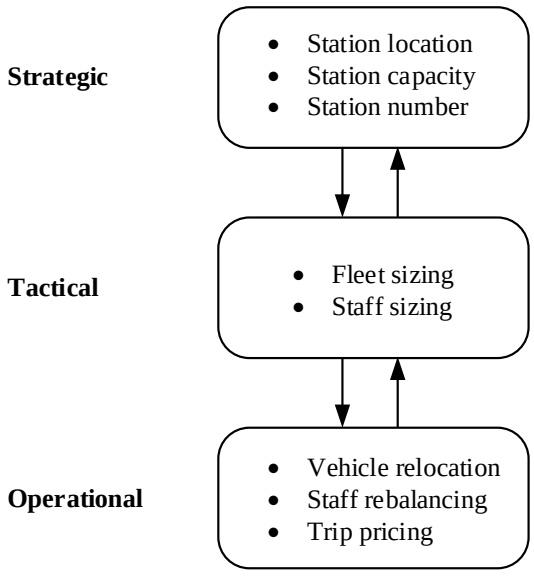

Figure 2.1 Three levels of decision-makings for CSSs

2.1 Strategic Station Planning

As the top-level decision-making, proper station planning for gasoline-powered CSSs or charging station planning for electric CSSs, which generally includes the determination of location, capacity, and number, is crucial to struggle a trade-off between enhancing service capability and reducing infrastructure construction cost. Table 2.1 summarizes the studies focusing on strategic station planning, which includes the type of service, the research objective, the formulated model, the solution method, and the evaluation approach. In the following, these studies are analyzed in more detail.

2.1.1 Station planning for gasoline-powered CSSs

A few studies have attempted to address the decision-makings on station planning in gasoline-powered CSSs. de Almeida Correia and Antunes (2012) developed an integer linear programming (ILP) model to deal with the depot (i.e., station) location problem in one-way station-based CSSs under three trip selection schemes. A case study on the municipality of Lisbon, Portugal was conducted to analyze the impact of depot location and trip selection schemes on the profitability of such systems. For the joint determination of station capacity and fleet size, Hu and Liu (2016) formulated a mixed queueing network model and a non-convex profit-maximization model. In the mixed queueing network model, they considered the road congestion and embedded the booking process to capture the vehicle idle time caused by the pick-up time window. A genetic algorithm was proposed to solve the non-convex optimization problem and two algorithms that belong to the class of mean value analysis were used to solve the equilibrium distribution of queuing network with a product-form solution. Huang et al. (2018) proposed an MINLP model to address the station location and station capacity problem. They used a logit model that determines the potential demand for CSSs to account for the competition with private cars and adopted a customized gradient algorithm to obtain near-optimal solutions in a reasonable time. In order to determine the parking planning and vehicle allocation for the one-way (including station-based and free-floating) CSSs, Lu et al. (2018) proposed a two-stage stochastic integer programming (IP) model and developed a branch-and-cut algorithm with mixed-integer, rounding-enhanced benders cuts to solve the model. Similarly, Zhang et al. (2021) introduced a two-stage risk-averse stochastic model for the determination of station location, station capacity, and fleet size. A branch-and-cut algorithm and a scenario decomposition algorithm were designed to solve the proposed model.

2.1.2 Charging station planning for electric CSSs

To cater to the needs of vehicle charging brought by the introduction of EVs into CSSs, some scholars have made great efforts to investigate the charging station planning for electric CSSs. For the determination of the service regions (i.e., non-designated stations) for a one-way free-floating carsharing system, He et al. (2017) established a mathematical programming model that incorporates details of both customer adoption behavior and fleet management, i.e., EV repositioning and charging, under imbalanced travel patterns. To overcome the possible ambiguity of data brought by the uncertain adoption patterns, they employed a distributionally robust optimization framework. With the demand uncertainty taken into account, both Brandstätter et al. (2017) and Çalık and Fortz (2019) dealt with a charging station location problem by a mixed-integer stochastic programming model. Cocca et al. (2019) proposed a data-driven & simulation-based optimization approach to determine the optimal placement of charging stations, and the smart vehicle return policies. A case study on Turin showed that few charging stations were enough to make the system self-sustainable. Deza et al. (2020) presented a mixed-integer linear programming (MILP) model and adopted a column generation approach to find the optimal locations of charging stations for one-way station-based electric CSSs among a large number of potential charging station locations. Taking the constraint of the limited cost of the company and the multiple influencing factors of carsharing to meet the maximum user demand into consideration, Sai et al. (2020) built up an MINLP model and designed a genetic algorithm for the corresponding model to determine the location of charging stations. Using the number of expected trips that can be accepted as a gauge of quality, Brandstätter et al. (2020) introduced an MILP model and heuristics for the determination of the optimal location and size of charging stations. Based on the survival analysis, Bi et al. (2021) constructed a bi-level optimization model that maximizes profit and service level respectively for the planning of station location, parking spots, charging piles. To determine the number and location of fast chargers to be deployed in one-way station-based electric carsharing systems, Bekli et al. (2021) proposed an IP model based on a time-space-battery level network and introduced three heuristics to cope with the computational intractability. The above-mentioned studies focused only on the decision-making of station planning.

In addition, several studies attempted to address the joint determination of station planning and fleet size and/or fleet management. Boyacı et al. (2015) developed a multi-objective MILP model for the planning of one-way station-based electric carsharing systems involving decision-makings of station location, station capacity, and fleet size. To scale to the problem

size, they transformed the proposed model into an aggregate one using the concept of the virtual hub. Hua et al. (2019) proposed an innovative framework for the joint determination of charging station location, fleet distribution, and real-time fleet operations considering demand uncertainty. A multi-stage stochastic model was built up to overcome the challenge brought by the demand uncertainty and an accelerated solution algorithm, which is based on lagrangian relaxation and the stochastic dual dynamic programming method, was designed to obtain the operation policy while checking the optimality gap to the optimum. Huang et al. (2020a) developed an MINLP model and a hybrid solution method of golden section line search approach and shadow price algorithm to optimize the station capacity and fleet size of one-way station-based electric CSSs.

2.1.3 Station planning for autonomous electric CSSs

With the advent of autonomous driving technology, it becomes possible for users to enjoy the autonomous CSSs in the foreseeable future. According to what we have reviewed, only a few studies have been dedicated to the charging station planning for autonomous electric CSSs. Kang et al. (2017) presented an integrated decision framework, which includes the decision makings of the charging station location and fleet size, for the design of autonomous electric carsharing systems. A case study for an autonomous fleet operation in Ann Arbor was conducted to compare autonomous electric CSSs and autonomous gasoline-powered CSSs in terms of profitability and feasibility for a variety of market scenarios. Lee et al. (2020) designed an autonomous electric carsharing system including charging station location and charging station capacity with the system uncertainty considered. A reliability-based design optimization approach was proposed to minimize the total cost of system design while satisfying the target reliability of the customer waiting time. Ma et al. (2021b) formulated an MINLP model to optimize the charging station location and vehicle routing for a location routing problem arising from the autonomous electric CSSs. Zhao et al. (2021) established a simulation-based optimization model to seek a near-optimum design of charging station location and vehicle deployment for autonomous electric carsharing systems.

In comparison to the human-driven CSSs, the vehicles in an autonomous carsharing system can relocate themselves to the users' locations without any human operations (Zhao et al., 2021). This provides users with more convenience and enables operators to save labor and decision-making effort of staff movement. At the same time, nevertheless, the advanced autonomous driving technology would inevitably increase capital investment. In addition, the more flexible operation mode of autonomous CSSs, which allows remote parking and en-route

pick-up and drop-off, would induce more decision-making problems. Particularly, for electric autonomous CSSs, it additionally involves the decision making of which station to charge for a vehicle before the vehicle drives to a location for picking up a user.

We can see from the summary in Table 2.1 that most of the studies focused on the human-driven station-based CSSs and it is quite common for these studies to set the objective as maximizing profit or minimizing cost. Based on the specific context of the station planning problem, the solution method can vary a lot from study to study.

Table 2.1 A summary of studies on the strategic station planning

(1) Station planning for gasoline-powered CSSs

Literature	Service type	Objective	Model	Solution method	Evaluation
de Almeida Correia and Antunes (2012)	One-way station-based	Profit maximization	ILP	Solver Xpress	Case study
Hu and Liu (2016)	One-way station-based	Profit maximization	Mixed queuing network model & MILP	Exact mean value analysis algorithm & Approximate Schweitzer-Bard mean value analysis algorithm	Computational experiments
Huang et al. (2018)	One-way station-based	Profit maximization	MINLP	Customized gradient algorithm	Case study
Lu et al. (2018)	One-way	Cost minimization	Two-stage stochastic IP	Branch-and-cut algorithm	Computational experiments
Zhang et al. (2021)	One-way station-based	Cost minimization	Two-stage risk-averse stochastic programming	Branch-and-cut algorithm & Scenario decomposition algorithm	Computational experiments

(2) Charging station planning for electric CSSs

Literature	Service type	Objective	Model	Solution Method	Evaluation
He et al. (2017)	One-way free-floating	Profit maximization	Mixed-integer second-order cone programming	Mixed-integer second-order cone programming approximation	Case study
Brandstätter et al. (2017)	One-way station-based	Profit maximization	Two-stage stochastic ILP	Heuristic	Computational experiments & case study
Çalık and Fortz (2019)	One-way station-based	Profit maximization	Mixed-integer linear stochastic programming	Benders decomposition algorithm	Case study

Cocca et al. (2019)	One-way free-floating	Service level maximization	Data-driven optimization	Heuristic & simulation-based approach	Case study
Deza et al. (2020)	One-way station-based	Service level maximization	MILP	Column generation approach	Case study
Sai et al. (2020)	One-way station-based	Service level maximization	Integer nonlinear programming	Genetic algorithm	Case study
Brandstätter et al. (2020)	One-way station-based	Profit maximization	ILP	Path-based heuristic & flow-based heuristic	Computational experiments & case study
Bi et al. (2021)	One-way station-based	Service level maximization & Profit maximization	MINLP	Bi-level heuristic	Case study
Bekli et al. (2021)	One-way station-based	Profit maximization	ILP	Heuristic	Computational experiments & case study
Boyacı et al. (2015)	One-way station-based	Profit maximization	Multi-objective MILP	Aggregate modeling method	Case study
Hua et al. (2019)	One-way station-based	Cost minimization	Multi-stage nonlinear integer stochastic programming	Accelerated solution algorithm	Computational experiments & case study
Huang et al. (2020a)	One-way station-based	Profit maximization	MINLP	Golden section line search method & shadow price algorithm	Case study

(3) Charging station planning for autonomous electric CSSs

Literature	Service type	Objective	Model	Solution Method	Evaluation
Kang et al. (2017)	Station-based	Profit maximization	MILP	Genetic algorithm & sequential quadratic programming	Case study
Lee et al. (2020)	Station-based	Cost minimization	Reliability-based design optimization model	Reliability-based design optimization	Computational experiments
Ma et al. (2021b)	Station-based	Cost minimization	MINLP	Genetic algorithm	Computational experiments

Zhao et al. (2021)	Station-based	Cost minimization	Stochastic, and nonlinear programming	Customized heuristic algorithm	Case study

2.2 Tactical Fleet Size & Staff Size and Trip Pricing

In this section, studies on the tactical fleet size & staff size will first be reviewed, followed by the trip pricing problem.

2.2.1 Fleet size & staff size

The determination of the number of vehicles put into use, i.e., fleet size, is an important tactical decision-making problem for CSSs. In particular, for one-way CSSs, the carsharing operators may choose to hire staff members to implement the vehicle relocation operations in order to deal with the vehicle imbalance issue across different stations, and staff size is another tactical decision-making problem in CSSs. Table 2.2 summarizes the related studies, in which, in comparison to Table 2.1, modeling technique and the involved specific tactical-level decision-makings are reported for each study.

Some studies have tried to tackle the tactical decision-making problems based on the time-space network (Boyacı et al., 2015; Huang et al., 2020a; Lu et al., 2018; Zhang et al., 2021). Specifically, Fan (2014) developed a multi-stage stochastic linear programming model to optimize the tactical allocation (i.e., deployment) of vehicles for one-way station-based CSSs with the demand uncertainty taken into account. Zhou et al. (2017) proposed a data-driven metamodel simulation-based optimization approach to determine the profit-optimal deployment of vehicle fleet across a large-scale network of round-trip carsharing stations. Xu et al. (2018) formulated a mixed-integer nonlinear and nonconvex programming model to solve an EV fleet size and trip pricing problem for one-way station-based CSSs. An effective global optimization method with several outer-approximation schemes was employed to find the global optimal or ε-optimal solution to the considered problem. Zhao et al. (2018) established an integrated framework to optimize the allocation plan of EVs and staff with the operational EV relocation and staff rebalancing decisions considered. To solve the considered problem efficiently, they proposed a Lagrangian relaxation-based solution approach to decompose the primal problem into several sets of computationally efficient subproblems and design a three-phase implementation algorithm based on dynamic programming according to the values of Lagrangian multipliers. Monteiro et al. (2021) proposed an MILP model to optimize the fleet size of a carsharing system for one-way and round-trip modes while simulating the clients' interaction. Huang et al. (2021) developed a two-stage stochastic programming model for the demand-supply imbalance problem of one-way station-based CSSs under demand uncertainty, with the fleet size and deployment determined at the first stage.

In addition to the time-space network approach, some other modeling techniques were also adopted in the existing studies. These modeling techniques include a connection-based multi-commodity formulation (Xu et al., 2021), a mixed queuing network approach (Hu and Liu, 2016), and a set partitioning formulation (Xu and Meng, 2019). Focusing on the autonomous carsharing systems, Ma et al. (2017) proposed a linear connection-based programming model to efficiently obtain the optimal solution to the fleet sizing problem. With the battery degradation considered, Xu et al. (2021) developed a connection-based MINLP model with concave and convex terms in the objective function to address the tactical EV fleet size problem faced by the CSS providers. A piecewise linear approximation approach and an outer-approximation method were employed to linearize the proposed model. As reviewed in Section 2.1, Hu and Liu (2016) formulated a one-way station-based carsharing system as a mixed queueing network model and built up a profit-maximization model for the joint design of fleet size and station capacity. Xu and Meng (2019) formulated a set partitioning model to determine the EV fleet size for one-way station-based CSSs by maximizing the profit of carsharing operators while taking into account the vehicle relocation operations and nonlinear charging profile of EVs. By taking into account the interplays among vehicle relocations, supply-demand dynamics, and travelers' multi-modal multiactivity schedules, Li and Liao (2020) proposed a bi-level system optimal model for the deployment of autonomous vehicles in the free-floating CSSs. A heuristic algorithm based on Lagrangian relaxation was developed to solve the considered problem.

From Table 2.2, it can be concluded that researchers are more interested in the fleet size problem in one-way CSSs and the time-space network approach is mostly adopted.

Table 2.2 A summary of studies on tactical decision-making problems

Literature	Service type	Fleet type	Modeling technique	Tactical-level decision-makings	Objective	Model	Solution method	Evaluation
Fan (2014)	One-way station-based	Gasoline-powered	Time-space network approach	Fleet size	Profit maximization	Multi-stage stochastic linear programming	Scenario-tree-based approach	Computational experiments
Boyacı et al. (2015)	One-way station-based	Electric	Time-space network approach	Fleet size & staff size	Profit maximization	Multi-objective MILP	Aggregate modeling method	Case study
Zhou et al. (2017)	Round-trip	Gasoline-powered	Time-space network approach	Fleet size	Profit maximization	Metamodel	Data-driven metamodel simulation-based optimization approach	Computational experiments & Case study
Lu et al. (2018)	One-way	Gasoline-powered	Time-space network approach	Fleet size	Cost minimization	Two-stage stochastic IP	Branch-and-cut algorithm	Computational experiments
Xu et al. (2018)	One-way station-based	Electric	Time-space network approach	Fleet size & staff size	Profit maximization	MINLP	Outer-approximation method	Case study
Zhao et al. (2018)	Station-based	Human-driven & electric	Time-space network approach	Fleet deploying; Staff deploying	Cost minimization	MILP	Lagrangian relaxation-based solution approach	Computational experiments & Case study
Huang et al. (2020a)	One-way station-based	Electric	Time-space network approach	Fleet size	Profit maximization	MINLP	Golden section line search method & shadow	Case study

Monteiro et al. (2021)	Round-trip and one-way	Gasoline-powered	Time-space network approach	Fleet size	Service level maximization	MILP	price algorithm Simulation-based optimization	Computational experiments
Zhang et al. (2021)	One-way station-based	Gasoline-powered	Time-space network approach	Fleet size	Cost minimization	Two-stage risk-averse stochastic programming	Branch-and-cut algorithm & Scenario decomposition algorithm	Computational experiments
Huang et al. (2021)	One-way station-based	Gasoline-powered	Time-space network approach	Fleet size	Profit maximization	A two-stage stochastic programming	Dedicated gradient search algorithm	Case study
Ma et al. (2017)	Free-floating	Autonomous & gasoline-powered	Connection-based formulation	Fleet sizing	Cost minimization	Linear programming	A linear programming approach	Case study
Xu et al. (2021)	One-way station-based	Electric	Connection-based formulation	Fleet size	Profit maximization	MINLP	Piecewise linear approximation & outer-approximation	Case study
Hu and Liu (2016)	One-way station-based	Gasoline-powered	Mixed queuing network approach	Fleet size	Profit maximization	Mixed queuing network model & MILP	Exact mean value analysis algorithm & Approximate Schweitzer-Bard mean value analysis algorithm	Computational experiments

Xu and Meng (2019)	One-way station-based	Electric	Set partitioning formulation	Fleet size	Profit maximization	Set partitioning model	Branch and price	Computational experiments & Case study
Li and Liao (2020)	Free-floating	Autonomous & gasoline-powered	Multi-state super-network representation	Fleet sizing & deploying	Profit maximization	Integer, time-dependent nonlinear programming with equilibrium constraints	Lagrangian relaxation-based heuristic	Computational experiments

2.2.2 Trip pricing

Setting service charge standard, i.e., trip pricing, is another significant tactical decision-making problem in CSSs. Table 2.3 summarizes the studies on the trip pricing problem in CSSs. It can be seen that the trip pricing problem has received little attention in comparison to the fleet size & staff size problem. Specifically, Jorge et al. (2015) developed an MINLP model for the pricing problem of the one-way CSSs. As reviewed in Subsection 2.2.1, Xu et al. (2018) formulated a mixed-integer nonlinear and nonconvex programming model to solve the EV fleet size and trip pricing problem for one-way CSSs. To determine the optimal pricing and operation strategy for a one-way electric carsharing system, Xie et al. (2019) established a bi-level model and reformulated it as a mixed-integer quadratic programming model through a global polyhedral approximation of second-order cones, primal-dual optimality condition, and product term linearization. Huang et al. (2021) proposed a two-stage stochastic programming model for the demand-supply imbalance problem of one-way CSSs under demand uncertainty, with the trip price optimized at the first stage.

Table 2.3 A summary of studies on the trip pricing problem

Literature	Service type	Fleet type	Objective	Model	Solution method	Evaluation
Jorge et al. (2015)	One-way station-based	Gasoline-powered	Profit maximization	MINLP	Iterated local search metaheuristic	Case study
Xu et al. (2018)	One-way station-based	Electric	Profit maximization	MINLP	Outer-approximation algorithm	Case study
Xie et al. (2019)	One-way station-based	Electric	Profit maximization	MINLP	Outer polyhedral approximation	Case study
Huang et al. (2021)	One-way station-based	Gasoline-powered	Profit maximization	A two-stage stochastic programming	Gradient search algorithm	Case study

2.3 Operational Vehicle Relocation

At the operational level, vehicle relocation is the most frequently encountered decision-making problems in CSSs. In comparison to round-trip CSSs, one-way CSSs provide users with more flexibility since they allow users to pick up and drop off vehicles at different stations. However, this flexibility would inevitably induce the vehicle imbalance issue among stations, i.e., the number of vehicles/parking spots available at a specific station cannot well match users' demand over a particular period. To solve this issue, vehicle relocation operations among stations are imperative for the carsharing operators (Boyacı et al., 2015; Nourinejad and Roorda, 2015; Xu and Meng, 2019). According to the relocation strategies concerned, two approaches are identified in the literature, i.e., the operator-based approach and the user-based approach (Gambella et al., 2018). As mentioned in Subsection 2.2.1, to deal with the vehicle imbalance problem, carsharing operators may choose to hire staff members to implement the vehicle relocation operations by driving vehicles from saturated stations to the ones that suffer from vehicle shortage. This belongs to the operator-based approach. Such vehicle relocation operations may result in the imbalanced distribution of staff members among stations (Yang et al., 2021; Zhao et al., 2018). Staff members need to self-rebalance by the movement among stations such that a series of relocation operations can be performed smoothly. Hence, staff rebalancing keeps as important decision-making in the operator-based relocation (Nourinejad et al., 2015; Xu et al., 2018). The user-based approach mainly incentivizes users to change their trips such that the carsharing systems can restore a balanced distribution of vehicles in the network. Table 2.4 and Table 2.5 summarize the studies on the operator-based vehicle relocation problem and the user-based vehicle relocation problem, respectively.

2.3.1 Operator-based vehicle relocation & staff rebalancing

The operator-based vehicle relocation problem has been investigated extensively by scholars. By incorporating a discrete choice model that depicts users' mode choice, Jian et al. (2018) proposed an MINLP model linking the supply and the demand to solve the vehicle relocation problem for station-based CSSs. Zakaria et al. (2018) presented a multi-objective ILP model for solving the one-way carsharing relocation problem. In order to allow substantially longer reservation times while keeping the system profitable and achieving high service quality, Molnar and de Almeida Correia (2019) proposed a relocation-based reservation enforcement method combining vehicle locking and relocation movements. By this method, a variable quality of service model was developed and an iterated local search metaheuristic

based on simulation was used to solve the model. These studies focused on gasoline-powered CSSs.

The introduction of EVs in CSSs creates additional managerial problems due to the limited driving range per battery charge (Brandstätter et al., 2016), and a large number of researchers have worked hard to deal with the vehicle relocation problem in the one-way electric CSSs by taking the battery-related restrictions into account. Bruglieri et al. (2014) established an MILP model to solve the vehicle relocation problem in the electric CSSs. Boyacı et al. (2017) developed an integrated multi-objective MILP model and a discrete event simulation framework for the optimization of vehicle relocation and personnel rebalancing in a carsharing system with reservations. A clustering procedure was adopted to deal with the dimensionality of the considered problem without compromising on the solution quality. Bruglieri et al. (2018) proposed a three-objective MILP model for the vehicle relocation problem to struggle a trade-off among the users' satisfaction, the staff's workload balance, and the carsharing provider's pursuit of profit. Gambella et al. (2018) introduced an exact relocation model to manage the daily relocation operations of an electric carsharing system. This model was also extended for the overnight relocations. Boyacı and Zografos (2019) presented an integrated modeling and computational framework, which consists of preprocessing, optimization, and simulation modules, for analyzing the effect of spatial and/or temporal flexibility and reservation processing type on the performance of one-way electric carsharing systems. To tackle the EV relocation problem in one-way CSSs, Bruglieri et al. (2019) specially developed an adaptive large neighbourhood search and a tabu search metaheuristic. In order to circumvent battery constraints and to improve vehicle utilization rates in one-way electric CSSs, Zhang et al. (2019) proposed a novel space-time-battery network flow model to determine the optimal assignment and relay decisions. Folkestad et al. (2020) developed a mathematical model to optimize the charging and repositioning of a fleet of EVs for CSSs. By considering a time-of-use charging pricing mechanism, Lai et al. (2020) established a framework to minimize the delivery time of customers and charging cost simultaneously while satisfying customer demands and working hour requirements. Lu et al. (2020) formulated a stochastic sequential decision programming model to investigate the charging and relocation problem for an electric carsharing system. Based on a static node-charge graph structure, Pantelidis et al. (2022) developed non-myopic idle vehicle rebalancing model, which considers queueing constraints applicable to EV charging, to jointly determine the relocation and routing decisions of vehicles under available

charging capacity. All the above studies assumed that the user demand is known a priori or can be estimated beforehand.

In order to take the inherent uncertainty of user demand into account, several studies have attempted to develop vehicle relocation strategies in a dynamic fashion or by a stochastic programming approach. Fan (2013) developed a multi-stage stochastic MILP model that can take the system uncertainty into account to address the dynamic vehicle allocation problem for CSSs. Wang et al. (2019) developed a new model, which consists of relocation needs computation and execution plan generation, for the relocation operations of one-way electric carsharing systems without advanced reservation information. Huo et al. (2020) constructed a data-driven optimization model considering demand uncertainty to improve the efficiency and profitability of CSSs. Yang et al. (2021) proposed an integrated model for the determination of the operations of vehicle relocation and dispatcher rebalancing. A hybrid solution method combining a rolling horizon algorithm with a customized decomposition algorithm was designed to solve the model. Huang et al. (2021) established a two-stage stochastic programming model for the demand-supply imbalance problem of one-way CSSs under demand uncertainty, with the vehicle relocation optimized at the second stage.

As the era of autonomous driving is upcoming, the potential application of autonomous vehicles in the CSSs would enable the vehicles to be relocated without staff. Several studies have pioneered the investigation of vehicle relocation problem for the autonomous CSSs in either static or dynamic setting. Iacobucci et al. (2019) proposed an MILP model to optimize charging schedules with vehicle-to-grid and vehicle routing & relocation at two different time scales by running two model-predictive control optimization algorithms. Ma et al. (2021a) developed an MILP model for the service optimization of autonomous carsharing systems, in which the objective was expressed by the weighted sum of the total travel distance, the total travel time, and the total energy consumption. Hyland and Mahmassani (2018) presented and compared six autonomous vehicle traveler assignment strategies for the operational problem associated with the on-demand autonomous CSSs. Li et al. (2021) proposed a minimum drift plus penalty scheduling policy for real-time vehicle dispatching in large-scale autonomous electric carsharing systems.

It can be observed from the summary in Table 2.4 that several studies proposed a multi-objective model for the operator-based relocation problem. This seems to be in line with the reality, as the carsharing operators, when providing services, may take multiple objectives into account instead of pursuing only profit.

2.3.2 User-based vehicle relocation

Regarding the user-based vehicle relocation problem, it has received much less attention compared with the operator-based vehicle relocation problem. In a user-based relocation problem setting where the users may accept to leave the car in a different location in exchange for fare discounts, Di Febbraro et al. (2018) formulated a two-stage optimization model for the determination of the alternative destinations proposed to users. Schiffer et al. (2021) introduced an IP model to optimize the assignment of user-based relocation strategies for the fleets in free-floating CSSs. Through the incentivization of customers and a predictive model for the state of the system, Stokkink and Geroliminis (2021) developed a user-based vehicle relocation approach to determine the optimal incentive as a trade-off between the cost of an incentive and the expected omitted demand loss. To mitigate the demand and supply imbalance problem and increase profits by means of combinatorial monetary incentives and surcharges, Wang et al. (2021a) proposed an optimization framework for the determination of the incentives and surcharges at different stations and times of day in one-way CSSs.

Instead of focusing on either the operator-based vehicle relocation or the user-based vehicle relocation, two studies have tried to factor in both of the two vehicle relocation strategies. With the time-varying SOC of vehicles tracked, Huang et al. (2020b) compared the efficiency of the operator-based and the user-based vehicle relocation strategies in a one-way station-based electric carsharing system. By combining operator-based and user-based relocation strategies, Wang et al. (2021b) developed an IP model to solve the vehicle imbalance problem in one-way electric CSSs.

As summarized in Table 2.5, in total, only six studies factored the user-based vehicle relocation problem for CSSs. This may indicate that there is a lot of room for future research on this problem.

Table 2.4 A summary of studies on the operator-based vehicle relocation problem

Literature	Fleet type	Operation-level decision-makings	Objective	Model	Solution method	Evaluation
Jian et al. (2018)	Gasoline-powered	Vehicle relocation	Profit maximization	MINLP	Model linearization	Case study
Zakaria et al. (2018)	Gasoline-powered	Vehicle relocation & staff rebalancing	Service level maximization; Staff size minimization; Relocation time minimization	Multi-objective ILP	Genetic algorithms	Computational experiments
Molnar and de Almeida Correia (2019)	Gasoline-powered	Vehicle relocation	Operators' preference maximization	Variable quality of service model	Iterated local search metaheuristic	Computational experiments & case study
Lu et al. (2022)	Gasoline-powered	Vehicle relocation	Distance minimization	MILP	Adaptive large neighbourhood search algorithm	Computational experiments & case study
Bruglieri et al. (2014)	Electric	Staff rebalancing	Service level maximization	MILP	Heuristic	Computational experiments
Boyacı et al. (2017)	Electric	Vehicle relocation & staff rebalancing	Service level maximization; Cost minimization	Multi-objective MILP	Clustering algorithm	Case study
Bruglieri et al. (2018)	Electric	Staff rebalancing	Staff size minimization; Relocation needs satisfaction maximization;	Multi-objective MILP	Randomized search heuristics	Computational experiments

			Route duration minimization			
Gambella et al. (2018)	Electric	Vehicle relocation & staff rebalancing	Profit maximization & battery level maximization	MILP	Heuristics	Computational experiments
Boyacı and Zografos (2019)	Electric	Vehicle relocation & staff rebalancing	Cost minimization	IP	Discrete-event simulation approach	Case study
Bruglieri et al. (2019)	Electric	Staff rebalancing	Profit maximization	MILP	Adaptive large neighbourhood search & tabu search metaheuristic	Computational experiments
Zhang et al. (2019)	Electric	Vehicle relocation	Profit maximization	IP	Diving heuristic	Case study
Folkestad et al. (2020)	Electric	Vehicle relocation & staff rebalancing	Cost minimization	IP	Genetic algorithm	Computational experiments
Lai et al. (2020)	Electric	Vehicle relocation	Sum of cost and time minimization	MILP	Solver CPLEX	Case study
Lu et al. (2020)	Electric	Vehicle relocation	Profit maximization	Stochastic sequential decision programming	Event-based strategy improvement approach	Computational experiments
Pantelidis et al. (2022)	Electric	Vehicle relocation	Cost minimization	MILP	Heuristic	Computational experiments & case study
Fan (2013)	Gasoline-powered	Vehicle relocation	Cost minimization	Multi-stage stochastic MILP	Simplex method/Interior point methods/Decomposition methods	Computational experiments

Wang et al. (2019)	Electric	Staff rebalancing	Relocation needs satisfaction maximization	ILP	Ruin-probability-based predictive approach & zoning scheme	Case study
Huo et al. (2020)	Electric	Vehicle relocation	Profit maximization	MINLP	Data-driving approach	Case study
Yang et al. (2021)	Gasoline-powered	Vehicle relocation & staff rebalancing	Cost minimization	ILP	Decomposition algorithm	Computational experiments & case study
Huang et al. (2021)	Gasoline-powered	Vehicle relocation	Profit maximization	A two-stage stochastic programming	Gradient search algorithm	Case study
Iacobucci et al. (2019)	Autonomous & electric	Vehicle relocation	Cost minimization	MILP	Model-predictive control optimization algorithms	Case study
Ma et al. (2021a)	Autonomous & electric	Vehicle relocation	Weighted sum of distance, time, and energy minimization	MILP	Adaptive large neighbourhood search	Computational experiments
Hyland and Mahmassani (2018)	Autonomous & gasoline-powered	Vehicle relocation	Distance minimization	ILP	Agent-based simulation approach	Computational experiments
Li et al. (2021)	Autonomous & electric	Vehicle relocation	Cost minimization	ILP	Minimum drift plus penalty approach	Case study

Table 2.5 A summary of studies on the user-based vehicle relocation problem

Literature	Fleet type	Objective	Model	Solution method	Evaluation
Di Febbraro et al. (2018)	Gasoline-powered	Profit maximization	ILP	Simulation-based approach	Case study

Schiffer et al. (2021)	Gasoline-powered	Profit maximization	ILP	Polynomial algorithm	Case study
Stokkink and Geroliminis (2021)	Gasoline-powered	Profit maximization	Predictive model	Learning algorithm	Case study
Wang et al. (2021a)	Gasoline-powered	Profit maximization	MINLP	Approximate algorithm	Case study
Huang et al. (2020b)	Electric	Profit maximization	MINLP	Rolling horizon method & ε-optimal algorithm & iterated local search algorithm	Case study
Wang et al. (2021b)	Electric	Profit maximization	ILP	Solver Gurobi	Case study

2.4 Research Gaps

From above literature review, two practically significant issues for electric CSSs that have received little attention can be identified. The two issues are described as follows.

(1) The battery degradation has not been considered

Although many studies on electric CSSs have considered the limited driving range and charging requirement of EVs, none of them considered the battery health and impact of battery degradation. In fact, these studies either assumed 'strict' charging strategy that an EV should stay at a station for a pre-specified time or should be charged to a certain level before it can be picked up by another user or relocator (Boyacı et al., 2015; Li et al., 2016; Xu et al., 2018), or adopted 'partial' charging strategy that an EV can be picked up by a user or a relocator as long as its SOC is feasible for the next trip (Boyacı et al., 2017; Gambella et al., 2018; Xu and Meng, 2019). In fact, these studies implicitly assumed that EVs will always remain charged as long as they stay at stations, disregarding how much electricity is actually needed for the next trip. This assumption may result in 'battery over-charged than needed', especially at the low-demand period, and unfavorably incur battery wear cost caused by battery degradation.

Take a carsharing system with one order requested from a user and one EV as an example. Suppose the SOC of the EV is 40% and this EV needs to serve an order with electricity consumption of 50%. The time allowed for charging is sufficient. To satisfy the order, two charging schemes are proposed. The first charging scheme requires the EV to be fully charged before being assigned to the order, whereas in the second charging scheme, this EV will be charged to 50% only and remain uncharged in the station until being picked up. It can be seen that both charging schemes make sure that the SOC of EV is feasible to serve the order. Figure 2.2 shows the profiles of SOC under the two schemes. According to Pelletier et al. (2017) and Han et al. (2014), the health of batteries is adversely affected by battery degradation occurring during charging and discharging processes corresponding to cycle aging, and the degradation of a battery will be more serious at high SOC, i.e., operating an EV at a higher value of SOC will lead to a higher battery wear cost. Therefore, the second charging scheme is better. This example demonstrates the necessity of designing an 'on-demand' charging strategy that not only allows flexible 'partial' charging but also charges EVs as per the need (instead of charging extensively as long as time allows), where the main concern is to reduce the battery degradation and wear cost for the sake of battery health as well as the profitability of CSSs in a long term.

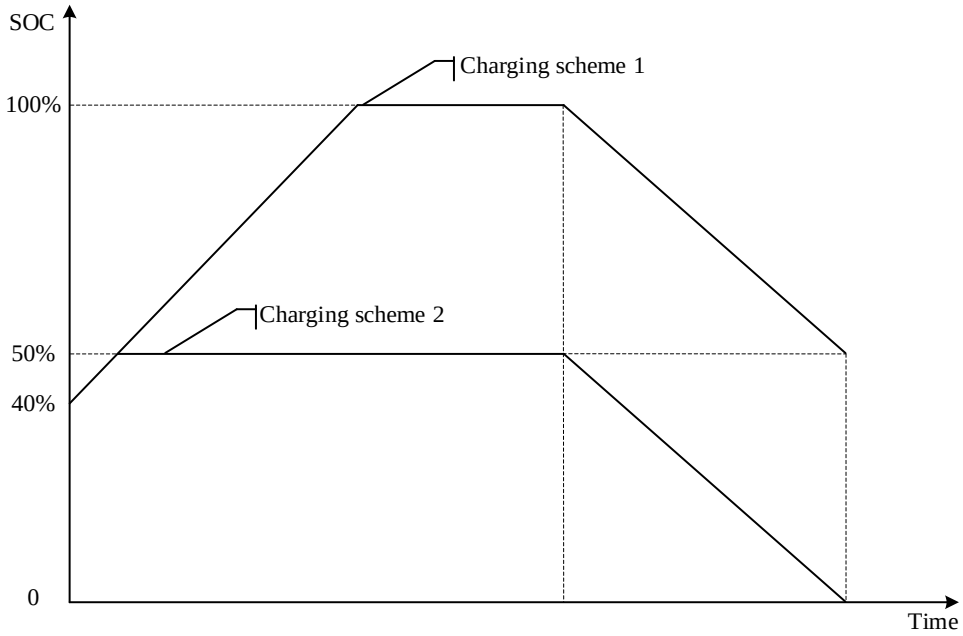

Figure 2.2 The SOC profiles of the EV under two charging schemes

Important as it is, to the best of our knowledge, no studies have ever considered the battery health or the 'on-demand' charging strategy in the electric CSSs. Chapter 3 will close this research gap by incorporating battery degradation from a cost perspective in the determination of EV fleet size for CSSs.

(2) Practical nonlinear charging and demand dynamics have been largely ignored

Most of the existing studies on carsharing adopted either the time-space network modeling approach or the connection-based multi-commodity formulation method, both of which have limitation in dealing with the vehicle charging. Although the two modeling techniques can model individual vehicle charging explicitly, the time-space network modeling approach only works with a linear charging profile and the connection-based multi-commodity formulation method is only applicable to a charging profile with a closed-form expression. Therefore, for the ease of vehicle charging modeling, an assumption of linear approximation of the practical nonlinear charging profile that has no closed-form expression is often made in the related studies (Boyacı and Zografos, 2019; Gambella et al., 2018; Xu et al., 2021; Zhao et al., 2018), which may reduce the credibility and quality of the solution. Xu and Meng (2019) made the first attempt to propose a branch-and-price approach in order to incorporate the practical nonlinear charging profile of EVs in the fleet size determination for one-way electric CSSs.

In addition, despite of the considerable research advancements made for electric CSSs, which can be reflected in the literature review, the demand dynamics is largely ignored. Most

studies assumed that the information of user requests is known a priori or can be estimated beforehand (Boyacı et al., 2017; Gambella et al., 2018; Xu and Meng, 2019; Xu et al., 2021). A few studies considered the stochastic demand (Brandstätter et al., 2017; Hua et al., 2019; Li et al., 2016; Lu et al., 2018; Ma et al., 2018). These studies either optimized operational relocation policies without considering demand dynamics or focused on strategic decision-makings, instead of addressing an ad-hoc carsharing system with dynamically reserved or canceled demands. For example, some users make a reservation just a few minutes before their departure time and the relocation and charging strategy obtained by existing models might become inefficient or even infeasible.

To the best of our knowledge, few studies have ever considered both realistic nonlinear charging profile and demand dynamics for an ad-hoc electric carsharing system with dynamically reserved or canceled demands. Chapter 4 will close the research gap by extending the study of Xu and Meng (2019) to a dynamic environment. Chapter 5 will further extend the study in Chapter 4 to include staff rebalancing.

2.5 Summary

This chapter comprehensively reviewed mathematical modeling-based studies on carsharing based on the three levels of decision-makings, i.e., strategic, tactical, and operational. Subsequently, two practically significant issues that remain to be addressed for electric CSSs were identified. The first issue is the consideration of battery degradation and the second issue is the involvement of both practical nonlinear charging profile and demand dynamics. To close the research gaps, Chapter 3 will tackle a fleet size problem for electric CSSs considering the on-demand charging strategy and battery degradation; Chapter 4 will deal with a real-time vehicle relocation and charging optimization for one-way electric CSSs considering practical nonlinear charging profile and demand dynamics; Chapter 5 will further extend the study in Chapter 4 to include staff rebalancing. The primary objective of the thesis is to address the decision-making challenges faced by carsharing operators due to vehicle electrification.

CHAPTER 3 ELECTRIC VEHICLE FLEET SIZE FOR CARSHARING SERVICES CONSIDERING ON-DEMAND CHARGING STRATEGY AND BATTERY DEGRADATION

This chapter addresses the tactical electric vehicle fleet size (EVFS) problem faced by CSS providers while considering vehicle assignment, vehicle relocation, vehicle charging strategy (i.e., the charging duration at each station), and battery degradation in pursuit of profit maximization. To alleviate battery degradation and achieve cost-saving in a long term, the on-demand charging strategy is proposed in the determination of fleet size. The novelty of this study lies in the incorporation of nonlinear battery wear cost incurred during the battery charging and discharging processes. An MINLP model with both concave and convex terms in the objective function is first developed for the EVFS problem. A piecewise linear approximation approach and an outer-approximation method are employed to linearize the proposed model. Numerical experiments based on EVCARD, a one-way electric carsharing operator in China, are conducted to demonstrate the efficiency of the proposed model and solution method, as well as the necessity of incorporating the battery degradation into the fleet size determination of CSSs. The impacts of several key parameters, i.e., the daily fixed cost of EV and battery price, battery cycle efficiency, service charge, and relocation cost on the performance of one-way electric CSSs are also analyzed.

The remainder of this chapter is organized as follows. Assumptions and problem statement are presented in Section 3.1. An MINLP model for the EVFS problem is formulated in Section 3.2. Section 3.3 discusses the model properties and linearizes the model by employing an outer-approximation method and a piecewise linear approximation approach. The resultant MILP model can be readily solved by available solvers to obtain the ε-optimal solution. The efficiency of the proposed model and solution method, as well as the necessity of incorporating the battery degradation into the fleet size determination of CSSs are demonstrated in Section 3.4 through numerical experiments based on EVCARD in China. Section 3.5 concludes this chapter. Finally, Appendix A presents the notations and the algorithms for model linearization involved in this chapter.

3.1 Assumptions and Problem Description

Consider a one-way CSS provider who operates a fleet of homogenous EVs among a number of predetermined stations in an urban area. At the beginning of the service operation, the EVs are initially distributed at different stations. During the operational period, users are allowed to pick up vehicles according to their reservations and return them later at another station different from their pick-up stations. The information of all rentals, i.e., CSS orders, requested from users is assumed to be known a priori by estimation/prediction or reservation. In order to achieve profit maximization, not all demands are to be satisfied due to the limited resources, and a penalty will be incurred if a customer is denied service. The distribution of EVs across stations will become imbalanced along with the flow dynamics of users. EVs will be relocated among these stations to address vehicle imbalance and demand asymmetry problems. Considering the limited driving range of EVs, it is assumed that sufficient parking spots equipped with charging facilities are provided in each station such that EVs can be charged when staying idle at stations. The battery will be discharged when relocated or under service. For simplicity, it is assumed that the SOC of EVs will increase/decrease linearly with charging/discharging time, with battery wear cost incurred according to a battery wear cost model to be introduced in Subsection 3.1.1. The EVFS problem aims to maximize the daily profit of CSS providers by determining the EV fleet size considering the vehicle assignment, vehicle relocation, vehicle charging strategy, and battery degradation.

3.1.1 Battery wear cost

Battery degradation occurs during charging and discharging processes corresponding to cycle aging. Based on the experimental cycle life data of EVs provided by the manufacturers, Han et al. (2014) proposed the following generic semi-empirical battery wear cost model for EVs:

$$WC = BS \times \int_{l_{init}}^{l_{ulti}} W(l) \left| dl \right| \tag{3.1}$$

where WC denotes the battery wear cost incurred during charging or discharging process when the SOC increases or decreases from l_{init} to l_{ulti}; BS represents the battery size measured in kWh; $W(l)$ is the battery wear density function that represents the battery wear cost per unit energy transfer at the SOC l, given by

$$W(l) = \frac{BP \times b}{2 \times BS \times \mu^2 \times a} \times (1-l)^{b-1} \tag{3.2}$$

where BP is the battery price of an EV; a and b are battery-dependent parameters, which are acquired experimentally, and they are $0<b<1$ and $a>0$; μ is the battery cycle efficiency.

It's easy to see that the battery wear density function $W(l)$ is a monotonically increasing function with respect to the SOC l. The wear cost per unit energy transfer is thus higher when a battery is operated at a higher value of SOC. By further substituting Eq. (3.2) into Eq. (3.1), with simple manipulation, the following explicit expression of battery wear function can be obtained:

$$WC = \frac{BP}{2\times\mu^2\times a}\times\left|(1-l_{init})^b-(1-l_{ulti})^b\right| \tag{3.3}$$

It can be seen that the battery wear cost depends on not only the charging/discharging amount, i.e., charging/discharging duration, but also the initial SOC before charging/discharging.

The consideration of battery wear cost would significantly affect the optimal vehicle assignment for cost minimization or profit maximization. This can be illustrated by a simple example with three stations, i.e., Station A, Station B, and Station C, two rentals, i.e., Rental 1 and Rental 2, and two EVs, i.e., EV 1 and EV 2. Suppose Rental 1 departs from Station A to Station B with electricity consumption of 30% and Rental 2 departs from Station A to Station C with electricity consumption of 40%. Both the two EVs are available at Station A, with initial SOCs 60% (EV 1) and 70% (EV 2), respectively. The greedy assignment strategy, i.e., Strategy 1, that assigns a rental with more electricity consumption to an EV with higher SOC is first considered. By this strategy, Rental 1 will be assigned to EV 1 while Rental 2 will be assigned to EV 2. The SOC profiles of the two EVs under Strategy 1 are illustrated in Figure 3.1 (a). On the other hand, if another strategy that assigns Rental 1 to EV 2 and Rental 2 to EV 1, referred to as Strategy 2, is chosen, the variations of SOC will become the profiles shown in Figure 3.1 (b). It can be seen that Rental 1 and Rental 2 can be satisfied in both strategies. Since $W(l)$ is an increasing function with respect to l, the total battery wear cost of Strategy 2 is less than Strategy 1. Therefore, Strategy 2 is better than Strategy 1 from the perspective of cost saving. Hence, with battery wear cost taking into consideration, the vehicle assignment for the cost minimization or profit maximization would be largely influenced.

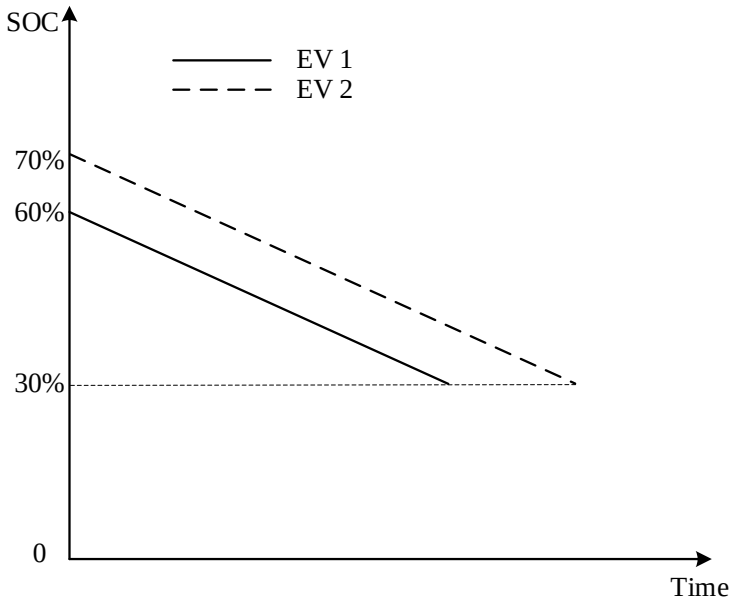

(a) The SOC profiles of the two EVs under Strategy 1

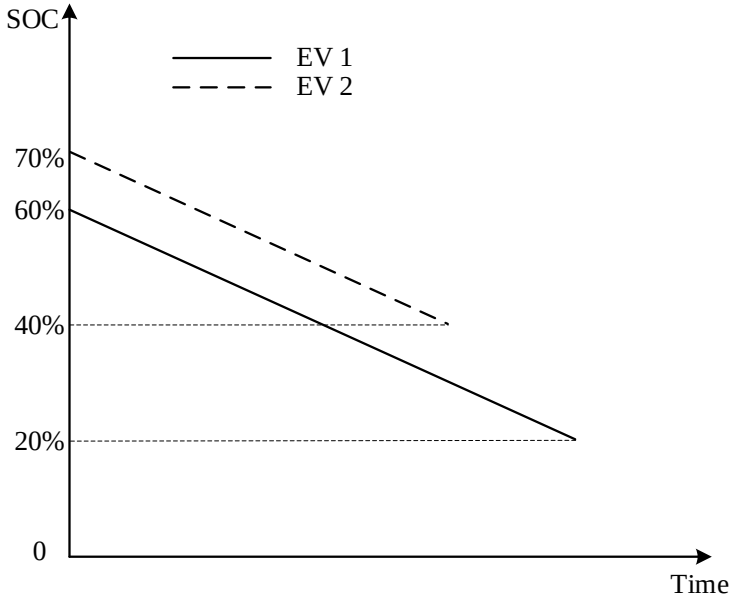

(b) The SOC profiles of the two EVs under Strategy 2

Figure 3.1 The SOC profiles of the two EVs under two vehicle assignment strategies

3.1.2 On-demand charging strategy

Apart from the vehicle assignment, the consideration of battery wear cost will also affect the schedule of vehicle relocation and vehicle charging. For example, suppose only one EV is in the CSS with three stations, i.e., Station A, Station B, and Station C. The EV is available at Station A from 1:30 pm onwards, with initial SOC of 10%. There will be a rental departing from Station B to Station C at 3:00 pm and the travel time is 30 min. To serve this rental,

relocation operation from Station A to Station B is needed. It is further assumed that the relocation time from Station A to Station B is 30 min and the charging and discharging rates are 10% SOC variation per 15 min. Excluding the relocation time, there are 60 min available for charging, either at Station A or Station B. Considering the electricity consumption during vehicle relocation, the EV should be charged at Station A for at least 15 min in order to have enough electricity for relocation operation. Three feasible schedules of vehicle relocation and vehicle charging in this example, i.e., Schedule 1, Schedule 2, and Schedule 3, are considered. Schedule 1 requires the EV to be charged at Station A for 60 min before the relocation operation to Station B, while under Schedule 2, after being charged for 15 min at Station A, the EV is relocated to Station B and charged at Station B for another 45 min. Unlike the aforementioned two schedules, under which the EV is charged as long as it stays idle at a station, Schedule 3 charges the EV as per the need, i.e., before and after the relocation operation, the EV is charged for 15 min and 30 min at Station A and Station B, respectively. Figure 3.2 shows the EV trajectories corresponding to the three schedules in a time-space coordinate system. The SOC profiles of EV under the three schedules are illustrated in Figure 3.3. It can be seen that the SOC of EV under Schedule 3 is averagely lower than the other two schedules, indicating that the battery wear cost under Schedule 3 is the least and thus Schedule 3 is the best.

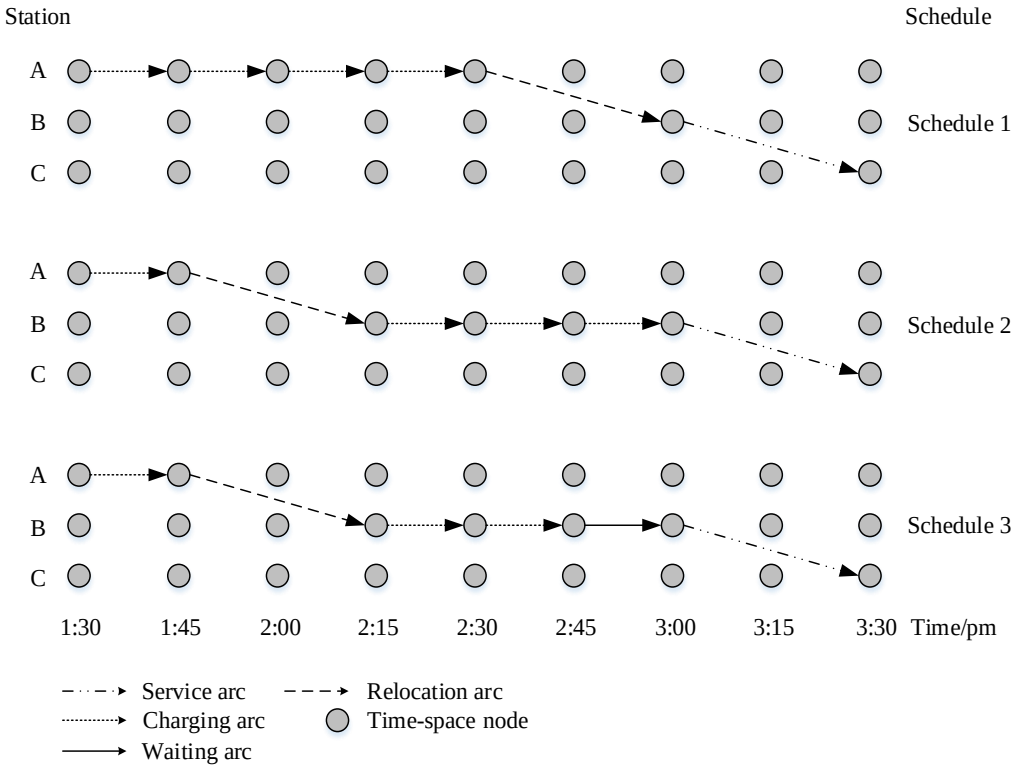

Figure 3.2 The EV trajectories under three schedules in a time-space coordinate system

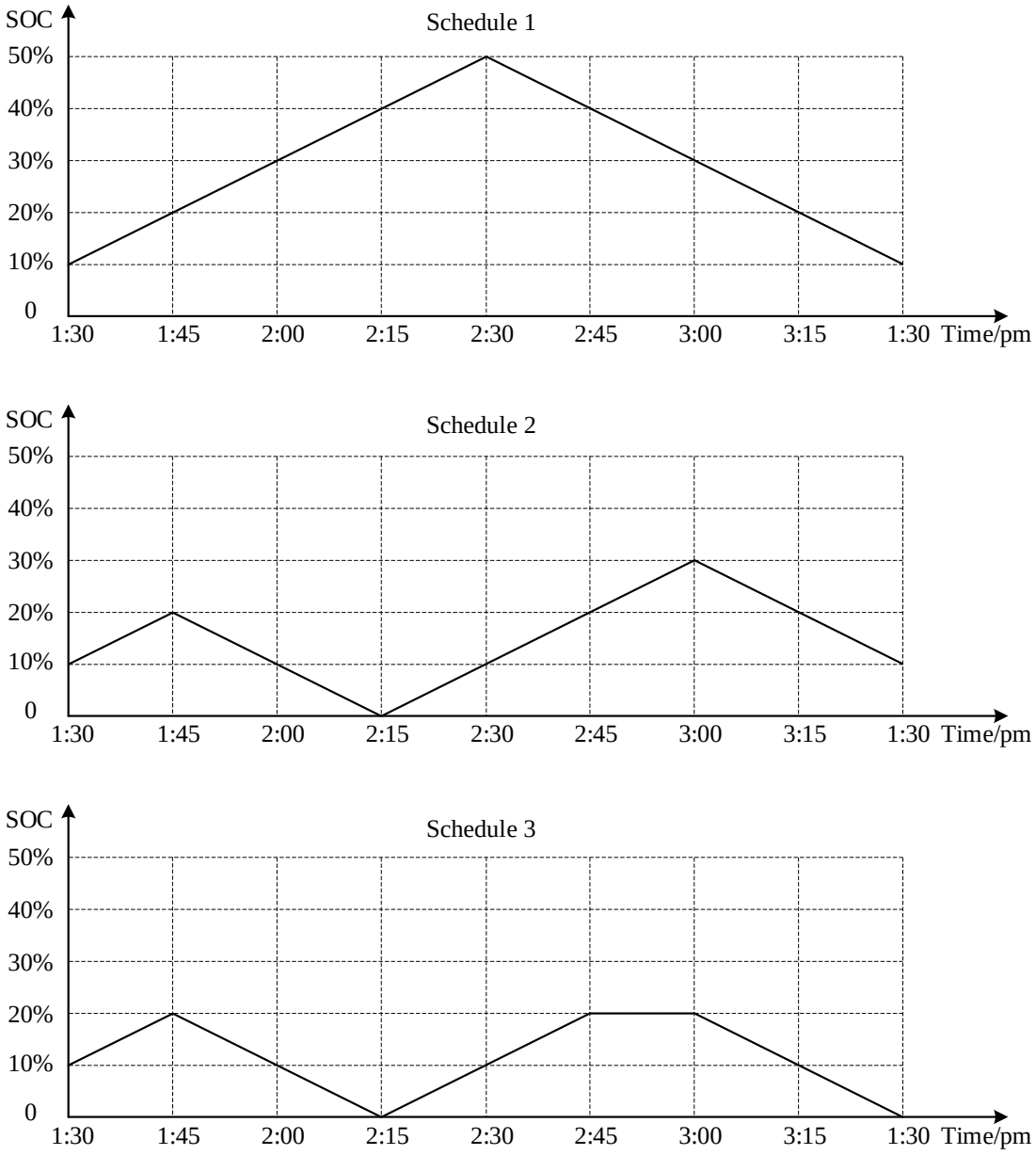

Figure 3.3 The SOC profiles of EV under three schedules

Instead of extensive charging whenever staying idle at stations, ‘on-demand’ charging strategy is considered, which not only allows ‘partial’ charging of EVs before they are picked up, but also charges the EVs as needed for the sake of battery health and cost saving. The amount of electricity to be charged at each station should be determined jointly with the vehicle assignment and vehicle relocation.

3.2 Optimization Model Building

3.2.1 Notations

To formulate the EVFS problem, let FC be the fixed amortized cost of an EV per day and I denote the set of rentals. Each rental $i \in I$ is described by a quadruplet $U_i = \{s_i^o, s_i^d, t_i^o, t_i^d\}$, where s_i^o and s_i^d denote the pick-up and drop-off stations of rental $i \in I$, t_i^o and t_i^d denote the departure and arrival time of rental $i \in I$. Let l_i, TP_i and PC_i be the electricity consumption, net profit and incurred penalty of rental $i \in I$, and l_{ij}, t_{ij} and RC_{ij} denote the electricity consumption, time, and cost of relocation operation from the drop-off station of rental i to the pick-up station of rental j, respectively. The electricity consumption and replenishment are measured by the variation of SOC of battery. Since linear charging and discharging process are assumed, both the charging and discharging rate, i.e., the uniform variation of SOC per unit of time, are represented by constants CR and DR, respectively. The usable battery capacity denoted by E is also measured by SOC, i.e., $E = 100\%$. Without loss of generality, it is assumed that $l_i \le E$, $\forall i \in I$. The minimum SOC value allowed for an EV is denoted by E_{min}.

For ease of model building, a dummy node denoted by n_0 is created, which all vehicles will depart from and return to at the beginning and end of the operational period, respectively. In this way, the fleet size is exactly the number of EVs originating from the node n_0. It is assumed that the attributes of the dummy node (i.e., the electricity consumption, time duration, net profit, and incurred penalty) and the links (i.e., the electricity consumption, time, and cost) connecting the dummy node and the physical stations are zero. Let A^0 denote the set of dummy links connecting the dummy node and all the rentals and A^r denote the set of relocation operations connecting any two rentals that are compatible both in terms of travel time and electricity consumption. In other words, a link (i, j), $\forall i \ne j \in I$ belongs to set A^r if it satisfies the following conditions:

$$t_{ij} \le t_j^o - t_i^d \tag{3.4}$$

$$min\left\{E, E - l_i + CR \times (t_j^o - t_i^d - t_{ij})\right\} \ge l_{ij} \tag{3.5}$$

$$min\left\{E, E - l_i - l_{ij} + CR \times (t_j^o - t_i^d - t_{ij})\right\} \ge l_j \tag{3.6}$$

As for the decision variables, let f be an integer decision variable representing the fleet size of EVs, z_i be a binary decision variable that equals 1 if rental $i \in I$ is satisfied (and 0 otherwise), and x_{ij} be a binary decision variable that equals 1 if an EV is relocated from the drop-off station of rental i to the pick-up station of rental j (and 0 otherwise). On a typical operation day, an EV will depart from the dummy node. It then serves a series of rentals and gets charged at traversed stations before finally returning to the dummy node. The activity trajectory of an EV, which can be seen as a trip chain r consisting of a dummy node and a series of rentals sorted in ascending order in terms of their departure time, i.e., n_0, i_1, i_2, i_3,…, i_{m_r}, n_0, as well as several relocation operations connecting these rentals, can be intuitively represented by

$$n_0 \Rightarrow s_{i_1}^o \rightarrow s_{i_1}^d \Rightarrow s_{i_2}^o \rightarrow s_{i_2}^d \Rightarrow \cdots \Rightarrow s_{i_k}^o \rightarrow s_{i_k}^d \Rightarrow \cdots \Rightarrow s_{i_{m_r}}^o \rightarrow s_{i_{m_r}}^d \Rightarrow n_0 \qquad (3.7)$$

where the single and double lined arrows denote the rentals and relocations from one station to another, respectively. To capture the SOC of EV and facilitate the formulation of 'on-demand' charging strategy, in addition to the aforementioned integer or binary variables, a set of continuous variables are defined: two SOC-state variables, R_i and Q_i, $\forall i \in I$, denoting the SOC of an EV rightly before serving the rental i and the relocation operation originated from the drop-off station of rental i, respectively; and two electricity-amount variables, e_i^o and e_i^d, $\forall i \in I$, denoting the amount of electricity charged at the pick-up station and drop-off station of rental $i \in I$, respectively. All the notations used throughout this chapter are provided in Appendix A.1 for readability.

Suppose that the amount of electricity charged at the dummy node is zero. The EV departs from the dummy node with SOC expressed by $R_{i_1} - e_{i_1}^o$. After arriving at station $s_{i_1}^o$, it is charged to R_{i_1}. The same vehicle is then picked up by a user and the SOC reduces to $R_{i_1} - l_{i_1}$ when being dropped off at station $s_{i_1}^d$. By making use of the dwell time at station $s_{i_1}^d$, the EV is charged to Q_{i_1}. After being relocated to station $s_{i_2}^o$, the SOC falls to $Q_{i_1} - l_{i_1 i_2}$, which also equals $R_{i_2} - e_{i_2}$. Figure 3.4 illustrates the trajectory of the EV in a time-space coordinate system and Figure 3.5 shows the correspondent profile of SOC over the same period of time. The above process happens iteratively and according to Eq. (3.3), there will be battery wear cost

each time the SOC varies. By simple manipulation, the following battery wear cost of an EV over the entire operational period can be obtained:

$$WC_r = \frac{BP}{\mu^2 \times a} \times \sum_{k=1}^{m_r} [(1-R_{i_k} + e^o_{i_k})^b - (1-R_{i_k})^b + (1-R_{i_k} + l_{i_k})^b - (1-Q_{i_k})^b] \tag{3.8}$$

Therefore, the total battery wear cost of all EVs is calculated by

$$TWC = C \sum_{i \in I} [(1-R_i + e^o_i)^b - (1-R_i)^b + (1-R_i + l_i)^b - (1-Q_i)^b] \tag{3.9}$$

where $C = \frac{BP}{\mu^2 \times a}$.

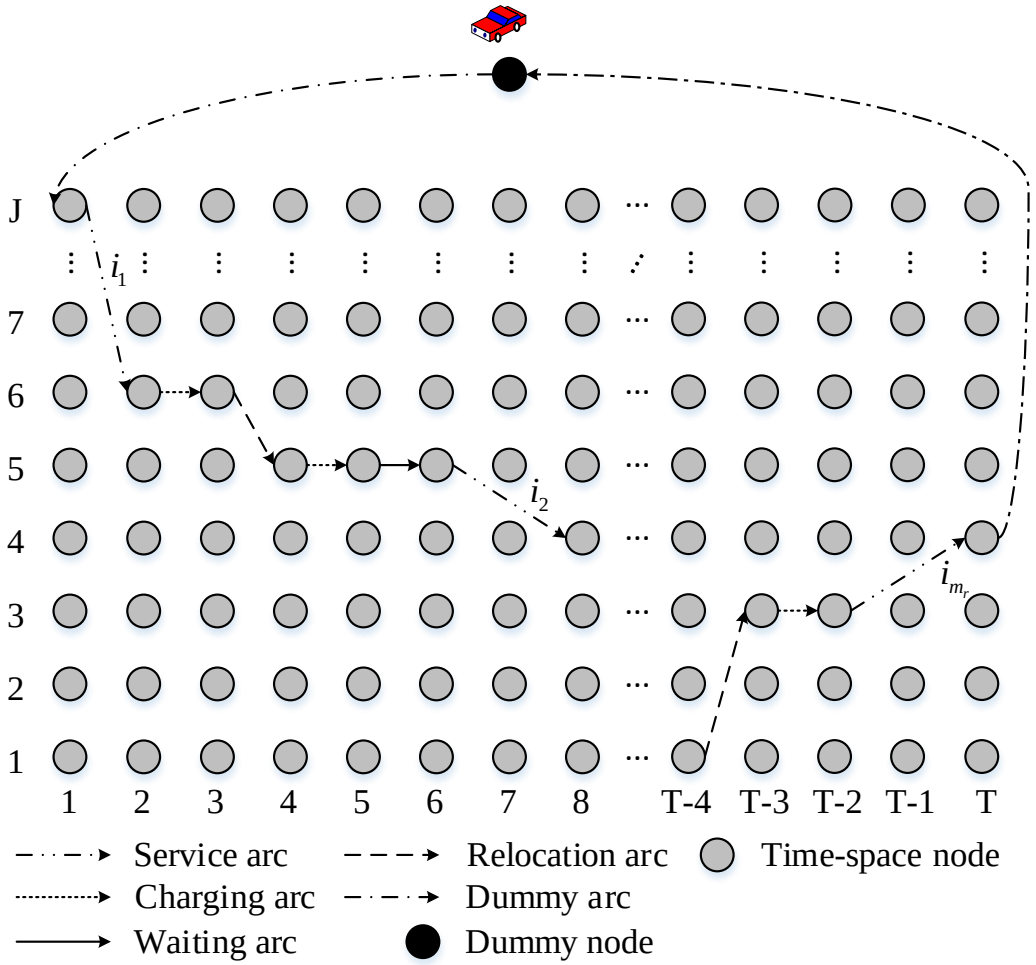

Figure 3.4 Trajectory of an EV in a time-space coordinate system over the operational period

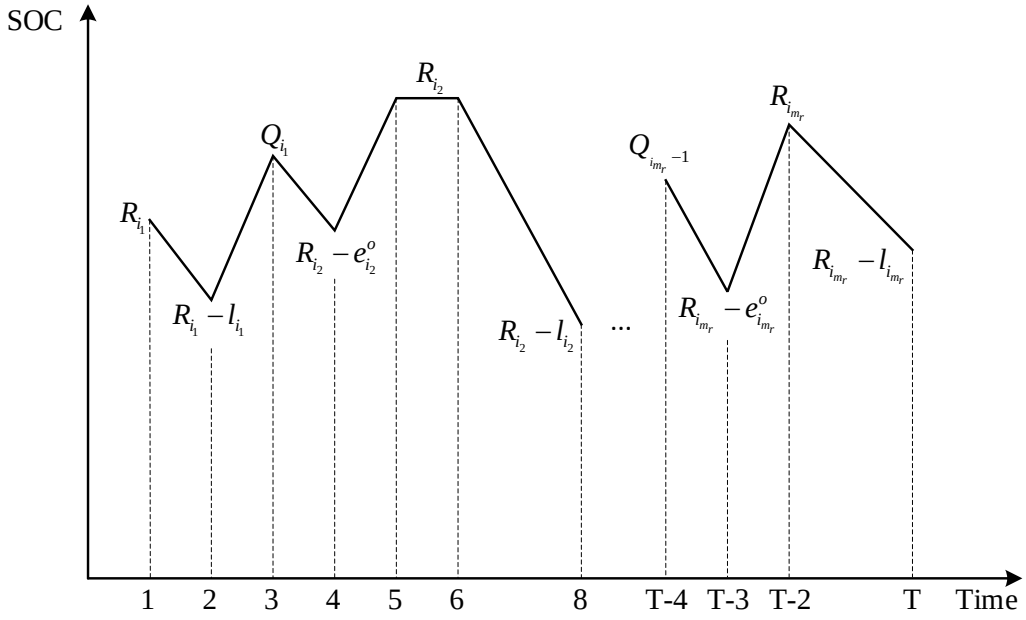

Figure 3.5 SOC profile of the EV in Figure 3.4

3.2.2 Model formulation

Given the above notations, the EVFS problem can be formulated as follows:

[EVFS]

$$\max_{\mathbf{x,z,f,R,Q,e}} PROFIT(\mathbf{x,z,f,R,Q,e}) = \sum_{i\in I} TP_i \times z_i - \sum_{i\in I} PC_i \times (1-z_i) - \sum_{(i,j)\in A^r} RC_{ij} \times x_{ij} - FC \times f - TWC \tag{3.10}$$

subject to Eq. (9) and

$$\sum_{i\in I\cup\{n_0\}:(i,j)\in A^0\cup A^r} x_{ij} = z_j, \qquad \forall j \in I \tag{3.11}$$

$$\sum_{i\in I\cup\{n_0\}:(i,j)\in A^0\cup A^r} x_{ij} - \sum_{i\in I\cup\{n_0\}:(j,i)\in A^0\cup A^r} x_{ji} = 0, \quad \forall j \in I \tag{3.12}$$

$$\sum_{i\in I} x_{n_0 i} \le f \tag{3.13}$$

$$R_i \ge l_i + E_{min}\ z_i, \ \forall i \in I \tag{3.14}$$

$$Q_i \ge (l_{ij} + E_{min}) x_{ij}, \quad \forall i \ne j \in I, (i,j) \in A^r \tag{3.15}$$

$$Q_i = R_i - l_i + e_i^d, \quad \forall i \in I \tag{3.16}$$

$$R_j \le Q_i - l_{ij} + e_j^o + M_1(1-x_{ij}), \quad \forall i \ne j \in I \bigcup \{n_0\}, (i,j) \in A^0 \bigcup A^r \tag{3.17}$$

$$t_i^d + \frac{e_i^d}{CR} + t_{ij}x_{ij} \le t_j^o - \frac{e_j^o}{CR} + M_2(1-x_{ij}), \quad \forall i \ne j \in I, (i,j) \in A^r \tag{3.18}$$

$$e_{n_0}^o = e_{n_0}^d := 0 \tag{3.19}$$

$$R_i, Q_i, e_i^o, e_i^d \in [0, E], \forall i \in I \bigcup \{n_0\} \tag{3.20}$$

$$f \in Z^+, x_{ij}, z_i \in \{0,1\}, \quad \forall (i,j) \in A^0 \bigcup A^r, i \in I \tag{3.21}$$

where $M_1 := E + max\{l_{ij}\}_{(i,j)\in A^r}$, $M_2 := max\{t_j^o\}_{j\in I} - min\{t_j^o\}_{j\in I} + E/CR$, and Z^+ denotes the set of non-negative integers.

The objective function shown by Eq. (3.10) is the daily profit of CSS providers, i.e., the difference of service revenue and total system cost. The cost is composed of four terms including the penalty for unserved rentals, the relocation cost (e.g., the electricity consumption cost), the capital investment of EV fleet, and the battery wear cost in sequence. Note that the battery wear cost in Eq. (3.10), i.e., TWC, is calculated by Eq. (3.9). Constraint (3.11) delineates the fulfillment of rentals, which ensures that there should be one EV arriving at the origin station of rental j if it is served, i.e., $z_j = 1$. Constraint (3.12) is the flow conservation constraint. Constraint (3.13) limits that the total number of EVs originating from the dummy node is not larger than the fleet size. Constraints (3.14)-(3.20) are constraints dedicated for the characteristics of EVs. Specifically, Constraints (3.14) and (3.15) ensure the feasibility of nodes (i.e., serving rentals) and links (i.e., relocation operations) in terms of the SOC of EV. Constraints (3.16) and (3.17) update the SOC upon the departure of EV to serve rentals and the relocation of EV to another station considering the charging and discharging processes, respectively. In particular, based on the recursion relationship, Constraint (3.17) updates the SOC-state variables of two rentals connected by a relocation operation. Note that since $M_1 = E + max\{l_{ij}\}_{(i,j)\in A^r}$, R_j will be $Q_i - l_{ij} + e_j^o$ at optimal if $x_{ij} = 1$. Constraint (3.18) ensures that the EVs are timely relocated in order to serve the next rental. Again, this constraint reduces to $t_i^d + \frac{e_i^d}{CR} + t_{ij} \le t_j^o - \frac{e_j^o}{CR}$ at optimal if $x_{ij} = 1$ because $M_2 = max\{t_j^o\}_{j\in I} - min\{t_j^o\}_{j\in I} + E/CR$.

Constraint (3.19) imposes that the amount of electricity charged at the dummy node is zero. Constraints (3.20) and (3.21) define the domains of variables x_{ij}, z_i, f, R_i, Q_i, e_i^o and e_i^d.

It is worth noting that the model [EVFS] can be easily extended to consider the users' range anxiety, which, if not taken into account properly, may lower the level of CSSs significantly. The range anxiety here refers to the fear of running out of electricity before reaching the destinations (Xu et al., 2020). To achieve this, an additional constraint can be added and expressed by

$$R_i \geq l_i + E_{comf} \times z_i, \qquad \forall i \in I \tag{3.22}$$

where E_{comf} denotes the minimum SOC value above which users are free from range anxiety.

3.3 Model Properties and Model Linearization

It can be seen that except for the total battery wear cost term in Eq. (3.10), all the constraints and the other terms in the objective function are linear. The consideration of battery health results in a nonlinear model that is not easily solvable by commercial solvers. To address this problem, another continuous variable, i.e., $G_i := R_i - e_i^o$, $\forall i \in I$, denoting the SOC of an EV rightly after arriving at the origin station of rental i, is first defined. Then the battery wear cost term in the objective function (3.10) will become

$$MTWC = C\sum_{i\in I}[-(1-G_i)^b + (1-R_i)^b - (1-R_i+l_i)^b + (1-Q_i)^b] \tag{3.23}$$

It should be noted that $MTWC$ denotes the minus of total battery wear cost, i.e., $MTWC = -TWC$, by further taking the minus sign in the objective function (3.10) into consideration. For the convenience of description, the minus of total battery wear cost will be referred to as MTWC for short. By digging further, it can be found that the MTWC in the above equation can be divided into three terms, i.e., $-(1-G_i)^b$, $(1-R_i)^b - (1-R_i+l_i)^b$ and $(1-Q_i)^b$. In other words, Eq. (3.23) can be rewritten as follows:

$$MTWC = C\left(\sum_{i\in I}\left(-(1-G_i)^b\right) + \sum_{i\in I}\left((1-R_i)^b - (1-R_i+l_i)^b\right) + \sum_{i\in I}(1-Q_i)^b\right) \tag{3.24}$$

Since $0<b<1$, it is not hard to prove that the term $-(1-G_i)^b$ is convex with respect to G_i, whereas $(1-R_i)^b - (1-R_i+l_i)^b$ and $(1-Q_i)^b$ are concave with respect to R_i and Q_i,

respectively. Therefore, the model [EVFS] is an MINLP model with both concave and convex terms in the objective function subject to many linear constraints. To linearize the model, a piecewise linear approximation approach and an outer-approximation method will be employed for the convex and concave terms, respectively. Details can be found in next subsections.

3.3.1 Piecewise linear approximation approach

This subsection describes the linearization of the convex term of the MTWC, i.e., $-(1-G_i)^b$ in Eq. (3.24), in the objective function of the model [EVFS]. The piecewise linear approximation approach is one of the most prevailing linearization techniques for nonlinear separable programming problems. It works by approximating any arbitrary continuous function using a piecewise linear function as illustrated in Figure 3.6. The error resulted from the approximation can be controlled by the number of linear segments. To apply the piecewise linear approximation approach for the model [EVFS], let $g(G_i)$ denote the convex term $-(1-G_i)^b$, i.e., $g(G_i) := -(1-G_i)^b$, $\forall G_i \in [0, E], \forall i \in I$. As shown in Figure 3.6, the interval $[0, E]$ is subdivided into smaller intervals by the point $G_i^{(k)}$, where $k \in K = \{1, 2, ..., N-1, N\}$ and $0 = G_i^{(1)} < G_i^{(2)} < ... < G_i^{(N-1)} < G_i^{(N)} = E$. K is the set of breakpoints for the linear segments of the curve $g(G_i)$. Appendix A.2 presents the generation of breakpoints for the linear segments such that the approximation of the function $g(G_i)$ can be controlled within a pre-specified tolerance $\hat{\varepsilon}$. Any point G_i in the interval $[G_i^{(k)}, G_i^{(k+1)}]$ can be thus uniquely expressed as $G_i = \lambda_i^k G_i^{(k)} + \lambda_i^{k+1} G_i^{(k+1)}$, where $\lambda_i^k + \lambda_i^{k+1} = 1$, $\lambda_i^k, \lambda_i^{k+1} \geq 0$. Then $\hat{g}(G_i) = \lambda_i^k g(G_i^{(k)}) + \lambda_i^{k+1} g(G_i^{(k+1)})$ gives a linear approximation of the function $g(G_i)$ in the interval $[G_i^{(k)}, G_i^{(k+1)}]$. The piecewise linear approximation of the function $g(G_i)$ over the interval $[0, E]$ can then be written as $\hat{g}(G_i) = \sum_{k=1}^{N} \lambda_i^k g(G_i^{(k)})$, where $G_i = \sum_{k=1}^{N} \lambda_i^k G_i^{(k)}$, $\sum_{k=1}^{N} \lambda_i^k = 1$, and at most two adjacent λ_i^k are positive (often referred to as 'special ordered sets of type 2' (SOS2) in the literature (Guéret et al., 2000).

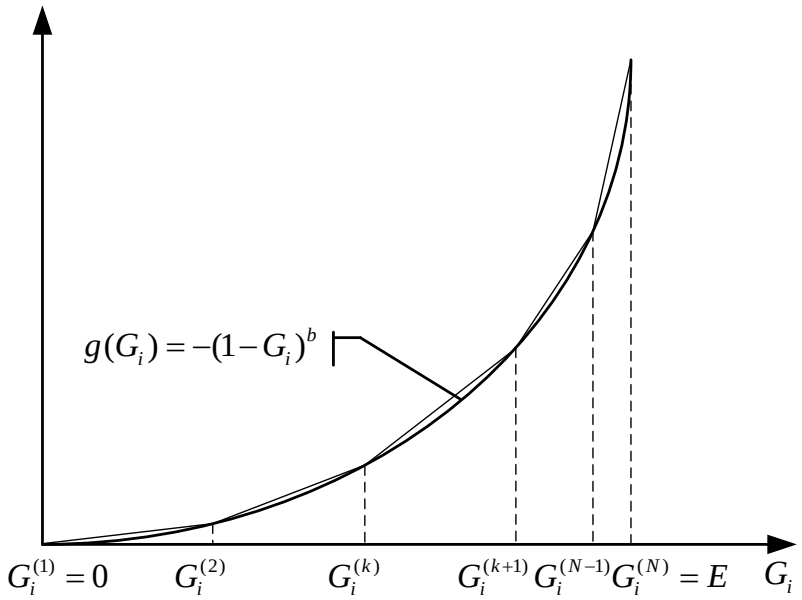

Figure 3.6 Illustration of the piecewise linear approximation approach

A reformulated model [EVFS-I] can be obtained by replacing the convex term $-(1-G_i)^b$ in the objective function of model [EVFS] with the piecewise linear approximation $\hat{g}(G_i)$ and enforcing the associated conditions, i.e., Constraints (3.11)-(3.21), and

$$\sum_{k=1}^{N} \lambda_i^k G_i^{(k)} = R_i - e_i^o \quad \forall i \in I \tag{3.25}$$

$$\sum_{k=1}^{N} \lambda_i^k = 1 \quad \forall i \in I \tag{3.26}$$

$$\sum_{k=1}^{N-1} \delta_i^k = 1 \quad \forall i \in I \tag{3.27}$$

$$\lambda_i^1 \le \delta_i^1 \quad \forall i \in I \tag{3.28}$$

$$\lambda_i^k \le \delta_i^{k-1} + \delta_i^k \quad \forall i \in I, k \in K \setminus \{1, N\} \tag{3.29}$$

$$\lambda_i^N \le \delta_i^{N-1} \quad \forall i \in I \tag{3.30}$$

$$\lambda_i^k \ge 0, \delta_i^k \in \{0,1\}, \quad \forall i \in I, k \in K \tag{3.31}$$

where δ_i^k, $\forall i \in I, k \in K \setminus \{N\}$ are binary variables defined to enforce the SOS2 condition through Constraints (3.27)-(3.30) that at most two adjacent λ_i^k, $\forall i \in I$ are positive and it is $\delta_i^k = 1$ if $G_i^{(k)} \le G_i \le G_i^{(k+1)}$, and $\delta_i^k = 0$ otherwise. Then the MTWC in the objective function of the model [EVFS-I] will be

$$MTWC^{\mathrm{I}} = C\left(\sum_{i \in I} \sum_{k=1}^{N} \lambda_i^k g(G_i^{(k)}) + \sum_{i \in I} \left((1-R_i)^b - (1-R_i+l_i)^b \right) + \sum_{i \in I} (1-Q_i)^b \right) \quad (3.32)$$

3.3.2 Outer-approximation method

The outer-approximation algorithm was initially proposed by Duran and Grossmann (1986) to find an ε-optimal solution to MINLP problems of a particular class. The main feature in the underlying mathematical structure of this particular class of problems (minimization problems) is the convexity of the nonlinear functions involving continuous variables. For a general MINLP problem with convex terms both in the objective function and constraints, this algorithm obtains its ε-optimal solution by generating a sequence of non-increasing upper and non-decreasing lower bounds at multiple iterations until their difference does not exceed the pre-specified tolerance ε. Particularly, for the considered maximization problem [EVFS-I], since the concave terms appear only in the objective function, the outer-approximation algorithm can be applied more efficiently. Specifically, the model [EVFS-I] will be further transformed into an MILP model by approximating the concave terms in the objective function, i.e., $(1-R_i)^b - (1-R_i+l_i)^b$ and $(1-Q_i)^b$ in Eq. (3.32), with multiple linear functions. The ε-optimal solution can be readily obtained by solving the resultant MILP model using state-of-the-art MILP solvers like Gurobi.

To apply the outer-approximation method, two auxiliary continuous variables A_i and B_i, $\forall i \in I$ are first defined as the proxy variables for $(1-R_i)^b - (1-R_i+l_i)^b$ and $(1-Q_i)^b$, respectively. The model [EVFS-I] can be rewritten by replacing $(1-R_i)^b - (1-R_i+l_i)^b$ and $(1-Q_i)^b$ in the objective function with A_i and B_i, and imposing Constraints (3.11)-(3.21), (3.25)-(3.31), and

$$A_i \le (1-R_i)^b - (1-R_i+l_i)^b, \quad \forall i \in I \quad (3.33)$$

$$B_i \le (1-Q_i)^b, \quad \forall i \in I \quad (3.34)$$

The MTWC in the objective function of the rewritten model can then be expressed by

$$MTWC^{\text{II}} = C\left(\sum_{i\in I}\sum_{k=1}^{N}\lambda_i^k g(G_i^{(k)}) + \sum_{i\in I}(A_i + B_i)\right) \tag{3.35}$$

For the sake of presentation, let $h(R_i)$ and $y(Q_i)$ denote the concave terms $(1-R_i)^b - (1-R_i+l_i)^b$ and $(1-Q_i)^b$, respectively, i.e., $h(R_i) := (1-R_i)^b - (1-R_i+l_i)^b$, $\forall R_i \in [0,E], \forall i \in I$ and $y(Q_i) := (1-Q_i)^b, \forall Q_i \in [0,E], \forall i \in I$. Constraints (3.33) and (3.34) can thereby be relaxed by replacing the functions $h(R_i)$ and $y(Q_i)$ with many linear functions that are tangent to the concave curves $h(R_i)$ and $y(Q_i)$. Figure 3.7 illustrates the linearization of function $h(R_i)$ as an example. Those linear functions are grouped into two sets denoted by $\Omega = \{1,2,...,M-1,M\}$ and $V = \{1,2,...,P-1,P\}$ for $h(R_i)$ and $y(Q_i)$, respectively. Again, the generation of tangent points for tangent lines such that the approximation of the function $h(R_i)$ and $y(Q_i)$ can be controlled within a pre-specified tolerance $\hat{\varepsilon}$ is presented in Appendix A.2. Let $a_i^{(k)}$ and $b_i^{(k)}$ be the slope and intercept of the k^{th} tangent line of the curve $h(R_i)$ at the point $R_i^{(k)}$, i.e., $a_i^{(k)} = h'(R_i^{(k)})$ and $b_i^{(k)} = h(R_i^{(k)}) - h'(R_i^{(k)})R_i^{(k)}$. Thus Constraint (3.33) can be relaxed to be

$$A_i \le a_i^{(k)} R_i + b_i^{(k)}, \quad \forall i \in I, k \in \Omega \tag{3.36}$$

Similarly, Constraint (3.34) can be relaxed to be

$$B_i \le \bar{a}_i^{(k)} Q_i + \bar{b}_i^{(k)}, \quad \forall i \in I, k \in V \tag{3.37}$$

where $\bar{a}_i^{(k)}$ and $\bar{b}_i^{(k)}$ are the slope and intercept of the k^{th} tangent line of curve $y(Q_i)$ at the point $Q_i^{(k)}$, i.e., $\bar{a}_i^{(k)} = y'(Q_i^{(k)})$ and $\bar{b}_i^{(k)} = y(Q_i^{(k)}) - y'(Q_i^{(k)})Q_i^{(k)}$.

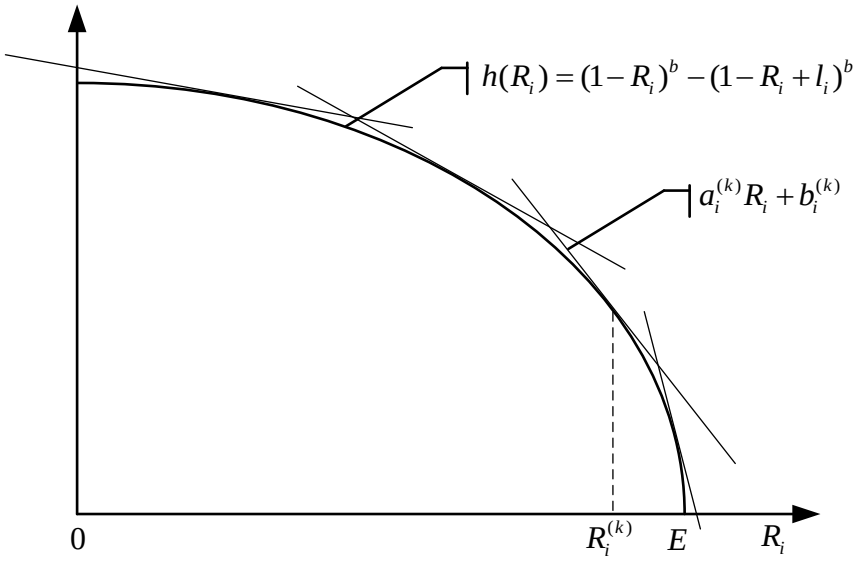

Figure 3.7 Illustration of the outer-approximation method

It can be seen that the original MINLP model [EVFS] has been transformed into the following MILP model by the piecewise linear approximation and outer-approximation methods, which can be efficiently solved by state-of-the-art MILP solvers like Gurobi:

[EVFS-II]

$$\max_{\mathbf{x,z,f,R,Q,e,\lambda,}\delta\mathbf{,A,B}} PROFIT^{\mathrm{II}}(\mathbf{x,z,f,R,Q,e,\lambda,}\delta\mathbf{,A,B}) = \sum_{i\in I} TP_i \times z_i - \sum_{i\in I} PC_i \times (1-z_i)$$
$$- \sum_{(i,j)\in A^r} RC_{ij} \times x_{ij} - FC \times f + C\left(\sum_{i\in I}\sum_{k=1}^{N} \lambda_i^k g(G_i^{(k)}) + \sum_{i\in I}(A_i + B_i) \right) \tag{3.38}$$

subject to Constraints (3.11)-(3.21), (3.25)-(3.31), and (3.36)-(3.37).

3.3.3 ε-optimal solution

This subsection demonstrates that an ε-optimal solution to the MINLP model [EVFS] can be obtained by solving the resultant MILP model [EVFS-II]. In the first place, the following proposition is introduced.

Proposition 1: Let $(\hat{\mathbf{x}},\hat{\mathbf{z}},\hat{\mathbf{f}},\hat{\mathbf{R}},\hat{\mathbf{Q}},\hat{\mathbf{e}},\hat{\boldsymbol{\lambda}},\hat{\delta},\hat{\mathbf{A}},\hat{\mathbf{B}})$ denote an optimal solution to the MILP model [EVFS-II] and $PROFIT^*$ denote the optimal objective value of the MINLP model [EVFS]. Then it is

$$PROFIT(\hat{\mathbf{x}},\hat{\mathbf{z}},\hat{\mathbf{f}},\hat{\mathbf{R}},\hat{\mathbf{Q}},\hat{\mathbf{e}}) \le PROFIT^* \le PROFIT^{\mathrm{II}}(\hat{\mathbf{x}},\hat{\mathbf{z}},\hat{\mathbf{f}},\hat{\mathbf{R}},\hat{\mathbf{Q}},\hat{\mathbf{e}},\hat{\boldsymbol{\lambda}},\hat{\delta},\hat{\mathbf{A}},\hat{\mathbf{B}}) \tag{3.39}$$

Proof. Firstly, since the nonlinear terms are only in the objective function of the model [EVFS], $(\hat{\mathbf{x}}, \hat{\mathbf{z}}, \hat{\mathbf{f}}, \hat{\mathbf{R}}, \hat{\mathbf{Q}}, \hat{\mathbf{e}})$ will always be a feasible solution to the model [EVFS]. Therefore, it is

$$PROFIT(\hat{\mathbf{x}}, \hat{\mathbf{z}}, \hat{\mathbf{f}}, \hat{\mathbf{R}}, \hat{\mathbf{Q}}, \hat{\mathbf{e}}) \le PROFIT^{*} \tag{3.40}$$

In addition, after adopting the piecewise linear approximation approach and the outer-approximation method, model [EVFS-II] can be interpreted as a relaxation of model [EVFS] defined as overestimating the objective function. Hence, its optimal objective value provides an upper bound on that of the model [EVFS]. Then it is

$$PROFIT^{*} \le PROFIT^{\mathrm{II}}(\hat{\mathbf{x}}, \hat{\mathbf{z}}, \hat{\mathbf{f}}, \hat{\mathbf{R}}, \hat{\mathbf{Q}}, \hat{\mathbf{e}}, \hat{\boldsymbol{\lambda}}, \hat{\delta}, \hat{\mathbf{A}}, \hat{\mathbf{B}}) \tag{3.41}$$

This completes the proof. □

Let $\hat{g}(G_i) = \sum_{k=1}^{N} \lambda_i^k g(G_i^{(k)})$, $\hat{h}(R_i) = \min_{k \in \Omega} \left\{ a_i^{(k)} R_i + b_i^{(k)} \right\}$, and $\hat{y}(Q_i) = \min_{k \in V} \left\{ \bar{a}_i^{(k)} Q_i + \bar{b}_i^{(k)} \right\}$ denote the corresponding piecewise linear approximation function for $g(G_i)$, $h(R_i)$, and $y(Q_i)$, respectively. The approximation error of the optimal solution can be controlled within a pre-specified tolerance $\varepsilon > 0$, i.e.,

$$PROFIT^{\mathrm{II}}(\hat{\mathbf{x}}, \hat{\mathbf{z}}, \hat{\mathbf{f}}, \hat{\mathbf{R}}, \hat{\mathbf{Q}}, \hat{\mathbf{e}}, \hat{\boldsymbol{\lambda}}, \hat{\delta}, \hat{\mathbf{A}}, \hat{\mathbf{B}}) - PROFIT(\hat{\mathbf{x}}, \hat{\mathbf{z}}, \hat{\mathbf{f}}, \hat{\mathbf{R}}, \hat{\mathbf{Q}}, \hat{\mathbf{e}}) \le \varepsilon \tag{3.42}$$

by properly selecting the breakpoints and tangent points for the piecewise linear segment and tangent line generation, respectively, such that $\hat{g}(G_i) - g(G_i) \le \hat{\varepsilon}$, $\hat{h}(R_i) - h(R_i) \le \hat{\varepsilon}$, and $\hat{y}(Q_i) - y(Q_i) \le \hat{\varepsilon}$, where $\hat{\varepsilon} \le \dfrac{\varepsilon}{3 \times |I|}$.

Eq. (3.42) together with Eq. (3.39) jointly suggest that the ε-optimal solution to the model [EVFS] can be obtained by the proposed approaches, as summarized in the following proposition:

Proposition 2: For any exogenously specified tolerance ε>0, the proposed methods can obtain the ε-optimal solution to the model [EVFS], i.e.,

$$PROFIT(\hat{\mathbf{x}}, \hat{\mathbf{z}}, \hat{\mathbf{f}}, \hat{\mathbf{R}}, \hat{\mathbf{Q}}, \hat{\mathbf{e}}) \le PROFIT^{*} \le PROFIT(\hat{\mathbf{x}}, \hat{\mathbf{z}}, \hat{\mathbf{f}}, \hat{\mathbf{R}}, \hat{\mathbf{Q}}, \hat{\mathbf{e}}) + \varepsilon \tag{3.43}$$

if the linear segments and tangent lines are generated subject to an error bound $\hat{\varepsilon} \le \dfrac{\varepsilon}{3 \times |I|}$.

As aforementioned, the algorithms to determine the breakpoints and tangent points for the linear segment and tangent line generation subject to a pre-specified error bound $\hat{\varepsilon}$, respectively, are presented in Appendix A.2 for the readers' reference.

3.4 Case Study of EVCARD

This section conducts the case study of EVCARD to evaluate the performance of the proposed model and solution method. The algorithm is coded in C++ calling Gurobi 9.0.0 on a personal computer with Intel (R) Core (TM) Duo 3.0 GHz CPU. The EVCARD in China and parameters setup are first introduced in Subsection 3.4.1. After that, the computational performance of the proposed solution method is assessed in Subsection 3.4.2. The necessity of incorporating the battery degradation into the fleet size determination of CSSs will be demonstrated in Subsection 3.4.3 in comparison with the model without considering battery degradation. Finally, sensitivity analysis of several key parameters on the system performance is examined in Subsection 3.4.4.

3.4.1 EVCARD in China and parameter setup

EVCARD, a popular one-way carsharing company in China, takes EV time-sharing rental as its core business. EVCARD operates more than 13,000 stations in about 65 cities with 50,000 new energy vehicles put into use at present, and the monthly order volume reaches 1.84 million. EVs can be rented by minute or day with different charge standards. In this study, the stations in three districts of Suzhou, namely, Kunshan, Xiangcheng, and Wujiang, are considered. The deployments of stations in the three districts are shown in Figure 3.8, with 70 stations in Kunshan, 27 stations in Xiangcheng, and 29 stations in Wujiang. Multiple stations are combined into one if the shortest path distances between them are within five-minute driving mileage, as it is assumed that there would be no rentals between these stations. This is implemented by Google Maps (Google, 2022) using the mode of 'driving' without considering traffic. After merging processing, 57 stations are obtained.

(a) Kunshan (b) Xiangcheng (c) Wujiang

Figure 3.8 Stations deployment in three districts of Suzhou

Let $\{1,2,...,57\}$ be the set of considered stations, from which the origin and destination stations of each rental $i \in I$, i.e., s_i^o and s_i^d, are randomly generated. It is assumed that the operational period is from 6 am to 10 pm considering that most of the users have vehicle rental needs during this period. Particularly, if 6 am is taken as the time benchmark and the time duration is measured in minutes, the departure time of each rental $i \in I$, i.e., t_i^o, is randomly generated from the integer set $\{0,1,...,960\}$ and the arrival time t_i^d is chosen as a uniformly random integer from the set $\{t_i^o + \Delta T_{min}, t_i^o + \Delta T_{min} + 1, ..., t_i^o + \Delta T_{max}\}$, where ΔT_{min} and ΔT_{max} are the minimum and maximum rental duration, respectively. Kindly note that the demand pattern variance over the operational period can be incorporated in the random generation for the departure time of a rental. If the destination station of the rental i is different from its origin station, ΔT_{min} is set to be the shortest travel time from the origin station to the destination station, which is obtained by Google Maps (Google, 2022). Otherwise ΔT_{min} is set to be 15 min to ensure the minimum profit from the perspective of a carsharing operator. All EVs are assumed to be equipped with a 16-kWh lithium-ion battery. The minimum SOC allowed for an EV, i.e., E_{min}, is assumed to be 0. With a fully charged battery, it is assumed that an EV can be driven for 150 min, with an average speed of 35 km per hour. ΔT_{max} is thus set to be 150 min, as it is assumed that the CSS is charged by rental duration and users would avoid leaving the EVs unused as much as possible during the rental period. A depleted battery is assumed to be fully charged in 150 min by a regular charging outlet. The charging and discharging rate of battery expressed in percentage are both assumed to be a constant, i.e., $\frac{1}{150}$/min, thus the charging amount and the electricity consumption are proportional to the charging and the trip

(i.e., rental and relocation) duration respectively. The parameters related to battery wear cost in Eq. (3.3), i.e., a=694, b=0.795, μ=0.95, are adopted from Han et al. (2014). The price of battery is assumed to be 20,000¥.

Without loss of generality, it is further assumed that the service charge is 0.5¥/min according to the website of EVCARD (https://www.evcard.com/). The penalty for rejecting a rental is assumed to be 0.25¥/min, which is the half of the revenue generated from the rental. The relocation cost and the daily fixed cost of an EV are set to be 0.3¥/min and 20¥/vehicle, respectively.

3.4.2 Computational performance of the proposed solution method

In this subsection, the proposed approach, i.e., solving the resultant MILP model [EVFS-II] with the prevailing MILP solver Gurobi after applying a piecewise linear approximation approach and an outer-approximation method, is compared with the MINLP approach which solves the model [EVFS] directly by using Knitro, an especially versatile nonlinear solver offering a range of state-of-the-art algorithms and options for working with smooth objective and constraint functions in continuous and integer variables. Problems of different sizes indicated by the number of rentals (#TotalRent) are used to test the performance of the proposed solution method and MINLP approach. For a particular-size problem, ten instances are randomly generated and the average results are reported. Moreover, different values of $\hat{\varepsilon}$ are adopted for the proposed approach to analyze its effects on the quality of solutions. The preliminary numerical experiments indicated that both the MINLP approach and the proposed approach can obtain the optimal solution in a few seconds under a relatively small demand (e.g., 10). Nevertheless, when the demand increases beyond a certain value (e.g., 25), the MINLP approach can no longer produce the optimal solution. In more detail, it obtains a feasible solution by the built-in heuristics in a few minutes and after the feasible solution is produced, it will not improve the solution quality even within the time limit of 12 hours. In regard to the proposed approach, for the problems with the number of rentals larger than a certain value (e.g., 50), no improvement in the solution quality could be made after 1 hour of running time because the solution values obtained within 1 hour and 12 hours are almost the same, and the difference between the solution values achieved within 15 minutes and 1 hour is not significant. Hence, the time limit is set to be 15 minutes to compare the solution values obtained by the two approaches. Specifically, two performance measures, i.e., the objective

value and the computation time (in seconds), are compared. Let Obj_Knitro and Obj_Gurobi be the objective value obtained by the MINLP approach and the proposed approach, respectively. For a more intuitive comparison, the ratio of Obj_Gurobi to Obj_Knitro, i.e., Obj_Gurobi/Obj_Knitro, is also reported. This value must be equal to 1 if both approaches can find an optimal solution within 15 min. A value larger than 1 indicates that the solution obtained by the proposed approach is better than that achieved by the MINLP approach, and vice versa.

The results are tabulated in Table 3.1. Overall, it shows that the proposed approach obtains much better solutions within 15 min compared with the MINLP approach except for the smallest-size instances with 10 rentals. This outcome demonstrates the superiority of the proposed approach. For the smallest-size problem, both approaches can obtain the optimal solution within the time limit, with the proposed approach taking much less time at the values of $\hat{\varepsilon}$ larger than 0.001. It is interesting that the computation time for the proposed approach dramatically decreases from hundreds of seconds to a fraction of a second when the value of $\hat{\varepsilon}$ increases to above 0.001. This can be explained by the fact that a smaller tolerance $\hat{\varepsilon}$ indicates more binary variables for the piecewise linear approximation approach in Subsection 3.3.1, which may dominate the computational efficiency for the small-size problems. For the larger-size problems, within the time limit of 15 min, the MINLP approach can no longer obtain the optimal solution. The proposed approach, however, can still find the optimal solution to the instances with 25 rentals at all values of $\hat{\varepsilon}$ except 0.001. For a specific-size problem, it can be observed that the objective value produced by the proposed approach is not sensitive to the tolerance $\hat{\varepsilon}$ when the value of it is not smaller than 0.25. However, this is not true for the values of $\hat{\varepsilon}$ not greater than 0.25 within which the highest objective value, indicating the best solution, can generally be obtained at the value of $\hat{\varepsilon}$=0.01, although there exist exceptions for the smallest-size instances with 10 rentals. Hence, $\hat{\varepsilon}$=0.01 will be employed to carry out the following analysis. Regarding the quality of solutions, the objective value achieved by the proposed approach is at least 1.43 times that of the MINLP approach without considering the problem with 10 rentals. Therefore, the proposed approach shows a visible advantage over the MINLP approach on the whole in solving the tactical problem proposed by this study.

Table 3.1 Comparison of computational performance between the MINLP approach and the proposed approach

#TotalRent	MINLP approach		Proposed approach			
	Obj_ Knitro	Comp_ Time	$\hat{\varepsilon}$	Obj_ Gurobi	Comp_ Time	Obj_Gurobi/ Obj_Knitro
10	309.45	1.22	0.001	309.98	128.89	1.00
			0.01	309.89	0.17	1.00
			0.1	309.29	0.03	1.00
			0.25	306.43	0.03	0.99
			0.5	306.43	0.03	0.99
25	545.48	900.08	0.001	795.09	900.02	1.46
			0.01	795.70	60.88	1.46
			0.1	792.91	6.74	1.45
			0.25	782.06	6.45	1.43
			0.5	782.06	6.42	1.43
50	984.43	900.15	0.001	1602.68	900.03	1.63
			0.01	1608.85	900.03	1.63
			0.1	1608.36	900.02	1.63
			0.25	1578.93	900.03	1.60
			0.5	1578.93	900.02	1.60
75	1524.83	900.21	0.001	2377.52	900.04	1.56
			0.01	2386.84	900.04	1.57
			0.1	2376.69	900.03	1.56
			0.25	2330.86	900.04	1.53
			0.5	2330.86	900.04	1.53
100	2060.40	900.11	0.001	3199.48	900.58	1.55
			0.01	3222.99	900.04	1.56
			0.1	3188.14	900.04	1.55
			0.25	3118.40	900.05	1.51
			0.5	3118.40	900.04	1.51
125	2547.99	900.14	0.001	3985.09	900.08	1.56
			0.01	3993.38	900.06	1.57
			0.1	3975.84	900.13	1.56
			0.25	3865.23	900.08	1.52
			0.5	3865.23	900.10	1.52

3.4.3 Impact of battery degradation consideration

In this subsection, how the incorporation of battery wear cost influences the tactical decision-making of fleet size, i.e., the main concern of this study, is explored, and the benefit of battery degradation consideration to the profitability of CSSs is justified. Then how the parameters in the battery wear function, i.e., the battery price and battery cycle efficiency,

affect the influence of battery degradation consideration on the profitability and fleet size of CSSs is investigated. A model that is similar to the model [EVFS] is formulated, but without taking the battery wear cost into account, referred to as [EVFS$^{w/o}$] thereafter. For ease of comparison, the model considering the battery degradation, i.e., [EVFS], is renamed as [EVFS^{w}] in this subsection. In addition, the parameter setting in this subsection is the same as that specified in Subsection 3.4.1, and ten instances are randomly generated for a particular number of rentals (#TotalRent) and the average results are reported. The computation time limit is set to be 15 min.

3.4.3.1 Impact on the fleet size determination

To investigate the impact of battery degradation consideration on the fleet size decision-making of CSSs, the model [EVFS^{w}] and the model [EVFS$^{w/o}$] were solved respectively by randomly generating the same instances and the fleet sizes obtained from the two models are compared. For the sake of presentation, let 'FleetSize^{w}' and 'FleetSize$^{w/o}$' be the fleet size obtained by solving the model [EVFS^{w}] and the model [EVFS$^{w/o}$], respectively. The ratio of FleetSize^{w} to FleetSize$^{w/o}$, i.e., FleetSize_Ratio, is adopted to evaluate the impact of the battery degradation consideration on the fleet size determination of CSSs.

Table 3.2 presents the impact of battery degradation consideration on the tactical decision-making of fleet size. It can be seen from Table 3.2 that all the ratios, i.e., FleetSize^{w}/FleetSize$^{w/o}$, are larger than 1.7, which implies that the consideration of battery degradation will result in the substantial expansion of fleet size. This suggests, when the battery degradation is further taken into account, the carsharing operator should adopt a larger fleet size to serve rentals, in order to avoid the extensive charging and discharging processes and thus circumvent the high battery wear cost, and realize the ultimate profit maximization. These findings demonstrate the necessity of incorporating the battery degradation into the fleet size determination of CSSs and hence validate the significance of this study.

Table 3.2 Impact of battery degradation consideration on the fleet size determination

#TotalRent	FleetSize^{w}	FleetSize$^{w/o}$	FleetSize_Ratio
10	7.4	4.6	1.75
25	17.0	9.7	1.83
50	31.1	17.0	1.94
75	44.9	23.1	1.85
100	57.1	30.8	1.86
125	69.2	37.3	1.75

3.4.3.2 Impact on the profitability improvement

In order to measure the profitability improvement simply brought by the battery degradation consideration during the operational period, the profits obtained from the model [EVFS^{w}] and the model [EVFS$^{w/o}$] are compared given the same fleet size. That's to say, under a certain demand, the number of EVs is set to be the same constant in the two models and the fleet investment is considered as a sunk cost. After the two models are solved by randomly generating the same instances, the battery wear cost for the model [EVFS$^{w/o}$] is calculated and then subtracted from the objective function value. Finally, the daily profits of the carsharing operator based on the two models can be obtained, both with the battery wear cost included. Again, let 'Profit^{w}' and 'Profit$^{w/o}$' denote the daily profit of the carsharing operator obtained from the model [EVFS^{w}] and the model [EVFS$^{w/o}$], respectively. The gap of profits indicated by 'Profit_Gap' is defined as '(Profit^{w} – Profit$^{w/o}$)/Profit^{w}'. It can be used to assess the benefit of the battery degradation consideration to the profitability of CSSs. Specifically, the fleet size is set to be 7, 16, 28, 40, 55, 70 under the demand of 10, 25, 50, 75, 100, 125, respectively.

The profitability improvement brought by the battery degradation consideration is shown in Table 3.3. It can be concluded from Table 3.3 that the consideration of battery degradation does enhance the profitability of CSSs because all the gaps of profits are larger than 7%. The largest gap in profit can be as high as 13.97% when the number of rentals is 50. It appears that the gap in profits generally shows an upward trend along with the rising of demand, although there exists a fluctuation in the scenario with 50 rentals. This may indicate that the profitability of CSSs can be improved more significantly by considering battery degradation when the demand is higher. This result further verifies the value of this study. However, it should be cautioned that the influence of battery degradation consideration on the profitability and fleet size of CSSs may largely depend on the parameters in the battery wear cost function. The values of these parameters should be carefully chosen based on empirical studies in the future. In Subsection 3.4.3.3, how the parameters in the battery wear cost function affect the impact of battery degradation consideration will continue to be tested.

Table 3.3 Impact of battery degradation consideration on the profitability of CSSs

#TotalRent	Profit^{w} (¥/day)	Profit$^{w/o}$ (¥/day)	Profit_Gap (%)
10	438.40	405.61	7.48
25	1095.14	1002.80	8.43

50	2141.90	1842.65	13.97
75	3198.89	2870.35	10.27
100	4339.47	3827.43	11.80
125	5484.27	4813.94	12.22

To further affirm the circumvention of the extensive charging and discharging processes brought by the consideration of battery degradation given a certain fleet size, three performance metrics, i.e., the total rental duration (TotalRentalTime), the total charging duration (TotalChargeTime), and the total relocation duration (TotalRelocationTime), are compared between the two models under the demand of 125. The results are illustrated in Figure 3.9. It shows that the total rental durations of the fleet obtained from the two models are almost the same. The total charging duration under the model [EVFS^{w}], however, shows a sharp decrease compared to the model [EVFS$^{w/o}$]. This is because when the battery wear cost is taken into account in the objective function, unnecessary charging processes will be circumvented for the sake of profit maximization. Regarding the total relocation duration, the result of the model [EVFS^{w}] is slightly higher than the model [EVFS$^{w/o}$]. These findings indicate that a comparable number of rentals are served in the two models and the battery degradation consideration results in the reduced charging processes, which contributes to the profitability improvement of CSSs.

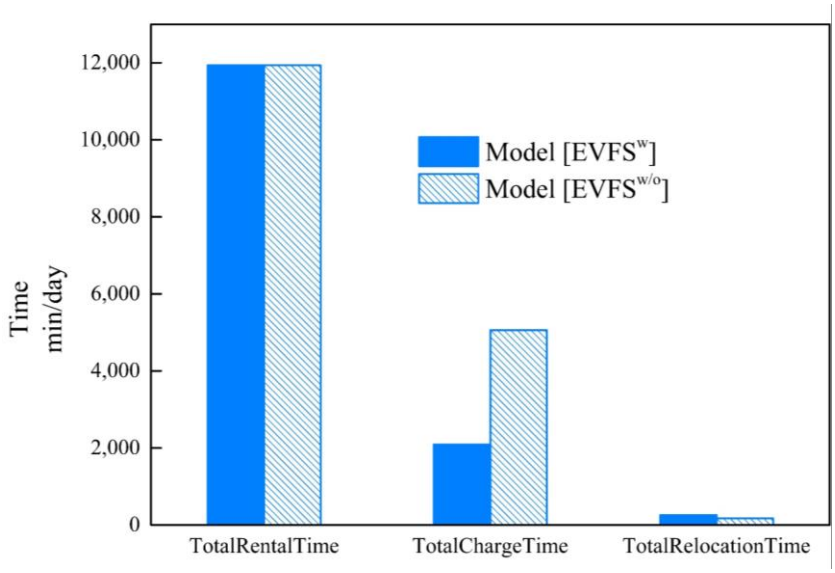

Figure 3.9 Comparison between the model [EVFS^{w}] and the model [EVFS$^{w/o}$] under the demand of 125

3.4.3.3 Impact of parameters in the battery wear cost function

In this subsection, we will investigate how the parameters in the battery wear cost function, i.e., the battery price and battery cycle efficiency, affect the impact of battery degradation consideration on the fleet size determination and profitability of CSSs. Due to the inter-dependency relationship between the battery price and the fixed cost of EVs, different battery prices should be associated with different EV fixed costs. More specifically, under the demand of 125, three values of battery price and daily fixed cost of EV, i.e., 12,000 & 12, 16,000 & 16, 20,000 & 20, and three values of battery cycle efficiency, i.e., 0.91, 0.93, 0.95, are adopted to test their effects on the influence of battery degradation consideration on the fleet size determination and profitability of CSSs.

Table 3.4 shows how the two parameters influence the impact of battery degradation consideration on the fleet size determination. It can be seen that with the increase of battery price & daily fixed cost of EV, the ratio of fleet size grows gradually, indicating that the battery degradation consideration has a greater effect on the fleet size determination under a higher value of battery price & daily fixed cost of EV. In addition, when the battery cycle efficiency decreases from 0.95 to 0.91, the ratio rises steadily. These results suggest that the impact of battery degradation on the fleet size determination of CSSs is largely influenced by battery price & daily fixed cost of EV and battery cycle efficiency.

Compared with the fleet size, the parameters in the battery wear cost function influence less the impact of battery degradation consideration on the profitability of CSSs. The results regarding how the impact of battery degradation consideration on the profitability of CSSs is affected by the two parameters in the battery wear cost function are presented in Table 3.5, where $Profit^{w}$ and $Profit^{w/o}$ are obtained by solving the model [$EVFS^{w}$] and the model [$EVFS^{w/o}$] under the fleet size of 70, respectively. It can be seen that the gap of profits increases along with the growth of battery price & daily fixed cost of EV, while it almost remains stable when the battery cycle efficiency varies. This implies that the profitability improvement brought by the battery degradation consideration is more significant when the battery price & daily fixed cost of EV is higher, and it appears not sensitive to the battery cycle efficiency.

Table 3.4 Impact on the influence of battery degradation consideration on the fleet size determination

Price&EVCost (¥&¥/vehicle/day)	Efficiency	FleetSize^{w}	FleetSize$^{w/o}$	FleetSize_Ratio
12,000&12	0.95	73.6	42.7	1.72
16,000&16	0.95	70.7	38.9	1.82
20,000&20	0.95	69.2	37.3	1.86
20,000&20	0.93	70.9	37.3	1.90
20,000&20	0.91	74.0	37.3	1.98

Table 3.5 Impact on the influence of battery degradation consideration on the profitability

Price&EVCost (¥&¥/vehicle/day)	Efficiency	Profit^{w} (¥/day)	Profit$^{w/o}$ (¥/day)	Profit_Gap
12,000&12	0.95	5659.60	5254.26	0.07
16,000&16	0.95	5570.97	5034.10	0.10
20,000&20	0.95	5482.78	4813.94	0.12
20,000&20	0.93	5461.82	4766.08	0.13
20,000&20	0.91	5442.88	4715.03	0.13

3.4.4 Sensitivity analysis

In this subsection, how the key parameters, i.e., the daily fixed cost of EV & battery price, battery cycle efficiency, service charge, and relocation cost, affect the performance of one-way electric CSSs will be investigated. Several performance indicators, which include the daily profit of carsharing operator, the number of satisfied rentals (#SatisRent), the satisfied ratio (#SatisRent/#TotalRent), the optimal EV fleet size (FleetSize), the usage rate of EV (#SatisRent/FleetSize), the daily battery wear cost per vehicle (WearCost), the daily rental duration per vehicle (RentalTime), the daily relocation duration per vehicle (RelocationTime) as well as the daily charging duration per vehicle (ChargeTime), are reported for ease of comparison and evaluation. Unless stated otherwise, the parameter setting is the same with Subsection 3.4.1 except that 10 instances with 125 rentals are randomly generated.

Effect of the daily fixed cost of EV & battery price

Since the high capital investment in EV fleet poses a major problem for many carsharing operators and the wear cost of the battery is closely related to the price of it, the effect of the daily fixed cost of EV & battery price on the performance of one-way electric CSSs is first explored. The results are tabulated in Table 3.6. It can be seen that the increase of daily fixed

cost of EV & battery price leads to the significantly decreased profit of CSSs, indicating the dominating impact of the daily fixed cost of EV & battery price on the profitability of CSSs. It is worth noting that the satisfied ratio is first stable at 1 and then decreases to 0.998 when the daily fixed cost of EV & battery price increases from 10&10,000 to 28&28,000, with the 26&26,000 being the turning point. This suggests that under the current parameter setting, all rentals would be served for the sake of profit maximization, even if the daily fixed cost of EV & battery price rises to 26&26,000. With the growth of the daily fixed cost of EV and battery price, the fleet size reduces with fluctuation while the rental, relocation, and charging duration generally increase significantly, eventually resulting in the overall upward trend of the usage rate and the significant increase of battery wear cost. It should be cautioned that the rising battery wear cost is the result of the dual effects of the growing daily fixed cost of EV & battery price and the time-related indicators. This demonstrates that the climbing daily fixed cost of EV & battery price may prompt the carsharing operators to acquire a smaller fleet size and serve rentals by more frequent relocation and charging operations.

Table 3.6 Effect of daily fixed cost of EV and battery price on the performance of one-way electric CSSs

EVCost&Price (¥/vehicle/day&¥)	Profit (¥/day)	#SatisRent	#SatisRent /#TotalRent	FleetSize	#SatisRent /FleetSize	WearCost (¥/vehicle/day)	RentalTime (min/vehicle/day)	RelocationTime (min/vehicle/day)	ChargeTime (min/vehicle/day)
10&10,000	5007.70	125.0	1.000	75.7	1.65	2.02	157.78	2.21	20.64
12&12,000	4807.04	125.0	1.000	73.6	1.70	2.85	162.32	3.07	24.48
14&14,000	4612.37	125.0	1.000	72.8	1.72	3.59	164.06	3.44	26.38
16&16,000	4407.60	125.0	1.000	70.7	1.77	4.81	169.05	4.25	31.09
18&18,000	4217.98	125.0	1.000	71.2	1.76	5.24	167.70	4.46	30.18
20&20,000	4003.10	125.0	1.000	69.2	1.81	6.88	172.68	5.13	35.69
22&22,000	3819.76	125.0	1.000	69.6	1.80	7.33	171.68	5.22	34.50
24&24,000	3639.43	125.0	1.000	69.9	1.79	7.85	171.15	5.13	33.99
26&26,000	3422.73	125.0	1.000	68.8	1.82	9.24	173.75	6.06	37.00
28&28,000	3212.94	124.8	0.998	67.0	1.87	11.26	178.40	6.29	41.62

Effect of battery cycle efficiency

As an important indicator of battery cycle life, cycle efficiency influences the battery wear cost greatly, as shown by Eq. (3.3). The variations of the performance indicators with respect to the growth of battery cycle efficiency are thus investigated, and the results are presented in Table 3.7. It illustrates that when the battery cycle efficiency rises, the profit shows a growing trend in general with the number of satisfied rentals remaining at 125. This indicates that under the current parameter setting, serving all rentals will be most conducive to profit maximization, even if the battery cycle efficiency is reduced to 0.9. The fleet size, however, decreases with minor fluctuations, leading to an overall upward trend of EV usage rate. All the time-related indicators averagely increase in a modest manner, and the battery wear cost grows gradually, in a fluctuating way, if any. This appears contrary to the fact that the increase of battery cycle efficiency should result in the declining battery wear cost, as indicated by Eq. (3.3). Kindly note that in addition to the battery cycle efficiency, charging and discharging processes corresponding to the time-related indicators are another two factors affecting the battery wear cost. A larger cycle efficiency means a lower battery wear cost under the same operating condition, which may allow longer charging and discharging (i.e., rental and relocation) duration per vehicle by smaller fleet size in pursuit of profit maximization. As a result, the battery wear cost shows an increasing trend under the combined effects of rising battery cycle efficiency and time-related indicators. It can be found that installing batteries with higher cycle efficiency in EVs has a similar positive effect on the profitability of CSSs to acquiring EVs with lower daily fixed cost & battery price to a certain degree. However, the variation magnitude of the profit is less than that resulted from the variation of the daily fixed cost of EV & battery price. The daily fixed cost of EV & battery price and the battery cycle efficiency should be considered comprehensively by the carsharing operators to increase the profitability.

Table 3.7 Effect of battery cycle efficiency on the performance of one-way electric CSSs

Efficiency	Profit (¥/day)	#SatisRent	#SatisRent /#TotalRent	FleetSize	#SatisRent /FleetSize	WearCost (¥/vehicle/day)	RentalTime (min/vehicle/day)	RelocationTime (min/vehicle/day)	ChargeTime (min/vehicle/day)
0.9	3990.44	125.0	1.000	74.1	1.69	5.41	161.20	4.31	25.24
0.91	3997.67	125.0	1.000	74.0	1.69	5.33	161.42	4.42	25.40
0.92	4007.41	125.0	1.000	73.5	1.70	5.54	162.87	4.48	26.66
0.93	4006.71	125.0	1.000	70.9	1.77	6.30	168.56	4.69	31.34
0.94	4008.01	125.0	1.000	70.5	1.77	6.36	169.72	5.06	32.47
0.95	4003.10	125.0	1.000	69.2	1.81	6.88	172.68	5.13	35.69
0.96	4017.75	125.0	1.000	68.3	1.84	7.02	175.19	5.34	37.17
0.97	4022.11	125.0	1.000	68.6	1.83	6.89	174.71	5.33	37.25
0.98	4039.08	125.0	1.000	67.4	1.86	7.05	177.14	5.22	38.88
0.99	4036.05	125.0	1.000	66.4	1.89	7.43	180.05	5.70	41.89

Effects of service charge and relocation cost

In addition to the daily fixed cost of EV and battery price and the battery cycle efficiency, how the variations of the service charge and relocation cost influence the performance of electric CSSs is also tested. The results are presented in Table 3.8 and Table 3.9. In Table 3.8, It can be seen that the carsharing companies would be in the red if the service charge is set to be below 0.18¥/min. With the increase of service charge, the satisfied ratio rises slowly until to 1 and profit grows dramatically, while the variations of time-related indicators, fleet size, EV usage rate, and battery wear cost, are somehow arbitrary. This indicates that the determination of fleet size, the main concern in this study, may be less affected by the charge standard under the current parameter setting. Compared with the service charge, the impacts of the relocation cost on the performance of electric CSSs are more significant. The variations of the above performance indicators with respect to the relocation cost are summarized in Table 3.9. It shows that all the performance indicators remain almost stable at a certain value when the relocation cost is not smaller than 1.5¥/min. Particularly, the relocation time is zero under this scenario, implying that if the relocation cost is high enough, no relocation operation would be implemented in pursuit of profit maximization. When the relocation cost increases from 0.1¥/min to 1.3¥/min, the profit appears to vary arbitrarily, with fewer rentals satisfied in general. This seems unreasonable as a higher relocation cost would result in a lower profit. Kindly note that the proposed method can only obtain the ε-optimal solution to the problem in question, the obtained profits may not be the global optimal values. Along with the increase of relocation cost within the value of 0.15¥/min, the trade-off effect between fleet size and vehicle relocation is distinct because their variation trends are opposite, i.e., when the relocation cost grows, the fleet size increases significantly while the relocation duration shows an obvious decrease. The carsharing operators are thus suggested to serve rentals by acquiring more EVs, i.e., less vehicle relocation, for the sake of profit maximization under a high relocation cost. Accordingly, a larger fleet size and less vehicle relocation lead to the lower usage rate of EVs, the reduced rental and charging duration, as well as the falling battery wear cost.

Table 3.8 Effect of service charge on the performance of one-way electric CSSs

Charge (¥/min)	Profit (¥/day)	#SatisRent	#SatisRent /#TotalRent	FleetSize	#SatisRent /FleetSize	WearCost (¥/vehicle/day)	RentalTime (min/vehicle/day)	RelocationTime (min/vehicle/day)	ChargeTime (min/vehicle/day)
0.1	-758.06	124.5	0.996	71.7	1.74	5.81	166.45	4.62	30.28
0.18	208.23	124.7	0.998	71.7	1.74	5.78	166.55	4.25	30.08
0.26	1145.37	124.9	0.999	70.4	1.78	6.40	169.92	4.95	33.32
0.34	2092.76	124.9	0.999	68.8	1.82	7.05	173.82	5.22	36.74
0.42	3056.31	125.0	1.000	69.5	1.80	6.67	172.12	5.19	34.57
0.5	4003.10	125.0	1.000	69.2	1.81	6.88	172.68	5.13	35.69
0.58	4970.81	125.0	1.000	69.7	1.80	6.58	171.44	4.85	34.04
0.66	5922.25	125.0	1.000	69.1	1.81	6.76	172.99	5.23	35.17
0.74	6874.74	125.0	1.000	68.9	1.82	6.91	173.44	5.08	35.74
0.82	7836.39	125.0	1.000	70.2	1.78	6.39	170.33	4.79	33.09

Table 3.9 Effect of relocation cost on the performance of one-way electric CSSs

RelocationCost (¥/min)	Profit (¥/day)	#SatisRent	#SatisRent /#TotalRent	FleetSize	#SatisRent /FleetSize	WearCost (¥/vehicle/day)	RentalTime (min/vehicle/day)	RelocationTime (min/vehicle/day)	ChargeTime (min/vehicle/day)
0.1	4025.51	125.0	1.000	67.8	1.86	8.12	177.28	7.72	42.16
0.3	4003.10	125.0	1.000	69.2	1.81	6.88	172.68	5.13	35.69
0.5	4042.01	124.9	0.999	73.2	1.71	4.85	163.18	2.92	24.86
0.7	4053.35	125.0	1.000	76.6	1.63	3.74	155.91	1.80	19.04
0.9	4042.04	124.7	0.998	79.3	1.57	3.03	150.53	1.35	15.45
1.1	4029.73	124.6	0.997	80.9	1.54	2.92	147.54	0.89	14.80
1.3	4018.45	124.5	0.996	84.0	1.48	2.73	142.13	0.30	13.88
1.5	4018.92	124.5	0.996	85.8	1.45	2.64	139.18	0.00	13.41
1.7	4018.30	124.5	0.996	86.0	1.45	2.59	138.84	0.00	13.17
1.9	4018.36	124.5	0.996	85.8	1.45	2.65	139.16	0.00	13.42

3.5 Concluding Remarks

This chapter deals with the EVFS problem for the one-way electric CSSs by taking battery degradation into account. Instead of charging the EVs as extensively as possible, the 'on-demand' charging strategy was proposed, which allows EVs to be charged as needed to reduce the battery wear cost incurred from battery degradation. An MINLP model with both concave and convex terms in the objective function was then developed to maximize the profit of carsharing operators by simultaneously determining the fleet size, vehicle relocation operations, and charging strategies of EVs. The consideration of nonlinear battery wear cost made the proposed model not easily solvable to optimality by commercial solvers. The considered model was thus linearized by applying a piecewise linear approximation approach and an outer-approximation method on the convex and concave terms, respectively. The resultant MILP model can finally be solved by state-of-the-art solvers like Gurobi. At last, numerical experiments based on the carsharing company EVCARD in China were conducted. In more detail, the computational performance of the proposed model and solution method was first demonstrated. Then a comparison between the proposed model and the one without taking the battery degradation into account was made. The comparison results indicate that the consideration of battery degradation will increase the profitability of the CSSs and expand the fleet size significantly. This finding demonstrates the necessity of incorporating the battery degradation into the fleet size determination of CSSs and hence validates the significance of this study. Finally, the effects of the daily fixed cost of EV & battery price, battery cycle efficiency, service charge, and relocation cost on the performance of electric CSSs were analyzed. The results reveal that the increase of daily fixed cost of EV & battery price may prompt the carsharing operators to acquire a smaller fleet size and serve rentals by more frequent relocation and charging operations; Installing batteries with higher cycle efficiency in EVs would lead to a decrease of fleet size and the growth of time-related indicators as well as daily battery wear cost per vehicle; Under a higher relocation cost, the carsharing operators should serve rentals by acquiring more EVs, i.e., less vehicle relocation, for the sake of profit maximization, while the service charge under the current parameter setting may have a less effect on the determination of fleet size.

CHAPTER 4 REAL-TIME VEHICLE RELOCATION AND CHARGING OPTIMIZATION FOR ONE-WAY ELECTRIC CARSHARING SYSTEMS

This chapter copes with a real-time vehicle relocation and charging strategy (RT-VR&CS) problem for the one-way electric CSSs considering demand dynamics and practical nonlinear charging profile. The RT-VR&CS problem aims to develop a fast yet robust algorithm to determine the real-time relocation and charging strategies for EVs (EVs) in pursuit of profit maximization of carsharing operators. A dynamic algorithmic framework based on a rolling time horizon is first established. Specifically, the entire planning horizon is divided into a series of sub-horizons, and a static vehicle relocation and charging strategy (S-VR&CS) problem is subsequently addressed over each sub-horizon in regard to the latest rental information known up to the beginning of the sub-horizon. For each static problem, a set-packing-type formulation and a column-generation-based solution method are employed. In particular, a multi-label method is developed to generate activity trajectories (i.e., columns) incorporating vehicle relocation and charging strategy for the first static problem, whereas the activity trajectories for the subsequent static problems are efficiently generated in an online environment by leveraging the existing activity trajectories generated for the previous static problem and employing a reactive column generation process. Numerical experiments on randomly generated instances and a case study based on a one-way carsharing company in China, i.e., EVCARD, are conducted to demonstrate the efficiency of the proposed solution method. The impacts of algorithm-related parameters, the demand dynamism, the service charge, and the relocation cost on the performance of one-way electric carsharing systems are also analyzed.

The remainder of this chapter is organized as follows. Assumptions, notations, and the description of the RT-VR&CS problem are elaborated in Section 4.1. A dynamic algorithmic framework for the RT-VR&CS problem is established in Section 4.2 based on a rolling time horizon. A column-generation-based approach is developed in Section 4.3 for solving a series of S-VR&CS problems defined over sub-horizons in the dynamic algorithmic framework. Numerical experiments on randomly generated instances and a case study of a carsharing company in China are carried out to evaluate the efficiency of the proposed solution method and explore managerial insights into the operations of electric CSSs in Section 4.4. Conclusions are presented in Section 4.5. Notations and propositions are shown in Appendix B.

4.1 Assumptions, Notations, and Problem Description

Consider a carsharing operator who operates the daily ad-hoc one-way CSSs using a fleet of homogeneous EVs among a number of designated stations located in an urban area over the operational period $[0,T]$. The set of EVs and stations are denoted by $\mathcal{V}$ and $\mathcal{S}$, respectively. Let $\mathcal{I}$ represent the set of rentals, i.e., orders requested from users. In the set $\mathcal{I}$, some rentals may have been known at the beginning of the operational period, while some rentals may be reserved and/or canceled dynamically over $[0,T]$. Since the ad-hoc CSSs that allow instant rental reservation and cancellation are considered, the information of these rentals can only be known after the users make reservations or cancellations through the reservation system, probably just a few minutes before their departure time. Vehicle relocation can be initiated from a station to another if there will be a user setting out from that station without operationally available EVs by his/her departure time. The parking spots of each station are equipped with charging facilities, and EVs can be charged when staying idle at stations. The SOC of EVs with respect to the charging duration follows a particular charging profile, which will be illustrated in detail in Subsection 4.1.2. During the daily operation of an EV, vehicle charging and vehicle relocation will be implemented between two adjacent rentals such that these trips are feasibly connected in terms of the travel time and driving range of EVs. To be applicable in an online context, the vehicle relocation and charging strategy should be constantly updated during the planning horizon, i.e., the operational period $[0,T]$, according to the latest known rentals. Given a limited fleet size, the objective is to relocate and charge EVs in a real-time fashion to serve both the already known rentals at the beginning of the planning horizon and the dynamically arriving rentals during the horizon so as to maximize the total profit of carsharing operators.

To fully present the RT-VR&CS problem, the following subsections will elaborate on the demand dynamics, EV charging, and vehicle activity trajectory. The notations used throughout this chapter can be found in Appendix B.1.

4.1.1 Demand dynamics

Each rental $i \in \mathcal{I}$ is described by a septuple $U_i = \{s_i^o, s_i^d, t_i^o, t_i^d, t_i^r, t_i^c, e_i\}$, where $s_i^o \in \mathcal{S}$ represents the pick-up station, $s_i^d \in \mathcal{S}$ stands for the drop-off station, t_i^o denotes the departure time from the pick-up station, t_i^d indicates the arrival time at the drop-off station, t_i^r and t_i^c ($t_i^c > t_i^r$) are the reservation and cancellation time epochs (if any) for the CSS via the reservation

system, respectively, and e_i is the electricity consumption. Let G_i denote the net profit collected from the rental $i \in \mathcal{I}$. To maximize the profit, the operators allow the rejection of rentals given the limited fleet size. A penalty denoted by E_i will be incurred if a rental $i \in \mathcal{I}$ is denied service.

To align with reality, it is assumed that the rentals grouped in set $\mathcal{I}_0 \subset \mathcal{I}$ have been reserved at the beginning of the planning horizon and their reservation information is known in advance. The rest portion of rentals, i.e., the rentals in the set $\mathcal{I} \setminus \mathcal{I}_0$, will arrive dynamically over time and space during the planning horizon $[0, T]$. The user may choose to cancel a rental reserved before or during the planning horizon some time later. The reservation and cancellation information of rentals can only be known by the time the users implement the corresponding operations via the reservation system. Note that the allowance of real-time rental reservation and cancellation can fully capture the instant changes of rentals, such as the changes of the service start time, the service end time, the pick-up station, and the drop-off station. That is to say, if a user makes a change to the reserved rental during the planning horizon, it can be considered that the original rental is canceled and the finalized one is newly reserved.

4.1.2 EV charging

The battery of an EV is generally charged with a constant current-constant voltage (CC-CV) or a constant power-constant voltage (CP-CV) scheme. Both schemes result in implicit and concave charging profiles expressed by differential equations that have no closed-form or analytical solutions (Marra et al., 2012; Xu and Meng, 2019). In this study, it is assumed without loss of generality that EVs are charged by the CC-CV scheme, under which a battery would first undergo the CC phase and then the CV phase. In the CC phase, the charging current holds constant so that the SOC would increase linearly with charging duration until the battery's terminal voltage reaches a threshold. After the CC phase, the charging process switches to the CV phase, in which the terminal voltage holds constant and the charging current decreases exponentially, thus resulting in the concavely increasing of SOC. Figure 4.1 illustrates the temporal variation of SOC when EVs are charged by the CC-CV scheme from the cut-off value SOC_{cutoff} enforced by the battery manufacturer to the maximum SOC achieved at the end of the CV phase denoted by $SOC_{\max}$. In real practice, the electric carsharing operator can achieve a more robust service by imposing a larger minimum SOC requirement,

i.e., the SOC of each EV shall not be less than a threshold $SOC_{\min} \geq SOC_{cutoff}$. It can be seen that the charging amount of an EV for a given period of time will not only depend on the charging duration but also the initial SOC before charging.

For ease of presentation, it is assumed that the final SOC of an EV, i.e., SOC_t, after charging for a period of time t from the initial SOC, i.e., SOC_0, is represented by an expression $\text{ExpSOC}(\bullet)$, namely:

$$SOC_t = \text{ExpSOC}(t \mid SOC_0) \tag{4.1}$$

In addition, the time t required to charge from SOC_0 to $SOC_t \geq SOC_0$ is calculated based on an expression $\text{ExpTime}(\bullet)$ as follows:

$$t = \text{ExpTime}(SOC_t \mid SOC_0) \tag{4.2}$$

Note that $\text{ExpSOC}(\bullet)$ and $\text{ExpTime}(\bullet)$ are introduced only for presentation purpose, as the closed-form expression of SOC_t and t cannot be written. In practice, the values of SOC_t and t can be obtained based on the numerical solution to the differential equation of the nonlinear charging profile. Detailed information on the battery model and charging profiles of EVs can be found in Marra et al. (2012), Pelletier et al. (2017), and Xu and Meng (2019). As for discharging, it is assumed for simplicity that EVs travel at speed without much variation such that the SOC of EVs decreases linearly with travel distance or time (Pelletier et al., 2017).

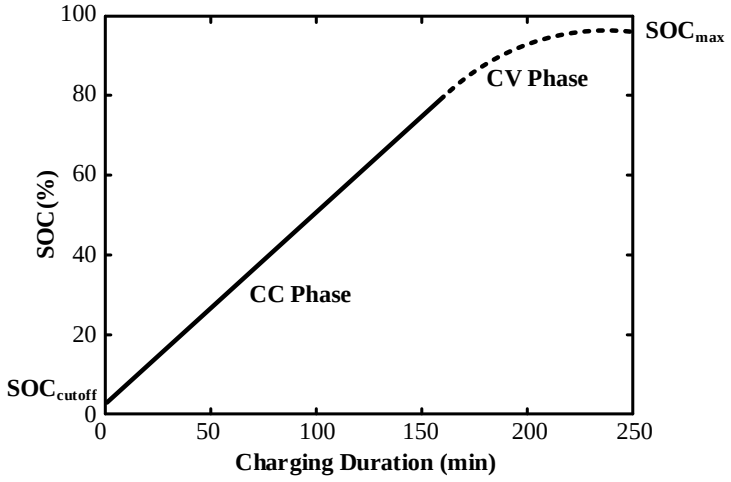

Figure 4.1 Illustration of the nonlinear charging profile by CC-CV scheme

4.1.3 Vehicle activity trajectory

At the beginning of the planning horizon $[0,T]$, EVs are distributed at different stations with certain SOCs. Let $\hat{s}_v^0$, $\hat{t}_v^0$, and $\hat{l}_v^0$ represent the initial location, time and SOC of an EV $v \in \mathcal{V}$, respectively. Departing from the initial location, an EV v may serve several rentals during the period $[0,T]$, and vehicle charging and relocation may be conducted between any two adjacent rentals, namely, i and j, to ensure that they are feasibly connected. Let $\tau(s_i^d, s_j^o)$, $e(s_i^d, s_j^o)$, and $RC(s_i^d, s_j^o)$ denote the relocation time, the electricity consumption, and the incurred relocation cost from the drop-off station of the rental i to the pick-up station of the rental j, respectively. Following the above notations, the relocation time, the electricity consumption, and the corresponding relocation cost from the initial location of an EV v, i.e., $\hat{s}_v^0$, to the pick-up station of a rental $j \in \mathcal{I}$ would be $\tau(\hat{s}_v^0, s_j^o)$, $e(\hat{s}_v^0, s_j^o)$, and $RC(\hat{s}_v^0, s_j^o)$, respectively.

For ease of elaboration, a series of activities (e.g., under service/relocation/charging) underwent in turn by an EV is referred to as an activity trajectory of that vehicle. An activity trajectory is deemed feasible for an EV if the vehicle can carry out all these activities in time without running out of electricity. Consider a simple electric carsharing system with five stations denoted by *A*, *B*, *C*, *D*, and *E*, and two rentals represented by *Rental 1* and *Rental 2* for example; Figure 4.2 shows the activity trajectory of an EV, i.e., '*Rental 1* (from *A* to *B*) → charging (at *B*) → relocation (from *B* to *C*) → *Rental 2* (from *C* to *D*)'. In fact, an activity trajectory of an EV illustrates a specific relocation and charging strategy for it. The profit of an activity trajectory is expressed by the difference between the net profit collected from the served rentals and the incurred total relocation cost.

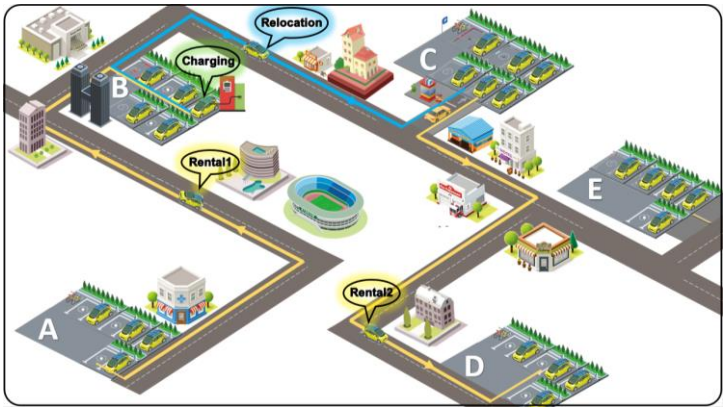

Figure 4.2 Illustration of an activity trajectory for an EV

Xu and Meng (2019) solved a static version of the problem considered in this chapter under the assumption that all demand information is known a priori. Inspired by their study, this study will consider the possible activity trajectories of vehicles instead of modeling every activity of vehicles in order to incorporate the realistic nonlinear and implicit charging profile. As such, the optimization of RT-VR&CS is equivalent to dynamically seeking among all the incumbent feasible activity trajectories the profitable one for each EV in the fleet such that every rental is covered by the selected activity trajectories at most once. The activity trajectories of EVs will be adjusted and updated based on the information of the latest rentals. Therefore, after dynamically identifying the promising activity trajectories for EVs, a good-quality solution to the RT-VR&CS problem can be obtained, which is extracted from the set of identified promising activity trajectories.

4.2 Dynamic Algorithmic Framework

To cope with the demand dynamics, a dynamic algorithmic framework for the RT-VR&CS problem based on a rolling time horizon is first developed. The entire planning horizon $[0,T]$ is discretized into a sequence of K sub-horizons denoted by $[t_1,T]$, $[t_2,T_2]$, …, $[t_{k-1},T]$, $[t_k,T]$, …, $[t_K,T]$. It is assumed that t_1, t_2, …, t_{k-1}, t_k, …, t_K are evenly spaced in time, i.e., $t_k=(k-1)\Delta$ where $\Delta=T/K$. The solution to the RT-VR&CS problem will be obtained by successively solving a series of S-VR&CS problems defined over these sub-horizons. At the time point t_{k-1}, the static problem defined over the sub-horizon $[t_{k-1},T]$, i.e., the $(k-1)^{th}$ S-VR&CS problem, is solved to optimize the vehicle relocation and charging strategy to cover unserved existing rentals, with all the information known up to this point of time. Unlike the offline static problem in Xu and Meng (2019) where time constraint is not a major concern, the online environment of the RT-VR&CS problem requires a timely response to the change of demand information. Therefore, a computation time limit τ is imposed for each static problem. By the time $t_{k-1}+\tau$, a solution to the $(k-1)^{th}$ S-VR&CS problem has been obtained for implementation over the time interval $[t_{k-1}+\tau,t_k+\tau]$. Figure 4.3 illustrates the proposed dynamic algorithmic framework, including the start time point t_k and the end time point T, the computation time limit τ, and the implementation period of the solution to the $(k-1)^{th}$ S-VR&CS problem $[t_{k-1}+\tau,t_k+\tau]$. For ease of illustration, the start time point t_k is referred to as a decision epoch hereafter.

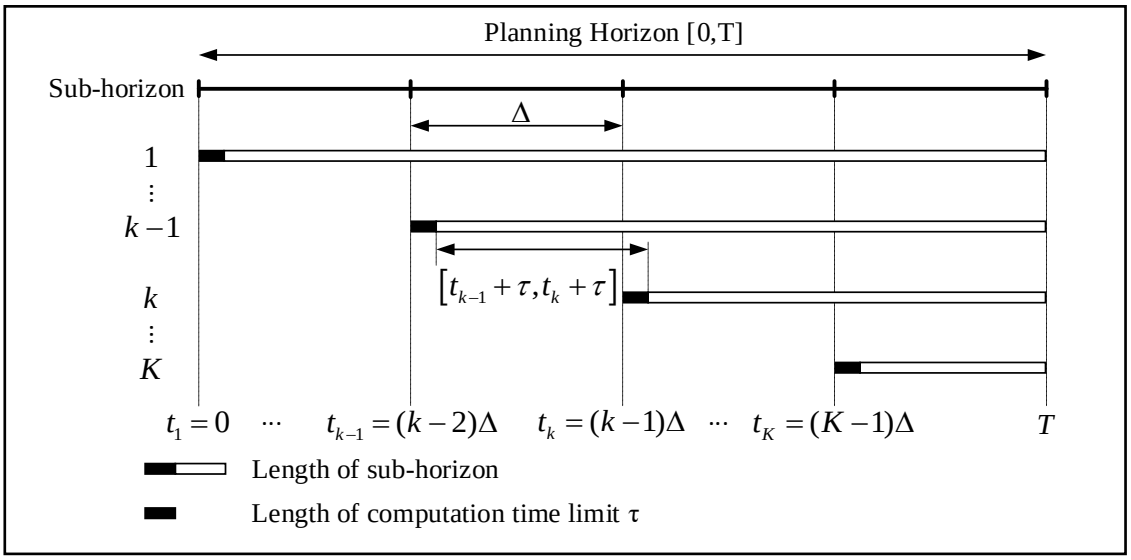

Figure 4.3 Illustration of the dynamic algorithmic framework

Specifically, the rentals considered in the k^{th} S-VR&CS problem should be the ones known up to the decision epoch t_k but with departure time no earlier than $t_k + \tau$. Let $\mathcal{I}_k$ denote the set of these rentals. It includes the rentals that are considered by the previous static problem but have not been satisfied by the time point $t_k + \tau$ and the newly arriving rentals during the period $[t_{k-1}, t_k)$, both of which have not been canceled by the decision epoch t_k. In other words, it is $\mathcal{I}_k = \left[(\mathcal{I}_{k-1} \setminus \bar{\mathcal{I}}_{k-1}) \cup \tilde{\mathcal{I}}_{k-1} \right] \setminus \hat{\mathcal{I}}_{k-1}$, where $\bar{\mathcal{I}}_{k-1}$ is the set of rentals with departure time falling in the period $[t_{k-1} + \tau, t_k + \tau)$; $\tilde{\mathcal{I}}_{k-1}$ and $\hat{\mathcal{I}}_{k-1}$ represent the set of rentals dynamically reserved and canceled during the time interval $[t_{k-1}, t_k)$, respectively. In particular, the rentals considered in the first static problem defined over the sub-horizon $[0, T]$ should be the ones that have been known at the beginning of the planning horizon, i.e., $\mathcal{I}_1 = \mathcal{I}_0$.

In addition to rental information, the vehicle information, which includes the earliest available time $\hat{t}_v$, the available location $\hat{s}_v$, and the corresponding SOC $\hat{l}_v$ of each EV $v \in \mathcal{V}$, is another important input to the k^{th} S-VR&CS problem. According to the solution to the $(k-1)^{th}$ static problem, an EV may be charging at a station, under service for a rental, or in the course of relocation to another station at the end of the corresponding implementation period, i.e., the time epoch $t_k + \tau$. Without loss of generality, it is assumed that the EV can be diverted to serve another rental according to the solution to the incumbent k^{th} S-VR&CS problem if it is under charging or in the course of relocation to another station at time $t_k + \tau$. However, if

the EV is still under service for a rental by time $t_k + \tau$, it is deemed unavailable until the current service is completed. Thus, once a solution to the $(k-1)^{th}$ static problem is obtained and implemented at the time point $t_{k-1} + \tau$, the earliest available time $\hat{t}_v$ and corresponding vehicle location $\hat{s}_v$ as well as SOC $\hat{l}_v$ of each EV $v \in \mathcal{V}$ for the k^{th} static problem can be known. For the first static problem, the available information of each EV $v \in \mathcal{V}$ should be its initial information at the beginning of the planning horizon, i.e., $\hat{t}_v = \hat{t}_v^0$, $\hat{s}_v = \hat{s}_v^0$, and $\hat{l}_v = \hat{l}_v^0$.

Given the information of each EV $v \in \mathcal{V}$ and the set of considered rentals $\mathcal{I}_k$, the k^{th} S-VR&CS problem is to relocate and charge these vehicles in $\mathcal{V}$ to serve the rentals in $\mathcal{I}_k$ so as to maximize the profit of carsharing operators over the sub-horizon $[t_k, T]$. It can be seen that the k^{th} S-VR&CS problem is solved to guide the vehicle relocation and charging strategy update in response to the reservations and/or cancellations received during the time interval $[t_{k-1}, t_k)$. Hence, the real-time response to the reservations and cancellations is realized by a short duration between t_{k-1} and t_k, i.e., a small Δ, in the proposed dynamic algorithmic framework.

4.3 Column-Generation-Based Approach

After establishing the dynamic algorithmic framework, the key to solving the RT-VR&CS problem lies in how to efficiently solve the S-VR&CS problem defined over each sub-horizon. Xu and Meng (2019) investigated a similar S-VR&CS problem and developed a branch-and-price (B&P) method to obtain the optimal solution to it. It was found that (i) the B&P method can solve small-sized instances, e.g., less than 50 rentals, within a few minutes, while as the number of rentals increases, e.g., 100 rentals, the computation time would increase rapidly; (ii) the overall efficiency of the B&P approach largely depends on the computational efficiency of column generation. The results demonstrate that the B&P approach proposed by Xu and Meng (2019) is not capable of generating a prompt demand-responsive operational vehicle relocation and charging strategy facing the sudden change of demand information in real time.

To overcome the computational difficulty, a heuristic-reinforced column generation method is developed, by which the activity trajectories, i.e., columns, are expected to be generated reactively in an online environment. To achieve this, a restricted set-packing-type model is first formulated for the static problem defined over each sub-horizon. A multi-label

method is then adopted to generate activity trajectories for the first static problem. The dynamic heuristic-reinforced column generation procedure for the subsequent S-VR&CS problems is elaborated thereafter. Details are described in the following subsections.

4.3.1 Set-packing-type model for each static problem

For the k^{th} S-VR&CS problem, given the available information of each EV $v \in \mathcal{V}$, i.e., $\hat{t}_v$, $\hat{s}_v$, and $\hat{l}_v$, and the set of rentals known up to the decision epoch t_k with departure time no earlier than $t_k + \tau$, i.e., $\mathcal{I}_k$, let $\mathcal{R}_k^v$ denote the set of feasible activity trajectories for the EV $v \in \mathcal{V}$, and P_r^v be the real profit of the activity trajectory $r \in \mathcal{R}_k^v$, i.e., the difference between the net profit collected from the served rentals and the incurred total relocation cost. Recall that E_i is defined as the penalty for rejecting a rental $i \in \mathcal{I}$. Then a set-packing-type formulation for the k^{th} S-VR&CS problem is developed as follows:

$$\max_{\boldsymbol{x}} \ PROFIT = \sum_{v \in \mathcal{V}} \sum_{r \in \mathcal{R}_k^v} P_r^v x_r^v - \sum_{i \in \mathcal{I}_k} (1 - \sum_{v \in \mathcal{V}} \sum_{r \in \mathcal{R}_k^v} \delta_{ir}^v x_r^v) E_i \tag{4.3}$$

subject to

$$\sum_{v \in \mathcal{V}} \sum_{r \in \mathcal{R}_k^v} \delta_{ir}^v x_r^v \le 1, \quad \forall i \in \mathcal{I}_k \tag{4.4}$$

$$\sum_{r \in \mathcal{R}_k^v} x_r^v \le 1, \quad \forall v \in \mathcal{V} \tag{4.5}$$

$$x_r^v \in \{0,1\}, \quad \forall v \in \mathcal{V}, r \in \mathcal{R}_k^v \tag{4.6}$$

where x_r^v, $\forall v \in \mathcal{V}, r \in \mathcal{R}_k^v$ is the binary decision variable that equals 1 if the EV v performs the activity trajectory r, and 0 otherwise; δ_{ir}^v is the rental-trajectory incidence coefficient that equals 1 if rental $i \in \mathcal{I}_k$ is covered by activity trajectory $r \in \mathcal{R}_k^v$, and 0 otherwise. The objective function expressed by Eq. (4.3) seeks to find a subset of single-vehicle activity trajectories from the set $\bigcup_{v \in \mathcal{V}} \mathcal{R}_k^v$ so that the profit of the k^{th} S-VR&CS problem is maximized. Constraint (4.4) ensures that each rental is covered by at most one activity trajectory. Constraint (4.5) imposes that each EV is assigned to at most one activity trajectory. Constraint (4.6) defines x_r^v as a binary variable. The IP model (4.3)-(4.6) can be equivalently expressed by

[S-VR&CS^k]

$$\max_{x_r^v} \; PROFIT^{new} = \sum_{v \in \mathcal{V}} \sum_{r \in \mathcal{R}_k^v} (P_r^v + \sum_{i \in \mathcal{I}_k} \delta_{ir}^v E_i) x_r^v \tag{4.7}$$

subject to Constraints (4.4)-(4.6), where the term $P_r^v + \sum_{i \in \mathcal{I}_k} \delta_{ir}^v E_i$ can be viewed as the profit of an activity trajectory $r \in \mathcal{R}_k^v$ considering the penalty for unserved rentals.

It should be noted that if $\mathcal{R}_k^v$ contains all feasible activity trajectories for each EV $v \in \mathcal{V}$, then the formulation [S-VR&CS^k] shows exactly the k^{th} static problem at the decision epoch t_k. Nevertheless, the huge number of feasible activity trajectories makes it challenging to solve the model [S-VR&CS^k] to optimality even for a small-sized problem, especially in an online environment where the change of demand information should be responded in a timely fashion. Moreover, since the aim is to maximize the profit in the whole planning horizon, solving the problem [S-VR&CS^k] to optimality does not necessarily generate a better solution to the entire problem than the case in which an approximate solution is obtained.

The solution method will seek to obtain a reasonably good feasible solution to the considered static problem in a limited amount of time. To achieve the goal, only a small subset of all the feasible activity trajectories for each EV $v \in \mathcal{V}$ will be generated, and the resultant restricted version of the problem [S-VR&CS^k] will be solved with state-of-the-art MILP solvers like Gurobi. The special structure of the set-packing-type formulation allows that the optimal solution can be obtained very efficiently. For example, the preliminary numerical experiments showed that a restricted set-packing-type model with 100 rows and about 40,000 columns could usually be solved to optimality within a few seconds. Next, an efficient column generation method for each static problem in the dynamic algorithmic framework will be designed.

4.3.2 Static problem over the first sub-horizon

For the static problem over the first sub-horizon $[0, T]$, the activity trajectories for each EV $v \in \mathcal{V}$ are generated before the decision epoch $t_1 = 0$. Since the initial set of rentals, i.e., $\mathcal{I}_0$, has been known before the beginning of the planning horizon, it is assumed that there is a sufficient amount of time to generate activity trajectories. In light of this, a customized multi-label method based on Laporte et al. (2011) is developed to generate activity trajectories for the first static problem, which is described in detail in the following subsections.

4.3.2.1 Network construction procedure

To implement the multi-label method, a directed pseudo-network denoted by $\mathcal{G} = (\mathcal{I}_0, \mathcal{A})$ needs to be constructed first. Each node $i \in \mathcal{I}_0$ associated with the profit $p_i = G_i + E_i$ and the electricity consumption e_i in the network represents a rental. Each link $ij \in \mathcal{A} \subseteq \mathcal{I}_0 \times \mathcal{I}_0$ from the node i to the node j associated with the profit $p_{ij} = -RC(s_i^d, s_j^o)$, the electricity consumption $e(s_i^d, s_j^o)$, and the travel time $\tau(s_i^d, s_j^o)$ indicates the relocation operation from the drop-off station of the rental i to the pick-up station of the rental j. Each path in the constructed pseudo-network is an EV activity trajectory. The objective to generate activity trajectories for each EV $v \in \mathcal{V}$ is thus equivalent to finding the paths that are feasible in terms of both travel time and electricity consumption for the EV v in the constructed network $\mathcal{G}$. It should be noted that the charging strategy of the EV (delineated by the charging duration/amount at each traversed station) implementing an activity trajectory in the network has been implicitly implied in the charging strategy of each link traversed by the corresponding path. Here the charging strategy of a link between two rentals refers to the charging duration/amount at the drop-off station of the preceding rental and the pick-up station of the succeeding rental. That is to say, for an activity trajectory represented by the sequence of the traversed rentals, the charging strategy of an EV can be derived from the charging strategy of each pair of preceding & succeeding rentals.

The network should be preprocessed to eliminate the infeasible nodes and links before applying the multi-label method in Subsection 4.3.2.2. Regarding the node feasibility, any node with the electricity consumption exceeding $SOC_{\max} - SOC_{\min}$ is removed from the constructed network and the corresponding links are removed accordingly. However, the link feasibility check in terms of both travel time and electricity consumption is not straightforward due to the sophisticated nonlinear and implicit charging profile. Fortunately, given the concavity of the charging profile, Xu and Meng (2019) have proposed a way to find a non-dominated charging strategy for an applicable link ij, by which the resultant SOC of the EV by the departure time

of the rental j is not less than that by any other feasible charging strategies[1]. Hence, the feasibility of a link will be checked by first examining the existence of non-dominated strategy and then verifying whether the EV is able to arrive at the drop-off station of the succeeding rental with SOC no less than $SOC_{\min}$ if the non-dominated charging strategy does exist.

Take a link ij shown in Figure 4.4 as an example. Recall that t_i^o, t_i^d, and e_i denote the departure time, arrival time, and electricity consumption of a rental i, respectively; and $\tau(s_i^d, s_j^o)$ and $e(s_i^d, s_j^o)$ represent the time and electricity consumption for the relocation operation from the drop-off station of a rental i to the pick-up station of a rental j, respectively. Let l_i^d be the SOC right after an EV arrives at the drop-off station of the rental i. The check of the existence of the non-dominated charging strategy, and under the non-dominated charging strategy if it does exist, the determination of the charging durations at the drop-off station of the rental i and the pick-up station of the rental j denoted by $\tau(s_i^d)$ and $\tau(s_j^o)$ respectively, and the SOC of the EV just before serving the rental j represented by l_j^o are discussed as follows:

(i) If $t_i^d + \tau(s_i^d, s_j^o) > t_j^o$ or $SOC_{\max} - e(s_i^d, s_j^o) < SOC_{\min}$, the non-dominated charging strategy does not exist and the link is infeasible; else continue the following discussion (ii) or (iii):

(ii) If $l_i^d - e(s_i^d, s_j^o) \geq SOC_{\min}$, the non-dominated charging strategy exists. The EV should be relocated directly to the pick-up station of the rental j without charging at the drop-off station of the rental i, i.e., $\tau(s_i^d) = 0$, and then charged at the pick-up station of the rental j from $l_i^d - e(s_i^d, s_j^o)$ for $\tau(s_j^o) = \min\left\{\text{ExpTime}\left(SOC_{\max} \mid l_i^d - e(s_i^d, s_j^o)\right), t_j^o - t_i^d - \tau(s_i^d, s_j^o)\right\}$. The SOC of the EV at the departure time of the rental j under the non-dominated charging strategy is calculated by $l_j^o = \text{ExpSOC}\left(\tau(s_j^o) \mid l_i^d - e(s_i^d, s_j^o)\right)$. The link is feasible only if

[1] If the non-dominated charging strategy does not exist, which means that there is no feasible charging strategy for link ij, the EV cannot reach the pick-up station of the succeeding rental j before the departure time t_j^o with SOC higher than or equal to $SOC_{\min}$.

$l_j^o - e_j \geq SOC_{\min}$.

(iii) If $l_i^d - e(s_i^d, s_j^o) < SOC_{\min}$, it is needed to calculate the duration required to charge the EV from l_i^d to $e(s_i^d, s_j^o) + SOC_{\min}$, i.e., $\text{ExpTime}\left(e(s_i^d, s_j^o) + SOC_{\min} \mid l_i^d\right)$. If $t_i^d + \text{ExpTime}\left(e(s_i^d, s_j^o) + SOC_{\min} \mid l_i^d\right) + \tau(s_i^d, s_j^o) > t_j^o$, the non-dominated charging strategy does not exist and the link is infeasible; otherwise, the non-dominated charging strategy exists and an EV should first be charged at the drop-off station of the rental i for $\tau(s_i^d) = \text{ExpTime}\left(e(s_i^d, s_j^o) + SOC_{\min} \mid l_i^d\right)$ and then relocated to the pick-up station of the rental j for further charging from $SOC_{\min}$ for $\tau(s_j^o) = \min\left\{\text{ExpTime}\left(SOC_{\max} \mid SOC_{\min}\right), t_j^o - t_i^d - \tau(s_i^d) - \tau(s_i^d, s_j^o)\right\}$. The SOC of the EV at the departure time of the rental j under the non-dominated charging strategy is calculated by $l_j^o = \text{ExpSOC}\left(\tau(s_j^o) \mid SOC_{\min}\right)$. The link is feasible only if $l_j^o - e_j \geq SOC_{\min}$.

For the details of non-dominated charging strategy of a link ij under the realistic concave EV charging profile, the interested readers can refer to the study by Xu and Meng (2019).

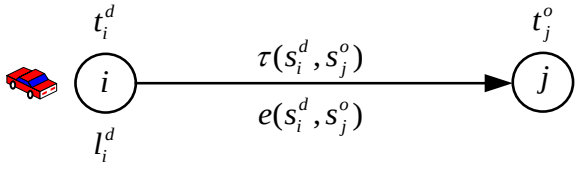

Figure 4.4 Two rentals with a link

Based on the above information, the network construction procedure is summarized as follows:

(i) Sort rentals in ascending order in terms of their pick-up time and name them in sequence as rental 1, rental 2, …, until rental $|\mathcal{I}_0|$;

(ii) Check the feasibility of each rental and remove the infeasible ones;

(iii) For each remaining rental i and rental $j > i$, generate the directed link ij if it is feasible given $l_i^d := SOC_{\max} - e_i$.

4.3.2.2 Multi-label method for generating activity trajectories

In this subsection, a multi-label method to generate activity trajectories for the first static

problem is developed based on the constructed network. Each node i will be associated with multiple labels representing partial paths starting from the initial location of an EV $v \in \mathcal{V}$, i.e., s_v^0, and ending at the drop-off station of the rental i, i.e., s_i^d. All labels associated with the EV v at the node i are grouped into a set denoted by $\mathcal{L}(v,i)$. Any label in the set $\mathcal{L}(v,i)$ can be coded as $l_k(v,i) := [\bar{p}_k, \bar{l}_k, n_k, m_k]$, where $\bar{p}_k$ represents the profit of the corresponding path and $\bar{l}_k$ denotes the SOC of the EV v right after arriving at the drop-off station of the rental i; n_k and m_k are the node and label indexes that precede label k respectively and are used to identify the traversed nodes of that path by backtracking.

The implementation procedure of the multi-label method to generate activity trajectories for the first static problem is summarized in Algorithm 4.1. The label set $\mathcal{L}(v, j)$, $\forall v \in \mathcal{V}$ and $j \in \mathcal{J}_0$ will be first initialized (Line 1). Labels directly from the initial location of each EV to each node will then be generated (Lines 2-9). Next, for each EV, labels from each node to any other node will be generated (Lines 10-27). Last, activity trajectories will be generated using backtracking based on the label set $\bigcup_{v \in \mathcal{V}, j \in \mathcal{J}_0} \mathcal{L}(v, j)$ (Lines 28-30). Note that NondominatedChargingStrategy in Algorithm 4.1 is the subfunction to find the non-dominated charging strategy for an EV when it departs from its initial location (Line 4) or the drop-off station of a rental (Line 15) to the pick-up station of another rental. As discussed in Subsection 4.3.2.1, given the initial SOC and time of EV v, i.e., $\hat{l}_v^0$ and $\hat{t}_v^0$, electricity consumption and time for the relocation operation from the initial location of EV v to the pick-up station of rental j, i.e., $e(\hat{s}_v^0, s_j^o)$ and $\tau(\hat{s}_v^0, s_j^o)$, and pick-up time of rental j, i.e., t_j^o, (or the SOC of EV v right after arriving at the drop-off station of the rental i along a path, i.e., $\bar{l}_k$, drop-off time of rental i, i.e., t_i^d, electricity consumption and time for the relocation operation from the drop-off station of rental i to the pick-up station of rental j, i.e., $e(s_i^d, s_j^o)$ and $\tau(s_i^d, s_j^o)$, and the pick-up time of rental j, i.e., t_j^o), the SOC of the EV before serving the rental j, i.e., l_j^o, under the non-dominated charging strategy can be easily found; otherwise, the subfunction will return zero as the value of l_j^o. Different from the exact algorithm design for a static problem in Xu and Meng (2019), the dominance test will not be conducted in the multi-label method because the dominated labels for the first sub-horizon have the potential to

become promising non-dominated labels after the dynamic addition and removal of rentals in subsequent sub-horizons. Moreover, given the large number of labels that could be generated at node j through a link $ij \in \mathcal{A}$, $\mathcal{L}(v, j)$ will be retained and augmented by at most a pre-specified number, i.e., N_{label}, of promising labels grouped in $\mathcal{W}$ among all the labels in the set $\mathcal{H}$, based on the weighted sum of the profit and SOC (Lines 20-24). This helps to strike a good balance between solution quality and computational efficiency and is realized by the subfunction PromisingLabels, where μ_1 and μ_2 are the weights for the profit and SOC, respectively (Line 21). The reason for incorporating SOC other than the profit in the determination of generated labels is that a label with a lower profit yet a higher SOC is likely to develop into activity trajectories that are more profitable by traversing rentals with larger electricity consumption. Finally, BackTracking is the subfunction to generate and return activity trajectories for the EV v by backtracking based on the set of labels $\bigcup_{j \in \mathcal{J}_0} \mathcal{L}(v, j)$ (line 29).

Algorithm 4.1: Pseudocode of the multi-label method to generate activity trajectories for the first static problem

Input: $\mathcal{G} = (\mathcal{J}_0, \mathcal{A})$ and $(\hat{t}_v^0, \hat{s}_v^0, \hat{l}_v^0)$, $\forall v \in \mathcal{V}$.

Output: $\mathcal{R}_1^v$, $\forall v \in \mathcal{V}$.

1 Initialize $\mathcal{L}(v, j) \leftarrow \varnothing$ for each $v \in \mathcal{V}$ and $j \in \mathcal{J}_0$;
2 **For** each EV $v \in \mathcal{V}$ Do
3 **For** each $j \in \mathcal{J}_0$ Do
4 $l_j^o \leftarrow \text{NondominatedChargingStrategy}(\hat{l}_v^0, \hat{t}_v^0, e(\hat{s}_v^0, s_j^o), \tau(\hat{s}_v^0, s_j^o), t_j^o)$;
5 **If** $l_j^o - e_j \geq SOC_{\min}$ Then
6 $\mathcal{L}(v, j) \leftarrow \mathcal{L}(v, j) \bigcup \{[-RC(\hat{s}_v^0, s_j^o) + p_j, l_j^o - e_j, 0, 0]\}$;
7 **EndIf**
8 **EndFor**
9 **EndFor**
10 **For** each EV $v \in \mathcal{V}$ Do
11 **For** each $i \in \mathcal{J}_0$ and $\mathcal{L}(v, i) \neq \varnothing$ Do
12 **For** each $j \in \mathcal{J}_0$ and $ij \in \mathcal{A}$ Do
13 $\mathcal{H} \leftarrow \varnothing$;
14 **For** $k = 1$ to $|\mathcal{L}(v, i)|$ Do
15 $l_j^o \leftarrow \text{NondominatedChargingStrategy}(\bar{l}_k, t_i^d, e(s_i^d, s_j^o), \tau(s_i^d, s_j^o), t_j^o)$;
16 **If** $l_j^o - e_j \geq SOC_{\min}$ Then
17 $\mathcal{H} \leftarrow \mathcal{H} \bigcup \{[\bar{p}_k + p_{ij} + p_j, l_j^o - e_j, i, k]\}$;

EndIf
EndFor
If $|\mathcal{H}| > N_{label}$ Then
$\mathcal{W} \leftarrow \text{PromissingLabels}(\mathcal{H}, N_{label}, \mu_1, \mu_2)$;
$\mathcal{L}(v, j) \leftarrow \mathcal{L}(v, j) \cup \mathcal{W}$;
Else $\mathcal{L}(v, j) \leftarrow \mathcal{L}(v, j) \cup \mathcal{H}$;
EndIf
EndFor
EndFor
EndFor
For each EV $v \in \mathcal{V}$ Do
$\mathcal{R}_1^v \leftarrow \text{BackTracking}(\bigcup_{j \in \mathcal{J}_0} \mathcal{L}(v, j))$;
EndFor

4.3.3 Static problems over the subsequent sub-horizons

For the k^{th} ($k \geq 2$) static problem, the activity trajectories for each EV $v \in \mathcal{V}$ are generated dynamically during the time interval $[t_{k-1} + \tau, t_k)$. Recall that $\bar{\mathcal{J}}_{k-1}$ is the set of rentals with departure times falling in period $[t_{k-1} + \tau, t_k + \tau)$, and $\tilde{\mathcal{J}}_{k-1}$ and $\hat{\mathcal{J}}_{k-1}$ represent the set of rentals dynamically reserved and canceled during time interval $[t_{k-1}, t_k)$, respectively. As mentioned in Section 4.2, immediately after a solution to the $(k-1)^{th}$ static problem is obtained and implemented at the time $t_{k-1} + \tau$, the earliest available time, the corresponding vehicle location, and the SOC of each EV $v \in \mathcal{V}$, i.e., $\hat{t}_v$, $\hat{s}_v$, and $\hat{l}_v$, for the k^{th} static problem can be known. Hence, at the beginning of the time interval $[t_{k-1} + \tau, t_k)$, all the vehicle information needed for generating activity trajectories for the k^{th} static problem is known. Regarding the rentals to be considered in the k^{th} static problem, i.e., $\mathcal{J}_k = \left[(\mathcal{J}_{k-1} \setminus \bar{\mathcal{J}}_{k-1}) \cup \tilde{\mathcal{J}}_{k-1} \right] \setminus \hat{\mathcal{J}}_{k-1}$, since the rentals in $\mathcal{J}_{k-1} \setminus \bar{\mathcal{J}}_{k-1}$ have arrived before the decision epoch t_{k-1}, they are known throughout the time interval $[t_{k-1} + \tau, t_k)$. Nevertheless, the rentals in $\tilde{\mathcal{J}}_{k-1} \cup \hat{\mathcal{J}}_{k-1}$ are dynamically reserved and/or canceled during the time interval $[t_{k-1}, t_k)$, the reservation and/or cancellation information of them is not available until they are reserved and/or canceled. Hence, in the process of dynamically generating activity trajectories for the k^{th} static problem over the time interval $[t_{k-1} + \tau, t_k)$, the rentals in $(\mathcal{J}_{k-1} \setminus \bar{\mathcal{J}}_{k-1}) \cup \tilde{\mathcal{J}}_{k-1}$ that have arrived but are not

canceled yet are considered. For ease of presentation, let $\mathcal{I}_{latest}$ denote the latest set of rentals that have arrived but are not canceled yet and $\mathcal{R}^v_{latest}$ be the corresponding latest set of activity trajectories generated for the EV $v \in \mathcal{V}$ that cover the rentals in $\mathcal{I}_{latest}$. In addition, it should be noted that the time-dependent travel time and electricity consumption can be well accommodated based on the latest traffic condition at time point $t_{k-1} + \tau$.

The flowchart of the dynamic process of generating activity trajectories for the k^{th} static problem is illustrated in Figure 4.5. First, $\mathcal{I}_{latest}$ will be initialized by $\mathcal{I}_{latest} \coloneqq \mathcal{I}_{k-1} \setminus \bar{\mathcal{I}}_{k-1}$ and $\bigcup_{v \in \mathcal{V}} \mathcal{R}^v_{latest}$ will be initialized by utilizing the activity trajectories generated for the previous static problem, i.e., the activity trajectories in the set $\bigcup_{v \in \mathcal{V}} \mathcal{R}^v_{k-1}$. Then, new activity trajectories will be generated in an iterative fashion for both existing and newly arriving rentals with updated $\mathcal{I}_{latest}$ and $\bigcup_{v \in \mathcal{V}} \mathcal{R}^v_{latest}$. Specifically, in each iteration, the linear programming (LP) relaxation of the restricted set-packing-type model [S-VR&CS^k] with $\mathcal{I}_{latest}$ and $\bigcup_{v \in \mathcal{V}} \mathcal{R}^v_{latest}$, namely, [LP-VR&CS], is first solved using state-of-the-art solver Gurobi such that the dual values and the optimal basis can be obtained. Then a pre-specified number of new activity trajectories are generated for the existing rentals in $\mathcal{I}_{latest}$ by applying fast local-search-based heuristics guided by the dual values on the activity trajectories in the optimal basis. The reason for leveraging the activity trajectories in the optimal basis is that these activity trajectories have zero reduced costs and they are likely to develop into new activity trajectories with positive reduced cost, which can result in a higher objective value if added to [LP-VR&CS]. Last, new activity trajectories will be generated for the newly arriving rentals, followed by the update of $\mathcal{I}_{latest}$ and $\bigcup_{v \in \mathcal{V}} \mathcal{R}^v_{latest}$.

In more detail, let λ_n denote the current time, i.e., the time epoch right after generating new activity trajectories for the existing rentals in $\mathcal{I}_{latest}$ in the n^{th} iteration. Then the time epoch right after generating new activity trajectories for the existing rentals in $\mathcal{I}_{latest}$ in the last iteration would be λ_{n-1}. Particularly, it is $\lambda_0 \coloneqq t_{k-1}$ if the current iteration is the first iteration. Let $\tilde{\mathcal{I}}[\lambda_{n-1}, \lambda_n)$ and $\hat{\mathcal{I}}[\lambda_{n-1}, \lambda_n)$ represent the sets of rentals that are newly reserved and

canceled during the time interval $[\lambda_{n-1}, \lambda_n)$, respectively; then in the n^{th} iteration, new activity trajectories are generated to cover the newly arriving rentals in $\tilde{\mathcal{I}}[\lambda_{n-1}, \lambda_n)$ by inserting each rental in $\tilde{\mathcal{I}}[\lambda_{n-1}, \lambda_n)$ into these already generated activity trajectories. The preliminary numerical experiments indicated that due to the strict insertion conditions imposed by the travel time and electricity consumption, a rental from the set $\tilde{\mathcal{I}}[\lambda_{n-1}, \lambda_n)$ often fails to be inserted into any activity trajectory in the optimal basis. Hence, in order to increase the probability of these new arrivals being successfully covered, when generating new activity trajectories to cover the newly arriving rentals in $\tilde{\mathcal{I}}[\lambda_{n-1}, \lambda_n)$ in each iteration, in addition to the activity trajectories in the optimal basis, the activity trajectories generated for the existing rentals in $\mathcal{I}_{latest}$ are also utilized. Afterwards, $\mathcal{I}_{latest}$ is updated by $\mathcal{I}_{latest} := \mathcal{I}_{latest} \bigcup \tilde{\mathcal{I}}[\lambda_{n-1}, \lambda_n) \setminus \hat{\mathcal{I}}[\lambda_{n-1}, \lambda_n)$, and $\bigcup_{v \in \mathcal{V}} \mathcal{R}^v_{latest}$ is updated by considering the rentals in $\tilde{\mathcal{I}}[\lambda_{n-1}, \lambda_n)$ and $\hat{\mathcal{I}}[\lambda_{n-1}, \lambda_n)$ successively. Then a new iteration is started until the decision epoch t_k. At the decision epoch t_k, a restricted set-packing-type formulation with the latest sets of rentals and activity trajectories, i.e., $\mathcal{I}_{latest}$ and $\bigcup_{v \in \mathcal{V}} \mathcal{R}^v_{latest}$, will be solved to obtain the binary assignment decisions for the k^{th} static problem.

In what follows, the initialization of activity trajectories will be first elaborated in Subsection 4.3.3.1. The detailed procedure of generating activity trajectories for the existing rentals in $\mathcal{I}_{latest}$ is illustrated in Subsection 4.3.3.2. At last, in Subsection 4.3.3.3, how to generate new activity trajectories to cover the newly arriving rentals in $\tilde{\mathcal{I}}[\lambda_{n-1}, \lambda_n)$ and how to update $\bigcup_{v \in \mathcal{V}} \mathcal{R}^v_{latest}$ by considering the rentals in $\tilde{\mathcal{I}}[\lambda_{n-1}, \lambda_n)$ and $\hat{\mathcal{I}}[\lambda_{n-1}, \lambda_n)$ successively are described.

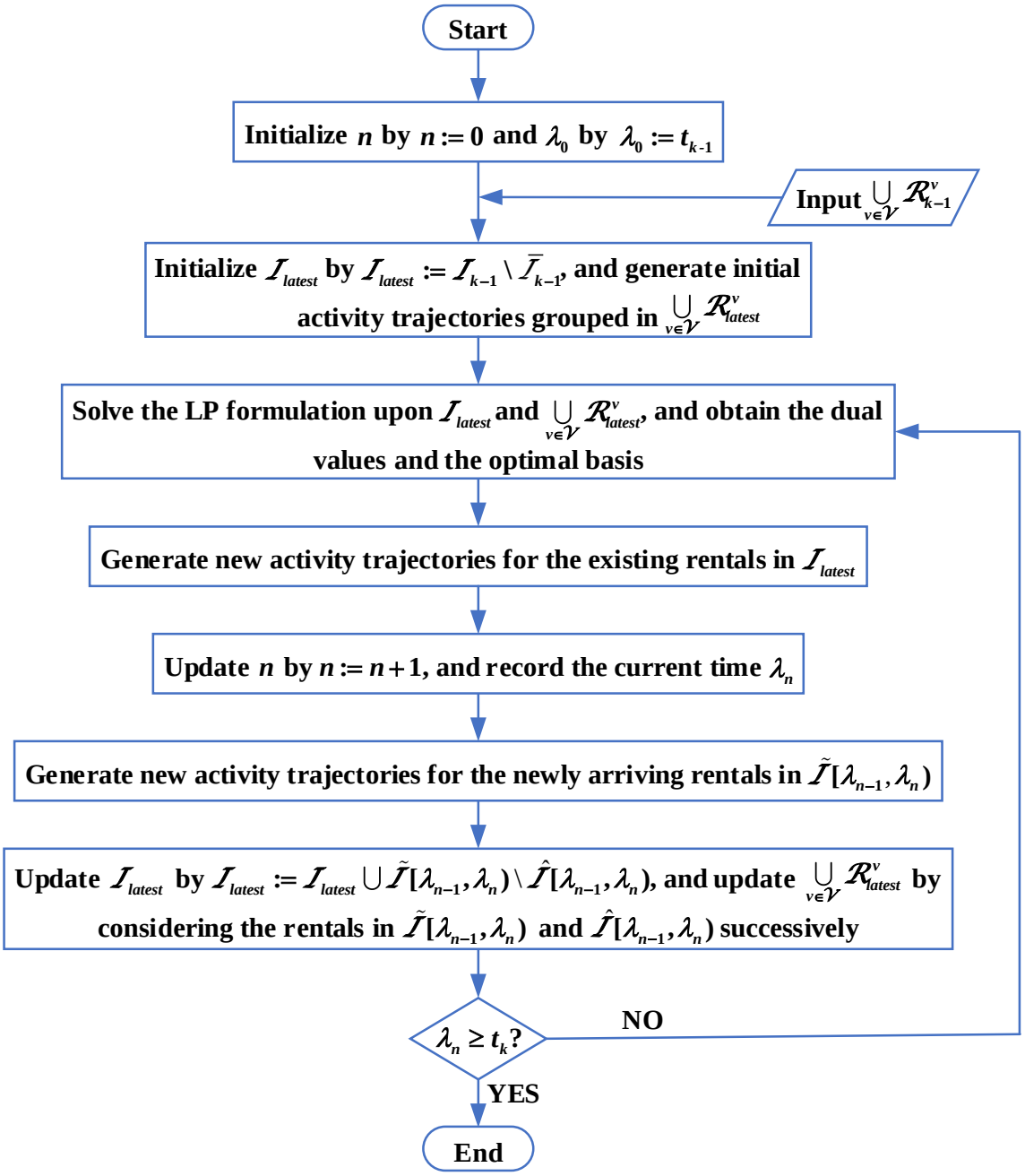

Figure 4.5 Flowchart of the dynamic column generation for the k[th] static problem

4.3.3.1 Activity trajectory initialization

Unlike the first static problem, only limited time is allowed to generate activity trajectories for the subsequent static problems in the online context. To speed up the column generation process, activity trajectories for the k^{th} static problem are first initialized by utilizing the activity trajectories generated for the $(k-1)^{th}$ static problem, i.e., the activity trajectories in set $\bigcup_{v \in \mathcal{V}} \mathcal{R}^v_{k-1}$. The process of generating initial activity trajectories starts as long as the solution to

the $(k-1)^{th}$ static problem is obtained and implemented at the time point $t_{k-1}+\tau$. The benefit of making use of existing activity trajectories will amplify as time goes by, offering the potential to generate a large number of activity trajectories in a short period of time.

For each EV $v \in \mathcal{V}$, let r_{k-1}^{v*} denote the optimal activity trajectory for it in the $(k-1)^{th}$ static problem, which is to be implemented over the time period $[t_{k-1}+\tau, t_k+\tau]$. Given the earliest available time $\hat{t}_v$, the location $\hat{s}_v$, and the SOC $\hat{l}_v$ of an EV v in the k^{th} static problem, the rentals to be served after the time epoch $t_k+\tau$ in an arbitrary activity trajectory $r \in \mathcal{R}_{k-1}^v \setminus \{r_{k-1}^{v*}\}$ may not be able to be served by the EV in view of the restrictions related to travel time and electricity consumption. Therefore, when the activity trajectory r is developed into an initial activity trajectory for the k^{th} static problem, the feasibility of the two constraints needs to be rechecked and restored if necessary. More specifically, when the EV attempts to depart from the location $\hat{s}_v$ to cover a succeeding rental j, the feasibility of the corresponding link should be checked (see Subsection 4.3.2.1). If the link is infeasible, the rental j will be removed from the activity trajectory, and the next adjacent rental will be checked until all the rentals have been examined.

Take an example to illustrate this process. Suppose r is an activity trajectory in the set $\mathcal{R}_{k-1}^v \setminus \{r_{k-1}^{v*}\}$ for an EV $v \in \mathcal{V}$, and *Rental 1*→*Rental 2*→*Rental 3* is the sequence of the rentals to be served after the time point $t_k+\tau$, based on which an initial activity trajectory for the k^{th} static problem is to be generated. Recall that l_i^d denote the SOC of the EV right after serving the rental i as defined in Subsection 4.3.2.1. Given the information of the EV v, including the available time $\hat{t}_v$, location $\hat{s}_v$, and SOC $\hat{l}_v$, whether the inequality $l_1^d = \text{NondominatedChargingStrategy}\left(\hat{l}_v, \hat{t}_v, e(\hat{s}_v, s_1^o), \tau(\hat{s}_v, s_1^o), t_1^o\right) - e_1 \geq SOC_{\min}$ holds, i.e., whether the EV can arrive at the drop-off station of *Rental 1* without violating the time and electricity consumption constraints by departing from its current location, will be first checked, If yes, the available time, the location, and the SOC of the EV v will be updated to be t_1^d, s_1^d, and l_1^d respectively after serving *Rental 1*; otherwise, *Rental 1* will be removed and the vehicle state will remain unchanged. Similar checking processes will be conducted for *Rentals 2* and *3*. Suppose that only *Rentals 1* and *3* are retained, then an initial activity trajectory represented

by the traversed rentals, i.e., *Rental 1*→*Rental 3*, will be generated for the EV v in the k^{th} static problem. On the other hand, if all the rentals are removed in the aforesaid process or there are no rentals after time point $t_k + \tau$ in the activity trajectory r, no activity trajectory for the k^{th} static problem will be generated from r.

Algorithm 4.2 outlines the procedure of generating the initial activity trajectories for the k^{th} ($k \geq 2$) static problem by utilizing the activity trajectories generated for the $(k-1)^{th}$ static problem, where r^{fst}, r^{last}, r_i^{sud}, and r^{num} are the first rental, the last rental, and the rental succeeding the rental i, and the total number of rentals covered by the activity trajectory r, respectively. Moreover, to facilitate illustration, the activity trajectory r will be augmented at the very beginning by a dummy rental o_v with the same pick-up and drop-off stations being $\hat{s}_v$, the same pick-up and drop-off times at $\hat{t}_v$, and 0 electricity consumption. This is implemented by the subfunction AugmentRental (Line 4). As such, the SOC of the EV v before serving the dummy rental o_v would be $\hat{l}_v$. Additionally, the subfunction RemoveRental is for the removal operation of a particular rental from an activity trajectory and it will return the resultant activity trajectory after the removal (Lines 9 and 19).

Algorithm 4.2: Pseudocode of generating initial activity trajectories for the k^{th} static problem

Input: $\bigcup_{v \in \mathcal{V}} \left(\mathcal{R}_{k-1}^v \setminus \{r_{k-1}^{v*}\} \right)$ and $(\hat{t}_v, \hat{s}_v, \hat{l}_v)$, $\forall v \in \mathcal{V}$.

Output: $\bigcup_{v \in \mathcal{V}} \mathcal{R}_{latest}^v$.

1 Initialize $\mathcal{R}_{latest}^v \leftarrow \varnothing$ for each EV $v \in \mathcal{V}$;
2 **For** each $v \in \mathcal{V}$ Do
3 **For** each $r \in \mathcal{R}_{k-1}^v \setminus \{r_{k-1}^{v*}\}$ Do
4 $r \leftarrow \text{AugmentRental}(r, o_v)$; $i \leftarrow r^{fst}$; $l_i^o \leftarrow \hat{l}_v$;
5 **While** $i \neq r^{last}$ Do
6 $j \leftarrow r_i^{sud}$;
7 $l_j^o \leftarrow \text{NondominatedChargingStrategy}(l_i^o - e_i, e(s_i^d, s_j^o), \tau(s_i^d, s_j^o), t_i^d, t_j^o)$;
8 **While** $l_j^o - e_j < SOC_{\min}$ Do
9 $r \leftarrow \text{RemoveRental}(r, j)$;
10 **If** $i \neq r^{last}$ Then
11 $j \leftarrow r_i^{sud}$;
12 $l_j^o \leftarrow \text{NondominatedChargingStrategy}(l_i^o - e_i, e(s_i^d, s_j^o), \tau(s_i^d, s_j^o), t_i^d, t_j^o)$;
13 **Else** $j \leftarrow i$; $l_j^o \leftarrow l_i^o$;

```
14          EndIf
15        EndWhile
16        i ← j; l_i^o ← l_j^o;
17      EndWhile
18      If r^num > 1 Then
19        r ← RemoveRental(r, o_v); R_latest^v ← R_latest^v ∪ {r};
20      EndIf
21    EndFor
22  EndFor
```

4.3.3.2 Generating new activity trajectories for the existing rentals

After solving [LP-VR&CS], the optimal basis and the optimal dual vector denoted by $\psi = (\alpha_1, ..., \alpha_i, ..., \alpha_{|\mathcal{I}_{latest}|}, \beta_1, ..., \beta_v, ..., \beta_{|\mathcal{V}|})$ are obtained, where α_i is the dual value for the rental $i \in \mathcal{I}_{latest}$, and β_v is the dual value for the EV $v \in \mathcal{V}$. Let $\mathcal{B}$ denote the set of the activity trajectories in the optimal basis. New activity trajectories with positive reduced cost are generated for the existing rentals in $\mathcal{I}_{latest}$, which remain to be added to $\bigcup_{v \in \mathcal{V}} \mathcal{R}_{latest}^v$, by applying the three-phase local-search-based heuristic on the activity trajectories from the set $\mathcal{B}$ one by one until the number of new activity trajectories reaches a pre-specified threshold Z. The three-phase local-search-based heuristic is composed of rental replacement, rental insertion, and rental deletion. For ease of illustration, let $\mathcal{C}^v$ denote the set of new activity trajectories generated for the EV $v \in \mathcal{V}$.

Particularly, for an arbitrary activity trajectory r from the set $\mathcal{B}$, the corresponding EV that is associated with it, i.e., v_r, is first confirmed. Then another activity trajectory, namely u, is defined and initialized to be r, i.e., $u := r$. Based on the activity trajectory u, the three-phase local search, i.e., rental replacement, rental insertion, and rental deletion, is performed. Specifically, in the first phase, with r being the benchmark activity trajectory, a rental $i \in \mathcal{I}(r)$ is picked, where $\mathcal{I}(r)$ denotes the set of rentals covered by the activity trajectory r, and all the feasible activity trajectories are generated by replacing the rental i in the activity trajectory u with a rental from the set $\mathcal{I}_{latest} \setminus \mathcal{I}(u)$. Among these feasible activity trajectories, qualified activity trajectories for the set $\mathcal{C}^{v_r}$, i.e., the activity trajectories with the reduced cost larger than zero, are identified, and the one with the maximum reduced cost u^* is determined.

Then u is updated to be u^*, i.e., $u := u^*$. Subsequently, another rental in the set $\mathcal{I}(r)$ is picked and the above replacement operations are repeated until all the rentals in the set $\mathcal{I}(r)$ have been examined. In the second phase, based on the activity trajectory u obtained in the first phase, all the feasible activity trajectories are generated by inserting a rental from the set $\mathcal{I}_{latest} \setminus \mathcal{I}(u)$ into u. Similar to the first phase, among these feasible activity trajectories, qualified activity trajectories for the set $\mathcal{C}^{v_r}$ are identified, and the one with the maximum reduced cost u^* is determined. Then u is updated to be u^*. The insertion operations are performed iteratively until no rental can be inserted into the activity trajectory u. In the third phase, based on the activity trajectory u resulted from the second phase, all the feasible activity trajectories are generated by removing a rental in the set $\mathcal{I}(u)$ from u. Again, among these feasible activity trajectories, qualified activity trajectories for the set $\mathcal{C}^{v_r}$ are identified, and the one with the maximum reduced cost u^* is determined. Then u is updated to be u^*. The deletion operations are repeated until no rental can be removed from u or $\mathcal{I}(u)$ has become a singleton.

The pseudocode of generating new activity trajectories for the existing rentals in $\mathcal{I}_{latest}$ is outlined in Algorithm 4.3. It should be noted that ReplaceRental (Line 8) in the first phase is the subfunction to replace the rental i in the activity trajectory u with the rental j and it returns the resultant activity trajectory $\hat{u}$ after the replacement operation. The subfunction CheckFeasibility (Lines 9, 24, and 39) checks the feasibility of the activity trajectory $\hat{u}$ for the EV v_r, given the available time, location, and SOC of the EV. This subfunction will return 'true' if feasible and 'false' otherwise. Given the dual vector ψ, IdentifyColumns (Lines 14, 30, and 44) and FindBstColumn (Lines 15, 31, and 45) return a set of activity trajectories with the reduced cost greater than a specific number, e.g., 0, and the activity trajectory with the maximum reduced cost in the set $\hat{\mathcal{C}}$, respectively. InsertSucceedingRental (Line 23) in the second phase is the subfunction to insert the rental j into the augmented activity trajectory $\bar{u}$ such that it succeeds the rental i. By this subfunction, the rentals covered by $\bar{u}$, i.e., the rentals in $\mathcal{I}(\bar{u})$, are checked one by one until a rental succeeding which the rental j can be feasibly inserted is found or all the rentals in $\mathcal{I}(\bar{u})$ have been checked. Kindly note that for the rental j, there exists at most one rental in $\mathcal{I}(\bar{u})$ succeeding which it can be feasibly inserted (see

Proposition 1 in Appendix B.2).

Algorithm 4.3**:** Pseudocode of generating new activity trajectories for the existing rentals in $\mathcal{I}_{latest}$

Input: $\mathcal{B}$, $\mathcal{I}_{latest}$, ψ, and $(\hat{t}_v, \hat{s}_v, \hat{l}_v)$, $\forall v \in \mathcal{V}$.

Output: $\bigcup_{v \in \mathcal{V}} \mathcal{C}^v$.

Initialize $\mathcal{C}^v \leftarrow \varnothing$ and $\mathcal{D}^v \leftarrow \varnothing$ for each EV $v \in \mathcal{V}$;
For each $r \in \mathcal{B}$ Do
  $u \leftarrow r$;
  // **First phase local search (Replacement)**
  For each $i \in \mathcal{I}(r)$ Do
    $\hat{\mathcal{C}} \leftarrow \varnothing$;
    For each $j \in \mathcal{I}_{latest} \setminus \mathcal{I}(u)$ Do
      $\hat{u} \leftarrow \text{ReplaceRental}(u, i, j)$;
      If CheckFeasibility$(\hat{u}, \hat{t}_{v_r}, \hat{s}_{v_r}, \hat{l}_{v_r})$ is true Then
        $\hat{\mathcal{C}} \leftarrow \hat{\mathcal{C}} \cup \{\hat{u}\}$;
      EndIf
    EndFor
    If $|\hat{\mathcal{C}}| > 0$ Then
      $\mathcal{X} \leftarrow \text{IdentifyColumns}(\hat{\mathcal{C}}, \psi, 0)$; $\mathcal{C}^{v_r} \leftarrow \mathcal{C}^{v_r} \cup \mathcal{X}$;
      $u \leftarrow \text{FindBstColumn}(\hat{\mathcal{C}}, \psi)$;
    EndIf
  EndFor
  // **Second phase local search (Insertion)**
  Do
    $\hat{\mathcal{C}} \leftarrow \varnothing$; $\bar{u} \leftarrow \text{AugmentRental}(u, o_{v_r})$;
    For each $j \in \mathcal{I}_{latest} \setminus \mathcal{I}(\bar{u})$ Do
      For each $i \in \mathcal{I}(\bar{u})$ Do
        $\hat{u} \leftarrow \text{InsertSucceedingRental}(\bar{u}, i, j)$;
        If CheckFeasibility$(\hat{u}, \hat{t}_{v_r}, \hat{s}_{v_r}, \hat{l}_{v_r})$ is true Then
          $\hat{u} \leftarrow \text{RemoveRental}(\hat{u}, o_{v_r})$; $\hat{\mathcal{C}} \leftarrow \hat{\mathcal{C}} \cup \{\hat{u}\}$; break;
        EndIf
      EndFor
    EndFor
    If $|\hat{\mathcal{C}}| > 0$ Then
      $\mathcal{X} \leftarrow \text{IdentifyColumns}(\hat{\mathcal{C}}, \psi, 0)$; $\mathcal{C}^{v_r} \leftarrow \mathcal{C}^{v_r} \cup \mathcal{X}$;
      $u \leftarrow \text{FindBstColumn}(\hat{\mathcal{C}}, \psi)$;
    EndIf
  While $|\hat{\mathcal{C}}| > 0$

```
// Third phase local search (Deletion)
While u^num > 1 Do
    Ĉ ← ∅;
    For each i ∈ I(u) Do
        û ← RemoveRental(u, i);
        If CheckFeasibility(û, t̂_{v_r}, ŝ_{v_r}, l̂_{v_r}) is true Then
            Ĉ ← Ĉ ∪ {û};
        EndIf
    EndFor
    If |Ĉ| > 0 Then
        X ← IdentifyColumns(Ĉ, ψ, 0); C^{v_r} ← C^{v_r} ∪ X;
        u ← FindBstColumn(Ĉ, ψ);
    Else break;
    EndIf
EndWhile
If |∪_{v∈V} C^v| ≥ Z
    break;
EndIf
EndFor
```

4.3.3.3 Generating new activity trajectories for the newly arriving rentals and updating the latest set of activity trajectories

As mentioned earlier, in addition to the activity trajectories from the optimal basis, i.e., the activity trajectories in set $\mathcal{B}$, the activity trajectories generated for the existing rentals in $\mathcal{I}_{latest}$ will be utilized to generate new activity trajectories for the newly arriving rentals in $\tilde{\mathcal{I}}[\lambda_{n-1}, \lambda_n)$. In view of the restrictive insertion conditions related to travel time and electricity consumption of a new arrival into an existing activity trajectory, it may still not be enough to leverage only the activity trajectories with positive reduced cost, i.e., the activity trajectories in the set $\bigcup_{v \in \mathcal{V}} \mathcal{C}^v$. Hence, when generating new activity trajectories for the existing rentals in $\mathcal{I}_{latest}$ in Subsection 4.3.3.2, another set of activity trajectories with the reduced cost greater than a pre-specified number $\varepsilon \leq 0$ are generated, specifically for the generation of new activity trajectories covering the newly arriving rentals in $\tilde{\mathcal{I}}[\lambda_{n-1}, \lambda_n)$. For ease of presentation, let $\mathcal{D}^v$ denote the set of activity trajectories for the EV $v \in \mathcal{V}$ with the reduced cost larger than ε.

$\bigcup_{v \in \mathcal{V}} \mathcal{D}^v$ can be obtained by replacing 0 in subfunction IdentifyColumns in Algorithm 4.3 with ε.

New activity trajectories for the newly arriving rentals in $\tilde{\mathcal{I}}[\lambda_{n-1}, \lambda_n)$ are generated by inserting each rental in $\tilde{\mathcal{I}}[\lambda_{n-1}, \lambda_n)$ into each possible activity trajectory in the set $\mathcal{B} \bigcup (\bigcup_{v \in \mathcal{V}} \mathcal{D}^v)$. The pseudocode is presented in Algorithm 4.4, where $\mathcal{M}^v$ denotes the set of the new activity trajectories generated for the EV $v \in \mathcal{V}$. In particular, for a rental i from $\tilde{\mathcal{I}}[\lambda_{n-1}, \lambda_n)$ and an activity trajectory r from $\mathcal{B} \bigcup (\bigcup_{v \in \mathcal{V}} \mathcal{D}^v)$ that i can be inserted into without violating the travel time and electricity consumption constraints, let $\bar{r}$ denote the resultant activity trajectory after i is inserted into r. For ease of illustration, let $\bar{P}_r$ and $\bar{P}_{\bar{r}}$ be the profits of the activity trajectory r and $\bar{r}$, respectively. If the profit increase of the activity trajectory r brought by the insertion of the rental i, i.e., $\bar{P}_{\bar{r}} - \bar{P}_r$, is not less than a pre-specified number σ, the activity trajectory $\bar{r}$ will be retained. It is worthwhile to note that although, in theory, activity trajectories with negative profit increase will not help boost the profit for the incumbent static problem (see Proposition 2 in Appendix B.2), they have the potential to develop into promising activity trajectories in later sub-horizons that can contribute to the overall profit maximization over the whole planning horizon. Hence, σ is set to be a non-positive number.

Algorithm 4.4: Pseudocode of generating new activity trajectories for the newly arriving rentals in $\tilde{\mathcal{I}}[\lambda_{n-1}, \lambda_n)$

Input: $\tilde{\mathcal{I}}[\lambda_{n-1}, \lambda_n)$, $\mathcal{B}$, $\bigcup_{v \in \mathcal{V}} \mathcal{D}^v$, and $(\hat{t}_v, \hat{s}_v, \hat{l}_v)$, $\forall v \in \mathcal{V}$.

Output: $\bigcup_{v \in \mathcal{V}} \mathcal{M}^v$.

Initialize $\mathcal{M}^v \leftarrow \varnothing$ for each EV $v \in \mathcal{V}$;
For each $i \in \tilde{\mathcal{I}}[\lambda_{n-1}, \lambda_n)$ Do
  For each $r \in \mathcal{B}$ Do
    $\hat{r} \leftarrow \text{ArgumentRental}(r, o_{v_r})$;
    For each $j \in \mathcal{I}(\hat{r})$ Do
      $\bar{r} \leftarrow \text{InsertSucceedingRental}(\hat{r}, j, i)$;
      If CheckFeasibility$(\bar{r}, \hat{t}_{v_r}, \hat{s}_{v_r}, \hat{l}_{v_r})$ is true and $\bar{P}_{\bar{r}} - \bar{P}_r \geq \sigma$ Then
        $\bar{r} \leftarrow \text{RemoveRental}(\bar{r}, o_{v_r})$; $\mathcal{M}^{v_r} \leftarrow \mathcal{M}^{v_r} \bigcup \{\bar{r}\}$; break;
      EndIf
    EndFor

EndFor
For each $v \in \mathcal{V}$ and $\left|\mathcal{D}^v\right| > 0$ Do
  For each $r \in \mathcal{D}^v$ Do
    $\hat{r} \leftarrow \text{AugmentRental}(r, o_v)$;
    For each $j \in \mathcal{I}(\hat{r})$ Do
      $\overline{r} \leftarrow \text{InsertSucceedingRental}(\hat{r}, j, i)$;
      If $\text{CheckFeasibility}(\overline{r}, \hat{t}_v, \hat{s}_v, \hat{l}_v)$ is true and $\overline{P}_{\overline{r}} - \overline{P}_r \geq \sigma$ Then
        $\overline{r} \leftarrow \text{RemoveRental}(\overline{r}, o_v)$; $\mathcal{M}^v \leftarrow \mathcal{M}^v \bigcup \{\overline{r}\}$; break;
      EndIf
    EndFor
  EndFor
EndFor
EndFor

As for the update of activity trajectories, if the new arrivals in $\tilde{\mathcal{I}}[\lambda_{n-1}, \lambda_n)$ are considered only, $\mathcal{R}^v_{latest}$, $\forall v \in \mathcal{V}$ will be updated by adding the new activity trajectories generated for the rentals in $\mathcal{I}_{latest}$ and $\tilde{\mathcal{I}}[\lambda_{n-1}, \lambda_n)$, i.e., $\mathcal{R}^v_{latest} := \mathcal{R}^v_{latest} \bigcup \mathcal{C}^v \bigcup \mathcal{M}^v$, $\forall v \in \mathcal{V}$. Different from the arrival of rentals in $\tilde{\mathcal{I}}[\lambda_{n-1}, \lambda_n)$, which will not affect the feasibility and profits of the already generated activity trajectories, the cancellation of the rentals in $\hat{\mathcal{I}}[\lambda_{n-1}, \lambda_n)$ will in most cases influence the profit and even make the already generated activity trajectories infeasible. Therefore, the consideration of rental cancellation requires rechecking the feasibility of each already generated activity trajectory covering any canceled rentals and updating the corresponding profit if it is feasible. Specifically, for each rental i in $\hat{\mathcal{I}}[\lambda_{n-1}, \lambda_n)$, each activity trajectory r covering i among the activity trajectories in $\bigcup_{v \in \mathcal{V}} \mathcal{R}^v_{latest}$ is found, and the feasibility of travel time and electricity consumption is rechecked for r after i is removed from it. If the activity trajectory r is no longer feasible, it will be removed from $\mathcal{R}^{v_r}_{latest}$; otherwise, it will be retained and the corresponding profit, i.e., $\overline{P}_r$, will be updated accordingly.

The algorithm design for the RT-VR&CS problem is finalized by packaging the solution methods developed in Section 4.3 into the dynamic algorithmic framework constructed in Section 4.2.

4.4 Numerical Experiments

In this section, random instances are generated to evaluate the performance of the

proposed solution method against two benchmark approaches. A case study created from EVCARD in China is conducted to further assess the efficiency of the proposed solution method when implemented in a real-world CSS, and explore how the algorithm-related parameters, the demand dynamism, the service charge, and the relocation cost affect the system performance. For the simplicity of algorithm implementation, when determining the available information of EVs for static problems, if an EV is in the course of relocation to another station, it is enforced to be available only when the current relocation operation is completed. The algorithms are coded in C++ calling Gurobi 9.0.0 on a personal computer with Intel (R) Core (TM) Duo 3.0 GHz CPU.

4.4.1 Computational performance of the proposed solution method

In this subsection, the benchmark approaches and the parameter settings of a series of representative random instances will be introduced. These instances will be used to evaluate the efficiency of the proposed solution method.

4.4.1.1 Benchmark approaches

To demonstrate the computational performance of the proposed solution method in terms of solution quality, an insertion-based approach and an optimality-based benchmark approach are further developed. Both the two benchmark approaches follow the same rolling time horizon framework as the dynamic algorithmic framework proposed in Section 4.2 but employ different techniques to solve the static problems. Specifically, the insertion-based approach employs a fast insertion-based heuristic, which is generalized from the study by Solomon (1987), to generate a solution to the k^{th} ($k \geq 2$) static problem based on the activity trajectories implemented by EVs in previous static problem. The optimality-based approach solves each static problem to optimality with an unlimited amount of time at each decision epoch to generate all the activity trajectories using the multi-label method with $N_{label} = +\infty$. Although it may not be implementable in the real-time setting, the optimality-based approach serves as a good reference to measure the solution quality of the proposed solution method. In what follows, the detailed procedure of the insertion-based approach is elaborated.

For the first static problem, same as the proposed solution method, the insertion-based approach generates activity trajectories for the rentals in the set $\mathcal{I}_0$ by using the multi-label method introduced in Subsection 4.3.2.2, and obtains a solution, i.e., a set of activity trajectories that are implemented by EVs in the set $\mathcal{V}$, by solving the restricted set-packing-

type model [S-VR&CS[1]] formulated upon these activity trajectories. For the k^{th} ($k \geq 2$) static problem, the solution is constructed within the time interval $[t_k, t_k + \tau]$ based on the solution to the $(k-1)^{th}$ static problem. For ease of presentation, let $\bar{\mathcal{R}}_{k-1}$ denote the set of activity trajectories that are implemented by EVs in the set $\mathcal{V}$ for the $(k-1)^{th}$ static problem. At the decision epoch t_k, for each $r \in \bar{\mathcal{R}}_{k-1}$, the rentals that have been satisfied during the time interval $[t_{k-1} + \tau, t_k + \tau]$ will be removed, the relative sequence of the remaining rentals from $t_k + \tau$ onward will be kept, and the resultant activity trajectory will be added into the set $\bar{\mathcal{R}}_k$. Following the notations defined in Subsection 4.3.3, let $\tilde{\mathcal{I}}[t_{k-1}, t_k)$ and $\hat{\mathcal{I}}[t_{k-1}, t_k)$ denote the set of new arrivals and canceled rentals during the time interval $[t_{k-1}, t_k)$, respectively. The following steps will be implemented to construct a solution to the k^{th} static problem.

Step 1: For each rental $i \in \tilde{\mathcal{I}}[t_{k-1}, t_k)$, try to insert it into every possible activity trajectory in the set $\bar{\mathcal{R}}_k$ and find the activity trajectory $r \in \bar{\mathcal{R}}_k$ that results in the maximum profit increase. Let $\bar{r}$ denote the resultant activity trajectory after the rental i is inserted into r. If the maximum profit increase is larger than zero, i.e., $\bar{P}_{\bar{r}} - \bar{P}_r > 0$, replace r in the set $\bar{\mathcal{R}}_k$ with $\bar{r}$, i.e., $\bar{\mathcal{R}}_k = \left(\bar{\mathcal{R}}_k \setminus \{r\}\right) \cup \{\bar{r}\}$; otherwise, reject the rental i. If all the rentals in $\tilde{\mathcal{I}}[t_{k-1}, t_k)$ have been checked, go to Step 2.

Step 2: For each rental $i \in \hat{\mathcal{I}}[t_{k-1}, t_k)$, if it is covered by an activity trajectory r in the set $\bar{\mathcal{R}}_k$, remove it from r. Since the feasibility of travel time and electricity consumption of the activity trajectory r after the rental i is removed may no longer be maintained, the method proposed in Subsection 4.3.3.1 is adopted to obtain a feasible activity trajectory $\bar{r}$ for the corresponding EV. The activity trajectory r in the set $\bar{\mathcal{R}}_k$ is replaced with $\bar{r}$, i.e., $\bar{\mathcal{R}}_k = \left(\bar{\mathcal{R}}_k \setminus \{r\}\right) \cup \{\bar{r}\}$. If all the rentals in $\hat{\mathcal{I}}[t_{k-1}, t_k)$ have been examined, go to Step 3.

Step 3: After implementing Step 2, an initial solution to the k^{th} static problem has been obtained. To improve this solution, local search is performed on the activity trajectories in the set $\bar{\mathcal{R}}_k$. The local search techniques applied in this step include 2-opt operator, exchange operator, and relocate operator. Specifically, the basic idea in 2-opt is to combine two activity

trajectories, namely, Trajectory 1 and Trajectory 2, such that the rentals served after a rental i in Trajectory 1 are inserted into Trajectory 2 after rental j, and the rentals after rental j in Trajectory 2 are moved to Trajectory 1 after rental i. The exchange operator swaps two rentals in two different activity trajectories. The relocate operator simply moves a rental from one activity trajectory to another. Kindly note that the feasibility of travel time and electricity consumption should be rechecked when applying the local search techniques.

4.4.1.2 Parameter setup

In order to create random instances, a transportation network in a Euclidean plane of 40 km by 40 km, where the travel distance between any two points is the Euclidean distance between them, is built up. Specifically, $|\mathcal{S}|$ stations are uniformly chosen from the Euclidean plane. The pick-up and drop-off stations of each rental $i \in \mathcal{I}$ and the initial location of each EV $v \in \mathcal{V}$ before the planning horizon, i.e., s_i^o, s_i^d, and $\hat{s}_v^0$, are randomly selected among these stations. The planning horizon is assumed to be 8 hours. If the time duration is measured by minutes, then the planning horizon will be $[0, 480]$. The time between two consecutive decision epochs and the computation time limit for each static problem, i.e., Δ and τ, are set to be 15 min and 2 min, respectively.

For a rental i, if it is reserved before the planning horizon, i.e., $i \in \mathcal{I}_0$, the pick-up time t_i^o is randomly chosen from the integer set $\{0, 1, 2, ..., 480\}$; otherwise, t_i^o is a random integer selected from the set $\{\Delta+\tau, \Delta+\tau+1, \Delta+\tau+2, ..., 480\}$. Accordingly, since the rentals in the set $\mathcal{I}_0$ have been known at the beginning of the planning horizon, the reservation times of them are uniformly set to be a negative number, e.g., -1. As for a rental $i \in \mathcal{I} \setminus \mathcal{I}_0$, the reservation time t_i^r is generated according to the following rule: if $t_i^o - \left\lfloor \frac{t_i^o}{\Delta} \right\rfloor \times \Delta \geq \tau$, t_i^r is a uniform random integer from the set $\left\{0, 1, ..., \left\lfloor \frac{t_i^o}{\Delta} \right\rfloor \times \Delta - 1\right\}$; otherwise, t_i^r is randomly generated from the set $\left\{0, 1, ..., \left(\left\lfloor \frac{t_i^o}{\Delta} \right\rfloor - 1\right) \times \Delta - 1\right\}$. The above rule also applies to the generation of cancellation time of a rental except that the start point of the integer set is $t_i^r + 1$. Valid reservation and cancellation times are generated in this way to ensure that they can be considered by the static

problems.

Let $d(s_i^o, s_i^d)$ denote the Euclidean distance between the pick-up station and the drop-off station of the rental $i \in \mathcal{I}$, and ς_i represent its minimum rental duration. The average travel speed of users is assumed to be $v = 40$ km/hr. For a rental i, if it is a one-way trip, i.e., the drop-off station is different from the pick-up station, the minimum rental duration would be $\varsigma_i = d(s_i^o, s_i^d)/v$; otherwise, ς_i is set to be 30 min to ensure the revenue gains of a carsharing operator. The arrival time of a rental $i \in \mathcal{I}$, i.e., t_i^d, is thus randomly generated from the integer set $\{t_i^o + \varsigma_i, t_i^o + \varsigma_i + 10 \text{ min}, t_i^o + \varsigma_i + 20 \text{ min}, ..., t_i^o + \varsigma_i + 60 \text{ min}\}$.

All the EVs are assumed to be equipped with a 20-kWh lithium-ion battery and the discharge rate of the battery, denoted by ξ, is set to be 30%/hr (Nissan, 2021). The electricity consumption of a rental $i \in \mathcal{I}$, i.e., e_i, is randomly generated from the interval $[\varsigma_i, t_i^d - t_i^o] \times \xi$. The initial SOC of all EVs in the set $\mathcal{V}$ is assumed to be uniformly distributed between 70% and $SOC_{\max}$. The relocation time from the drop-off station of a rental $i \in \mathcal{I}$ to the pick-up station of a rental $j \in \mathcal{I}$, i.e., $\tau(s_i^d, s_j^o)$, is calculated by $\tau(s_i^d, s_j^o) = d(s_i^d, s_j^o)/v$ and the corresponding electricity consumption would be $e(s_i^d, s_j^o) = \tau(s_i^d, s_j^o) \times \xi$. The minimum allowable SOC, i.e., $SOC_{\min}$, in the carsharing system is set to be 0.1. The parameters in the nonlinear charging profile are adopted from the numerical example of Pelletier et al. (2017).

Without loss of generality, it is assumed that the CSSs are charged by rental duration and the service charge is set to be 0.3 \$/min. The penalty for rejecting a rental due to the limited fleet size is assumed to be 0.15 \$/min, i.e., half of the revenue generated from the rental. The relocation cost is set to be 0.3 \$/min. The algorithm-related parameters are set as follows: $N_{label} = 2$, $\mu_1 = 1$ (i.e., $\mu_2 = 0$), $\varepsilon = 0$, $\sigma = 0$, and $Z = 1000$.

4.4.1.3 Assessment of the proposed solution method

To evaluate the efficiency of the proposed solution method, given the total number of rentals (#Demand) and the number of cancellations (#Cancellation), i.e., #Demand=200 and #Cancellation=10, three instances with different combinations of the number of stations (#Station), the fleet size (#EV), and the number of arrivals during the planning horizon (#Arrival), i.e., $\#\text{Station} \in \{30, 60\}$, $\#\text{EV} \in \{35, 70\}$, and $\#\text{Arrival} \in \{80, 130, 180\}$, are

randomly generated and the average results are reported. It should be noted that the number of arrivals during the planning horizon reflects the degree of dynamism when both the total number of rentals and the number of cancellations are fixed.

Table 4.1 compares the performance of the proposed solution method and the two benchmark approaches, i.e., the insertion-based approach (INS) and the optimality-based approach (OPT), in terms of the number of satisfied rentals (#SR) and the system profitability. In order to have a more intuitive comparison, the difference in satisfied rentals (Diff_SR) between the proposed solution method and the benchmark approaches and the relative increase of profit (Diff_Profit) by the proposed solution method with respect to the benchmark approaches are also reported. It shows that all the numbers of satisfied rentals and the profits achieved by the proposed solution method are larger than that obtained by the insertion-based approach. Notably, the difference in the number of served rentals and the relative gap in profit reach as high as 9.0 and 35.6%, respectively. This suggests the obvious advantage of the proposed solution method over the insertion-based approach. As for the comparison between the proposed solution method and the optimality-based approach, it can be seen that under most combinations of #Station, #EV, and #Arrival, the proposed solution method serves fewer rentals and produces less profit than the optimality-based approach. Nevertheless, the number of satisfied rentals and profit achieved by the proposed solution method are at most 4.0 and 5.59% lower than that obtained by the optimality-based approach respectively. It is worth noting that under 3 out of 12 combinations of #Station, #EV, and #Arrival, the proposed solution method obtains equivalent or higher numbers of satisfied rentals and/or profits. This indicates that the optimality-based approach, which solves each static problem to optimality, not necessarily produces a better solution over the entire planning horizon than the proposed solution method, which seeks to obtain a good-quality solution to each static problem. Overall, the above results demonstrate the efficiency of the proposed solution method in solving the RT-VR&CS problem.

Table 4.1 Comparison of the proposed solution method and the benchmark approaches based on randomly generated instances

#Station	#EV	#Arrival	INS		OPT		Proposed method		Comparison			
			#SR	Profit ($)	#SR	Profit ($)	#SR	Profit ($)	$Diff\_SR^{INS}$	$Diff\_Profit^{INS}$ (%)	$Diff\_SR^{OPT}$	$Diff\_Profit^{OPT}$ (%)
30	35	80	140.0	1,789	149.3	2,336	148.3	2,299	8.3	28.5	-1.0	-1.58
30	35	130	140.0	1,670	149.0	2,267	149.0	2,262	9.0	35.4	0.0	-0.22
30	35	180	140.3	1,721	145.7	2,207	144.7	2,162	4.4	25.6	-1.0	-2.04
30	70	80	186.3	3,287	189.0	3,443	188.3	3,395	2.0	3.3	-0.7	-1.39
30	70	130	185.0	3,219	188.0	3,371	187.0	3,333	2.0	3.5	-1.0	-1.13
30	70	180	181.7	3,155	188.0	3,365	184.0	3,177	2.3	0.7	-4.0	-5.59
60	35	80	138.0	1,694	147.0	2,263	144.7	2,186	6.7	29.0	-2.3	-3.40
60	35	130	134.3	1,471	140.7	1,984	140.7	1,995	6.4	35.6	0.0	0.55
60	35	180	135.0	1,475	139.7	1,930	140.7	1,924	5.7	30.4	1.0	-0.31
60	70	80	184.3	3,097	188.3	3,293	187.3	3,271	3.0	5.6	-1.0	-0.67
60	70	130	183.0	3,061	187.0	3,220	186.0	3,179	3.0	3.9	-1.0	-1.27
60	70	180	182.0	3,076	186.7	3,247	185.0	3,130	3.0	1.8	-1.7	-3.60

4.4.2 Case study of EVCARD

Initiated in 2015, EVCARD is the first one-way carsharing company in China that provides EV CSSs. It has deployed more than 13,000 stations in 65 cities of China with 50,000 vehicles put into use. In this study, the CSS of EVCARD in three districts of Suzhou, namely, Kunshan, Xiangcheng, and Wujiang, are considered. Figure 4.6 depicts the deployment of stations in the three districts, with 70 stations in Kunshan, 27 stations in Xiangcheng, and 29 stations in Wujiang. The configuration of these stations, e.g., the shortest travel time between each station pair, is obtained from Google Maps (Google, 2022). In addition, multiple stations are merged into one if the shortest travel time between them is within 5 min. After the merging process, 57 stations are obtained. It is assumed that 50 EVs are provided in these stations. Unless stated otherwise, the parameter settings are the same with Subsection 4.4.1.2.

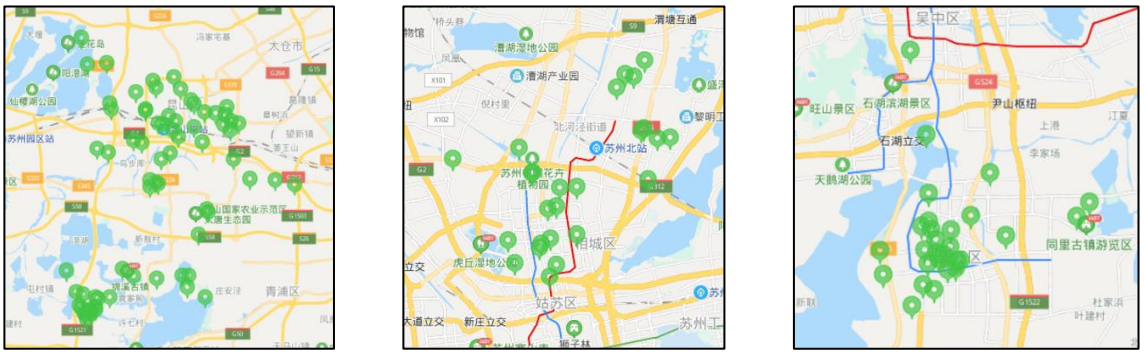

(a) Kunshan (b) Xiangcheng (c) Wujiang

Figure 4.6 Station deployment in three districts of Suzhou

4.4.2.1 Assessment of the proposed solution method in EVCARD

To assess the performance of the proposed solution method in the real-world CSS of EVCARD, this subsection compares it with the two benchmark approaches. Totally five groups of instances with a total of 200 rentals are generated, and three levels of dynamism characterized by different numbers of arrivals during the planning horizon, i.e., 80, 130, and 180, are considered for each instance group. The number of cancellations is set to be 10. Different from Table 4.1, which presents the average results that hide much of the variability, Table 4.2 shows the results of each individual instance.

It can be seen that the minimum and the maximum numbers of satisfied rentals obtained by the proposed solution method in the total 15 instances are 159 and 174 respectively, greatly larger than 150 and 160 achieved by the insertion-based approach and comparable to 161 and 174 produced by the optimality-based approach. In addition, the proposed solution method

serves at least 6 rentals more than the insertion-based approach and the largest gap in the number of satisfied rentals reaches 19. As for the comparison to the optimality-based approach in terms of service level, the proposed solution method obtains at most 6 rentals fewer than the optimality-based approach among the 15 instances; in 4 out of the 15 instances, the proposed solution method serves more rentals than the optimality-based approach. Regarding the profitability, the insertion-based approach and the optimality-based approach obtain a profit of around $2,200 and $2,800 in majority of the 15 instances respectively, whereas the proposed solution method produces a profit of about $2,700. As a result, the relative gap of profit between the proposed solution method and the insertion-based approach is larger than 7.5% in all of the 15 instances and the maximum reaches as high as 29.5%; the proposed solution method achieves less profit than the optimality-based approach by at most 9.1% and it performs better in 2 out of the 15 instances. These results prove the efficiency of the proposed solution method in a real-world application.

In addition, it can also be observed from Table 4.2 that the proposed solution method obtains different numbers of satisfied rentals and daily profits. When the number of arrivals during the planning horizon grows from 80 to 180 with an increment of 50, the daily profit first decreases and then rises in the five groups of instances. The reason for this obtained result may be as follows. On one hand, when more users make reservations during the planning horizon, the number of rentals known before the system operation declines. Hence, fewer promising activity trajectories would be generated at the beginning of the planning horizon, which may exert negative influence on the daily profit. On the other hand, as the demand dynamism increases, a larger number of activity trajectories would be generated during the planning horizon, which could contribute to the profitability improvement. Therefore, when the number of arrivals during the planning horizon rises, if the negative aspect dominates, the daily profit would reduce, and vice versa. In Subsection 4.4.2.2, how the demand dynamism affects the system performance will be explored in more detail.

Table 4.2 Comparison of the proposed solution method and the benchmark approaches on EVCARD

InstanceGroup	#Arrival	INS		OPT		Proposed method		Comparison			
		#SR	Profit ($)	#SR	Profit ($)	#SR	Profit ($)	$Diff\_SR^{INS}$	$Diff\_Profit^{INS}$ (%)	$Diff\_SR^{OPT}$	$Diff\_Profit^{OPT}$ (%)
1	80	158	2,429	167	2,902	165	2,814	7	15.9	-2	-3.0
	130	155	2,178	170	2,745	168	2,736	13	25.6	-2	-0.3
	180	159	2,599	171	2,984	174	2,918	15	12.3	3	-2.2
2	80	160	2,316	173	2,937	174	2,876	14	24.2	1	-2.1
	130	152	2,210	167	2,842	165	2,725	13	23.3	-2	-4.1
	180	155	2,336	166	2,783	168	2,878	13	23.2	2	3.4
3	80	153	2,156	174	2,828	172	2,783	19	29.1	-2	-1.6
	130	155	2,270	173	2,898	168	2,734	13	20.4	-5	-5.7
	180	155	2,212	171	2,858	169	2,817	14	27.4	-2	-1.4
4	80	153	2,171	168	2,753	171	2,812	18	29.5	3	2.1
	130	153	2,298	168	2,861	162	2,602	9	13.2	-6	-9.1
	180	156	2,330	172	2,739	168	2,604	12	11.8	-4	-4.9
5	80	157	2,404	169	2,847	163	2,690	6	11.9	-6	-5.5
	130	151	2,195	161	2,488	159	2,369	8	7.9	-2	-4.8
	180	150	2,021	163	2,588	162	2,534	12	25.4	-1	-2.1

4.4.2.2 Sensitivity analysis

In this subsection, extensive numerical experiments are conducted to investigate how the algorithm-related parameters (including N_{label}, μ_2, ε, and σ), the demand dynamism, the service charge, and the relocation cost affect the performance of the one-way electric carsharing system. Through these numerical experiments, the concern of the carsharing operator, i.e., how these parameters affect the system profitability and service level, is addressed. Hence, the daily profit and the satisfied ratio, an indicator that reflects the service level of the carsharing system and is defined as the ratio of the number of satisfied rentals to the total number of rentals that are not canceled during the planning horizon (#SR/#Rental), are reported. For the readers' interest in the time allocation of EVs, the rental time per vehicle (RentalTime), the relocation time per vehicle (RelocationTime), and the idle time per vehicle for charging (ChargeTime) are also reported. Again, three instances with 200 rentals are generated and the average results are presented. Unless specified otherwise, the number of dynamic arrivals is set to be 160.

Impact of N_{label} and μ_2

The maximum number of labels generated for a node through a specific link, i.e., N_{label}, and the weight of SOC, i.e., μ_2, in the proposed multi-label method jointly determine the number and quality of the activity trajectories generated for the first static problem. These activity trajectories fundamentally decide the quality of activity trajectories generated for the subsequent static problems to some extent. Therefore, different values of N_{label} and μ_2 will induce different performances of a one-way electric carsharing system. Hence, the variations of the performance indicators with respect to the above two parameters are tested. The number of dynamic arrivals is set to be 70 considering that the impact of the two parameters on the performance of the carsharing system may be more visible when the already-known rentals before the planning horizon account for a relatively large proportion.

Figure 4.7 plots the variations of the performance indicators when N_{label} increases from 2 to 10. It can be seen that blindly increasing N_{label} may not improve the system profitability, as the daily profit decreases when N_{label} increases from 2 to 4 and 6 to 10. In fact, compared with a lower value of N_{label}, a higher one generally means that more and diverse activity trajectories will be generated for the first static problem, which serve as the base activity trajectories for

the subsequent static problems. On the other hand, these activity trajectories require more time to solve the LP problem in each iteration of the dynamic column generation process, and thus negatively influence the quality of activity trajectories generated for the subsequent static problems. Hence, along with the increase of N_{label}, if the negative effect dominates the positive effect, the daily profit would reduce. As for the satisfied ratio, an interesting phenomenon is that it follows the opposite trend with the daily profit when N_{label} grows from 4 to 8. This may be because a larger daily profit not necessarily means a higher service level when more profitable but fewer rentals are served, and vice via. Overall, under the current parameter settings, a preferable solution for both the operator and users can be obtained by setting N_{label} to be 2, under which the carsharing system can simultaneously obtain relatively high daily profit and provide high-quality service. Regarding the time allocation of EVs, the time-related indicators remain relatively insensitive to N_{label}, although there exists a slight drop and growth for the relocation time and charging time respectively when N_{label} increases from 4 to 6. Roughly, 51%, 41%, and 8% of the operational period is used for rental service, charging operation, and relocation operation, respectively.

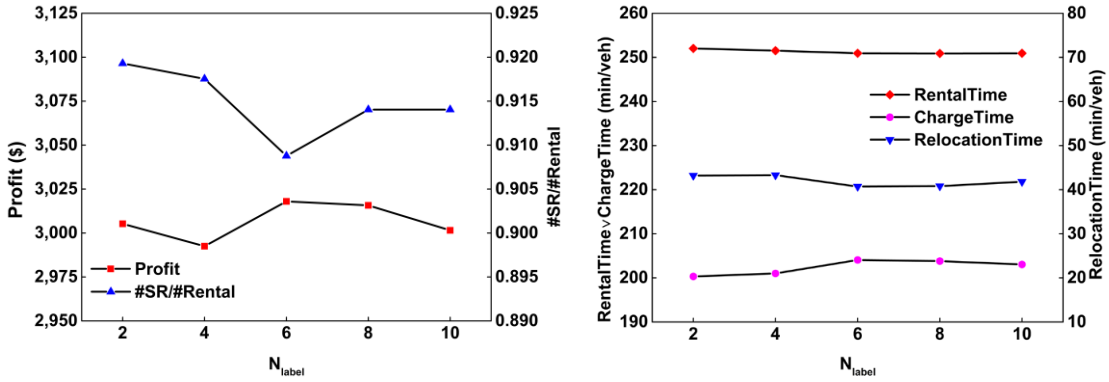

(a) Impact on daily profit and satisfied ratio (b) Impact on time-related indicators

Figure 4.7 Impact of N_{label} on the performance of a one-way electric carsharing system

Unlike N_{label} that limits the number of labels, μ_2 reflects the emphasis on SOC relative to profit when generating the labels. The variations of the performance indicators with respect to μ_2 are plotted in Figure 4.8. It shows that the satisfied ratio and the daily profit reach the maximum values of about 0.923 and \$3,060 at μ_2=0.5 and μ_2=0.25 respectively. By weighing the pros and cons, under the current parameter settings, letting the weight of SOC to be 0.25 may be the best choice considering the operator's pursuit of profit and the users' desire

for high-quality service. An interesting observation is that when μ_2 increases from 0 to 0.25, the satisfied ratio remains almost stable, while the daily profit shows an obvious growth. For the obtained result, it is guessed that when implementing the multi-label method, if the labels with higher SOC are given higher priority by increasing μ_2 from 0 to 0.25, EVs are likely to perform more profitable activity trajectories. This is consistent with the expectation that a label at a node with a lower profit but a higher SOC is likely to develop into activity trajectories that are more profitable by traversing rentals with higher electricity consumption, and justifies the incorporation of SOC other than profit in the determination of generated labels in Algorithm 4.1. Another phenomenon is that when μ_2 is further increased from 0.25 to 0.5, the satisfied ratio grows, whereas the daily profit shows an obvious decline. This may be because that although the higher priority for SOC allows EV to perform activity trajectories with more rentals, the lower priority for profit of labels would exert negative influence on the profits of these activity trajectories. If the negative influence dominates, the daily profit may decrease. Regarding the time-related indicators, both the relocation time and charging time fluctuate slightly with respect to μ_2, and the rental time remain relatively stable.

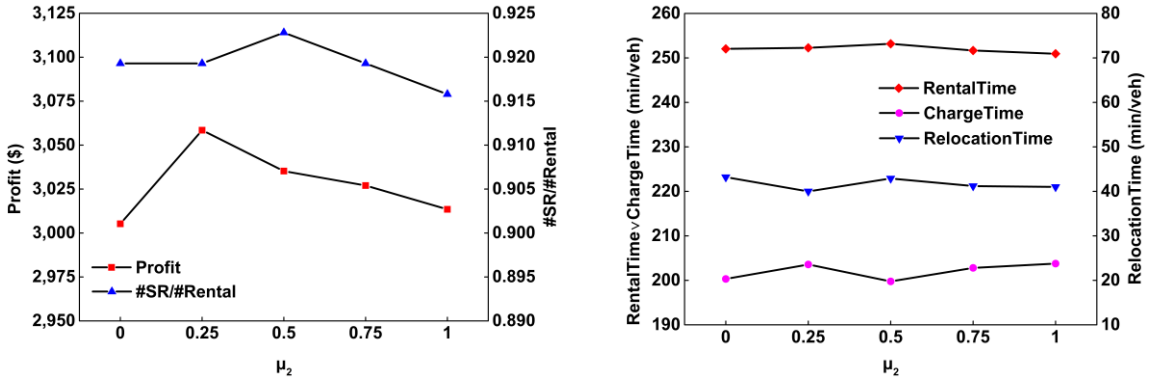

(a) Impact on daily profit and satisfied ratio (b) Impact on time-related indicators

Figure 4.8 Impact of μ_2 on the performance of a one-way electric carsharing system

Impact of ε and σ

Different from N_{label} and μ_2, which affect the activity trajectories generated for all static problems by initially altering the activity trajectories generated for the first static problem, the thresholds for the reduced cost of activity trajectories and the profit difference of activity trajectories, i.e., ε and σ, exert an effect on the activity trajectories generated for the subsequent static problems by influencing the dynamic column generation process. More specifically, in each iteration of the dynamic column generation process, ε determines the

activity trajectories that can be inserted by the newly arriving rentals and σ elects which ones among the activity trajectories that the newly arriving rentals can be feasibly inserted into are finally generated. Hence, in a real-time context, different values of ε and σ will affect the dynamic column generation process, and thus distinctive activity trajectories for the subsequent static problems will be generated. Therefore, how the performance indicators vary with respect to the two parameters is examined.

Figure 4.9 and Figure 4.10 illustrate the variations of the performance indicators when ε and σ increase from -160 to 0 and -40 to 0 respectively. Figure 4.9 shows that the satisfied ratio and the daily profit decrease with the growth of ε except that there exists a fluctuation for the latter at $\varepsilon = -80$, and both of them achieve the maximum value at $\varepsilon = -160$. Hence, -160 can be a suitable threshold for the reduced cost to determine the activity trajectories that can be inserted by the newly arriving rentals. Along with the rise of ε, the rental time shows insensitivity, whereas the relocation time and charging time fluctuate marginally. Figure 4.10 reveals that under the current parameter setting, -30 is an appropriate threshold for profit difference between two activity trajectories in the dynamic column generation process, as the system profitability and service level simultaneously peak at $\sigma = -30$. In addition, all the time-related indicators remain relatively stable with respect to σ. According to the initial expectation, lower values of ε and σ generally mean that more activity trajectories are generated for the newly arriving rentals, and activity trajectories that are more profitable are likely to be generated in later sub-horizons to improve the overall profitability of a carsharing system. However, it can be seen from Figure 4.9 and Figure 4.10 that lower values of ε and σ lead to lower daily profits in some cases. For the obtained result, the reason may be as follows: Under smaller values of ε and σ, more activity trajectories covering the newly arriving rentals can be generated in general in each iteration of dynamic column generation process. On one hand, these activity trajectories are likely to positively develop into more promising ones in later sub-horizons that can contribute to the total profit maximization over the whole planning horizon. On the other hand, these activity trajectories would negatively affect the efficiency of column generation and fewer dynamic iterations can be performed to generate new activity trajectories. The insufficient number of iterations may bring about the lowered quality of the activity trajectories generated in later sub-horizons, which may reduce the overall profitability of the carsharing system. Hence, when ε and σ decrease, if the negative aspect outweighs the positive aspect, the daily profit would decline.

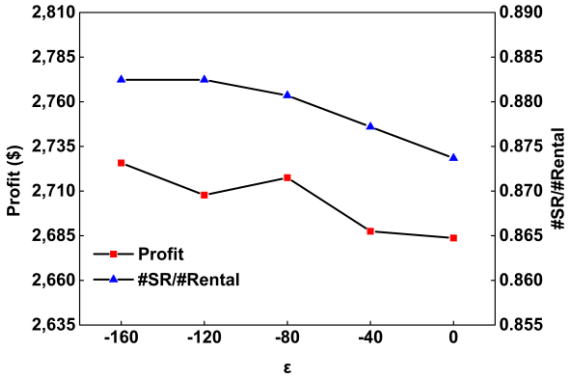

(a) Impact on daily profit and satisfied ratio

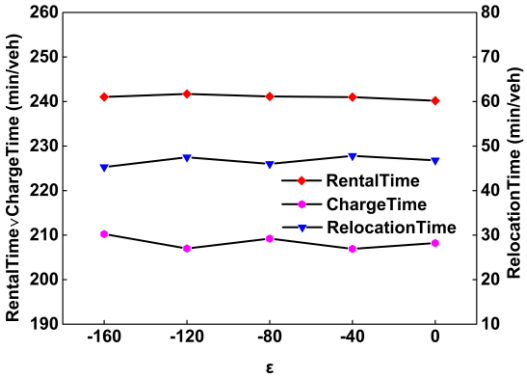

(b) Impact on time-related indicators

Figure 4.9 Impact of ε on the performance of a one-way electric carsharing system

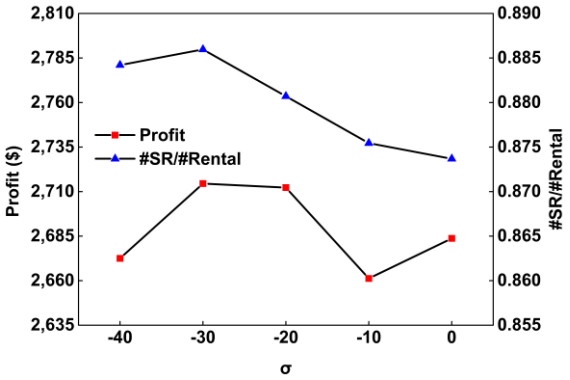

(a) Impact on daily profit and satisfied ratio

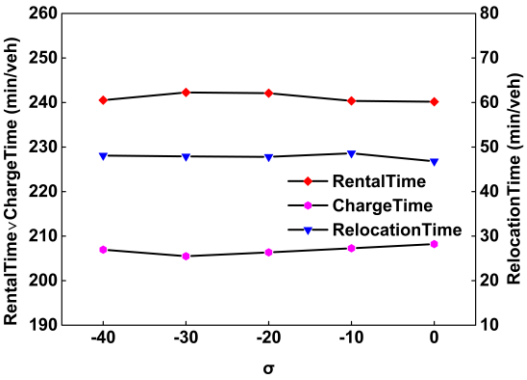

(b) Impact on time-related indicators

Figure 4.10 Impact of σ on the performance of a one-way electric carsharing system

Impact of demand dynamism

As was revealed in Subsection 4.4.2.1, a carsharing system performs differently in terms of service level and profitability under different demand dynamisms. Hence, how the performance of the carsharing system created from the real-world EVCARD is affected by the demand dynamism is explored in more detail. The results are plotted in Figure 4.11, where the number of arrivals during the planning horizon increases from 40 to 160. It can be seen that all the performance indicators are far more sensitive to demand dynamism in comparison to the algorithm-related parameters. Specifically, the increase of demand dynamism leads to the decrease of satisfied ratio and thus the general decline of rental time, whereas the relocation time grows with tiny fluctuations. This may suggest that when more users make ad-hoc reservations during the planning horizon, the proposed solution method would serve less of them by more time-consuming relocation operations. As a result, along with the growth of demand dynamism, the achieved profit decreases, and the charging time fluctuates.

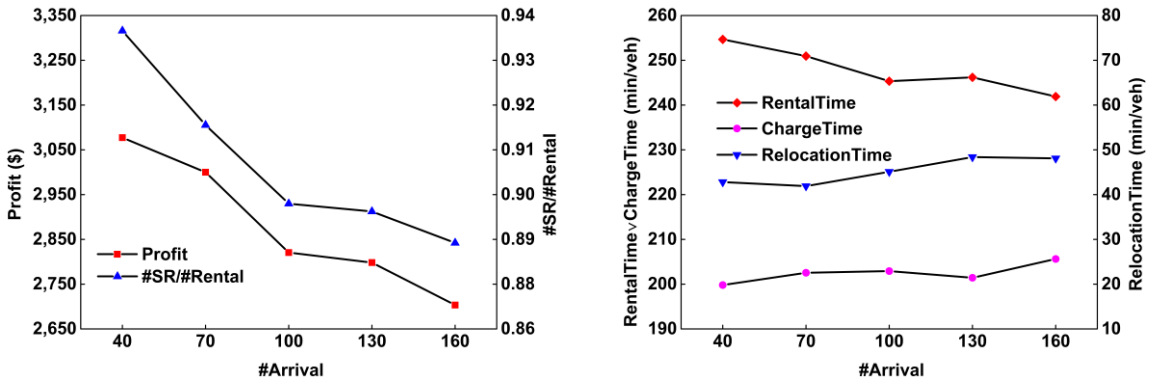

(a) Impact on daily profit and satisfied ratio (b) Impact on time-related indicators

Figure 4.11 Impact of demand dynamism on the performance of a one-way electric carsharing system

Impact of service charge and relocation cost

Last but not the least, the impacts of the two money-related parameters, i.e., service charge and relocation cost, on the performance of the carsharing system are further examined. The results are presented in Figure 4.12 and Figure 4.13. As expected, they demonstrate the significant effects of service charge and relocation cost on the profitability of CSSs. Figure 4.12 shows that if the service charge is set to be 0.1 $/min, the operator will only obtain a profit of about $300. A higher service charge would make all the rentals more profitable, and each EV would serve more users, generally with more time for relocation and less time (available) for charging. As a result, the daily profit grows almost linearly with the increase of service charge. In addition, a striking phenomenon is that when the service charge increases from 0.1 $/min to 0.15 $/min, there exists a relatively sharp growth in the satisfied ratio. For this result, it is guessed that when the service charge is relatively low, e.g., 0.1 $/min, most profit differences between two activity trajectories in the dynamic column generation process are lower than the pre-specified threshold, i.e., σ. This would cause that a number of rentals fail to be covered by any activity trajectory and thus cannot be served by EVs. When the service charge is increased to 0.15 $/min, majority of these rentals become more profitable and are served by EVs, which leads to the relatively sharp growth in the satisfied ratio. Figure 4.13 indicates that the increase of relocation cost exerts a diametrically opposite influence on the system performance compared with the service charge.

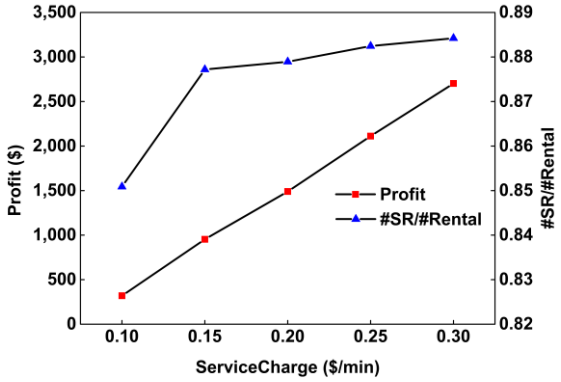

(a) Impact on daily profit and satisfied ratio

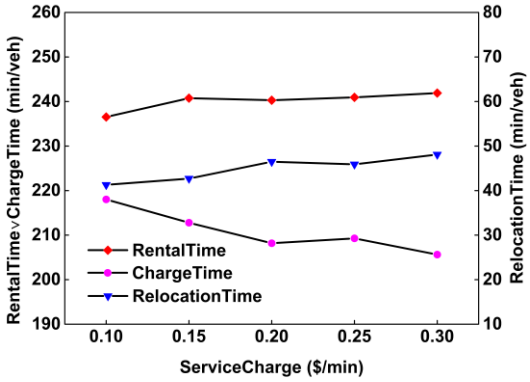

(b) Impact on time-related indicators

Figure 4.12 Impact of service charge on the performance of a one-way electric carsharing system

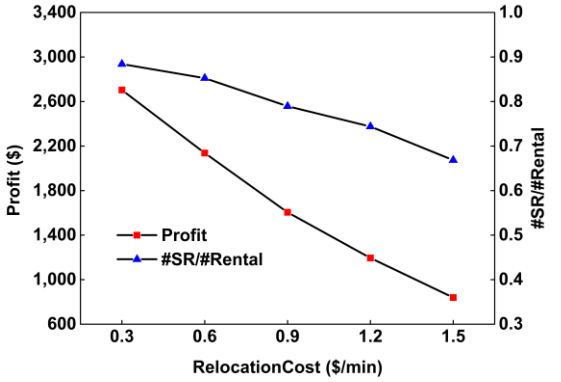

(a) Impact on daily profit and satisfied ratio

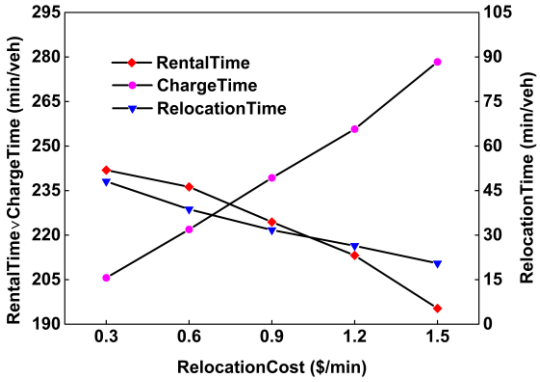

(b) Impact on time-related indicators

Figure 4.13 Impact of relocation cost on the performance of a one-way electric carsharing system

4.5 Concluding Remarks

This chapter addressed the RT-VR&CS problem for one-way electric CSSs considering demand dynamics and nonlinear charging profile. A dynamic algorithmic framework based on a rolling time horizon was established, in which the entire planning horizon was divided into a series of sub-horizons and an S-VR&CS problem was subsequently developed over each sub-horizon with respect to the latest information known up to the beginning of the sub-horizon. A set-packing-type formulation and a column-generation-based solution method were employed for each static problem. The multi-label method was proposed to generate activity trajectories for the first static problem. The activity trajectories for the subsequent static problems were efficiently generated in an online environment by utilizing existing activity trajectories generated for the previous static problem and three-phase local-search-based heuristic composed of rental replacement, rental insertion, and rental deletion. Based on numerical

experiments on randomly generated instances and a case study of EVCARD in China, several conclusions can be obtained. First, the proposed solution method shows obvious advantage over the insertion-based approach, which has been commonly adopted in the literature for various dynamic routing problems either as a main algorithm or as a benchmark for evaluating more sophisticated approaches. Second, in comparison to the optimality-based approach, which solves each S-VR&CS problem to optimality by taking an unlimited amount of time at each decision epoch and cannot be implemented in a real-time setting, the proposed solution method can obtain comparable-quality solutions. Third, the proposed solution method performs well in terms of robustness to algorithm-related parameters.

CHAPTER 5 REAL-TIME VEHICLE RELOCATION AND STAFF REBALANCING PROBLEM FOR ONE-WAY ELECTRIC CARSHARING SYSTEMS

This chapter proposes a real-time vehicle relocation and staff rebalancing (RT-VR&SR) problem for one-way electric CSSs considering demand dynamics and practical nonlinear charging profile of EVs. The RT-VR&SR problem aims to determine the strategies of vehicle relocation, vehicle charging, and staff rebalancing in a real-time fashion by maximizing the profit of carsharing operators. The RT-VR&SR problem is first formulated as an MDP. Subsequently, an efficient concurrent-scheduler-based policy is proposed for the MDP. Given the nonlinear charging profile, an innovative constrained non-dominated charging strategy considering scheduling restriction of staff is put up to facilitate the implementation of the policy. Numerical experiments on randomly generated instances and a case study based on a one-way electric carsharing company in China, i.e., EVCARD, are conducted to demonstrate the efficiency of the proposed policy and to analyse the impact of staff rebalancing. The results indicate that the proposed policy improves the service level and profitability greatly compared to a decomposition-based benchmark policy and ignoring staff rebalancing in the decision-making of vehicle relocation could cause the overestimation of service level and profitability. Finally, the effects of the demand dynamism, service charge, electricity cost, rebalancing cost, and rebalancing efficiency on the performance of one-way electric carsharing systems are analysed.

The remainder of this chapter is organized as follows. Assumptions, notations, and description of the RT-VR&SR problem are elaborated in Section 5.1. An MDP formulation is developed for the RT-VR&SR problem in Section 5.2. A concurrent-scheduler-based policy is proposed in Section 5.3. Section 5.4 conducts numerical experiments to assess the efficiency of the proposed policy, to analyse the impact of staff rebalancing, and to explore managerial insights. Conclusions are summarized in Section 5.5. Appendix C lists the notations used in this chapter.

5.1 Assumptions, Notations, and Problem Description

Consider a carsharing operator who provides daily ad-hoc one-way CSSs by managing a fleet of homogenous EVs and a crew of dedicated staff among a number of pre-determined stations located in an urban area over an operational period. Customers will reserve or cancel orders through a software-supporting platform anytime during the operational period. The

orders' reservation and/or cancellation information can only be known after the customers make the corresponding operations. An EV can be picked up by a customer or relocated from one station to another by a staff member. A staff member can perform a relocation task for an EV or self-rebalance between two stations by another transportation mode (e.g., bicycle and taxi). All the parking spots at a station are equipped with charging facilities for EV charging in idle times. Facing the dynamically changed order information, the carsharing operator needs to update the strategies of vehicle relocation, vehicle charging, and staff rebalancing to maximize the total profit. In the following subsections, the order information, EV activity trajectory & staff trip chain, and nonlinear charging profile of EVs will be elaborated. The notations used throughout this chapter can be found in Appendix C.

5.1.1 Order information

Let $\mathcal{S}$ denote the set of stations. Each order i is described by a quintuple $[s_i^o, s_i^d, t_i^o, t_i^d, e_i]$, where $s_i^o \in \mathcal{S}$ represents the pick-up station, $s_i^d \in \mathcal{S}$ denotes the drop-off station, t_i^o stands for the departure time from the pick-up station, t_i^d indicates the arrival time at the drop-off station, and e_i is the electricity consumption. The order i can be dynamically reserved and/or cancelled during the operational period $[0, T]$, and the reservation or cancellation information of it can only be known after the customer implements the corresponding operation through the platform. The fulfillment of the order i would generate profit represented by G_i. Nevertheless, given the limited number of EVs and staff members, the order i may be rejected, which would incur a penalty E_i. In addition, it is assumed without loss of generality that some orders grouped in the set $\mathcal{I}_0$ have been reserved before the operation.

5.1.2 EV activity trajectory & staff trip chain

At the beginning of the operational period, EVs grouped in the set $\mathcal{V}$ are distributed at different stations with different initial values of SOC. The initial location and SOC of an EV $v \in \mathcal{V}$ are denoted by s_v^0 and l_v^0, respectively. During the operational period, an EV may serve several orders, and vehicle charging and vehicle relocation may be implemented between any two adjacent orders, such as i and j, to ensure that they can be served successfully without violating the travel time and electricity consumption constraints. The travel time, the electricity

consumption, and the incurred operating cost for the relocation operation from the drop-off station of the order i to the pick-up station of the order j are represented by $\tau(s_i^d, s_j^o)$, $e(s_i^d, s_j^o)$, and $c(s_i^d, s_j^o)$ respectively. For ease of elaboration, a series of activities, e.g., under service/relocation/charging, underwent in turn by an EV is referred to as an *activity trajectory* of that vehicle. An activity trajectory illustrates a specific relocation and charging strategy of an EV and is regarded feasible if the EV can serve all the orders covered by it in time with SOC no lower than a threshold $SOC_{\min}$ imposed by the carsharing operator. The profit of an EV activity trajectory is expressed by the difference between the profit collected from the covered orders and the incurred EV relocation cost.

Similarly, staff members grouped in the set $\mathcal{F}$ are distributed at different stations at the beginning of the operational period. The initial location of a staff member $f \in \mathcal{F}$ is denoted by $\bar{s}_f^0$. A staff member may perform several relocation tasks during the daily operation. For ease of illustration, let a quadruple $[\bar{s}_m^o, \bar{s}_m^d, \bar{t}_m^o, \bar{t}_m^d]$ describe a given relocation task m, where $\bar{s}_m^o \in \mathcal{S}$ is the origin station, $\bar{s}_m^d \in \mathcal{S}$ represents the destination station, $\bar{t}_m^o$ denotes the departure time from the origin station, and $\bar{t}_m^d$ stands for the arrival time at the destination station. When performing these relocation tasks, a staff member may self-rebalance between two adjacent relocation tasks, namely, m and n, by taking another transport mode so that they can be performed feasibly in terms of travel time. The travel time and the incurred cost for the rebalancing operation from the destination station of the relocation task m to the origin station of the relocation task n are denoted by $\bar{\tau}(\bar{s}_m^d, \bar{s}_n^o)$ and $\bar{c}(\bar{s}_m^d, \bar{s}_n^o)$ respectively. Without loss of generality, it is assumed that a staff member will immediately self-rebalance to another station for the next relocation task after completing a relocation task. A series of relocation tasks and rebalancing operations performed in turn by a staff member is referred to as a *trip chain* of that staff member. A trip chain depicts a particular rebalancing strategy for a staff member and is deemed feasible if a staff member can perform all the relocation tasks covered by it in time. The cost of a trip chain is the sum of the cost incurred by the embedded rebalancing operations.

Consider a small electric carsharing system with eight stations (i.e., A-H), two EVs (i.e., EV 1 and EV 2), one staff member (i.e., Staff 1), and four orders (i.e., Order 1-4); Figure 5.1 shows the activity trajectories for the two EVs, i.e., 'Order 1 (from A to B) $\rightarrow$ relocation (from B to C) $\rightarrow$ charging (at C) $\rightarrow$ Order 2 (from C to D)' (for EV 1) and 'Order 3 (from E to F)

→ charging (at F) → relocation (from F to G) → Order 4 (from G to H)' (for EV 2), and a trip chain for the staff member, i.e., 'Task 1 (from B to C) → rebalancing (from C to F) → Task 2 (from F to G)'. It can be seen that EV activity trajectories and staff trip chains couple through vehicle relocation, as the relocation operations in EV activity trajectories serve as tasks in staff trip chains.

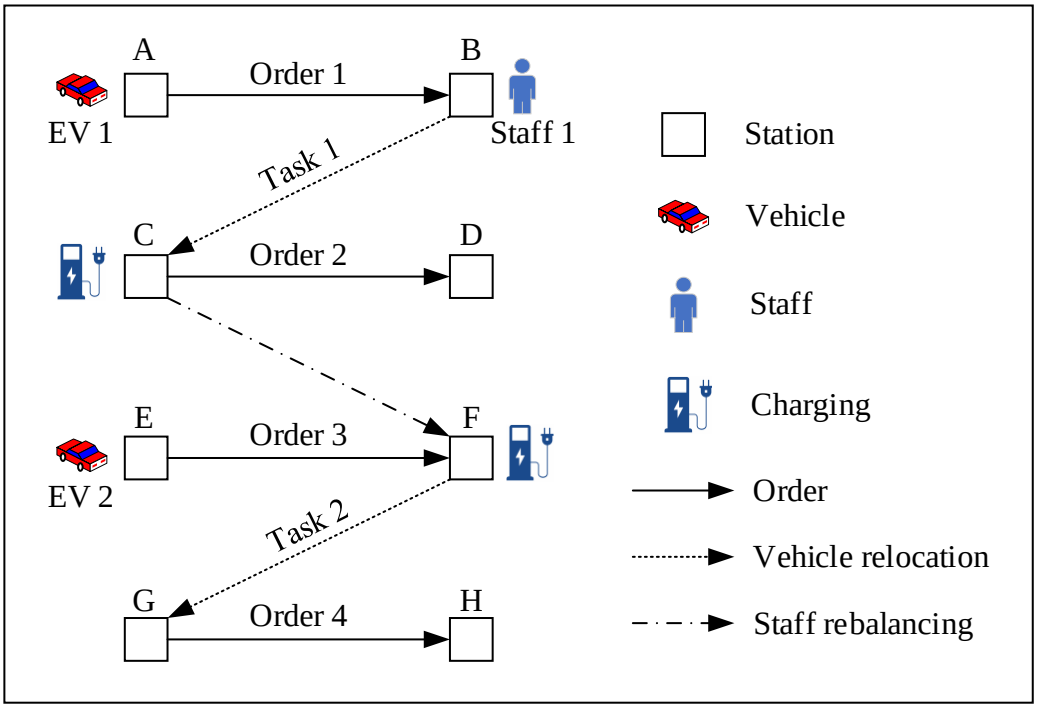

Figure 5.1 Illustration of vehicle relocation and staff rebalancing

5.1.3 Nonlinear charging profile

In practical applications, a constant current-constant voltage (CC-CV) or constant power-constant voltage (CP-CV) scheme is usually adopted to charge the battery of EVs to circumvent overcharging degradation (Liu, 2013). Under both realistic charging schemes, the SOC of an EV increases in a nonlinear manner regarding the charging duration, with the profile expressed by an implicit differential equation that has no analytical solutions (Marra et al., 2012; Pelletier et al., 2017). The temporal variations of SOC under the CC-CV and CP-CV schemes can be found in Figure 5.2. It can be observed that the charging amount of an EV is jointly determined by the charging duration and the initial SOC before charging, as SOC does not increase at the same rate. Same as we did in Chapter 4, we assume the final SOC of an EV, i.e., SOC_t, after the charging duration t from the initial SOC, i.e., SOC_0, is determined by an implicit function $FunSOC(\bullet)$, namely:

$$SOC_t = FunSOC(t \mid SOC_0) \tag{5.1}$$

Accordingly, the duration t required to charge an EV from SOC_0 to $SOC_t \geq SOC_0$ is calculated by an implicit function $FunTime(\bullet)$ as follows:

$$t = FunTime(SOC_t \mid SOC_0) \tag{5.2}$$

The values of SOC_t and t in the above two functions can be obtained based on the numerical solution to the differential equation of the charging profile. For the details of charging profiles of EVs, the interested readers can refer to the studies of Marra et al. (2012) and Pelletier et al. (2017).

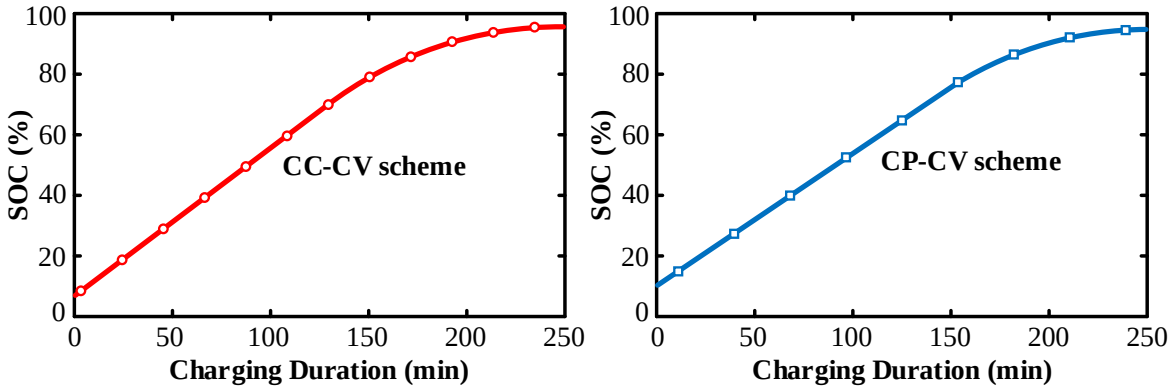

Figure 5.2 Illustration of nonlinear charging profiles by CC-CV and CP-CV schemes

5.2 MDP Formulation

In this section, the proposed RT-VR&SR problem is formulated as an MDP, which consists of decision epochs, state space, action space, transition dynamics, rewards, and objective function. In what follows, these elements are elaborated.

Decision epochs & state space. During the operational period $[0,T]$, a series of decision epochs are triggered in sequence by the random reservations or cancellations of customer orders. The system state at the k^{th} decision epoch triggered by an order reservation or cancellation is represented by $\mathcal{S}_k = (\boldsymbol{V}_k, \boldsymbol{F}_k, \mathcal{I}_k)$, where $\boldsymbol{V}_k = (V_{kv})_{v \in \mathcal{V}}$ and $\boldsymbol{F}_k = (F_{kf})_{f \in \mathcal{F}}$ are vectors of EV and staff available information at the k^{th} decision epoch respectively, and $\mathcal{I}_k$ is the set of unserved orders with departure time no earlier than the k^{th} decision epoch. The available information of each EV $v \in \mathcal{V}$ includes the earliest available time t_{kv}, available station s_{kv}, and corresponding SOC l_{kv}, i.e., $V_{kv} = (t_{kv}, s_{kv}, l_{kv})$. The available information of

each staff member $f \in \mathcal{F}$ comprises the earliest available time $\bar{t}_{kf}$ and available station $\bar{s}_{kf}$, i.e., $F_{kf} = (\bar{t}_{kf}, \bar{s}_{kf})$. All possible system states constitute the state space.

Action space. Given the available information of an EV $v \in \mathcal{V}$ and the set of unserved orders, i.e., V_{kv} and $\mathcal{I}_k$, let $\mathcal{P}_{kv}$ denote the set of all feasible activity trajectories for the EV v. All physically real relocation tasks, i.e., the relocation tasks with different origin and destination stations, embedded in an activity trajectory $p \in \mathcal{P}_{kv}$ for an EV $v \in \mathcal{V}$ is grouped in set $\mathcal{M}_{kvp}$. Then $\bigcup_{v \in \mathcal{V}, p \in \mathcal{P}_{kv}} \mathcal{M}_{kvp}$ is the set of all the relocation tasks possibly implemented by staff members. Given the information of a staff member $f \in \mathcal{F}$ and the set of relocation tasks, i.e., F_{kf} and $\bigcup_{v \in \mathcal{V}, p \in \mathcal{P}_{kv}} \mathcal{M}_{kvp}$, let $\mathcal{Q}_{kf}$ denote the set of all feasible trip chains for the staff member f. Then an action at the k^{th} decision epoch is described by $a_k = (\boldsymbol{x}, \boldsymbol{y})$, where $\boldsymbol{x} = (x_{vp})_{v \in \mathcal{V}, p \in \mathcal{P}_{kv}}$ is the vector of EV-trajectory decision, and x_{vp} equals 1 if the EV v implements the activity trajectory $p \in \mathcal{P}_{kv}$, and 0 otherwise; $\boldsymbol{y} = (y_{fq})_{f \in \mathcal{F}, q \in \mathcal{Q}_{kf}}$ is the vector of staff-chain decision and y_{fq} equals 1 if the staff member f performs the trip chain $q \in \mathcal{Q}_{kf}$, and 0 otherwise. To define the allowable actions under the system state s_k, the following constraints are introduced:

$$\sum_{p \in \mathcal{P}_{kv}} x_{vp} \leq 1, \quad \forall v \in \mathcal{V} \tag{5.3}$$

$$\sum_{v \in \mathcal{V}} \sum_{p \in \mathcal{P}_{kv}} \alpha_{vp}^{i} x_{vp} \leq 1, \quad \forall i \in \mathcal{I}_k \tag{5.4}$$

$$\sum_{q \in \mathcal{Q}_{kf}} y_{fq} \leq 1, \quad \forall f \in \mathcal{F} \tag{5.5}$$

$$\sum_{f \in \mathcal{F}} \sum_{q \in \mathcal{Q}_{kf}} \beta_{fq}^{m} y_{fq} = x_{vp}, \quad \forall v \in \mathcal{V},\ p \in \mathcal{P}_{kv},\ m \in \mathcal{M}_{kvp} \tag{5.6}$$

$$x_{vp} \in \{0,1\}, \quad \forall v \in \mathcal{V},\ p \in \mathcal{P}_{kv} \tag{5.7}$$

$$y_{fq} \in \{0,1\}, \quad \forall f \in \mathcal{F},\ q \in \mathcal{Q}_{kf} \tag{5.8}$$

where α_{vp}^{i} is the order-trajectory incidence coefficient that equals 1 if the order i is covered by activity trajectory $p \in \mathcal{P}_{kv}$, and 0 otherwise; β_{fq}^{m} is the task-chain incidence coefficient that

equals 1 if the relocation task m is covered by a trip chain $q \in \mathcal{Q}_{kf}$, and 0 otherwise. Constraint (5.3) ensures that each EV implements at most one activity trajectory. Constraint (5.4) limits that each order is covered by at most one EV. Constraint (5.5) imposes that each staff member performs at most one trip chain. Constraint (5.6) indicates that if an EV v implements an activity trajectory $p \in \mathcal{P}_{kv}$, then each physically real relocation task embedded in the activity trajectory p will be performed by a staff member, and vice versa. Constraints (5.7) and (5.8) define the domains of decisions. All allowable actions under all possible system states from the state space form the action space.

Transition dynamics. After the k^{th} decision epoch, another random order reservation or cancellation may trigger the $(k+1)^{th}$ decision epoch and the system state transits to s_{k+1}. Let $\xi_{k+1} = (t_{k+1}, i_{k+1}, \tilde{\mathcal{I}}_{k+1})$ denote the exogenous information that becomes known at the $(k+1)^{th}$ decision epoch, where t_{k+1} is the time point of the $(k+1)^{th}$ decision epoch, i_{k+1} represents the reserved or cancelled order at the $(k+1)^{th}$ decision epoch, $\tilde{\mathcal{I}}_{k+1}$ is the set of orders with the departure time between the k^{th} and the $(k+1)^{th}$ decision epochs. Then s_{k+1} is jointly determined by the state s_k, the action a_k, and the exogenous information ξ_{k+1} through the state transition function $S^M(\bullet)$:

$$s_{k+1} = S^M(s_k, a_k, \xi_{k+1}) \tag{5.9}$$

In the above state transition function, the available information of an EV $v \in \mathcal{V}$ and a staff member $f \in \mathcal{F}$ at the $(k+1)^{th}$ decision epoch, i.e., $V_{(k+1)v}$ and $F_{(k+1)f}$, is determined by the available information and action at the k^{th} decision epoch, i.e., V_{kv}, F_{kf}, and a_k, and the time point of the $(k+1)^{th}$ decision epoch, i.e., t_{k+1}. Specifically, given the available information V_{kv} and F_{kf} and the action a_k, at the time point t_{k+1}, the EV v may be charging at a station, under service for an order, or in the course of relocation to another station, whereas the staff member f may be waiting at a station, performing a relocation task, or self-rebalancing to another station. It is assumed that an EV is available instantly if it is at a station, whereas if an EV is serving a customer or under relocation to another station, it is available only when the service or relocation operation is completed. The same also applies to staff: a staff member is regarded available instantly if he/she is at a station; otherwise, he/she is deemed available only when the

relocation task or rebalancing operation is completed. As such, the available information of the EV v and the staff member f at the $(k+1)^{th}$ decision epoch can be obtained. Regarding the set of unserved orders by the $(k+1)^{th}$ decision epoch, i.e., $\mathcal{I}_{k+1}$, it can be obtained by $\mathcal{I}_{k+1} = (\mathcal{I}_k \setminus \tilde{\mathcal{I}}_{k+1}) \bigcup \{i_{k+1}\}$ if i_{k+1} is a newly reserved order, and $\mathcal{I}_{k+1} = (\mathcal{I}_k \setminus \tilde{\mathcal{I}}_{k+1}) \setminus \{i_{k+1}\}$ otherwise.

Rewards and objective function. As a result of choosing action a_k in state s_k under a specific decision rule, a function mapping state space into action space, the carsharing operator receives a one-period reward $r_k(s_k, a_k)$. The one-period reward $r_k(s_k, a_k)$ is defined as the expected profit of the carsharing system between the k^{th} and the $(k+1)^{th}$ decision epochs and its value depends on the time point of the $(k+1)^{th}$ decision epoch, i.e., t_{k+1}. On the one hand, according to what have been discussed earlier, given the action a_k in state s_k, the time point t_{k+1} determines the available information of each EV at the $(k+1)^{th}$ decision epoch, and thus the activity trajectory of each EV from the available time at the k^{th} decision epoch to the available time at the $(k+1)^{th}$ decision epoch. Here the activity trajectory of an EV from its available time at the k^{th} decision epoch to its available time at the $(k+1)^{th}$ decision epoch is referred to as the activity trajectory of it between the k^{th} and the $(k+1)^{th}$ decision epochs. The above expressions for activity trajectories of EVs also apply to the trip chains of staff members. On the other hand, the time point t_{k+1} determines the set of orders with the departure time between the k^{th} and the $(k+1)^{th}$ decision epochs, i.e., $\tilde{\mathcal{I}}_{k+1}$. Then the profit of the carsharing system between the k^{th} and the $(k+1)^{th}$ decision epochs can be calculated based on three terms: the profit generated from activity trajectories of EVs between the k^{th} and the $(k+1)^{th}$ decision epochs, the rebalancing cost incurred by trip chains of staff members between the k^{th} and the $(k+1)^{th}$ decision epochs, and the penalty for unserved orders in $\tilde{\mathcal{I}}_{k+1}$. Subsequently, the objective is to find a Markov policy z^*, which specifies the decision rule to be used at each decision epoch and is thus a sequence of decision rules, to maximize the expected total reward throughout the operational period by cumulating the one-period rewards:

$$\max_{z \in \mathcal{Z}} \mathbb{E}^{z} \left\{ \sum_{k=0}^{K} r_k(\mathcal{S}_k, a_k) \middle| \mathcal{S}_0 \right\} \tag{5.10}$$

where $\mathcal{Z}$ is the set of all possible Markov policies, K denotes the number of decision epochs by the end of the operational period, and $\mathcal{S}_0 = (\boldsymbol{V}_0, \boldsymbol{F}_0, \mathcal{I}_0)$ represents the initial state of the carsharing system at the beginning of the operational period with $V_{0v} = (0, s_v^0, l_v^0)$, $\forall v \in \mathcal{V}$ and $F_{0f} = (0, \bar{s}_f^0)$, $\forall f \in \mathcal{F}$.

The formulated MDP can be solved by the traditional dynamic programming method based on the Bellman operator iterations. However, due to the three notorious curses of dimensionality, i.e., the explosion of state space, outcome space, and action space, this method can become computationally intractable even for a small-sized problem (Powell, 2007). To overcome this computational intractability, an effective concurrent-scheduler-based policy is developed for the MDP. Details are described in the next section.

5.3 Concurrent-scheduler-based Policy

The concurrent-scheduler-based policy is developed based on the concurrent scheduler algorithm in Xu and Meng (2019) for the joint determination of vehicle relocation and staff rebalancing strategies. Under the concurrent-scheduler-based policy, the action at each decision epoch, i.e., the activity trajectory implemented by each EV and the trip chain performed by each staff member, is determined by extending the concurrent scheduler algorithm in Xu and Meng (2019) to factor in the staff rebalancing. More specifically, to determine the action at a particular decision epoch, pairs of EVs and staff members are jointly dispatched for fulfilling unserved orders such that the orders and relocation tasks can be assigned to EVs and staff members respectively in a parallel way. Here, a pair of an EV and a staff member is referred to as a *combination*. When dispatching a specific combination for serving a particular order, feasibility check will be conducted and incremental profit will be calculated if it is feasible. A feasible combination with the highest and positive incremental profit will be the decision for serving that order.

Take the action determination at the k^{th} decision epoch under the concurrent-scheduler-based policy as an example. Let p_{kv} and q_{kf} denote the activity trajectory implemented by an EV $v \in \mathcal{V}$ and the trip chain performed by a staff member $f \in \mathcal{F}$ at the k^{th} decision epoch, respectively. Recall that the system state at the k^{th} decision epoch is described by

$\mathcal{S}_k = (\boldsymbol{V}_k, \boldsymbol{F}_k, \mathcal{I}_k)$. To determine p_{kv} and q_{kf}, the orders in $\mathcal{I}_k$ are picked one by one in ascending order of their departure time. For a picked order, namely, j, a decision on which EV is relocated by which staff member to the pick-up station of the order j so that the order j can be served is first made. To achieve this, for each combination of an EV in $\mathcal{V}$ and a staff member in $\mathcal{F}$, its feasibility for serving the order j in terms of travel time and electricity consumption is checked, and the incremental profit is calculated if feasible. A feasible combination associated with the highest and positive incremental profit to carsharing operators, namely, v^* and f^*, will be the final decision for serving the order j. Given v^* and f^*, the order j is assigned to the EV v^* and the corresponding relocation task, if necessary, is assigned to the staff member f^*. If there exists no such combination, the order j will be rejected.

Considering the coordination between EVs and staff members and the implicit concave charging profile, the feasibility check of a combination, v and f for example, for serving the order j is not straightforward. Xu and Meng (2019) proposed a non-dominated charging strategy for a pair of preceding & succeeding orders, by which the resultant SOC of an EV at the departure time of the succeeding order is not less than that by any other feasible charging strategies. Here, the charging strategy for a pair of preceding & succeeding orders refers to the charging durations at the preceding order's drop-off station and the succeeding order's pick-up station. If the non-dominated charging strategy does not exist, it implies that an EV cannot arrive at the pick-up station of the succeeding order no later than its departure time with SOC higher than or equal to $SOC_{\min}$. In this study, the non-dominated charging strategy in Xu and Meng (2019) is extended to a constrained non-dominated charging strategy (CNCS) by factoring in the scheduling restriction of staff. For ease of illustration, let i_v represent the last order assigned to the EV v and $l_{i_v}^d$ be the corresponding SOC of the EV after it arrives at the drop-off station of the order i_v. If no order in $\mathcal{I}_k$ has yet been assigned to the EV v, it is assumed that the last order assigned to the EV v is a dummy one denoted by o_{kv} with the same pick-up and drop-off times at its earliest available time t_{kv}, the same pick-up and drop-off stations being its available station s_{kv}, and 0 electricity consumption. Thus, the SOC of the EV v after arriving at the drop-off station of the dummy order would be l_{kv}. In a similar vein, let

m_f represent the last relocation task assigned to the staff member f. If no relocation task has yet been assigned to the staff member f, whose earliest available time and the corresponding available station are $\overline{t}_{kf}$ and $\overline{s}_{kf}$ respectively, a dummy relocation task denoted by $\overline{o}_{kf}$, with departure and arrival times being $\overline{t}_{kf}$ and origin and destination stations being $\overline{s}_{kf}$, is assumed to be the last assigned relocation task. The feasibility of the combination v and f for serving the order j will be checked by examining the existence of the CNCS for the pair of orders i_v and j considering the scheduling restriction of the staff member f, and verifying whether the EV v can arrive at the drop-off station of the order j with SOC no less than $SOC_{\min}$ if the CNCS does exist. Figure 5.3 illustrates the combination v and f to serve the order j.

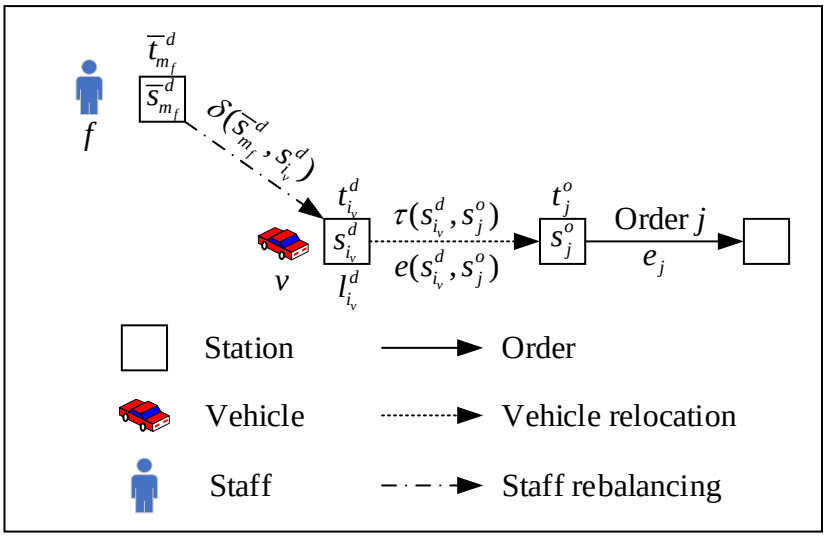

Figure 5.3 Illustration of the combination v and f to serve the order j

Given the picked order j, if the combination v and f is tentatively dispatched for serving it, let Δ^{pre}_{vf} and Δ^{suc}_{vf} denote the charging durations at the drop-off station of the order i_v and the pick-up station of the order j, and l^{suc}_{vf} be the resultant SOC by the departure time of the order j. Then the feasibility check, which includes (i) the existence examination of the CNCS for the pair of orders i_v & j considering the scheduling restriction of the staff member f and (ii) the determination of the values of Δ^{pre}_{vf}, Δ^{suc}_{vf}, and l^{suc}_{vf} under the CNCS if it exists, is elaborated as follows.

Restricted by the scheduling, the EV v and the staff member f arrive at the drop-off station of the order i_v at $t_{i_v}^d$ and $\left[\overline{t}_{m_f}^d + \delta(\overline{s}_{m_f}^d, s_{i_v}^d)\right]$, respectively. Then the earliest possible time t^{elst} at which the EV v can be picked up by the staff member f for relocation is the larger one in $t_{i_v}^d$ and $\left[\overline{t}_{m_f}^d + \delta(\overline{s}_{m_f}^d, s_{i_v}^d)\right]$, i.e., $t^{elst} = \max\left\{t_{i_v}^d, \overline{t}_{m_f}^d + \delta(\overline{s}_{m_f}^d, s_{i_v}^d)\right\}$. The corresponding SOC l^{elst} is calculated by $l^{elst} = \text{FunSOC}\left(t^{elst} - t_{i_v}^d \mid l_{i_v}^d\right)$. That is, the EV v should be charged at the drop-off station of the order i_v for at least $\Delta_{vf}^{pre1} = t^{elst} - t_{i_v}^d$, where Δ_{vf}^{pre1} is the charging duration at the drop-off station of the order i_v until the time point t^{elst}. Then Δ_{vf}^{pre} can be determined by the charging duration at the drop-off station of the order i_v after the time point t^{elst}, i.e., Δ_{vf}^{pre2}, as it is the sum of Δ_{vf}^{pre1} and Δ_{vf}^{pre2}.

Next, the key issue is to determine Δ_{vf}^{pre2} and Δ_{vf}^{suc} that maximize l_{vf}^{suc}, if any. In fact, this is equivalent to seeking the non-dominated charging strategy for a pair of preceding & succeeding orders, where the preceding order is a dummy one with drop-off station being $s_{i_v}^d$, drop-off time at t^{elst}, and the corresponding EV SOC being l^{elst}, and the succeeding order, naturally, is the order j. Therefore, according to Xu and Meng (2019), the following elaboration is introduced.

(i) If $t^{elst} + \tau(s_{i_v}^d, s_j^o) > t_j^o$ or $SOC_{\max} - e(s_{i_v}^d, s_j^o) < SOC_{\min}$, the CNCS does not exist and the combination v and f is infeasible for serving the order j; otherwise, go to step (ii) or (iii).

(ii) If $l^{elst} - e(s_{i_v}^d, s_j^o) \geq SOC_{\min}$, the CNCS exists. The EV v should be relocated directly to the pick-up station of the order j without further charging at the drop-off station of the order i_v, i.e., $\Delta_{vf}^{pre2} = 0$, and then charged at the pick-up station of the order j from $\left[l^{elst} - e(s_{i_v}^d, s_j^o)\right]$ for $\Delta_{vf}^{suc} = t_j^o - t^{elst} - \tau(s_{i_v}^d, s_j^o)$. The SOC of the EV v at the departure time of the order j under the CNCS is calculated by $l_{vf}^{suc} = FunSOC\left(\Delta_{vf}^{suc} \mid l^{elst} - e(s_{i_v}^d, s_j^o)\right)$. The combination v and f is feasible for serving the order j only if $l_{vf}^{suc} - e_j \geq SOC_{\min}$.

(iii) If $l^{elst} - e(s_{i_v}^d, s_j^o) < SOC_{\min}$, the duration required to charge the EV v from l^{elst} to $\left[e(s_{i_v}^d, s_j^o) + SOC_{\min}\right]$, i.e., $\Delta_{vf}^{pre2} = FunTime\left(e(s_{i_v}^d, s_j^o) + SOC_{\min} \mid l^{elst}\right)$, is further needed to be

calculated. If $t^{elst} + \Delta_{vf}^{pre2} + \tau(s_{i_v}^d, s_j^o) > t_j^o$, the CNCS does not exist and the combination v and f is infeasible for serving the order j; otherwise, the CNCS exists, and the EV v should be relocated to the pick-up station of the order j after the charging duration Δ_{vf}^{pre2} and charged from $SOC_{\min}$ for $\Delta_{vf}^{suc} = t_j^o - t^{elst} - \Delta_{vf}^{pre2} - \tau(s_{i_v}^d, s_j^o)$. The SOC of the EV v at the departure time of the order j under the CNCS is calculated by $l_{vf}^{suc} = FunSOC\left(\Delta_{vf}^{suc} \mid SOC_{\min}\right)$. The combination v and f is feasible for serving the order j only if $l_{vf}^{suc} - e_j \geq SOC_{\min}$.

Remark. If the drop-off station of the order i_v, i.e., $s_{i_v}^d$, and the pick-up station of the order j, i.e., s_j^o, are the same physical station, it can be regarded that there still exists a relocation operation for the EV v from $s_{i_v}^d$ to s_j^o, yet a dummy one that is free from the implementation of a staff member. In this way, the above elaboration on checking the feasibility of the combination v and f for serving the order j still applies, but with $t^{elst} = t_{i_v}^d$, $l^{elst} = l_{i_v}^d$, and $\Delta_{vf}^{pre1} = 0$.

If the combination v and f is feasible for serving the order j, the corresponding incremental profit $PROFIT_{vf}^{incremental}$ will be calculated by $PROFIT_{vf}^{incremental} = G_j + E_j - c(s_{i_v}^d, s_j^o) - \bar{c}(\bar{s}_{m_f}^d, s_{i_v}^d)$. In addition, given the combination v^* and f^*, it is $\Delta_{i_{v^*}}^d = \Delta_{v^* f^*}^{pre}$ and $\Delta_j^o = \Delta_{v^* f^*}^{suc}$, where $\Delta_{i_{v^*}}^d$ and Δ_j^o denote the finally determined charging durations at the drop-off station of the order i_{v^*} and the pick-up station of the order j respectively. Accordingly, a relocation task, with origin station being $s_{i_{v^*}}^d$, destination station being s_j^o, departure time being $t_{i_{v^*}}^d + \Delta_{i_{v^*}}^d$, and arrival time being $t_{i_{v^*}}^d + \Delta_{i_{v^*}}^d + \tau(s_{i_{v^*}}^d, s_j^o)$, will be assigned to the staff member f^*.

Algorithm 5.1 outlines the procedure of determining the action at the k^{th} decision epoch under the concurrent-scheduler-based policy, where $\hat{\mathcal{J}}_k$ denotes the set of orders that remain to be picked. It should be noted that *PickEarliestOrder* is the subfunction to pick the order with the earliest departure time from the set $\hat{\mathcal{J}}_k$, and it returns the picked order and the resultant set of orders after the picking operation. *CNCS* is the subfunction to determine the CNCS

when a combination v and f is dispatched for serving the order j. As discussed earlier, given the values of $t_{i_v}^d$, $l_{i_v}^d$, $\bar{t}_{m_f}^d$, $\delta(\bar{s}_{m_f}^d, s_{i_v}^d)$, $\tau(s_{i_v}^d, s_j^o)$, $e(s_{i_v}^d, s_j^o)$, and t_j^o, the charging durations at the drop-off station of the order i_v and the pick-up station of the order j, i.e., Δ_{vf}^{pre} and Δ_{vf}^{suc}, and the resultant SOC by the departure time of the order j, i.e., l_{vf}^{suc}, under the CNCS can be found if it exists; otherwise, the subfunction will return zero as the values of Δ_{vf}^{pre}, Δ_{vf}^{suc}, and l_{vf}^{suc}. Kindly note that if the drop-off station of the order i_v / i_{v^*} and the pick-up station of the order j are the same physical station, no vehicle relocation and staff member are needed.

Algorithm 5.1: Pseudocode of determining the action at the k^{th} decision epoch under the concurrent-scheduler-based policy

Input: s_k.

Output: p_{kv}, $\forall v \in \mathcal{V}$ and q_{kf}, $\forall f \in \mathcal{F}$.

Initialize $\hat{\mathcal{I}}_k \leftarrow \mathcal{I}_k$, $i_v \leftarrow o_{kv}$ and $l_{i_v}^d \leftarrow l_{kv}$ for each $v \in \mathcal{V}$, and $m_f \leftarrow \bar{o}_{kf}$ for each $f \in \mathcal{F}$.
While $\hat{\mathcal{I}}_k \neq \varnothing$ Do
  $[j, \hat{\mathcal{I}}_t] \leftarrow PickEarliestOrder(\hat{\mathcal{I}}_t)$;
  For each $v \in \mathcal{V}$ Do
    For each $f \in \mathcal{F}$ Do
      $[\Delta_{vf}^{pre}, \Delta_{vf}^{suc}, l_{vf}^{suc}] \leftarrow CNCS\left(t_{i_v}^d, l_{i_v}^d, \bar{t}_{m_f}^d, \delta(\bar{s}_{m_f}^d, s_{i_v}^d), \tau(s_{i_v}^d, s_j^o), e(s_{i_v}^d, s_j^o), t_j^o\right)$;
      If $l_{vf}^{suc} - e_j \geq SOC_{\min}$ Then
        If $s_{i_v}^d \neq s_j^o$ Then
          $PROFIT_{vf}^{incremental} \leftarrow G_j + E_j - c(s_{i_v}^d, s_j^o) - \bar{c}(\bar{s}_{m_f}^d, s_{i_v}^d)$;
        Else $PROFIT_{vf}^{incremental} \leftarrow G_j + E_j$;
        EndIf
      Else $PROFIT_{vf}^{incremental} \leftarrow -\infty$;
      EndIf
    EndFor
  EndFor
  $[v^*, f^*] \leftarrow \arg\max_{v \in \mathcal{V}, f \in \mathcal{F}} PROFIT_{vf}^{incremental}$;
  If $PROFIT_{v^* f^*}^{incremental} > 0$ Then
    $\Delta_{i_{v^*}}^d \leftarrow \Delta_{v^* f^*}^{pre}$; $\Delta_j^o \leftarrow \Delta_{v^* f^*}^{suc}$;
    If $s_{i_{v^*}}^d \neq s_j^o$ Then
      $m_{f^*} \leftarrow [s_{i_{v^*}}^d, s_j^o, t_{i_{v^*}}^d + \Delta_{i_{v^*}}^d, t_{i_{v^*}}^d + \Delta_{i_{v^*}}^d + \tau(s_{i_{v^*}}^d, s_j^o)]$;
    EndIf

22 | | $i_{v^*} \leftarrow j$; $l^d_{i_{v^*}} \leftarrow l^{suc}_{v^* f^*} - e_j$;
23 | **EndIf**
24 **EndWhile**

5.4 Numerical Experiments

In this section, numerical experiments on randomly generated instances and a case study of EVCARD in China are conducted. The main objective of these experiments is to assess the performance of the proposed concurrent-scheduler-based policy, to demonstrate the necessity of staff rebalancing consideration in the decision-making of vehicle relocation, and to explore the managerial insights into the operations of electric CSSs. The algorithms are coded in C++ on a personal computer with Intel (R) Core (TM) Duo 3.0 GHz CPU.

5.4.1 Computational performance of the proposed policy

In this subsection, a series of representative random instances are generated to evaluate the performance of the proposed concurrent-scheduler-based policy. Before that, a decomposition-based benchmark policy and the parameter settings for these random instances are first introduced.

5.4.1.1 Benchmark policy

To demonstrate the efficiency of the proposed policy in terms of solution quality, a decomposition-based benchmark policy is further developed. The idea of decomposition in the benchmark policy has been commonly utilized to solve the vehicle relocation and staff rebalancing problem for gasoline-powered CSSs (Nourinejad et al., 2015; Yang et al., 2021). The benchmark policy determines the action at each decision epoch by assigning orders to EVs and relocation tasks to staff members in a separate way. That is, at each decision epoch, the activity trajectory of each EV is obtained first, and the relocation tasks embedded in the activity trajectories are then utilized to determine the trip chain of each staff member. Considering that there may exist relocation tasks that staff members cannot perform due to the travel time restriction, an adjustment is likely to be made for an obtained EV activity trajectory. The notations defined in Section 5.3 will be used for consistency.

To be more specific, at the k^{th} decision epoch for example, given the vector of EV available information $\boldsymbol{V}_k$ and the set of orders $\mathcal{J}_k$, a simplified Algorithm 5.1 that disregards

staff members is applied to obtain the activity trajectory p_{kv} for each EV $v \in \mathcal{V}$. In this way, the relocation tasks embedded in the activity trajectories are obtained by implementing the non-dominated charging strategy for each pair of preceding & succeeding orders. The trip chain q_{kf} for each staff member $f \in \mathcal{F}$ is attempted to be obtained in a similar way. That is, the physically real relocation tasks embedded in activity trajectories are assigned to staff members one by one. The relocation task, namely, n, with the earliest departure time among the ones that remain to be picked for assignment is picked. For the relocation task n, the feasibility of each staff member to perform it is examined and the corresponding incremental cost is calculated if feasible. The relocation task n will be assigned to a feasible staff member with the lowest incremental cost.

There exists the possibility that no staff member is feasible to perform the task n. In other words, the inequality $\overline{t}_{m_f}^{d} + \delta(\overline{s}_{m_f}^{d}, \overline{s}_{n}^{o}) \le \overline{t}_{n}^{o}$ may not hold for each $f \in \mathcal{F}$ and the EV in the task n cannot be relocated accordingly. In this case, an adjustment is made for the activity trajectory of the EV in the task n. For ease of illustration, let v_n denote the EV that is relocated in the task n, i_n^{pre} and i_n^{suc} be the preceding and succeeding orders that the task n connects in the activity trajectory p_{kv_n} respectively. Since the task n cannot be performed due to that the inequality $\overline{t}_{m_f}^{d} + \delta(\overline{s}_{m_f}^{d}, \overline{s}_{n}^{o}) \le \overline{t}_{n}^{o}$ cannot hold for each $f \in \mathcal{F}$, delaying the departure time of the task n, i.e., $\overline{t}_{n}^{o}$, is considered by extending the charging duration of the EV v_n at the drop-off station of the order i_n^{pre}, i.e., $s_{i_n^{pre}}^{d}$ ($\overline{s}_{n}^{o}$). To achieve this, the staff member that is most likely to ensure that the EV v_n can serve the order i_n^{suc} feasibly in terms of travel time and electricity consumption is first identified. Let $f^{\times}$ denote the staff member and $f^{\times}$ would be the one that arrives at the origin station of the task n, i.e., $\overline{s}_{n}^{o}$ ($s_{i_n^{pre}}^{d}$), at the earliest time, i.e., $f^{\times} := \arg\min_{f \in \mathcal{F}} (\overline{t}_{m_f}^{d} + \delta(\overline{s}_{m_f}^{d}, \overline{s}_{n}^{o}))$. Limited by the scheduling of the staff member $f^{\times}$, the charging of the EV v_n at the drop-off station of the order i_n^{pre} will be extended to the time $\overline{t}_{m_{f^{\times}}}^{d} + \delta(\overline{s}_{m_{f^{\times}}}^{d}, \overline{s}_{n}^{o})$. With this restriction, the feasibility of the EV v_n to serve the succeeding order i_n^{suc} needs to be rechecked. If feasible, the charging durations of the EV v_n at the drop-off station of the order i_n^{pre} and the pick-up station of the order i_n^{suc} will be adjusted, and the

relocation task n will be assigned to the staff member $f^{\times}$ after the departure and arrival times of it are delayed accordingly; otherwise, the order i_n^{suc} will be removed from the activity trajectory p_{kv_n}. No matter what the result is, either the charging durations are adjusted or the order i_n^{suc} is removed, the change made to the activity trajectory p_{kv_n} requires updating the remaining activity trajectory. To achieve this, when the EV v_n attempts to depart from the drop-off station of the order i_n^{suc} (for the case that charging durations are adjusted) or the order i_n^{pre} (for the case that the order i_n^{suc} is removed) to serve a succeeding order, its feasibility should be checked. If it is infeasible, the succeeding order will be removed from the activity trajectory p_{kv_n}, and the next adjacent order will be checked until all the orders have been examined. Subsequently, the next relocation task is picked and the process is repeated until no relocation task remains to be picked for assignment.

5.4.1.2 Parameter setup

In order to generate the random instances for the assessment of the proposed policy, a transportation network in a Euclidean plane of 50 km by 50 km, where the travel distance between any two points is the Euclidean distance between them, is built up. To be specific, $|\mathcal{S}|$ stations are uniformly generated in the Euclidean plane. The pick-up and drop-off stations of an order i, i.e., s_i^o and s_i^d, and the initial locations of each EV $v \in \mathcal{V}$ and each staff member $f \in \mathcal{F}$, i.e., s_v^0 and $\overline{s}_f^0$, are randomly chosen from these generated stations. It is assumed that the duration of the operational period is 10 hours. If the time duration is measured in minutes, the operational period would be $[0, 600]$. For an order i, if it is reserved before the operational period, the pick-up time t_i^o is randomly selected from the integer set $\{0, 1, 2, ..., 600\}$ and the reservation time denoted by t_i^r is set to be a negative number, e.g., -1; otherwise, t_i^o is a random integer chosen from the set $\{1, 2, 3, ..., 600\}$ and t_i^r is randomly generated from the integer set $\{0, 1, 2, ..., t_i^o - 1\}$. As for an order i that is cancelled during the operational period, the cancellation time represented by t_i^c is chosen as a random integer from the set $\{t_i^r + 1, t_i^r + 2, ..., t_i^o - 1\}$. Let $d(s_i^o, s_i^d)$ be the Euclidean distance between the pick-up station and drop-off stations of the order i, and ω_i denote its minimum duration. The average travel

speed of customers denoted by υ is assumed to be 40 km/hr. If the order i is a one-way trip, which suggests that its drop-off station is different from its pick-up station, the minimum duration would be $\omega_i = d(s_i^o, s_i^d)/\upsilon$; otherwise, ω_i is set to be 40 min to ensure the minimum profit gains of a carsharing operator. Thus, the drop-off time of the order i, i.e., t_i^d, is randomly chosen from the integer set $\{t_i^o + \omega_i, t_i^o + \omega_i + 10\text{ min}, t_i^o + \omega_i + 20\text{ min}, ..., t_i^o + \omega_i + 60\text{ min}\}$.

All EVs are assumed to be equipped with a 30-kWh lithium-ion battery and charged by a CC-CV scheme. All the CC-CV charging scheme parameters are adopted from the numerical example presented by Pelletier et al. (2017). The initial SOC of all EVs is assumed to be randomly distributed between 70% and $SOC_{\max}$, where $SOC_{\max}$ is the maximum value of SOC achieved by the CC-CV charging scheme. The battery's discharging rate η is set at 30%/hr (Nissan, 2021), and the minimum allowable SOC in a carsharing system, i.e., $SOC_{\min}$, is assumed to be 0.1. The electricity consumption of an order i, i.e., e_i, is randomly generated from the interval $[\omega_i, t_i^d - t_i^o] \times \eta$. The travel time and electricity consumption for the relocation operation from the drop-off station of an order i to the pick-up station of an order j are calculated by $\tau(s_i^d, s_j^o) = d(s_i^d, s_j^o)/\upsilon$ and $e(s_i^d, s_j^o) = \tau(s_i^d, s_j^o) \times \eta$, respectively. The rebalancing time from the destination station of a relocation task m to the origin station of a relocation task n is calculated by $\delta(\bar{s}_m^d, \bar{s}_n^o) = d(\bar{s}_m^d, \bar{s}_n^o)/\bar{\upsilon}$, where $\bar{\upsilon}$ is the average travel speed of the transport mode for rebalancing and is assumed to be 30 km/hr.

It is assumed without loss of generality that the CSS is charged by the service duration of orders, and the service charge is set at 0.3 \$/min. The penalty for rejecting an order is set at half of the service charge, i.e., 0.15 \$/min. The operating cost of EVs incurred by order trips and relocation trips only depends on the amount of electricity consumption, and the electricity cost is set at 0.7 \$/kWh. The rebalancing cost of staff members is set at 0.1 \$/min.

5.4.1.3 Assessment of the proposed policy

Given the total number of orders (#Demand), the number of arrivals (#Arrival), and the number of cancellations (#Cancellation) during the operational period, i.e., #Demand=300, #Arrival=200, and #Cancellation=10, different combinations of the number of stations (#Station), EVs (#EV), and staff members (#Staff), i.e., #Station $\in \{20, 40, 60\}$,

$\#\text{EV} \in \{40, 50, 60\}$, and $\#\text{Staff} \in \{10, 20, 30\}$, are used to assess the performance of the proposed concurrent-scheduler-based policy. Ten instances are randomly generated for a particular combination and the average results are reported.

Table 5.1 compares the performance of the proposed concurrent-scheduler-based policy (CP) and the decomposition-based benchmark policy (DP) in terms of service level indicated by the number of satisfied orders (#SatisOrder) and profitability. To have a more intuitive comparison, the difference of satisfied orders (Diff_SatisOrder) and the relative increase of profit (Diff_Profit) by the proposed policy with respect to the benchmark policy are also reported. It can be seen that both the proposed policy and the benchmark policy serve fewer orders and thus obtain less profit when #Station increases. This is probably because a higher #Station would increase the diversity of spatial distribution of EVs, staff members, and orders, which may reduce the likelihood of an order being successfully served. Unlike #Station, a larger #EV, on the contrary, contributes to a higher profit by serving more orders. Regarding #Staff, its impact on service level and profitability is jointly influenced by #Station and #EV. Specifically, as #Staff increases, the proposed policy and the benchmark policy serve more orders in seven out of nine and six out of nine combinations, respectively, and both policies achieve a higher profit in eight out of nine combinations. It is interesting to find that when #Staff grows from 20 to 30 in some combinations of #Station and #EV (e.g., #Station=60 and #EV=50), the number of satisfied orders and profit show little sensitivity. This may be because the staff members have been saturated under the current demand and combination of #Station and #EV. As for the comparison between the proposed policy and the benchmark policy, it can be seen that the numbers of satisfied orders obtained by the proposed policy are higher than those achieved by the benchmark policy in most combinations of #Station, #EV, and #Staff. Besides, the proposed policy can serve as high as 18.1 orders more than the benchmark policy. In only four combinations of #Station, #EV, and #Staff, the proposed policy satisfies fewer orders than the benchmark policy by at most 1.7. In regards to the profitability, all the profits produced by the proposed policy are larger than those obtained by the benchmark policy and the largest relative gap in profit reaches 47.5% when #Station=60, #EV=40, and #Staff=10. Overall, the results demonstrate that the proposed policy outperforms the benchmark policy in solving the RT-VR&SR problem.

Table 5.1 Comparison between the proposed policy and the benchmark policy on the average results of ten randomly generated instances

#Station	#EV	#Staff	DP		CP		Comparison	
			#Satis Order	Profit ($)	#Satis Order	Profit ($)	Diff_Satis Order	Diff_Profit (%)
20	40	10	194.1	1,272	195.6	1,372	1.5	7.8
20	40	20	196.2	1,295	196.9	1,378	0.7	6.4
20	40	30	196.3	1,293	196.9	1,353	0.6	4.6
20	50	10	225.2	2,194	228.0	2,340	2.8	6.7
20	50	20	232.0	2,256	231.7	2,369	-0.3	5.0
20	50	30	231.7	2,308	233.4	2,410	1.7	4.4
20	60	10	250.6	2,927	253.8	3,118	3.2	6.5
20	60	20	260.6	3,153	259.6	3,242	-1.0	2.8
20	60	30	260.6	3,199	261.0	3,276	0.4	2.4
40	40	10	174.2	776	184.2	936	10	20.6
40	40	20	186.8	820	187.9	941	1.1	14.8
40	40	30	187.6	891	187.1	956	-0.5	7.2
40	50	10	202.5	1,604	215.1	1,881	12.6	17.3
40	50	20	219.7	1,683	222.1	1,934	2.4	14.9
40	50	30	221.1	1,761	222.0	1,939	0.9	10.1
40	60	10	222.8	2,214	239.3	2,580	16.5	16.5
40	60	20	249.0	2,562	250.7	2,818	1.7	10.0
40	60	30	252.7	2,736	251.0	2,825	-1.7	3.2
60	40	10	162.9	513	175.8	757	12.9	47.5
60	40	20	179.7	642	180.4	791	0.7	23.3
60	40	30	180.3	691	181.1	793	0.8	14.8
60	50	10	190.9	1,371	206.1	1,652	15.2	20.5
60	50	20	213.2	1,539	215.1	1,731	1.9	12.5
60	50	30	213.9	1,562	216.4	1,760	2.5	12.7
60	60	10	212.9	1,988	231.0	2,421	18.1	21.8
60	60	20	242.1	2,353	244.2	2,651	2.1	12.7
60	60	30	243.5	2,437	246.1	2,685	2.6	10.2

5.4.2 Case study of EVCARD

EVCARD, started up in 2015, is the first one-way electric carsharing company in China. It provides three types of rental services, i.e., hourly rent, daily rent, and monthly rent, and more than ten million users have registered it by 2021 (EVCARD, 2022). In this study, the hourly rental service of EVCARD in three districts of Suzhou, namely, Kunshan, Xiangcheng, and Wujiang, are considered. The station deployment in the three districts, with 70 stations in Kunshan, 27 stations in Xiangcheng, and 29 stations in Wujiang, is depicted in Figure 5.4. The configuration of these stations, e.g., the shortest travel time between each pair of stations, is obtained from Google Maps (Google, 2022). Multiple stations are combined into one if the shortest travel time between them is within 5 min. After the combination process, 57 stations are obtained. To distinguish the transport modes by which staff members self-rebalance and

perform relocation tasks, it is assumed that the rebalancing time between two stations is χ times the corresponding relocation time (i.e., the shortest travel time), where χ is referred to as the rebalancing coefficient. Analogous to Subsection 5.4.1.3, ten instances of orders with #Demand=300 and #Cancellation = 10 are randomly generated from 8 am to 6 pm, and the average results are reported. Unless stated otherwise, the rebalancing coefficient and the number of arrivals during the operational period, i.e., χ and #Arrival, are set to be 1.4 and 200 respectively, and the other parameter settings are the same as Subsection 5.4.1.2.

(a) Kunshan (b) Xiangcheng (c) Wujiang

Figure 5.4 Station deployment in three districts of Suzhou

5.4.2.1 Impact analysis of staff rebalancing

As reviewed in Chapter 2, no study has ever considered staff rebalancing for the real-time vehicle relocation problem of electric CSSs. This subsection explores how staff rebalancing affects the system service level and profitability. To this end, a real-time vehicle relocation (RT-VR) problem considering demand dynamics and nonlinear charging profile for the one-way electric CSSs is first considered. As previously done for the proposed RT-VRSR problem, the RT-VR problem is first formulated as an MDP and then solved by the simplified concurrent-scheduler-based policy without factoring in staff rebalancing. Here staff rebalancing is not factored in refers to that an EV can always be relocated no matter whether or not a staff member is available. For ease of presentation, let $\#SatisOrder^{w/o}$ and $Profit^{w/o}$ be the obtained number of satisfied orders and profit for the RT-VR problem, respectively. Accordingly, let $\#SatisOrder^{w}$ and $Profit^{w}$ denote the number of served orders and profit excluding the rebalancing cost for the RT-VR&SR problem, respectively. The difference between $\#SatisOrder^{w}$ and $\#SatisOrder^{w/o}$, i.e., Diff_SatisOrder, and the ratio of $Profit^{w}$ to $Profit^{w/o}$, i.e., ProfitRatio, are adopted to evaluate the impact of staff rebalancing on the service level and profitability.

Table 5.2 summarizes the results under different combinations of #EV and #Staff, i.e., $\#EV \in \{50, 55, 60\}$ and $\#Staff \in \{5, 6, 7, 8, 9, 10\}$. The results show that the obtained number of served orders and profit for the RT-VR&SR problem are always smaller than that achieved for the RT-VR problem, as Diff_SatisOrder is negative and ProfitRatio is lower than 1. This can be explained by the fact that restricted by the availability of staff members, some relocation operations cannot be successfully performed and thus a number of orders cannot be served, which results in the loss of profit. The largest difference in the number of satisfied orders can be as high as 60.7 when #EV=60 and #Staff=5, and the corresponding profit ratio is 0.57. As #Staff increases while fleet size is constant, more relocation operations can be performed and accordingly more orders would be served, leading to the decreasing difference in the number of satisfied orders and the growing profit ratio. It is interesting to find that when fleet size increases under a constant number of staff members, the difference in the number of satisfied orders rises, whereas the profit ratio generally declines. This may indicate that expanding fleet size should be accompanied by increasing the number of staff members to earn more money by serving more orders. It can be concluded from these results that staff rebalancing plays an important role in improving the service level and profitability, and ignoring it in the decision-making of vehicle relocation could cause the overestimation of service level and profitability. This demonstrates the significance of this study.

Table 5.2 Impact of staff rebalancing on the system service level and profitability

#EV	#Staff	#Satis Order$^{w/o}$	Profit$^{w/o}$ ($)	#Satis Order^{w}	Profit^{w} ($)	Diff_ SatisOrder	ProfitRatio (%)
50	5	213.1	1,789	166.2	1,065	-46.9	0.60
50	6	213.1	1,789	175.6	1,249	-37.5	0.70
50	7	213.1	1,789	181.2	1,360	-31.9	0.76
50	8	213.1	1,789	185.4	1,461	-27.7	0.82
50	9	213.1	1,789	194.7	1,650	-18.4	0.92
50	10	213.1	1,789	200.2	1,774	-12.9	0.99
55	5	230.2	2,284	177.1	1,383	-53.1	0.61
55	6	230.2	2,284	185.6	1,563	-44.6	0.68
55	7	230.2	2,284	193.0	1,724	-37.2	0.75
55	8	230.2	2,284	200.0	1,880	-30.2	0.82
55	9	230.2	2,284	205.2	1,980	-25.0	0.87
55	10	230.2	2,284	212.1	2,096	-18.1	0.92
60	5	246.1	2,750	185.4	1,561	-60.7	0.57
60	6	246.1	2,750	193.5	1,727	-52.6	0.63
60	7	246.1	2,750	202.2	1,960	-43.9	0.71
60	8	246.1	2,750	206.8	2,025	-39.3	0.74
60	9	246.1	2,750	214.5	2,206	-31.6	0.80

60	10	246.1	2,750	220.9	2,319	-25.2	0.84

5.4.2.2 Sensitivity analysis

In this subsection, how the demand dynamism indicated by the number of arrivals during the operational period, the service charge, the electricity cost (EleCost), the rebalancing cost (RebCost), and the rebalancing efficiency reflected by the coefficient χ affect the performance of the one-way electric carsharing system is investigated. To conduct these numerical experiments, it is assumed that 60 EVs and 15 staff members are provided in the carsharing system. In addition to the two concerns that the carsharing operator most cares about, i.e., the daily profit and the number of satisfied orders, several other performance indicators, i.e., the service duration per vehicle (SerDuration), the relocation duration per vehicle (RelDuration), the charging duration per vehicle (ChargeDuration), the total number of performed relocation tasks (#PerforTask), the task duration per staff member (TaskDuration), the rebalancing duration per staff member (RebDuration), and the waiting duration per staff member (WaitDuration) approximated by subtracting the sum of task and rebalancing duration from the operational period, are also reported to cater to the readers' interests.

Impact of demand dynamism

Since the problem focused on in this study is a real-time dynamic problem, how the demand dynamism affects the above-mentioned performance indicators is first explored. The results are shown in Table 5.3. It can be seen that when the demand dynamism increases from 20% (i.e., #Arrival=60) to 80% (i.e., #Arrival=240), both the daily profit and the number of satisfied orders decrease with fluctuations, whereas the two performance indicators decline no more than 8.5% and 4.5% respectively. This demonstrates the robustness of the proposed policy to the demand dynamism in terms of profitability and service level. On average, each EV serves about 4 orders and the carsharing operator makes a profit of around 10 $ per order. The amounts of time allocated to each EV for serving users and relocation & charging are approximately fifty-fifty in general. As for the staff aspect, the number of performed relocation tasks is smaller than that of satisfied orders. This is consistent with the perception that fulfilling an order would generate at most one relocation task. Averagely, a staff member performs about 10 relocation tasks. Dissimilar to the time allocation of EVs, each staff member waits at stations for more than 2.5 hours and the time spent on performing relocation tasks and self-rebalancing

is comparable. The carsharing operator is suggested to improve the system efficiency by assigning tasks other than vehicle relocation, e.g., vehicle maintenance, to staff members when they stay waiting at stations.

Impact of service charge

The effect of the service charge on the performance of the one-way electric carsharing system is continued to be investigated. The results are presented in Table 5.4. It shows that if the service charge is below 0.18 $/min, the carsharing company would be in the red[2]. Setting a larger service charge makes the orders more profitable, and the carsharing operator begins to earn money. As the service charge increases from 0.03 $/min to 0.30 $/min with an increment of 0.03, the variation amplitude from 0.03 $/min to 0.06 $/min is the largest for all the performance indicators excluding the daily profit. When the service charge is higher than 0.12 $/min, some of the performance indicators, e.g., #SatisOrder, remain almost stable with respect to the service charge. This is because if the service charge is relatively low, e.g., 0.03 $/min, limited by that only a feasible combination of an EV and a staff member with the maximum and positive profit increment can be dispatched for serving an order, some orders may be rejected due to the negative profit increments of all feasible combinations of an EV and a staff member. When the service charge is increased to 0.06 $/min, these negative profit increments may become positive, resulting in the visible growth of the number of satisfied orders and thus the relatively obvious variations of other performance indicators. If the service charge is high enough, e.g., 0.15 $/min, the profit increment exerts little influence on the fulfillment of orders, and then the performance indicators generally show less sensitivity to the variation of service charge. These results indicate that under the adopted concurrent-scheduler-based policy, the carsharing operator should set the service charge higher than 0.12 $/min to circumvent unnecessary service level drop brought by the profit increments of combinations of an EV and a staff member.

Impact of electricity cost

In addition to the service charge, the effect of electricity cost on the performance of the one-way electric carsharing system is also examined. Table 5.5 summarizes the results. As expected, it demonstrates the significant impact of electricity cost on the profitability of the

[2] The profit can be negative due to the penalty for unserved orders.

carsharing system. If the unit electricity cost is higher than 1.7 $, the carsharing operator would be at a loss. A notable phenomenon is that the variations of all EV-related and staff-related performance indicators appear arbitrary when the unit electricity cost is no more than 1.5 $. However, when the unit electricity cost is larger than 1.5 $, a higher value of it leads to a smaller number of satisfied orders, lower service and relocation durations, and thus higher charging duration. Accordingly, the number of relocation tasks performed by staff members and the task duration decrease visibly, while the rebalancing duration fluctuates, resulting in the increasing waiting duration. For these obtained results, it is guessed that the increase of the unit electricity cost from 0.3 $ to 1.5 $ probably influences the assignment decision of orders, as a feasible combination of an EV and a staff member with the maximum and positive profit increment, which includes the electricity-related terms, is the final decision for serving an order. The change in the assignment decisions of orders eventually alters activity trajectories of EVs and trip chains of staff members over the whole operational period, causing the arbitrary variations of the performance indicators. If the unit electricity cost is further increased, the profit increments of all feasible combinations of an EV and a staff member may turn negative for some orders, leading to the declining number of satisfied orders concerning unit electricity cost and the corresponding variations of other performance indicators. Hence, it should be understood by the carsharing operator that if the proposed concurrent-scheduler-based policy is adopted, unit electricity cost no larger than 1.5 $ will exert little impact on the system service level.

Impact of rebalancing cost

Variations of these performance indicators concerning the rebalancing cost are further tested. Table 5.6 tabulates the results. It can be seen that compared to the electricity cost, the rebalancing cost has a more significant impact on the system service level, as the number of satisfied orders decreases by more than 25% when the unit rebalancing cost increases from 0.1 $ to 1.9 $. The declining number of satisfied orders leads to fewer relocation tasks performed by staff members. As a result, all the time-related performance indicators excluding the charging and waiting durations generally decrease when the unit rebalancing cost rises. An interesting phenomenon is that the profit, instead of keeping falling with the growth of unit rebalancing cost, drops first and then increases. When the unit rebalancing cost is increased from 1.7 $ to 1.9 $, the carsharing system dramatically turns from loss to profit. For this result, it should be cautioned that the net profit of the carsharing system is determined by two variable

terms, i.e., the total profit generated from the activity trajectories, including the penalty for unserved orders, and the total rebalancing cost incurred by the trip chains. When the unit rebalancing cost increases, the total profit generated from the activity trajectories of EVs would normally decrease due to the falling number of satisfied orders. Nevertheless, the variation of the total rebalancing cost incurred by the trip chains of staff members, which is the product of unit rebalancing cost and rebalancing duration, is uncertain in light of the declining rebalancing duration. Hence, if the total rebalancing cost reduces and the reduction magnitude is greater than that of the total profit produced by the activity trajectories of EVs, the net profit of the carsharing system would grow. This has been confirmed by experimental data.

Impact of rebalancing efficiency

Last, how rebalancing efficiency, which can be indicated by the rebalancing coefficient χ, affects the performance of the one-way electric carsharing system is investigated. The results are reported in Table 5.7. It can be observed that both the system profitability and service level would be negatively influenced if the transport mode for rebalancing is inefficient. When the rebalancing efficiency is halved by increasing χ from 1 to 2, the daily profit and the number of satisfied orders decrease by 13.3% and 4.6% respectively. This is because, as shown by the results in Table 5.7, if the transport mode for rebalancing is less efficient, more rebalancing duration will be required, which could result in fewer relocation tasks to be performed. Consequently, a number of orders will fail to be served and thus some profits will be lost. Accordingly, as χ increases, staff members spend less time performing tasks and waiting at stations. Regarding the time allocation of EVs, less time is needed for service and relocation, and more time is used for charging, in general. Considering that a more efficient transport mode for rebalancing generally means a higher unit rebalancing cost, which can negatively influence the profitability and service level of the carsharing system, the operator should weigh the benefit and the cost when choosing the transport mode for rebalancing.

Table 5.3 Impact of demand dynamism on the performance of the one-way electric carsharing system

#Arrival	Profit ($)	#SatisOrder	SerDuration (hr/veh)	RelDuration (hr/veh)	ChargeDuration (hr/veh)	#PerforTask	TaskDuration (hr/mem)	RebDuration (hr/mem)	WaitDuration (hr/mem)
60	2,554	247	4.79	0.86	4.24	151	3.45	3.79	2.77
80	2,563	247	4.79	0.84	4.26	148	3.38	3.70	2.93
100	2,483	243	4.73	0.86	4.28	148	3.42	3.65	2.94
120	2,484	243	4.74	0.85	4.30	150	3.40	3.79	2.81
140	2,438	241	4.71	0.84	4.38	147	3.37	3.77	2.86
160	2,354	238	4.63	0.84	4.50	146	3.35	3.69	2.96
180	2,428	239	4.67	0.83	4.51	147	3.33	3.61	3.07
200	2,377	239	4.64	0.84	4.43	147	3.35	3.57	3.08
220	2,280	235	4.57	0.84	4.55	148	3.35	3.59	3.06
240	2,338	237	4.59	0.80	4.55	143	3.21	3.30	3.49

Table 5.4 Impact of service charge on the performance of the one-way electric carsharing system

Charge ($/min)	Profit ($)	#SatisOrder	SerDuration (hr/veh)	RelDuration (hr/veh)	ChargeDuration (hr/veh)	#PerforTask	TaskDuration (hr/mem)	RebDuration (hr/mem)	WaitDuration (hr/mem)
0.03	-2,076	230	4.59	0.78	4.53	139	3.11	3.03	3.86
0.06	-1,590	236	4.65	0.81	4.44	145	3.23	3.31	3.46
0.09	-1,098	238	4.66	0.83	4.44	147	3.30	3.36	3.34
0.12	-621	238	4.65	0.85	4.43	146	3.39	3.44	3.18
0.15	-96	240	4.68	0.84	4.43	148	3.36	3.49	3.15
0.18	405	239	4.67	0.83	4.44	147	3.31	3.51	3.19
0.21	882	239	4.66	0.84	4.45	147	3.36	3.60	3.04
0.24	1,375	239	4.65	0.84	4.45	147	3.38	3.58	3.05
0.27	1,881	239	4.65	0.84	4.43	148	3.35	3.57	3.08
0.30	2,377	239	4.64	0.84	4.43	147	3.35	3.57	3.08

Table 5.5 Impact of electricity cost on the performance of the one-way electric carsharing system

EleCost ($/kWh)	Profit ($)	#SatisOrder	SerDuration (hr/veh)	RelDuration (hr/veh)	ChargeDuration (hr/veh)	#PerforTask	TaskDuration (hr/mem)	RebDuration (hr/mem)	WaitDuration (hr/mem)
0.3	3,264	237	4.60	0.91	4.41	146	3.64	3.64	2.72
0.5	2,909	240	4.68	0.83	4.45	147	3.34	3.54	3.13
0.7	2,377	239	4.64	0.84	4.43	147	3.35	3.57	3.08
0.9	1,897	239	4.65	0.84	4.45	147	3.36	3.58	3.07
1.1	1,494	241	4.72	0.78	4.46	151	3.13	3.99	2.88
1.3	996	239	4.68	0.76	4.48	148	3.04	3.88	3.08
1.5	522	237	4.68	0.77	4.47	148	3.07	3.88	3.05
1.7	52	236	4.68	0.76	4.48	148	3.03	3.85	3.13
1.9	-425	232	4.63	0.73	4.55	145	2.90	3.88	3.22
2.1	-793	228	4.61	0.67	4.67	139	2.66	3.46	3.88

Table 5.6 Impact of rebalancing cost on the performance of the one-way electric carsharing system

RebCost ($/min)	Profit ($)	#SatisOrder	SerDuration (hr/veh)	RelDuration (hr/veh)	ChargeDuration (hr/veh)	#PerforTask	TaskDuration (hr/mem)	RebDuration (hr/mem)	WaitDuration (hr/mem)
0.1	2,377	239	4.64	0.84	4.43	147	3.35	3.57	3.08
0.3	1,683	236	4.60	0.89	4.43	146	3.57	3.47	2.96
0.5	1,164	234	4.57	0.87	4.47	142	3.47	3.18	3.35
0.7	645	229	4.48	0.84	4.56	138	3.37	2.92	3.72
0.9	426	227	4.47	0.81	4.60	130	3.23	2.54	4.23
1.1	123	218	4.30	0.75	4.80	122	3.00	2.18	4.83
1.3	-53	212	4.19	0.70	4.95	113	2.79	1.89	5.32
1.5	-170	206	4.09	0.62	5.10	100	2.48	1.65	5.87
1.7	-63	194	3.85	0.53	5.35	84	2.11	1.20	6.70
1.9	95	178	3.50	0.41	5.78	67	1.62	0.74	7.64

Table 5.7 Impact of transport mode for rebalancing on the performance of the one-way electric carsharing system

χ	Profit ($)	#SatisOrder	SerDuration (hr/veh)	RelDuration (hr/veh)	ChargeDuration (hr/veh)	#PerforTask	TaskDuration (hr/mem)	RebDuration (hr/mem)	WaitDuration (hr/mem)
1.1	2,491	241	4.70	0.87	4.36	154	3.47	3.00	3.53
1.2	2,464	241	4.69	0.86	4.40	151	3.43	3.19	3.38
1.3	2,437	240	4.67	0.84	4.44	149	3.36	3.34	3.30
1.4	2,377	239	4.64	0.84	4.43	147	3.35	3.57	3.08
1.5	2,326	237	4.61	0.82	4.50	143	3.28	3.70	3.02
1.6	2,314	236	4.61	0.81	4.53	145	3.25	3.92	2.83
1.7	2,285	236	4.59	0.79	4.56	141	3.16	4.10	2.74
1.8	2,220	234	4.55	0.78	4.61	139	3.13	4.25	2.63
1.9	2,201	232	4.54	0.76	4.64	136	3.03	4.37	2.60
2.0	2,160	230	4.51	0.75	4.67	135	2.99	4.45	2.56

5.5 Concluding Remarks

This chapter addressed a RT-VR&SR problem for one-way electric CSSs by taking into account the demand dynamics and practical nonlinear charging profile. An MDP formulation was first developed for the RT-VR&SR problem. An efficient concurrent-scheduler-based policy, which incorporates a novel CNCS, was subsequently proposed. Numerical experiments on randomly generated instances and a case study of EVCARD in China were conducted to assess the efficiency of the proposed policy against a decomposition-based benchmark policy, to demonstrate the necessity of considering staff rebalancing in the decision-making of vehicle relocation, and to explore the managerial insights of the carsharing system. The results indicated that the proposed concurrent-scheduler-based policy has an obvious advantage over the benchmark policy in solving the RT-VR&SR problem, and ignoring staff rebalancing in the vehicle relocation problem of CSSs will cause the overestimation of service level and profitability. In addition, the carsharing operator should well weigh the benefit and the cost when choosing the transport mode for rebalancing; staff members can be assigned to do some other works, such as cleaning EVs, when staying waiting at stations; the long waiting time of staff members at stations suggest that the number of staff members should be carefully determined to avoid waste of labor.

CHAPTER 6 CONCLUSIONS AND RECOMMENDATIONS

6.1 Overview and Research Contributions

The thesis addresses three problems of electric CSSs: a tactical fleet size problem considering on-demand charging strategy and battery degradation, an operational RT-VR problem taking into account demand dynamics and nonlinear charging profiles of EVs, and a further extended operational RT-VR&SR problem.

Chapter 3 tackles the tactical fleet size problem. This study makes the first attempt to incorporate the battery degradation into the mathematical modeling of electric CSSs in the form of battery wear cost. The battery wear cost is incurred during the battery charging and discharging processes. The incorporation of battery degradation also enables the consideration of the novel on-demand charging strategy, which allows EVs to be charged as per the need. Meanwhile, the consideration of battery degradation results in an MINLP model with both concave and convex terms in the objective function. To deal with the nonlinearity, a hybrid solution method is employed to realize model linearization. Using the proposed hybrid solution method, a global ε-optimal solution can be obtained. Numerical experiments demonstrate the efficiency of the proposed model and solution method.

Chapter 4 deals with the RT-VR&CS problem considering demand dynamics and realistic nonlinear charging profile. This is a novel research topic with practical significance. In order to cope with the demand dynamics, a dynamic algorithmic framework based on a rolling time horizon is first established. The entire planning horizon is divided into a series of sub-horizons, and the complicated RT-VR&CS problem is subsequently transformed into successively solving a series of S-VR&CS problems defined over these sub-horizons. Based on the notion of EV activity trajectory, which illustrates a specific relocation and charging strategy for an EV by enabling the incorporation of implicit nonlinear charging profile, a set-packing-type model and a novel column-generation-based solution method are employed to solve each static problem. Specifically, for the first static problem, the activity trajectories are generated by a developed multi-label method. For each static problem from the second one onward, we reuse existing activity trajectories generated for the previous static problem and employ a reactive column generation process; we generate activity trajectories in an online environment until the underlying decision epoch, by which a set-packing-type formulation consisting of the activity trajectories generated up to this time point is solved. The benefit of making use of existing

activity trajectories will amplify as time goes, offering the potential to generate a large number of activity trajectories in a short period of time. The proposed solution method is numerically proved to be efficient in solving the proposed complicated RT-VR&CS problem.

Chapter 5 makes an extension for the study in Chapter 4 such that staff rebalancing is included. The ignorance of staff rebalancing in the study of Chapter 4 hinders the applicability to a real-world carsharing system, as it assumes that a vehicle can always be relocated between two stations disregarding whether a staff member is available to perform the relocation operation. The additional consideration of staff rebalancing in Chapter 5 closes this research gap. To cope with the intractability caused by staff rebalancing consideration, an MDP is first formulated for the RT-VR&SR problem. In the MDP formulation, the activity trajectories of EVs and trip chains of staff members, which explicitly describe the vehicle relocation & vehicle charging strategy and staff rebalancing strategy respectively, are utilized to express the action taken at each decision epoch. To overcome the computational intractability caused by the three notorious curses of dimensionality, i.e., the explosion of state space, outcome space, and action space, in an online environment, an efficient concurrent-scheduler-based policy is proposed for the MDP formulation. Under the concurrent-scheduler-based policy, the action at each decision epoch, i.e., the activity trajectory implemented by each EV and the trip chain performed by each staff member, is determined by dispatching combinations of EVs and staff members to unserved orders and assigning orders and relocation tasks to EVs and staff members respectively in a parallel way. A novel CNCS, which considers scheduling restriction of staff, is incorporated to facilitate the implementation of the policy. The good performance of the proposed policy is validated by the numerical experiments.

The three studies investigated in the thesis help carsharing operators address the decision-making challenges caused by vehicle electrification.

6.2 Recommendations for Future Studies

In this section, several possible future research directions are highlighted. Broadly speaking, these research directions can be classified into two categories. The first category concerns research directions related to the limitations of the three studies investigated in the thesis. The second category involves research directions reflected in the literature review. In the following, the research directions are discussed based on the two categories.

(1) Research directions related to the limitations of the studies investigated in the thesis

All of the three studies investigated in the thesis assumed that users always pick up and drop off vehicles according to the time they have reserved. However, users are more likely to pick up and drop off vehicles within a time window containing the time epoch they have reserved. Considering the time window of orders would be more align with reality. Furthermore, current studies consider the profit maximization as the optimization objective. Future studies can consider the service quality as the optimization objective. As for the battery characteristics, in addition to the battery degradation and nonlinear charging profile considered in the thesis, battery capacity deserves more attention. On the one hand, a larger battery capacity generally means a higher EV cost. On the other hand, a larger battery capacity induces a higher electricity consumption rate; the battery capacity and the electricity consumption rate jointly influence the service capability of an EV. Hence, determining the optimal battery capacity is another crucial decision-making problem for electric CSSs. Particularly, for the fleet size problem in Chapter 3, efficient algorithms or heuristics remain to be developed for implementation in large-scale problems in the future; for the real-time problems in Chapter 4 and Chapter 5, the vehicle relocation and/or staff rebalancing strategies are optimized without incorporating the probabilistic or forecasted features of demand that may appear in the future, and some degree of demand stochasticity can be incorporated to improve the real-time decision-makings in electric CSSs.

(2) Research directions reflected in the literature review

First, the literature review reveals that very few studies have pioneered dealing with the decision-making problems arising from the autonomous CSSs. In comparison to the traditional CSSs with human-driven vehicles, CSSs with autonomous vehicles automize users' walking to vehicles and driving for parking or refueling and thus provide users with more convenience. The convenience, however, makes it impossible to solve the decision-making problems arising from the autonomous CSSs directly by utilizing the models and solution methods for the decision-makings of human-driven CSSs. This is because the operation mode of autonomous CSSs allows remote parking and en-route pick-up and drop-off, which would induce more decision-makings. Particularly, in an autonomous electric carsharing system, decision-making about which station to charge for a vehicle before the vehicle drives to a location for picking up a user needs to be additionally made. Therefore, for the smooth and efficient operation of the autonomous CSSs in the near future, considerable efforts are highly anticipated for the decision-making problems of autonomous CSSs.

Second, almost all the existing studies considered CSSs with a single fleet type, e.g., human-driven gasoline-powered vehicles, human-driven EVs, and autonomous EVs. In reality, however, a carsharing system may contain both gasoline-powered vehicles and EVs. Moreover, it is highly likely that the autonomous vehicles will be applied in CSSs by replacing part of the human-driven vehicles. The investigation on the operations of CSSs with hybrid fleet type will be more in line with the reality.

Third, the optimization models formulated for the CSS operations in the existing literature largely ignored the user behavior. In fact, in a carsharing system, the users, as the enjoyers of the service, usually show their subjective behavior. For example, in human-driven electric CSSs, users may select vehicles with certain battery levels according to their mileage and preferences. The users may also choose to advance or postpone the pick-up/drop-off time based on their own needs. Incorporating these subjective user behaviors into the model formulation would be a challenging research direction in the future.

Fourth, for the vehicle relocation problem, little attention has been paid to the user-based strategy, although it may also be a practically effective approach to tackle the vehicle imbalance problem in one-way CSSs. Hence, in the future, more efforts should be made for the user-based vehicle relocation problem. Besides, the joint implementation of the operator-based vehicle relocation and user-based vehicle relocation strategies may be a potentially good way to cope with the vehicle imbalance problem.

Fifth, for the trip pricing problem, the investigation on it in the existing literature is insufficient, although it is an important decision-making problem for CSSs. The decision-making of trip pricing deserves more attention in the future. Last but not the least, several pioneering studies have adopted the data-driven approach to solve the CSS operation problems by making use of the massive historical data. In the era of big data, utilizing the historical data to deal with the decision-making problems arising from CSSs would be an inevitable trend.

APPENDIX A NOTATIONS AND SUPPLEMENT FOR CHAPTER 3

A.1 Notations

I	Set of rentals
A^r	Set of relocation operations connecting any two rentals that are compatible both in terms of travel time and electricity consumption
A^0	Set of dummy links connecting the dummy node and all the rentals
i, j	Indices for rental
(i, j)	Index for link
n_0	Index for the dummy node
FC	The fixed daily amortized cost of an EV
s_i^o	Pick-up station of rental i
s_i^d	Drop-off station of rental i
t_i^o	Departure time of rental i
t_i^d	Arrival time of rental i
l_i	Electricity consumption of rental i
TP_i	Net profit of rental i
PC_i	Incurred penalty for rejecting rental i
l_{ij}	Electricity consumption of relocation operation from the drop-off station of rental i to the pick-up station of rental j
t_{ij}	Relocation time from the drop-off station of rental i to the pick-up station of rental j
RC_{ij}	Relocation cost from the drop-off station of rental i to the pick-up station of rental j
CR	Charging rate
DR	Discharging rate
M_1, M_2	Big numbers
E	The usable battery capacity
E_{min}	The minimum SOC allowed for an EV
E_{comf}	The minimum SOC value above which users are free from range anxiety
WC	Battery wear cost incurred during charging or discharging process
WC_r	Battery wear cost of an EV over the entire operational period
TWC	The total battery wear cost of all EVs over the entire operational period
$W(l)$	Battery wear density function with respect to the SOC l that represents the battery wear cost per unit energy transfer at the SOC l
l_{init}	The initial SOC of battery before the charging or discharging process
l_{ulti}	The ultimate SOC of battery after the charging or discharging process
BP	Battery price
BS	Battery size

μ	Battery cycle efficiency
a, b	Battery-dependent parameters that are acquired experimentally
$\varepsilon, \hat{\varepsilon}$	Pre-specified tolerances
$g(G_i)$	Denote the convex term $-(1-G_i)^b$, i.e., $g(G_i) := -(1-G_i)^b$, $\forall G_i \in [0, E],\ \forall i \in I$
$h(R_i)$	Denote the concave term $(1-R_i)^b - (1-R_i+l_i)^b$, i.e., $h(R_i) := (1-R_i)^b - (1-R_i+l_i)^b,\ \forall R_i \in [0, E],\ \forall i \in I$
$y(Q_i)$	Denote the concave term $(1-Q_i)^b$, i.e., $y(Q_i) := (1-Q_i)^b$, $\forall Q_i \in [0, E],\ \forall i \in I$
$\hat{g}(G_i)$	Piecewise linear approximation function for the curve $g(G_i)$
$\hat{h}(R_i)$	Piecewise linear approximation function for the curve $h(R_i)$
$\hat{y}(Q_i)$	Piecewise linear approximation function for the curve $y(Q_i)$
$a_i^{(k)}$	The slope of the k^{th} tangent line of the curve $h(R_i)$
$b_i^{(k)}$	The intercept of the k^{th} tangent line of the curve $h(R_i)$
$\bar{a}_i^{(k)}$	The slope of the k^{th} tangent line of the curve $y(Q_i)$
$\bar{b}_i^{(k)}$	The intercept of the k^{th} tangent line of the curve $y(Q_i)$
K	Set of breakpoints for the linear segments of the curve $g(G_i)$
Ω	Set of tangent lines of the curve $h(R_i)$
V	Set of tangent lines of the curve $y(Q_i)$
k	Index for breakpoint of the curve $g(G_i)$ or tangent line of the curves $h(R_i)$ and $y(Q_i)$
N	Number of breakpoints for the linear segments of the curve $g(G_i)$
M	Number of tangent lines of the curve $h(R_i)$
P	Number of tangent lines of the curve $y(Q_i)$
f	Integer decision variable representing fleet size of EVs
z_i	Binary decision variable that equals 1 if rental i is satisfied, and 0 otherwise
x_{ij}	Binary decision variable that equals 1 if an EV is relocated from the drop-off station of rental i to the pick-up station of rental j, and 0 otherwise
R_i	Continuous decision variable denoting SOC of an EV rightly before serving the rental i
Q_i	Continuous decision variable denoting SOC of an EV rightly before the relocation operation originated from the drop-off station of rental i
e_i^o	Continuous decision variable denoting amount of electricity charged at the pick-up station of rental i
e_i^d	Continuous decision variable denoting amount of electricity charged at the drop-off station of rental i

G_i	Continuous variable denoting the SOC of an EV rightly after arriving at the origin station of rental i
λ_i^k, δ_i^k	Binary variables for the application of the piecewise linear approximation approach
A_i	Proxy variable for the concave term $(1-R_i)^b - (1-R_i+l_i)^b$ in the objective function (3.24)
B_i	Proxy variable for the concave term $(1-Q_i)^b$ in the objective function (3.24)
ΔT_{min}	The minimum rental duration
ΔT_{max}	The maximum rental duration

A.2 Algorithms for Model Linearization

The determination of the breakpoints for linear segments of the convex terms in the objective function (3.10) is shown in Algorithm A.1. *FindSegmentPoint* is a recursive function to find the set of breakpoints for the linear segments of the convex curve $g(G_i)$. In each recursion step, this function will return a unique point in the domain $G_i \in [G_i^{(L)}, G_i^{(U)}]$ with the maximum error for approximating the convex function $g(G_i)$ using the linear segment specified by the two endpoints of the interval, if the maximum error is larger than $\hat{\varepsilon}$. The sub-function *SegmentLine* will return the slope and intercept of the line across points $(G_i^{(L)}, g(G_i^{(L)}))$ and $(G_i^{(U)}, g(G_i^{(U)}))$. *SlopeEquivalentPoint* returns the point with the maximum error for approximating the convex function $g(G_i)$ using the linear segment specified by the above two endpoints. *ApproximationValue* calculates the approximate value for the function $g(G_i)$ at this unique point.

Algorithm A.1: Pseudocode for finding the set of breakpoints $\boldsymbol{P}$ for linear segment generation.

1 Initialize $\boldsymbol{P} \leftarrow \{G_i^{(L)}, G_i^{(U)}\}$;
2 Function $[\boldsymbol{P}] = FindSegmentPoint(G_i^{(L)}, G_i^{(U)}, \boldsymbol{P})$
3 $[s, c] = SegmentLine(G_i^{(L)}, G_i^{(U)})$;
4 $G_i = SlopeEquivalentPoint(g(G_i), s)$;
5 $\hat{g}(G_i) = ApproximationValue(s, c, G_i)$;
6 $Error = \hat{g}(G_i) - g(G_i)$;
7 If $Error > \hat{\varepsilon}$, then \\ If the maximal error is larger than the threshold, add the corresponding point to

set $\boldsymbol{P}$, and execute the above procedure for two subintervals $[G_i^{(L)}, G_i]$, $[G_i, G_i^{(U)}]$

$\boldsymbol{P} \leftarrow G_i$;

$[\boldsymbol{P}] = FindSegmentPoint(G_i^{(L)}, G_i, \boldsymbol{P})$

$[\boldsymbol{P}] = FindSegmentPoint(G_i, G_i^{(U)}, \boldsymbol{P})$

End if

End function

Analogously, the procedure for determining the tangent points for tangent lines of the concave terms in the objective function (3.10) is presented in Algorithm A.2, taking the function $h(R_i)$ as an example. *FindTangentPoint* is a recursive function to determine the set of tangent points in the domain $R_i \in [R_i^{(L)}, R_i^{(U)}]$ for the tangent lines of the concave curve $h(R_i)$. Due to the infinite slope of the curve $h(R_i)$ at the point $R_i = E$, *FindTangentPoint* first returns a new $R_i^{(U)}$ that ensures the approximation error at the point $R_i = E$ is no larger than $\hat{\varepsilon}$, which is determined by the sub-function $FindNewR_i^{(U)}$. The function *TangentLine* returns the slope and intercept of the tangent lines at points $(R_i^{(L)}, h(R_i^{(L)}))$ and $(R_i^{(U)}, h(R_i^{(U)}))$. *Intersection* calculates the coordinate value of the intersection of the above two tangent lines. The function *FindTangentPoint* will return the point corresponding to the intersection, i.e., the point at which the error for approximating the concave function $h(R_i)$ using the outer-approximation envelope formulated by the above two tangent lines is maximal when $R_i^{(L)} \le R_i \le R_i^{(U)}$, if the approximation error at the point is larger than $\hat{\varepsilon}$.

Algorithm A.2: Pseudocode for finding the set of tangent points $\boldsymbol{T}$ for tangent line generation.

Initial $\boldsymbol{T} \leftarrow \{R_i^{(L)}, R_i^{(U)}\}$;

Function $[\boldsymbol{T}] = FindTangentPoint(R_i^{(L)}, R_i^{(U)}, \boldsymbol{T})$

If $R_i^{(U)} = E$, then \\ Since the slope of curve $h(R_i)$ at point E is infinite, we need to find a new $R_i^{(U)}$ if $R_i^{(U)} = E$ to ensure the approximation error at point E is no larger than $\hat{\varepsilon}$.

$[R_i^0] = FindNewR_i^{(U)}(h(R_i), E, \hat{\varepsilon})$;

End if

$R_i^{(U)} \leftarrow R_i^0$

$[s_1, c_1] = TangentLine(R_i^{(L)})$;

$[s_2, c_2] = TangentLine(R_i^{(U)})$;

$[R_i, \hat{h}(R_i)] = Intersection(s_1, c_1, s_2, c_2)$;

10 $Error = \hat{h}(R_i) - h(R_i)$;

11 If $Error > \hat{\varepsilon}$, then \\ If the error is larger than the threshold value, add the corresponding point R_i to set $\boldsymbol{P}$, and execute the above procedure for the two subintervals $[R_i^{(L)}, R_i]$ and $[R_i, R_i^{(U)}]$.

12 $\boldsymbol{T} \leftarrow R_i$;

13 $[\boldsymbol{T}] = FindTangentPoint(R_i^{(L)}, R_i, \boldsymbol{T})$

14 $[\boldsymbol{T}] = FindTangentPoint(R_i, R_i^{(U)}, \boldsymbol{T})$

15 End if

16 End function

APPENDIX B NOTATIONS AND SUPPLEMENT FOR CHAPTER 4

B.1 Notations

T	Duration of the planning horizon
$\mathcal{I}$	Set of rentals
i, j	Indices for rental
$\mathcal{V}$	Set of EVs
v	Index for EV
$\mathcal{S}$	Set of stations
s_i^o	Pick-up station of the renal i
s_i^d	Drop-off station of the rental i
t_i^o	Departure time of the rental i
t_i^d	Arrival time of the rental i
t_i^r	Reservation time of the rental i
t_i^c	Cancellation time of the rental i
e_i	Electricity consumption of the rental i
G_i	Net profit collected from the rental i
E_i	Penalty for the rental i if it is denied service
$\mathcal{I}_0$	Set of rentals known at the beginning of the planning horizon
SOC_0	Initial SOC of EV before charging
$SOC_{\max}$	Maximum SOC achieved at the end of the CV phase
$SOC_{\min}$	Minimum SOC allowed in a carsharing system
SOC_{cutoff}	Cut-off value of SOC
$\hat{s}_v^0$	Initial location of the EV v at the beginning of the planning horizon
$\hat{t}_v^0$	Initial time of the EV v at the beginning of the planning horizon

$\hat{l}_v^0$	Initial SOC of the EV v at the beginning of the planning horizon
$\tau(s_i^d, s_j^o)$	Relocation time from the drop-off station of rental i to the pick-up station of rental j
$e(s_i^d, s_j^o)$	Electricity consumption for the relocation operation from the drop-off station of rental i to the pick-up station of rental j
$RC(s_i^d, s_j^o)$	Incurred relocation cost from the drop-off station of rental i to the pick-up station of rental j
$\tau(\hat{s}_v^0, s_j^o)$	Relocation time from the initial location of the EV v to the pick-up station of rental j
$e(\hat{s}_v^0, s_j^o)$	Electricity consumption for the relocation operation from the initial location of the EV v to the pick-up station of rental j
$RC(\hat{s}_v^0, s_j^o)$	Incurred relocation cost from the initial location of the EV v to the pick-up station of rental j
K	Number of sub-horizons
t_k	Start time point of the k^{th} sub-horizon
Δ	Time interval between two decision epochs
τ	Computation time limit for each static problem
$\mathcal{I}_k$	Set of rentals known up to the decision epoch t_k but with departure time no earlier than $t_k + \tau$
$\bar{\mathcal{I}}_{k-1}$	Set of rentals with departure time lying in the period $[t_{k-1} + \tau, t_k + \tau)$
$\tilde{\mathcal{I}}_{k-1}$	Set of rentals newly received during the period $[t_{k-1}, t_k)$
$\hat{\mathcal{I}}_{k-1}$	Set of rentals canceled by users during the period $[t_{k-1}, t_k)$
$\hat{t}_v$	Earliest available time of the EV v for the static problems
$\hat{s}_v$	Available location of the EV v for the static problems
$\hat{l}_v$	Available SOC of the EV v for the static problems
$\mathcal{R}_k^v$	Set of activity trajectories associated with the EV v for the k^{th} static problem
r, u	Indices for activity trajectory
P_r^v	Real profit of the activity trajectory $r \in \mathcal{R}_k^v$ for the k^{th} static problem
x_r^v	Binary decision variable that equals 1 if an EV v performs the activity trajectory r, and 0 otherwise
δ_{ir}^v	Rental-trajectory incidence coefficient that equals 1 if a rental i is covered by the activity trajectory $r \in \mathcal{R}_k^v$ in the k^{th} static problem, and 0 otherwise
$\mathcal{G} = (\mathcal{I}_0, \mathcal{A})$	Constructed pseudo-network for generating activity trajectories of the first static problem
ij	Index for link
p_i	Profit for the node i in the constructed pseudo-network
p_{ij}	Profit for the link ij in the constructed pseudo-network
$\tau(s_i^d)$	Charging duration at the drop-off station of the rental i
$\tau(s_j^o)$	Charging duration at the pick-up station of the rental j
l_i^d	SOC of an EV right after arriving at the drop-off station of the rental i

l_j^o	SOC of an EV just before serving the rental j
$\mathcal{L}(v,i)$	Set of labels associated with the EV v at the node i
$l_k(v,i)$	Label k associated with the EV v at the node i, $l_k(v,i) := [\bar{p}_k, \bar{l}_k, n_k, m_k]$, where $\bar{p}_k$ and $\bar{l}_k$ are the profit and SOC of the path k ending at the drop-off station of node/rental i, respectively; n_k and m_k are the node and label indexes that precede label k
N_{label}	The maximum number of labels generated for a node through a specific link
μ_1	Weight for path profit
μ_2	Weight for SOC of EV
$\mathcal{R}_{latest}^v$	Set of latest activity trajectories generated for the EV v in the dynamic column generation process for the subsequent static problems
$\mathcal{I}_{latest}$	Set of latest known rentals in the dynamic column generation process for the subsequent static problems
λ_n	The time epoch right after generating new activity trajectories for the rentals in $\mathcal{I}_{latest}$ in the n^{th} iteration
$\tilde{\mathcal{I}}[\lambda_{n-1}, \lambda_n)$	Set of rentals that are newly reserved during the time interval $[\lambda_{n-1}, \lambda_n)$
$\hat{\mathcal{I}}[\lambda_{n-1}, \lambda_n)$	Set of rentals that are canceled during the time interval $[\lambda_{n-1}, \lambda_n)$
r_{k-1}^{v*}	The selected activity trajectory for the EV v in the $(k-1)^{th}$ static problem to be implemented over the time period $[t_{k-1}+\tau, t_k+\tau]$
r^{fst}	First rental covered by the activity trajectory r
r^{last}	Last rental covered by the activity trajectory r
r_i^{sud}	The rental that succeeds the rental i in the activity trajectory r
o_v	A created dummy rental corresponding to the EV v
ψ	The optimal dual vector of the formulation [LP-VR&CS] and $\psi = (\alpha_1, ..., \alpha_i, ..., \alpha_{\lvert\mathcal{I}_{latest}\rvert}, \beta_1, ..., \beta_v, ..., \beta_{\lvert\mathcal{V}\rvert})$, where α_i is dual variable value for the rental i and β_v is the dual variable value for the EV v
$\mathcal{B}$	Set of activity trajectories in the optimal basis
Z	A pre-specified threshold for the number of activity trajectories generated for the rentals in $\mathcal{I}_{latest}$
$\mathcal{C}^v$	Among the activity trajectories generated for the rentals in $\mathcal{I}_{latest}$, set of the ones associated with the EV v with the reduced cost lager than zero
ε	Threshold for the reduced cost to determine the activity trajectories that can be inserted by the newly arriving rentals in the dynamic column generation process
$\mathcal{D}^v$	Among the activity trajectories generated for the rentals in $\mathcal{I}_{latest}$, set of the ones associated with the EV v with the reduced cost larger than ε
v_r	The EV covering the activity trajectory r
$\mathcal{I}(r)$	Set of rentals covered by the activity trajectory r
$\mathcal{M}^v$	Set of activity trajectories associated with the EV v generated for the rentals in $\tilde{\mathcal{I}}[\lambda_{n-1}, \lambda_n)$

$\bar{P}_r$	Profit of the activity trajectory r with the penalty for unserved rentals considered
σ	Threshold for the profit difference between two activity trajectories to determine the activity trajectories generated for the newly arriving rentals in the dynamic column generation process

B.2 Propositions

Proposition 1. For the rental j, there exists at most one rental in the set $\mathcal{N}(\bar{u})$ succeeding which it can be feasibly inserted.

Proof. The proposition can be proved by contradiction. Suppose that there exist two such rentals, namely, i and l. Since both i and l are covered by $\bar{u}$ and without loss of generality, it is assumed that the rental i is served before the rental l. Since the rental j can be feasibly inserted into $\bar{u}$ such that it succeeds the rental i, i.e., the rental j is served after the rental i and before the rental l. This contradicts to that the rental j can be feasibly inserted into $\bar{u}$ such that it succeeds the rental l, i.e., the rental j is served after the rental l.

This concludes the proof. □

Proposition 2. If the profit increase of the activity trajectory r brought by the insertion of the rental i is less than zero, i.e., $\bar{P}_{\bar{r}} - \bar{P}_r < 0$, the activity trajectory $\bar{r}$ will not be an optimal activity trajectory for the restricted set-packing-type formulation of the considered static problem.

Proof. The proposition can be proved by contradiction. Suppose that $\bar{r}$ is an optimal activity trajectory in the restricted set-packing-type formulation of the considered static problem. Since the activity trajectory r covers the same rentals as the activity trajectory $\bar{r}$ except for the rental i, the activity trajectory r can also be implemented by the EV performing the activity trajectory $\bar{r}$. Since $\bar{P}_r > \bar{P}_{\bar{r}}$, the implementation of the activity trajectory r will yield a higher objective value, which contradicts to the assumption that $\bar{r}$ is an optimal activity trajectory for the restricted set-packing-type formulation of the considered static problem.

This concludes the proof. □

APPENDIX C NOTATIONS FOR CHAPTER 5

$\mathcal{S}$	Set of stations
i, j	Indices for an order
s_i^o	Pick-up station of the order i
s_i^d	Drop-off station of the order i
t_i^o	Departure time from the pick-up station of the order i
t_i^d	Arrival time at the drop-off station of the order i
e_i	Electricity consumption of the order i
T	Duration of the operational period
G_i	Revenue collected from the order i
E_i	Penalty for rejecting the order i
$\mathcal{I}_0$	Set of orders that have been reserved at the beginning of the operational period
$\mathcal{V}$	Set of EVs
v	Index for an EV
s_v^0	Initial location of the EV v
l_v^0	Initial SOC of the EV v
$\tau(s_i^d, s_j^o)$	Travel time for the relocation operation from the drop-off station of the order i to the pick-up station of the order j
$e(s_i^d, s_j^o)$	Electricity consumption for the relocation operation from the drop-off station of the order i to the pick-up station of the order j
$\mathrm{c}(s_i^d, s_j^o)$	Operating cost for the relocation operation from the drop-off station of the order i to the pick-up station of the order j
$SOC_{\min}$	The minimum SOC allowed in the electric carsharing system
$\mathcal{F}$	Set of staff members
f	Index for a staff member
$\overline{s}_f^0$	Initial location of the staff member f
m, n	Indices for a relocation task
$\overline{s}_m^o$	Origin station of the relocation task m
$\overline{s}_m^d$	Destination station of the relocation task m
$\overline{t}_m^o$	Departure time from the origin station of the relocation task m
$\overline{t}_m^d$	Arrival time at the destination station of the relocation task m
$\overline{\tau}(\overline{s}_m^d, \overline{s}_n^o)$	Travel time for the rebalancing operation from the destination station of the relocation task m to the origin station of the relocation task n
$\overline{c}(\overline{s}_m^d, \overline{s}_n^o)$	Incurred cost for the rebalancing operation from the destination station of the relocation task m to the origin station of the relocation task n
$\mathcal{S}_k$	System state at the k^{th} decision epoch
$\boldsymbol{V}_k$	Vector of EV available information at the k^{th} decision epoch
V_{kv}	Available information of the EV v at the k^{th} decision epoch

$\boldsymbol{F}_k$	Vector of staff available information at the k^{th} decision epoch
F_{kf}	Available information of the staff member f at the k^{th} decision epoch
$\mathcal{I}_k$	Set of orders with departure time no earlier than the k^{th} decision epoch
t_{kv}	The earliest available time of the EV v at the k^{th} decision epoch
s_{kv}	The available station of the EV v at the k^{th} decision epoch
l_{kv}	The available SOC of the EV v at the k^{th} decision epoch
$\overline{t}_{kf}$	The earliest available time of the staff member f at the k^{th} decision epoch
$\overline{s}_{kf}$	The available station of the staff member f at the k^{th} decision epoch
$\mathcal{P}_{kv}$	Set of feasible activity trajectories for the EV v at the k^{th} decision epoch
p	Index for an EV activity trajectory
$\mathcal{M}_{kvp}$	Set of physically real relocation tasks embedded in the activity trajectory $p \in \mathcal{P}_{kv}$ at the k^{th} decision epoch
$\mathcal{Q}_{kf}$	Set of feasible trip chains for the staff member f at the k^{th} decision epoch
q	Index for a staff trip chain
a_k	Action at the k^{th} decision epoch
$\boldsymbol{x}$	Vector of EV-trajectory decisions
x_{vp}	A decision that equals 1 if the EV v implements the activity trajectory p, and 0 otherwise
$\boldsymbol{y}$	Vector of staff-chain decisions
y_{fq}	A decision that equals 1 if the staff member f performs the trip chain q, and 0 otherwise
α_v^{ip}	Order-trajectory incidence coefficient that equals 1 if order i is covered by activity trajectory $p \in \mathcal{P}_{kv}$, and 0 otherwise
β_f^{mq}	Task-chain incidence coefficient that equals 1 if relocation task m is covered by trip chain $q \in \mathcal{Q}_{kf}$, and 0 otherwise
ξ_{k+1}	Exogenous information that becomes known at the $(k+1)^{th}$ decision epoch
t_{k+1}	Time point of the $(k+1)^{th}$ decision epoch
i_{k+1}	Reserved or cancelled order at the $(k+1)^{th}$ decision epoch
$\tilde{\mathcal{I}}_{k+1}$	Set of orders with the departure time between the k^{th} and the $(k+1)^{th}$ decision epochs
$r_k(s_k, a_k)$	A reward received by the carsharing operator at the k^{th} decision epoch as a result of choosing action a_k in state s_k
$\mathcal{Z}$	Set of all possible Markov policies
z	Index for a Markov policy
K	Number of decision epochs before the end of the operational period
s_0	Initial system state
$\boldsymbol{V}_0$	Vector of EV initial information

V_{0v}	Initial information of the EV v
$\boldsymbol{F}_0$	Vector of Staff initial information
F_{0f}	Initial information of the staff member f
p_{kv}	The activity trajectory implemented by the EV v at the k^{th} decision epoch
q_{kf}	The trip chain performed by the staff member f at the k^{th} decision epoch
v^* and f^*	The combination of an EV and a staff member associated with the highest and positive incremental profit
i_v	The last order assigned to the EV v
$l_{i_v}^d$	SOC of the EV v after it arrives at the drop-off station of the order i_v
o_{kv}	A dummy order with the same pick-up and drop-off stations being s_{kv}, the same pick-up and drop-off times at t_{kv}, and 0 electricity consumption
m_f	The last relocation task assigned to the staff member f
$\overline{o}_{kf}$	A dummy relocation task with origin and destination stations being $\overline{s}_{kf}$ and departure and arrival times at $\overline{t}_{kf}$
Δ_{vf}^{pre}	Charging duration at the drop-off station of the order i_v if the combination v and f is tentatively dispatched for serving a picked order
Δ_{vf}^{suc}	Charging duration at the pick-up station of a picked order if the combination v and f is tentatively dispatched for serving the order
l_{vf}^{suc}	EV SOC by the departure time of a picked order if the combination v and f is tentatively dispatched for serving the order
t^{elst}	The earliest possible time at which the EV v is picked up by the staff member f for relocation if a combination v and f is tentatively dispatched for serving a picked order
l^{elst}	The corresponding EV SOC at the time t^{elst}
Δ_{vf}^{pre1}	Charging duration at the drop-off station of the order i_v until the time point t^{elst}
Δ_{vf}^{pre2}	Charging duration at the drop-off station of the order i_v after the time point t^{elst}
$PROFIT_{vf}^{incremental}$	Incremental profit if a combination v and f is tentatively dispatched for serving an order
$\Delta_{i_{v^*}}^d$	Determined charging duration at the drop-off station of the order i_{v^*}
Δ_j^o	Determined charging duration at the pick-up station of the order j
$\widehat{\mathcal{I}}_k$	Set of orders that remain to be picked for assignment when determining the action at the k^{th} decision epoch

REFERENCES

Balac, M., Ciari, F., Axhausen, K.W., 2017. Modeling the impact of parking price policy on free-floating carsharing: case study for Zurich, Switzerland. *Transportation Research Part C: Emerging Technologies* 77, 207-225.

Barré, A., Deguilhem, B., Grolleau, S., Gérard, M., Suard, F., Riu, D., 2013. A review on lithium-ion battery ageing mechanisms and estimations for automotive applications. *Journal of Power Sources* 241, 680-689.

Bekli, S., Boyacı, B., Zografos, K.G., 2021. Enhancing the performance of one-way electric carsharing systems through the optimum deployment of fast chargers. *Transportation Research Part B: Methodological* 152, 118-139.

Bi, J., Sai, Q., Xie, D., Zhao, X., 2021. Bi-level optimisation model for one-way electric carsharing stations based on survival model. *Sustainable Cities Society* 65, 102528.

Board, T.R., National Academies of Sciences, E., Medicine, 2005. *Car-sharing: where and how it Succeeds*. The National Academies Press, Washington, DC.

Boyacı, B., Zografos, K.G., 2019. Investigating the effect of temporal and spatial flexibility on the performance of one-way electric carsharing systems. *Transportation Research Part B: Methodological* 129, 244-272.

Boyacı, B., Zografos, K.G., Geroliminis, N., 2015. An optimization framework for the development of efficient one-way car-sharing systems. *European Journal of Operational Research* 240, 718-733.

Boyacı, B., Zografos, K.G., Geroliminis, N., 2017. An integrated optimization-simulation framework for vehicle and personnel relocations of electric carsharing systems with reservations. *Transportation Research Part B: Methodological* 95, 214-237.

Brandstätter, G., Gambella, C., Leitner, M., Malaguti, E., Masini, F., Puchinger, J., Ruthmair, M., Vigo, D., 2016. Overview of optimization problems in electric car-sharing system design and management, *Dynamic Perspectives on Managerial Decision Making*. Springer, pp. 441-471.

Brandstätter, G., Kahr, M., Leitner, M., 2017. Determining optimal locations for charging stations of electric car-sharing systems under stochastic demand. *Transportation Research Part B: Methodological* 104, 17-35.

Brandstätter, G., Leitner, M., Ljubić, I., 2020. Location of charging stations in electric car sharing systems. *Transportation Science* 54, 1408-1438.

Bruglieri, M., Colorni, A., Luè, A., 2014. The relocation problem for the one-way electric vehicle sharing. *Networks* 64, 292-305.

Bruglieri, M., Pezzella, F., Pisacane, O., 2018. A two-phase optimization method for a multiobjective vehicle relocation problem in electric carsharing systems. *Journal of Combinatorial Optimization* 36, 162-193.

Bruglieri, M., Pezzella, F., Pisacane, O., 2019. An adaptive large neighborhood search for relocating vehicles in electric carsharing services. *Discrete Applied Mathematics* 253, 185-200.

Çalık, H., Fortz, B., 2019. A benders decomposition method for locating stations in a one-way electric car sharing system under demand uncertainty. *Transportation Research Part B: Methodological* 125, 121-150.

Cocca, M., Giordano, D., Mellia, M., Vassio, L., 2019. Free floating electric car sharing design: data driven optimisation. *Pervasive Mobile Computing* 55, 59-75.

Condliffe, J., 2017. China and India want all new cars to be electric, MIT Technology Review. https://www.technologyreview.com/2017/09/11/149226/china-and-india-want-all-new-cars-to-be-electric/ (accessed 15.06.2022).

Crabtree, G., 2019. The coming electric vehicle transformation. *Science* 366, 422-424.

de Almeida Correia, G.H., Antunes, A.P., 2012. Optimization approach to depot location and trip selection in one-way carsharing systems. *Transportation Research Part E: Logistics Transportation Review* 48, 233-247.

Deza, A., Huang, K., Metel, M.R., 2020. Charging station optimization for balanced electric car sharing. *Discrete Applied Mathematics*.

Di Febbraro, A., Sacco, N., Saeednia, M., 2018. One-way car-sharing profit maximization by means of user-based vehicle relocation. *IEEE Transactions on Intelligent Transportation Systems* 20, 628-641.

Duran, M.A., Grossmann, I.E., 1986. An outer-approximation algorithm for a class of mixed-integer nonlinear programs. *Mathematical Programming* 36, 307-339.

EIA, 2021. International energy outlook 2021, U.S. Energy Information Administration. https://www.eia.gov/outlooks/ieo/pdf/IEO2021_Narrative.pdf (accessed 14.06.2022).

EVCARD, 2022. https://www.evcard.com (accessed 01.03.2022).

Fan, W., 2013. Management of dynamic vehicle allocation for carsharing systems: stochastic programming approach. *Transportation Research Record* 2359, 51-58.

Fan, W.D., 2014. Optimizing strategic allocation of vehicles for one-way car-sharing systems under demand uncertainty, *Journal of the Transportation Research Forum*.

Ferrero, F., Perboli, G., Rosano, M., Vesco, A., 2018. Car-sharing services: an annotated review. *Sustainable Cities and Society* 37, 501-518.

Folkestad, C.A., Hansen, N., Fagerholt, K., Andersson, H., Pantuso, G., 2020. Optimal charging and repositioning of electric vehicles in a free-floating carsharing system. *Computers Operations Research* 113, 104771.

Gambella, C., Malaguti, E., Masini, F., Vigo, D., 2018. Optimizing relocation operations in electric car-sharing. *Omega* 81, 234-245.

Golalikhani, M., Oliveira, B.B., Carravilla, M.A., Oliveira, J.F., Antunes, A.P., 2021a. Carsharing: a review of academic literature and business practices toward an integrated decision-support framework. *Transportation Research Part E: Logistics transportation review* 149, 102280.

Golalikhani, M., Oliveira, B.B., Carravilla, M.A., Oliveira, J.F., Pisinger, D., 2021b. Understanding carsharing: a review of managerial practices towards relevant research insights. *Research in Transportation Business Management* 41, 100653.

Google, 2022. Google Maps. https://www.google.com.hk/maps (accessed 01.03.2022).

Guéret, C., Prins, C., Sevaux, M., 2000. Applications of optimization with Xpress-MP. http://citeseerx.ist.psu.edu/viewdoc/download?doi=10.1.1.69.9634&rep=rep1&type=pdf (accessed 15.09.2020).

Han, S., Han, S., Aki, H., 2014. A practical battery wear model for electric vehicle charging applications. *Applied Energy* 113, 1100-1108.

Hao, M., Yamamoto, T., 2018. Shared autonomous vehicles: a review considering carsharing and autonomous vehicles. *Asian Transport Studies* 5, 47-63.

He, L., Mak, H.-Y., Rong, Y., Shen, Z.-J.M., 2017. Service region design for urban electric vehicle sharing systems. *Manufacturing Service Operations Management* 19, 309-327.

Hu, L., Liu, Y., 2016. Joint design of parking capacities and fleet size for one-way station-based carsharing systems with road congestion constraints. *Transportation Research Part B: Methodological* 93, 268-299.

Hua, Y., Zhao, D., Wang, X., Li, X., 2019. Joint infrastructure planning and fleet management for one-way electric car sharing under time-varying uncertain demand. *Transportation Research Part B: Methodological* 128, 185-206.

Huang, K., An, K., de Almeida Correia, G.H., 2020a. Planning station capacity and fleet size of one-way electric carsharing systems with continuous state of charge functions. *European Journal of Operational Research* 287, 1075-1091.

Huang, K., An, K., de Almeida Correia, G.H., Rich, J., Ma, W., 2021. An innovative approach to solve the carsharing demand-supply imbalance problem under demand uncertainty. *Transportation Research Part C: Emerging Technologies* 132, 103369.

Huang, K., An, K., Rich, J., Ma, W., 2020b. Vehicle relocation in one-way station-based electric carsharing systems: a comparative study of operator-based and user-based methods. *Transportation Research Part E: Logistics Transportation Review* 142, 102081.

Huang, K., Correia, G.H.D.A., An, K., 2018. Solving the station-based one-way carsharing network planning problem with relocations and non-linear demand. *Transportation Research Part C: Emerging Technologies* 90, 1-17.

Huo, X., Wu, X., Li, M., Zheng, N., Yu, G., 2020. The allocation problem of electric car-sharing system: a data-driven approach. *Transportation Research Part D: Transport Environment* 78, 102192.

Hyland, M., Mahmassani, H.S., 2018. Dynamic autonomous vehicle fleet operations: Optimization-based strategies to assign AVs to immediate traveler demand requests. *Transportation Research Part C: Emerging Technologies* 92, 278-297.

Iacobucci, R., McLellan, B., Tezuka, T., 2019. Optimization of shared autonomous electric vehicles operations with charge scheduling and vehicle-to-grid. *Transportation Research Part C: Emerging Technologies* 100, 34-52.

IEA, 2021a. Global EV outlook 2021, International Energy Agency. https://www.iea.org/reports/global-ev-outlook-2021 (accessed 15.06.2022).

IEA, 2021b. New energy automobile industry development plan (2021-2035), International Energy Agency. https://www.iea.org/policies/13099-new-energy-automobile-industry-development-plan-2021-2035 (accessed 15.06.2022).

Jian, S., Rey, D., Dixit, V., 2018. An integrated supply-demand approach to solving optimal relocations in station-based carsharing systems. *Networks and Spatial Economics* 19, 611-632.

Jittrapirom, P., Caiati, V., Feneri, A.-M., Ebrahimigharehbaghi, S., Alonso González, M.J., Narayan, J., 2017. Mobility as a service: a critical review of definitions, assessments of schemes, and key challenges. *Urban Planning* 2, 13–25.

Jorge, D., Molnar, G., de Almeida Correia, G.H., 2015. Trip pricing of one-way station-based carsharing networks with zone and time of day price variations. *Transportation Research Part B: Methodological* 81, 461-482.

Jung, A., 2014. Carsharing services in emerging economies. *Sustainable Urban Transport Project.* https://sutp.org/publications/carsharing-services-in-emerging-economies/ (accessed in 07,06,2022).

Kang, N., Feinberg, F.M., Papalambros, P.Y., 2017. Autonomous electric vehicle sharing system design. *Journal of Mechanical Design* 139, 011402.

Kim, J., Rasouli, S., Timmermans, H., 2017. Satisfaction and uncertainty in car-sharing decisions: an integration of hybrid choice and random regret-based models. *Transportation Research Part A: Policy Practice* 95, 13-33.

Lage, M., Machado, C., Berssaneti, F., Quintanilha, J., 2018. A method to define the spatial stations location in a carsharing system in São Paulo–Brazil. *International Archives of the Photogrammetry, Remote Sensing and Spatial Information Sciences* 4, 27-32.

Lai, K., Chen, T., Natarajan, B., 2020. Optimal scheduling of electric vehicles car-sharing service with multi-temporal and multi-task operation. *Energy* 204, 117929.

Laporte, G., Pascoal, M.M., Research, O., 2011. Minimum cost path problems with relays. *Computers & Operations Research* 38, 165-173.

Lee, U., Kang, N., Lee, I., 2020. Shared autonomous electric vehicle design and operations under uncertainties: a reliability-based design optimization approach. *Structural Multidisciplinary Optimization* 61, 1529-1545.

Li, L., Pantelidis, T., Chow, J.Y., Jabari, S.E., 2021. A real-time dispatching strategy for shared automated electric vehicles with performance guarantees. *Transportation Research Part E: Logistics Transportation Review* 152, 102392.

Li, Q., Liao, F., 2020. Incorporating vehicle self-relocations and traveler activity chains in a bi-level model of optimal deployment of shared autonomous vehicles. *Transportation Research Part B: Methodological* 140, 151-175.

Li, Q., Liao, F., Timmermans, H.J., Huang, H., Zhou, J., 2018. Incorporating free-floating car-sharing into an activity-based dynamic user equilibrium model: a demand-side model. *Transportation Research Part B: Methodological* 107, 102-123.

Li, X., Ma, J., Cui, J., Ghiasi, A., Zhou, F., 2016. Design framework of large-scale one-way electric vehicle sharing systems: a continuum approximation model. *Transportation Research Part B: Methodological* 88, 21-45.

Liu, W., 2013. *Introduction to hybrid vehicle system modeling and control*. John Wiley & Sons.

Lu, M., Chen, Z., Shen, S., 2018. Optimizing the profitability and quality of service in carshare systems under demand uncertainty. *Manufacturing Service Operations Management* 20, 162-180.

Lu, X., Zhang, Q., Peng, Z., Shao, Z., Song, H., Wang, W., 2020. Charging and relocating optimization for electric vehicle car-sharing: an event-based strategy improvement approach. *Energy* 207, 118285.

Lu, Y., Wang, K., Yuan, B., 2022. The vehicle relocation problem with operation teams in one-way carsharing systems. *International Journal of Production Research* 60, 3829-3843.

Ma, B., Hu, D., Chen, X., Wang, Y., Wu, X., 2021a. The vehicle routing problem with speed optimization for shared autonomous electric vehicles service. *Computers Industrial Engineering* 161, 107614.

Ma, B., Hu, D., Wu, X., 2021b. The Location Routing Problem of the Car-Sharing System with Autonomous Electric Vehicles. *KSCE Journal of Civil Engineering* 25, 3107-3120.

Ma, J., Li, X., Zhou, F., Hao, W., 2017. Designing optimal autonomous vehicle sharing and reservation systems: A linear programming approach. *Transportation Research Part C: Emerging Technologies* 84, 124-141.

Ma, W., Wang, L., Li, L., 2018. Vehicle relocation triggering thresholds determination in electric carsharing system under stochastic demand. *Journal of Advanced Transportation* 2018.

Machado, C.A.S., de Salles Hue, N.P.M., Berssaneti, F.T., Quintanilha, J.A., 2018. An overview of shared mobility. *Sustainability* 10, 4342.

Marra, F., Yang, G.Y., Træholt, C., Larsen, E., Rasmussen, C.N., You, S., 2012. Demand profile study of battery electric vehicle under different charging options, *2012 IEEE Power and Energy Society General Meeting*. IEEE, pp. 1-7.

Molnar, G., de Almeida Correia, G.H., 2019. Long-term vehicle reservations in one-way free-floating carsharing systems: a variable quality of service model. *Transportation Research Part C: Emerging Technologies* 98, 298-322.

Monteiro, C.M., Machado, C.A.S., de Oliveira Lage, M., Berssaneti, F.T., Davis Jr, C.A., Quintanilha, J.A., 2021. Optimization of carsharing fleet size to maximize the number of clients served. *Computers, Environment Urban Systems* 87, 101623.

Münzel, K., Boon, W., Frenken, K., Blomme, J., van der Linden, D., 2020. Explaining carsharing supply across western European cities. *International Journal of Sustainable Transportation* 14, 243-254.

Nicholas, M., Bernard, M.R., 2021. Success factors for electric carsharing. Working Paper 2021-30, International Council on Clean Transportation.

Nissan, 2021. Nissan Leaf. http://www.nissanusa.com/electric-cars/leaf/ (accessed 31/05/2021).

Nourinejad, M., Roorda, M.J., 2015. Carsharing operations policies: a comparison between one-way and two-way systems. *Transportation* 42, 497-518.

Nourinejad, M., Zhu, S., Bahrami, S., Roorda, M.J., 2015. Vehicle relocation and staff rebalancing in one-way carsharing systems. *Transportation Research Part E: Logistics and Transportation Review* 81, 98-113.

Pantelidis, T.P., Li, L., Ma, T.-Y., Chow, J.Y., Jabari, S.E.G., 2022. A node-charge graph-based online carshare rebalancing policy with capacitated electric charging. *Transportation Science* 56, 654-676.

Pelletier, S., Jabali, O., Laporte, G., Veneroni, M., 2017. Battery degradation and behaviour for electric vehicles: review and numerical analyses of several models. *Transportation Research Part B: Methodological* 103, 158-187.

Phillips, S., Gopal, V., Azarcon, L., Rafferty, A., 2021. Electric carsharing whitepaper. https://movmi.net/blog/electric-carsharing-whitepaper-2021/ (accessed 14.06.2022).

Powell, W.B., 2007. *Approximate dynamic programming: solving the curses of dimensionality*. John Wiley & Sons.

Sai, Q., Bi, J., Chai, J., 2020. Optimal model for carsharing station location based on multi-factor constraints. *Algorithms* 13, 43.

Schiffer, M., Hiermann, G., Rüdel, F., Walther, G., 2021. A polynomial-time algorithm for user-based relocation in free-floating car sharing systems. *Transportation Research Part B: Methodological* 143, 65-85.

Shaheen, S., Chan, N., Bansal, A., Cohen, A., 2015. Shared mobility: a sustainability & technologies workshop: definitions, industry developments, and early understanding. *Transportation Sustainability Research Center, University of California, Berkeley.* https://escholarship.org/uc/item/2f61q30s (accessed 05.06.2022).

Shaheen, S., Cohen, A., Jaffee, M., 2018. Worldwide carsharing growth. *Transportation Sustainability Research Center, University of California, Berkeley.* *https://escholarship.org/content/qt61q03282/qt61q03282_noSplash_74ac9b5438b71e5b2f3250e6c1e14099.pdf (accessed 04.10.2021).*

Shaheen, S.A., Cohen, A.P., Roberts, J.D., 2006. Carsharing in north America: market growth, current developments, and future potential. *Transportation Research Record* 1986, 116-124.

Solomon, M.M., 1987. Algorithms for the vehicle routing and scheduling problems with time window constraints. *Operations Research* 35, 254-265.

Statista, 2022. https://www.statista.com/ (accessed 13.06.2022).

Stokkink, P., Geroliminis, N., 2021. Predictive user-based relocation through incentives in one-way car-sharing systems. *Transportation Research Part B: Methodological* 149, 230-249.

Wang, L., Liu, Q., Ma, W., 2019. Optimization of dynamic relocation operations for one-way electric carsharing systems. *Transportation Research Part C: Emerging Technologies* 101, 55-69.

Wang, L., Ma, W., Wang, M., Qu, X., 2021a. Demand control model with combinatorial incentives and surcharges for one-way carsharing operation. *Transportation Research Part C: Emerging Technologies* 125, 102999.

Wang, N., Guo, J., Liu, X., Liang, Y., 2021b. Electric vehicle car-sharing optimization relocation model combining user relocation and staff relocation. *Transportation Letters* 13, 315-326.

Waserhole, A., Jost, V., 2012. Vehicle sharing system pricing regulation: a fluid approximation. https://hal.archives-ouvertes.fr/hal-00727041 (accessed 10.06.2022).

Xie, R., Wei, W., Wu, Q., Ding, T., Mei, S., 2019. Optimal service pricing and charging scheduling of an electric vehicle sharing system. *IEEE Transactions on Vehicular Technology* 69, 78-89.

Xu, M., 2018. Modeling and optimization for battery electric vehicle operations. *Ph.D. Dissertation, University of Singapore*.

Xu, M., Meng, Q., 2019. Fleet sizing for one-way electric carsharing services considering dynamic vehicle relocation and nonlinear charging profile. *Transportation Research Part B: Methodological* 128, 23-49.

Xu, M., Meng, Q., Liu, Z., 2018. Electric vehicle fleet size and trip pricing for one-way carsharing services considering vehicle relocation and personnel assignment. *Transportation Research Part B: Methodological* 111, 60-82.

Xu, M., Wu, T., Tan, Z., 2021. Electric vehicle fleet size for carsharing services considering on-demand charging strategy and battery degradation. *Transportation Research Part C: Emerging Technologies* 127, 103146.

Xu, M., Yang, H., Wang, S., 2020. Mitigate the range anxiety: siting battery charging stations for electric vehicle drivers. *Transportation Research Part C: Emerging Technologies* 114, 164-188.

Yang, S., Wu, J., Sun, H., Qu, Y., Li, T., 2021. Double-balanced relocation optimization of one-way car-sharing system with real-time requests. *Transportation Research Part C: Emerging Technologies* 125, 103071.

Zakaria, R., Dib, M., Moalic, L., 2018. Multiobjective car relocation problem in one-way carsharing system. *Journal of Modern Transportation* 26, 297-314.

Zhang, D., Liu, Y., He, S., 2019. Vehicle assignment and relays for one-way electric car-sharing systems. *Transportation Research Part B: Methodological* 120, 125-146.

Zhang, K., Takano, Y., Wang, Y., Yoshise, A., 2021. Optimizing the strategic decisions for one-way station-based carsharing systems: a mean-CVaR approach. *IEEE Access* 9, 79816-79828.

Zhao, D., Li, X., Cui, J., 2021. A simulation‐based optimization model for infrastructure planning for electric autonomous vehicle sharing. *Computer‐Aided Civil Infrastructure Engineering* 36, 858-876.

Zhao, M., Li, X., Yin, J., Cui, J., Yang, L., An, S., 2018. An integrated framework for electric vehicle rebalancing and staff relocation in one-way carsharing systems: model formulation and lagrangian relaxation-based solution approach. *Transportation Research Part B: Methodological* 117, 542-572.

Zhou, T., Osorio, C., Fields, E., 2017. A data-driven discrete simulation-based optimization algorithm for large-scale two-way car-sharing network design. *Massachusetts Inst. Technol., Boston, MA, USA, Tech. Rep*.